Investigating the effect of emetic and aversive compounds on *Dictyostelium* identifies a novel non-sentient model for bitter tastant research

Steven Jann Robery

Research thesis submitted for the degree of Doctor of Philosophy at Royal Holloway University of London in July 2013

Declaration of Authorship

I, Steven Robery, hereby declare that this thesis and the work presented in it is entirely my own. Where I have consulted the work of others, this is always clearly stated.

Signed:

Date:

Acknowledgements

First and foremost, I would like to thank my supervisors, Professor Robin Williams and Professor Paul Andrews. I would like to thank Robin for providing me with the support and direction he has given me over the past few years, as well as teaching me to critique my own work to make me a better scientist. I would like to thank Paul for providing me with support, advice and passion throughout my PhD. Your meetings were always inspirational. I would also like to thank my laboratory colleagues for all of the help, support and banter whilst I have been at Royal Holloway.

Secondly, I would like to thank my funding body, Universities Federation for Animal Welfare. Without you I would not have been given a PhD and been able to undertake this exciting project, nor would I have been able to contribute to the world of science in the way that I have.

I would also like to thank my friends and family for all of the support you have given me over the years. In particular I would like to thank my girlfriend Annabelle, for putting up with me and for providing me with laughs and generally being there for me when I needed her to be. I would also like to thank my parents, Peter and Elisabeth, as well as my sister, Nina for providing me with all the support and encouragement I needed. I would also like to thank my all my friends, providing me with the banter and encouraging me to “get a move on” and complete my PhD. Finally, I can’t forget my dog, Plato, who let me know time and again whilst I was writing that it is time to clear my mind and go for a much needed walk.

Abstract

Nausea and vomiting are common but serious side effects associated with many therapeutic drugs. Whilst the physiological mechanisms behind the generation of the vomiting response are well characterised, the range of emetic stimuli that can generate the response are poorly understood. The potential of using *Dictyostelium discoideum*, a eukaryotic amoeba, as a model for predicting emetic liability was examined in this thesis. The effects of a range of known emetic and aversive compounds on *Dictyostelium* cell behaviour was investigated, resulting in the identification of a small number that strongly inhibited cell migration in a concentration-dependent and reversible manner. These active compounds included a range of bitter compounds and the pungent tastant, capsaicin. A *Dictyostelium* mutagenesis screen was then used to identify genes controlling sensitivity to bitter tastants. This screen identified a mutant containing a disrupted *grlJ* gene as showing partial resistance to phenylthiourea in growth and behavioural changes in movement. GrlJ is a G-protein coupled receptor that regulates a phenylthiourea-dependent effect by inhibition of a phosphatidylinositol (PIP_3) signalling pathway. A search for proteins sharing homology to GrlJ identified an uncharacterised $GABA_B$-like receptor, Q8NHA5, involved in the detection of phenylthiourea in *Dictyostelium*. This thesis has therefore identified *Dictyostelium* as a potentially useful model for the identification of bitter and pungent tastants. In addition, this thesis has identified the *Dictyostelium* protein, GrlJ, as well as an uncharacterised human protein, Q8NHA5, involved in the detection of the bitter tastant, phenylthiourea.

Table of Contents

List of Figures and Tables

Abbreviations

$5\text{-}HT_3$	5-hydroxytryptamine receptor 3
$5\text{-}HT_4$	5-hydroxytryptamine receptor 4
ATP	adenosine triphosphate
BLAST	basic local alignment search tool
cAMP	cyclic adenosine monophosphate
cAR	cAMP receptor
CCK	cholecystokinin
cDNA	complementary DNA
cGMP	cyclic guanosine monophosphate
DAG	diacylglycerol
DMN	dorsal motor vagal nucleus
DMSO	dimethylsulphoxide
dNTPs	deoxynucleotide triphosphatases
DVC	dorsal vagal complex
GABA	gamma aminobutyric acid
$GABA_B$	gamma aminobutyric acid receptor B
GAP	guanine activating protein

gDNA	genomic DNA
GDP	guanosine diphosphate
GEF	guanine exchange factor
GFP	green fluorescent protein
GTP	guanosine triphosphate
IC_{50}	50% inhibitory concentration
IP_3	inositol triphosphate
IP_3R	inositol triphosphate receptor
NK_1	neurokinin receptor 1
NT	neurotransmitter
NTS	nucleus tractus solitarius
P1X	pannexin-1
P2X	pannexin-2
PCR	polymerase chain reaction
PDE	phosphodiesterase
PI3K	phosphatidylinositol-3-kinase
PIP_2	phosphatidylinositol-4,5-phosphate
PIP_3	phosphatidylinositol-3,4,5-phosphate
PKB/Akt	protein kinase B

PKC	protein kinase C
PKD	protein kinase D
PLC	phospholipase C
PTEN	phosphatase and tensin homologue
REMI	restriction enzyme-mediated integration
SCAR	suppressor of cAR
SDS	sodium dodecyl sulphate
SDS-PAGE	sodium dodecyl sulphate polyacrylamide gel electrophoresis
sGC	soluble guanylyl cylcase
SSRI	selective serotonin reuptake inhibitor
T2R	taste type II receptor
TEMED	N,N,N'N' – Tetramethyl-ethylene-1,2-diamine
TORC2	target of rapamycin complex 2
TRPM5	transient receptor potential melastatin 5
TRPV1	transient receptor potential vanilloid 1
VNUT	vesicular ATP transporter
WASP	Wiskott-Aldrich syndrome protein

Chapter 1

Introduction

Aspects of the physiology and pharmacology of nausea and vomiting will be reviewed in this introduction to provide background for the potential use of *Dictyostelium* as a model for the replacement of sentient species in the identification of emetic liability of novel chemical entities. In addition, some of the key compounds involved in the induction of these responses will be discussed. Current sentient models used in emetic research will then be outlined, before exploring alternative non-sentient approaches that have the potential to reduce or possibly replace the number of animals involved in emetic research. Finally, the use of a single celled social amoeba, *Dictyostelium discoideum*, has as a potential biomedical model in emetic research will be introduced.

1.1. Nausea and Vomiting

Many therapeutic drugs that are marketed today have gastrointestinal side effects, of which nausea (over 50% of drugs) and vomiting (emesis) (over 33% of drugs) are the most common (Holmes et al., 2009). Nausea is an "unpleasant sensation of sickness, which is often followed by the urge to vomit" (Parkinson et al., 2011). This sensation predominantly but not exclusively precedes the physical action of vomiting, which can be described as the forceful expulsion of gastric contents from the stomach through the mouth (Parkinson et al., 2011). Nausea and vomiting can be caused by gastrointestinal upset, an unpleasant smell, concussion, anticipation of fear, imbalance of the vestibular system and various drug treatments (Sanger and Andrews, 2006).

During drug treatment, nausea and vomiting are severe side effects that can adversely affect clinical response when administered orally, due to prevention of efficient absorption of drugs from the gastrointestinal tract into the

systemic circulation (Parkinson et al., 2011). Anticipatory nausea and vomiting, which is commonly seen in patients receiving cancer chemotherapy, can also hinder patient compliance during drug treatments (Parkinson et al., 2011). In addition, the highly unpleasant nature of the experience can also discourage patients from taking their treatments, which may also result in poor treatment efficacy.

1.2. Physiology of Nausea and Vomiting

In considering the biological process of vomiting (emesis), the physiological process of vomiting will firstly be examined. The emetic response occurs in 3 phases consisting of a pre-ejection, ejection and a post-ejection phase (Lindley and Andrews, 2005).

1.2.1. Pre-ejection phase

Upon detection of nauseating or emetic stimuli, numerous physiological changes occur, known as the pre-ejection phase. This phase has been associated with increased plasma levels of the hormones vasopressin (associated with the induction of nausea) and adrenaline (associated with stress) (Andrews and Rudd, 2004; Lindley and Andrews, 2005). The pre-ejection phase is also characterised by relaxation of the proximal stomach to delay gastric emptying and facilitating space for intestinal contents (Andrews and Rudd, 2004). This is followed by a giant retrograde contraction originating in the small intestine, forcing intestinal contents into the relaxed stomach (Andrews and Rudd, 2004). In addition, other physical symptoms characterised by the pre-ejection phase include retching, the onset of tachycardia (accelerated heart rate), cutaneous vasoconstriction, pallor (pale skin),

salivation and cold sweating (Andrews and Rudd, 2004; Lindley and Andrews, 2005).

1.2.2. Ejection phase

Vomiting is characterised by rhythmic contractions of the diaphragm, external intercostal and abdominal muscles, which compress the stomach (Andrews and Rudd, 2004; Lindley and Andrews, 2005). Simultaneously, the crural fibres of the diaphragm surrounding the oesophagus (usually in a contracted state) relax facilitating the expulsion of gastric contents (Holmes et al., 2009). This combination of abdominal contractions generate an extremely high pressure in the stomach, resulting in vomiting (Andrews and Rudd, 2004).

1.2.3. Post-ejection phase

Once vomiting has occurred, the subject often suffers numerous exhaustive physical symptoms, characterised by a subject feeling exhausted, dehydrated and weak, due to the respective violent contractions and fluid loss that have just occurred (Richards and Andrews, 2007).

1.3. Pharmacology of Nausea and Vomiting

In order to survive exposures to ingested harmful substances, humans and many animals developed an emetic response (Andrews and Sanger, 1993). The mucosal lining of the gastrointestinal tract is sensitive to a range of stimuli, resulting in neurotransmitter release by enterochromaffin cells and causing activation of afferent fibres in the vagus nerve (Sanger and Andrews, 2006). One of the primary mediators involved in generating the emetic response is 5-hydroxytryptamine (serotonin), which is stored and released by enterochromaffin cells, activating 5-hydroxytryptamine$_3$ (5-HT$_3$) receptors on afferent vagal termini (Andrews et al., 1988) **(Figure 1.1)**. It is proposed that

emetic compounds, such as chemotherapeutic agents, activate enterochromaffin cells by generating reactive oxygen species (such as the superoxide anion (O_2^-)), causing increased intracellular calcium and thus facilitating extracellular serotonin release (Andrews and Rudd, 2004). Orally administered emetic compounds such as copper sulphate and ipecac (a mixture of plant alkaloids) are proposed to initiate serotonin release from enterochromaffin cells, which subsequently initiates the acute onset of vomiting (Sanger and Andrews, 2006). In cancer chemotherapy, radiation therapy and injected chemotherapeutic agents can also result in the enterochromaffin cell-mediated acute onset of vomiting (Andrews and Davis, 1993; Andrews et al., 1988) **(Figure 1.1)**. The 5-HT_3 receptor is now the target of antiemetic drugs, designed to block receptor activation (such as granisetron, ondansetron, palonosetron) (Ryan, 2012; Bhandari et al., 1992), resulting in vagal transmission involved in the acute onset of vomiting.

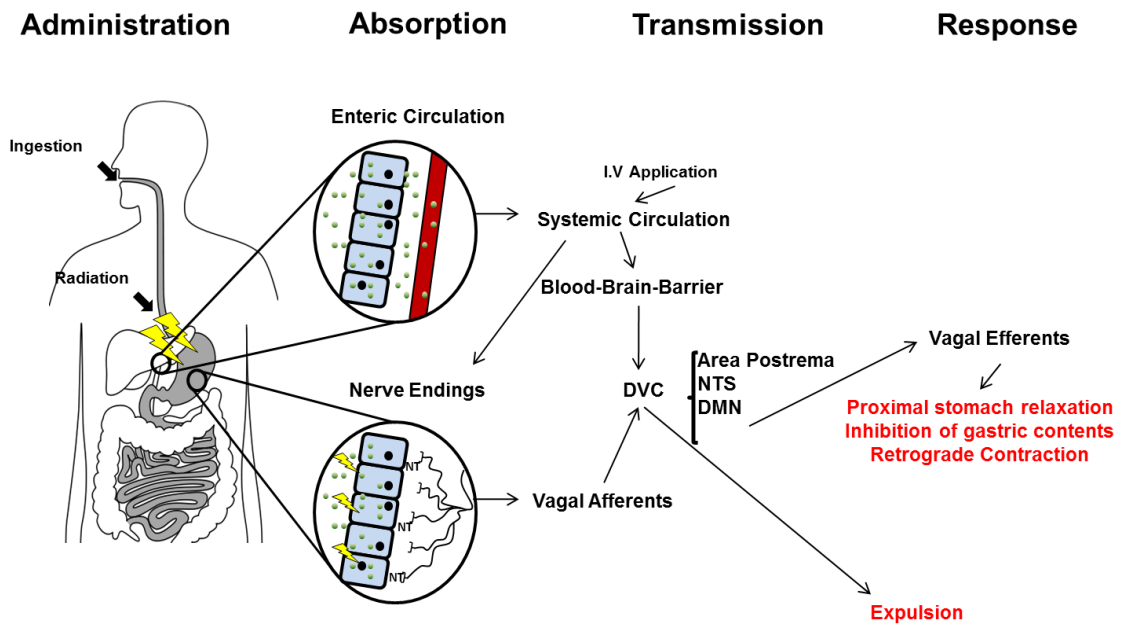

Figure 1.1. The emetic response generated by ingested toxins, radiotherapy and intravenous agents. Orally-ingested emetic compounds or radiation can induce vomiting by initiating serotonin (NT) release from enterochromaffin cells located throughout the gastrointestinal tract. Serotonin acts on abdominal vagal afferent nerve endings, which terminate in the nucleus tractus solitarius (NTS). This forms part of the dorsal vagal complex (DVC), which also consists of the area postrema and the dorsal motor vagal nucleus (DMN). In addition, compounds absorbed into hepatic portal veins that subsequently enter the systemic circulation can generate the emetic reflex by acting on receptors located in the area postrema (which is located outside of the blood-brain barrier) or initiating serotonin release from enterochromaffin cells (from the blood side). Receptor activation in the dorsal vagal complex results in signalling through vagal efferent fibres, involved in relaxation of the proximal stomach, inhibiting the transit of gastric contents and initiating a giant retrograde contraction of the small intestine. Activation in the dorsal vagal complex also mediates expulsion of gastric contents through nerves other than the vagus.

Abdominal vagal afferent fibres terminate in the dorsal vagal complex, located in the hindbrain (Andrews and Rudd, 2004), which comprises the nucleus tractus solitarius (part of a group of nuclei known as the emetic central pattern generator) the dorsal motor vagal nucleus (the site of origin of vagal efferent neurones) as well as the area postrema (Miller and Leslie, 1994; Hornby, 2001) **(Figure 1.1)**. The nucleus tractus solitarius is regarded as a key integrator, receiving inputs from multiple organs and inducing the activation of emetic motor outputs (Andrews and Rudd, 2004). The dorsal vagal complex as

a whole contains a variety of receptors, which include primary emetic mediatory receptors 5-HT_3 and neurokinin (NK_1) (Costall and Naylor, 1992; Saito et al., 2003).

In addition to 5-HT_3 receptor activation through enterochromaffin cell-mediated serotonin release, injected or orally ingested emetic compounds that enter the systemic circulation can diffuse into the area postrema, which is located outside the blood-brain barrier **(Figure 1.1)** (Andrews et al., 1988). The area postrema (also known as the chemoreceptor trigger zone) acts as a chemoreceptor for multiple compounds, since it contains numerous receptors (Andrews and Rudd, 2004). Upon detection of emetic compounds (such as the opioid receptor agonist loperamide) in the area postrema, neurones terminating in the nucleus tractus solitarius are activated, resulting in the induction of emetic motor outputs (Andrews and Rudd, 2004; Miller and Leslie, 1994; Bhandari et al., 1992). Lesion of the area postrema eliminates the vomiting response caused by cytotoxic agents such as cisplatin (delayed phase vomiting) (Percie du Sert et al., 2009), apomorphine (a dopamine D_2 receptor agonist) and morphine (an opioid receptor agonist) (Andrews and Rudd, 2004; Miller and Leslie, 1994)**.**

1.4. Emetic Compounds

Although the physiological and pharmacological mechanisms involved in the emetic response have been partially characterised, the individual molecular and receptor targets remain poorly understood. Various receptors and channels are responsible for the generation of the emetic response, which include ligand-gated ion channels, ion channels and G-protein coupled receptors (Costall and Naylor, 1992; Storr and Sharkey, 2007) **(Figure 1.2)**. A

range of receptors and channels associated with the induction of vomiting as well as the targets of drugs involved in interacting with these receptors will now be discussed.

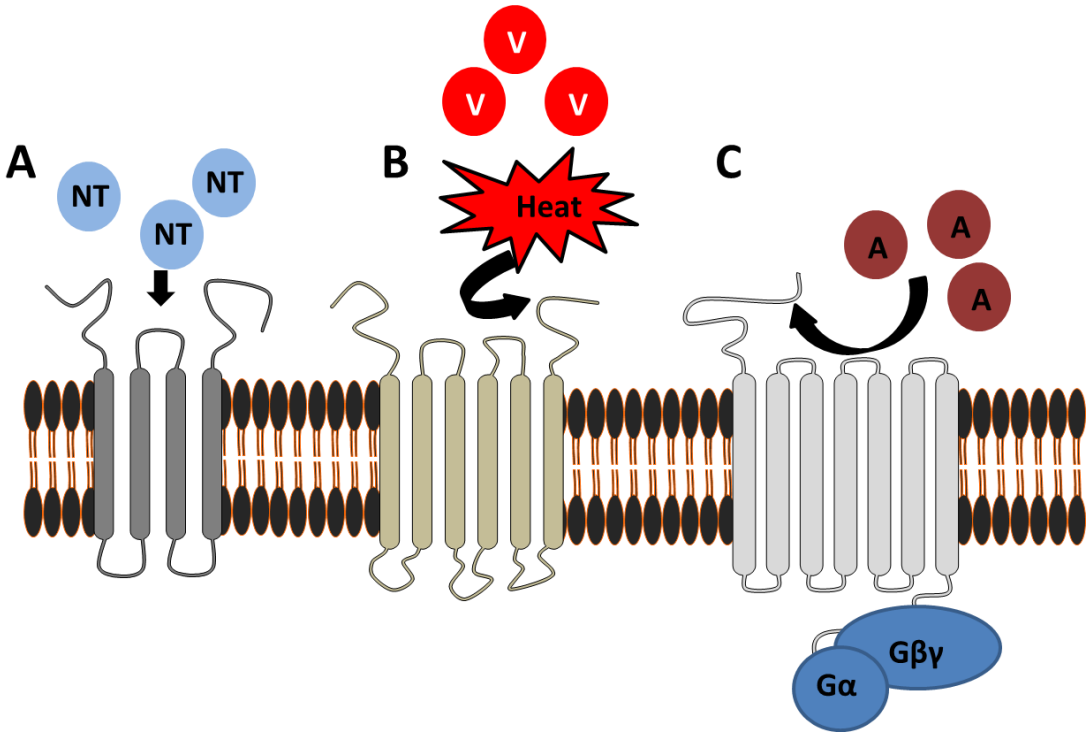

Figure 1.2. Principal receptors and channels involved in the emetic response. Emetic compounds that activate cell surface receptors predominantly fall into three distinct groups: (A) Ligand gated ion channels such as the 5-HT_3 receptor, which is activated by the neurotransmitter (NT), serotonin. (B) Ion channels that include the TRPV1 receptor, a calcium permeable cation channel activated by vanilloid binding (V) or heat detection on the C-terminal. Cells expressing the TRPV1 receptor are located in throughout the body. (C) G-protein coupled receptors, activated by agonists (A) binding to the N-terminal region causing dissociation of heterotrimeric α, β and γ subunits, which mediate a cascade of intracellular pathways. Specific receptors such as the $neurokinin_1$ receptor, activated by Substance P, and predominantly located in the dorsal vagal complex, are shown to induce emesis.

1.4.1. Ligand gated ion channels

Activation of ligand gated ion channels results in neurotransmission (Alexander et al., 2011) These channels contain a pore that allows ions to travel across the cell membrane upon receptor activation by neurotransmitters (**Figure 1.2)** (Alexander et al., 2011).

1.4.1.1. 5-HT_3 receptor

Located in the dorsal vagal complex as well as afferent vagal fibres originating near the gastrointestinal tract, the 5-HT_3 receptor has been identified as one of the principal receptors involved in the emetic response to chemo- and radiotherapy (Fujiwara-Sawada et al., 2003; Javid and Naylor, 2002; Torii et al., 1991). To block emetic side effects as a result of these therapies, clinically available anti-emetic drugs, such as granisetron, ondansetron and paolonosetron, are 5-HT_3 receptor antagonists (Ryan, 2012). Activation of this receptor by serotonin or by metformin-induced release of serotonin (as used in the treatment of diabetes), induces emesis in the *Suncus murinus* (Fujiwara-Sawada et al., 2003; Cubeddu et al., 2000).

Enterochromaffin cell-mediated serotonin release can be caused by metallic elements such as copper, which is shown to act through the 5-HT_3 (Fukui et al., 1993b) and possibly 5-HT_4 receptor (Fukui et al., 1994). At high concentrations, copper has been shown to induce emesis in the ferret and dog (Makale and King, 1992; Kayashima et al., 1978b; Kayashima et al., 1978b). Whilst it is shown that the gastro-duodenal luminal concentration of copper is a vital inducing factor in emesis in dogs, little is understood about the molecular mechanism involved in copper-induced emesis (Cushny, 1918; Kayashima et al., 1978b). Copper is also an essential element required in the human diet. However, due to its emetic properties, guidelines for the permitted concentration of copper in drinking water have been generated (Araya et al., 2001; Olivares et al., 2001).

Reactive oxygen species generated in enterochromaffin cells are also shown to cause serotonin release, resulting in abdominal vagus nerve activation

(Andrews et al., 2000a; Torii et al., 1994). The oral ingestion of pyrogallol, a generator of the destructive superoxide anion, O_2^-, induces vomiting in the *Suncus murinus*, which is subsequently abolished upon abdominal vagotomy (a process where the abdominal vagus nerve is severed) (Torii et al., 1994).

Selective serotonin reuptake inhibitors (SSRIs) are effective treatments for depression and anxiety, which also have reduced side effects in comparison to other anti-depressants. Fluoxetine, an SSRI has however been shown to have potent emetic properties in the *Suncus murinus* (Fujiwara-Sawada et al., 2003). Whilst SSRIs cause emesis, episodes can be reduced with the gradual development of tolerance (Fujiwara-Sawada et al., 2003). Increased brain serotonin levels due to reduced reuptake into cells may lead to generation of the emetic response via activation of 5-HT_3 receptors (Fujiwara-Sawada et al., 2003).

1.4.1.2. Nicotinic acetylcholine receptor

Nicotine, a natural plant alkaloid and the addictive component in tobacco, is a highly toxic substance with potent emetic properties in dogs and cats (Yamamoto et al., 2004; Torii et al., 1991; Laffan and Borison, 1957). Evidence has also shown the nicotinic receptor, which is activated by acetylcholine, is also located both peripherally and centrally, as ablation of the area postrema still leads to the onset of emesis in cats (Laffan and Borison, 1957).

1.4.2. Ion Channels

Activation of ion channels can be initiated by voltage (voltage-gated ion channels) or by second messengers (Alexander et al., 2011), resulting in the release of ions. These channels contain a pore, for ion transport (Alexander et al., 2011).

1.4.2.1. Voltage-gated sodium channel

Voltage gated sodium channels are located predominantly in excitable cells. Veratridine, a voltage-gated sodium channel activator induces emesis in the cat by vagal activation, which may originate centrally in the nodose ganglion of the vagus nerve, located in the cervical region of the spine (Borison and Fairbanks, 1952).

1.4.2.2. TRPV1 Receptor

Transient receptor potential vanilloid 1 (TRPV1) channels belong to a superfamily of calcium permeable cation channels located on the cell membrane (Dong et al., 2010). Members of this family can be by subdivided into 6 sub-families: canonical, vanilloid, melastatin, mucolipin, polycystin and ankyrin channels (Alexander et al., 2011). TRPV1 channels are six transmembrane domain containing proteins, containing intracellular N and C termini that interact to form homo- or heterotetramers (Alexander et al., 2011). Activation of this receptor is initiated by extracellular binding of vanilloid compounds, naturally found in plants, or detection of heat in the C-terminus (Brauchi et al., 2007) **(Figure 1.2)**.

The TRPV1 receptor is primarily expressed in neurones distributed throughout the body and is responsible for sensations of heat, pain and burning (Pingle et al., 2007). The receptor is highly conserved across mammalian

species and causes emesis in the *Suncus murinus* by initiating release of substance P from neurones (Smith et al., 2002; Rudd and Wai, 2001; Andrews et al., 2000a; Andrews et al., 2000b). Upon activation, TRPV1 channels allow calcium influx, which drives substance P release through activation of intracellular phosphatidylinositol 4,5-bisphosphate (PIP_2) (Brauchi et al., 2007).

Two principal agonists involved in inducing TRPV1 receptor mediated emesis are capsaicin (the "hot" component of chillies) and its ultra-potent analogue, resiniferatoxin, which are believed to act directly on the nucleus tractus solitarius (Andrews et al., 2000b). In addition to the burning sensation experienced by TRPV1 activation, the receptor has also been associated with metallic taste in artificial sweeteners and salts (Riera et al., 2007; Riera et al., 2009).

1.4.3. G Protein-Coupled Receptors

Receptors belonging to the family of G protein-coupled receptors consist of an extracellular N-terminal "binding" domain, followed by a central looping seven-transmembrane α-helical domain as well as an intracellular C-terminal domain (Schioth et al., 2007) **(Figure 1.2)**. G-protein coupled receptors arrange themselves in a tertiary structure where the α-helical regions are organised into an anticlockwise "barrel" shape (Schioth et al., 2007). Upon receptor activation, heterotrimeric α, β and γ subunits dissociate from the membrane, resulting in an intracellular signalling cascade, ultimately inducing neurotransmission and subsequent vomiting.

1.4.3.1. Neurokinin receptor

The neurokinin (NK_1) receptor, is a G-protein coupled receptor, activated by substance P and induces emesis in dogs (Andrews and Rudd, 2004). NK_1 receptors are located throughout the dorsal vagal complex (Costall and Naylor, 1992; Saito et al., 2003), where receptor activation triggers efferent fibres to initiate the emetic response (Saito et al., 2003; Andrews and Rudd, 2004). This receptor is pivotal in the induction of emesis since a range of stimuli, which include nicotine, opioids, ipecac, radiation, chemotherapy, motion and anaesthesia (Andrews and Rudd, 2004).

1.4.3.2. Dopamine receptor

Non-selective dopamine receptor agonists can activate any of four specific dopamine G-protein coupled receptors isoforms, D_1-D_4. Stimulation of these receptors with compounds such as apomorphine, a D_2 receptor agonist, has been used as symptomatic treatments for neurodegenerative disorders such as Parkinson's disease and psychosis (Depoortere et al., 2008). Dopamine receptor agonists activate receptors located in the area postrema, where D_2 receptor agonism specifically is responsible for generation of the emetic response in ferrets (Storr and Sharkey, 2007; Osinski et al., 2005).

1.4.3.3. Opioid receptor

Four different subtypes of opioid receptor exist, delta, kappa, mu and noiciceptin, of which mu activation by compounds such as morphine (Andrews et al., 1996) and loperamide (used in treatment for diarrhoea) (Bhandari et al., 1992) in the area postrema (Bhandari et al., 1992) induces emesis. Loperamide has a long half-life and takes time to be metabolised and cleared from the body. Upon treatment with loperamide in ferrets, emetic episodes

occur, which decrease as a tolerance is shown to develop upon repeat dosing (Bhandari et al., 1992).

1.4.3.4. Prostanoid receptor

Numerous prostaglandins such as prostaglandins E_2 and $F_{2\alpha}$ cause vomiting with varying potencies in ferrets by activating the prostanoid receptor (Kan et al., 2002; Kan et al., 2003). It is unclear how the prostanoid receptor is involved in the induction of emesis as precise mechanisms of action are currently unknown.

1.4.3.5. T2R Receptor

A final group of GPCRs located throughout epithelia, including taste buds, the stomach as well as the lungs, are taste (type II) receptors (T2R), responsible for the perception of bitter taste (Kinnamon, 2011). At higher concentrations, T2R receptor ligands can cause emesis upon ingestion (Sibert and Frude, 1991). In addition, some emetic chemotherapeutic agents have been associated with inducing the sensation of bitter taste, which may in part be responsible for nausea and/or vomiting (Peyrot des et al., 2011; Fetting et al., 1985).

Genes encoding proteins responsible for bitter taste detection have been identified in humans since a pre-Neanderthal age, providing a conserved mechanism for identifying potentially toxic substances (Lalueza-Fox et al., 2009a). These receptors are found along the gastric mucosa and in taste buds located on the tongue and in the lungs (Kinnamon, 2011; Wu et al., 2002). Upon activation of T2R receptors, heterotrimeric G-proteins (G_{α}-gustducin and $G_{\beta\gamma}$ subunits) dissociate from the membrane, where $G_{\beta\gamma}$ activates phospholipase $C_{\beta 2}$ ($PLC_{\beta 2}$). Increased $PLC_{\beta 2}$ activity catalyses the cleavage of

PIP_2 to release inositol triphosphate (IP_3) and sn-diacylglycerol (DAG) (Kinnamon, 2011). The second messenger DAG activates protein kinases C and D (PKC, PKD respectively), both of which trigger the release of gastrointestinal peptides (Rozengurt and Sternini, 2007). IP_3 acts on the IP_3 receptor (IP_3R_3) to facilitate the release of Ca^{2+} from intracellular stores, activating a mucolipin channel, TRPM5 **(Figure 1.3)** (Clapp et al., 2008; Sternini, 2007; Chen et al., 2006; Sawano et al., 2005; Caicedo and Roper, 2001). This channel activation facilitates membrane depolarisation and ATP release through the Pannexin-1 (P1X) receptor, resulting in the generation of action potentials though neurotransmitters serotonin and noradrenaline (Kinnamon, 2011; Huang et al., 2008). A third receptor, vesicular ATP transporter (VNUT) may also be involved in the facilitation of ATP release (Kinnamon, 2011).

The GPCR subunit, G_{α}-gustducin, maintains a basal active state in taste receptor cells, enabling fast signal transduction upon stimulation (Clapp et al., 2008) **(Figure 1.3)**. The G-protein increases phosphodiesterase (PDE) activity, which in turn reduces intracellular cAMP (Kinnamon, 2011). Decreased cAMP levels subsequently down-regulate protein kinase A (PKA) activity, an enzyme that reduces $PLC_{\beta 2}$ activity, leading to hydrolysis of PIP_2 and decreasing downstream Ca^{2+} release (Clapp et al., 2008; Kinnamon, 2011). In addition to stimulation of T2R receptors, denatonium benzoate has been shown to induce neural signal transduction in a pathway independent of G-protein activation by inducing calcium release from intracellular stores (Sawano et al., 2005). Intracellular calcium release by bitter compounds denatonium benzoate and phenylthiourea also results in discharge of the hormone, cholecystokinin (CCK)

from enteroendocrine cells, which is a known regulator of gastric motility (Chen et al., 2006).

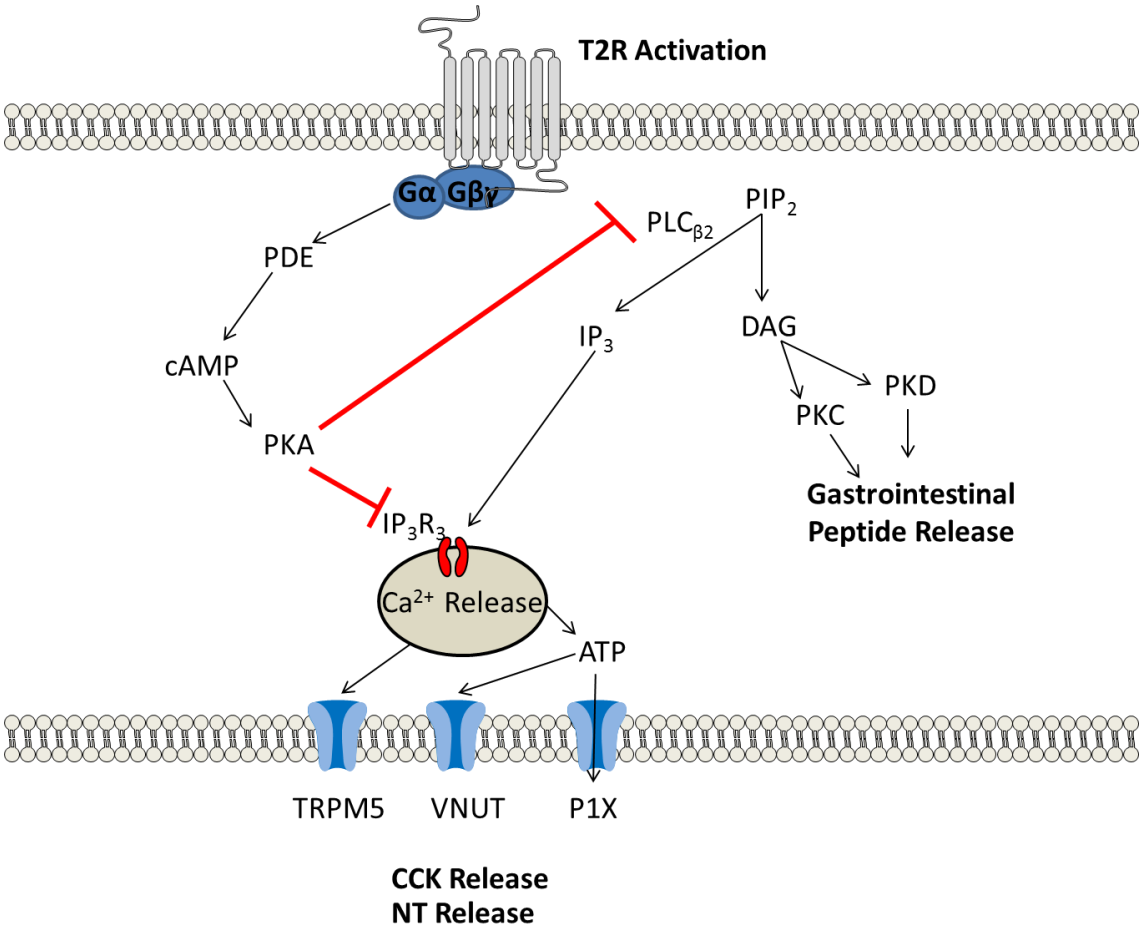

Figure 1.3. Bitter tastants function through activation of T2R receptors located in taste cells throughout the digestive tract. Upon activation, the $G_{\beta\gamma}$ subunit dissociates from the cell membrane activating phospholipase $C_{\beta 2}$ ($PLC_{\beta 2}$), which increases PIP_2 phosphorylation into inositol triphosphate (IP_3) and sn-diacylglycerol (DAG). IP_3 subsequently binds to its respective receptor, IP_3R_3, mediating calcium release from intracellular stores, which is subsequently released from the cell by TRMP5 receptors, driving membrane depolarisation. In addition to calcium release from the cell, ATP is also released through P1X and VNUT receptors, driving cholecystokinin (CCK) (from enteroendocrine cells) and neurotransmitter (NT) (from taste buds) release. DAG is believed to drive the activation of protein kinases C and D (PKC and PKD), which mediates the release of gastrointestinal peptides from the cell. The G_{α} subunit is plays a role in regulation of calcium within the cell whereby it activates phosphodiesterases (PDE) to reduce cAMP within the cell. This in turn reduces protein kinase A activity, which leads to reduced activity of $PLC_{\beta 2}$ and the binding of IP_3 to IP_3R_3.

The T2R family of receptors is encoded by 25 different genes, which share a 30-70% homology (Adler et al., 2000; Chandrashekar et al., 2000). These different receptors show ligand specificity where 6-nitrosaccharin and denatonium both activate human *TAS2R44* receptors, whereas for example *TAS2R61* receptors are 6-nitrosaccharin specific (Pronin et al., 2004). This specificity has also been shown to be dependent upon bitter ligand binding, as measured by varying calcium release from cells (Caicedo and Roper, 2001).

Phenylthiourea and 6-n-propylthiouracil are both compounds that are perceived as extremely bitter or not at all in 70% and 30% of humans respectively. This phenomenon is due to the activity of a principal bitter receptor gene, the *hTAS2R38*, which contains single nucleotide polymorphisms (Bufe et al., 2005). Amino acid substitutions can occur on this gene, giving rise to five different haplotypes resulting in three distinct taster statuses, known as supertaster, taster and non-taster (Tepper et al., 2009; Bufe et al., 2005). Two more alleles for the human T2R genes, *TAS2R43* and *TAS2R44,* are also shown to cause hypersensitivity to bitter tastants found in plants as well as finding saccharin, an artificial sweetener, bitter (Pronin et al., 2007). Recent evidence has also shown genetic bitter taster status plays a role in sensitivity to motion sickness and nausea (Benson et al., 2012) as well as possible links with epilepsy (Pal et al., 2004).

Bitter tastants are perceived as being toxic, where animals commonly display “hard-wired” food aversive behaviour upon detection (Kinnamon, 2011; Yarmolinsky et al., 2009). This aversive behaviour has even been exploited to aid the survival of the northern quoll, an endangered species (O'Donnel et al., 2010). Aside from the behavioural response of aversion to bitter taste, bitter

tastants also cause physiological responses such as delayed gastric emptying (Glendinning et al., 2008).

1.4.4. Transporters and Enzymes

In addition to receptors, the emetic response can be generated by various transporters and enzymes. Membrane transporters require ATP to actively transport compounds across the hydrophobic cell membrane against a diffusion gradient (Alexander et al., 2011). In addition to transporters, numerous drugs often target enzyme inhibition in order to prevent a specific cellular function (Alexander et al., 2011).

1.4.4.1. Emetic compound transport into cells

Whilst G protein-coupled receptors are the largest family of membrane proteins in the human genome, solute carrier transporters are the second largest (Alexander et al., 2011). Many therapeutic drugs are transported across the plasma membrane via solute carrier transporters; emetic compounds include cytotoxic agents such as 5-fluorouracil, cisplatin, and methotrexate (Alexander et al., 2011). Chemotherapeutic agents administered orally or intravenously include a wide variety of chemical structures that are cytotoxic to dividing cells and used to treat cancer. Cytotoxic compounds prescribed during chemotherapy such as 5-fluorouracil and cisplatin have strong emetic effects in multiple animal models including the ferret (Bannink et al., 2008; Percie du Sert et al., 2010; Fetting et al., 1985).

1.4.4.2. Enzyme inhibitors

Digoxin is a cardiac glycoside used in the treatment of numerous heart conditions and is also taken into cells by solute carrier transporters (Alexander et al., 2011). Treatment of patients with high doses often results in digoxin

poisoning, a common symptom of which is vomiting in cats (Parsons and Summers, 1971). Little is known about the mechanism for the induction of emesis by cardiac glycosides, however it has been shown that they act upon the area postrema to induce emesis (Parsons and Summers, 1971).

Cyclic nucleotides are a part of second messenger systems, which are created by cyclases (Alexander et al., 2011). Phosphodiesterases are involved in the hydrolysis of cyclic adenosine monophosphate (cAMP) or cyclic guanosine mononphosphate (cGMP). Compounds such as the phosphodiesterase IV inhibitors, rolipram (an anti-inflammatory treatment) are associated with emetic side effects in ferrets (Aoki et al., 2001). These agents inhibit phosphodiesterase activity, which is responsible for the degradation of 3,5-adenosine cyclic monophosphate (cAMP) (Aoki et al., 2001).

1.5. Animal Models in Emetic Research

Whilst the physiological mechanisms of the emetic response is clearly understood, many specific molecular targets of emetic compounds remain diverse and uncharacterised, which has resulted in extensive animal research (Andrews and Horn, 2006). This has subsequently led to the development of several sentient models for studying the vomiting response. Animals used in emetic research can be divided into those that do not have a vomiting reflex (mice, rats) and those that do (ferret, pig, dog, cat and primates). Non-vomiting species such as the rat cannot vomit as they may lack the neural pathways or anatomical features to do so (a narrow oesophagus for example) (Andrews and Horn, 2006; Sanger et al., 2011; Horn et al., 2013). Conversely, animals that can vomit display sensitivity to emetic stimuli, which varies between species. It therefore makes it difficult to establish a single animal model that is most

indicative of emesis in humans for newly developed therapeutic drugs (Holmes et al., 2009).

Animals lacking the emetic reflex demonstrate an alternative behaviour known as pica where they ingest kaolin (a form of clay) in response to potentially toxic substances (Andrews and Horn, 2006; Holmes et al., 2009). Kaolin slows gastric emptying and absorbs harmful toxic substances (Liu et al., 2005). Pica can however be induced by non-emetic stimuli and may therefore not always be predictive of emetic liability, giving rise to false positive or negative results (Andrews and Horn, 2006). Non-emetic species are also used in conditioned taste aversion/food avoidance experiments, where animals avoid substances associated with toxicity (Andrews and Horn, 2006). A recent study has however underlined the importance of genetics, species difference and the physiology behind the vomiting response, where it was suggested rodents such as the rat could be vital in understanding molecular targets in emetic research (Sanger et al., 2011).

Animal research requires the implementation of the 3 R's: Refinement, Reduction, Replacement (Holmes et al., 2009). In investigating the specific physiology involved in the induction of vomiting, no single sentient model exists, as different animals' exhibit varying sensitivities to the same compound (Percie du Sert et al., 2012), apomorphine being a prime example (Andrews and Rudd, 2004). In addition, repeated animal experimentation with emetic stimuli is presumed to induce a large amount of suffering (Holmes et al., 2009; Parkinson et al., 2011). This presumption can be based upon the unpleasant feelings humans experience during episodes of nausea and vomiting. In addition, whilst newly developed compounds may not actually cause emesis themselves,

animals cannot be monitored for unpleasant symptoms such as nausea, which precede vomiting (Parkinson et al., 2011; Holmes et al., 2009).

To refine, reduce and replace the use of animals in emetic research, a tiered approach to these tests has been suggested. This incorporates preliminary literature searches and *in vitro* mammalian tests followed by the use of a reduced number of *in vivo* experiments using sentient models as proposed by Holmes and colleagues (**Figure 1.4)**.

Less complex models such as implementing non-sentient organisms in emetic research could be extremely beneficial in assisting this research. The ease of manipulating non-sentient organisms through genetic mutations and using readily available molecular markers could also provide valuable information about currently unknown molecular mechanisms in emetic research. In addition, early identification of emetic liability in non-sentient models during drug development would be of substantial benefit, because this would reduce the number of animals involved as well as the cost of research. Use of non-sentient models in emetic research could also provide fast and potentially high throughput results. The second part of this introduction discusses the properties that a potential non-sentient model, *Dictyostelium discoideum*, may have for use in emetic research.

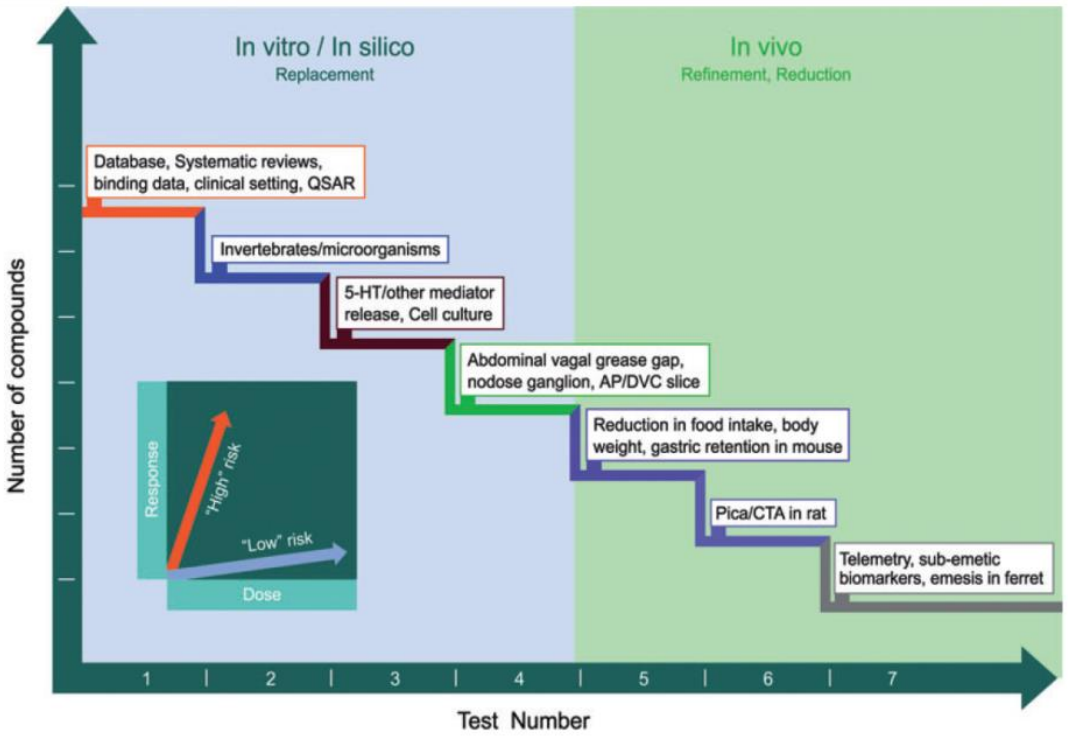

Figure 1.4. A Proposed Novel Tiered Model for Reducing Animals used in Testing for Emetic Liability. This diagram suggests a novel approach to developing therapeutic drugs for emetic liability. This method employs database searching and tests to reduce *in vitro* animal models. The number of *in vivo* models used to predict emetic liability would then be substantially reduced. This figure is from a review by Holmes et al. (2009).

1.6. *Dictyostelium discoideum*

First discovered in 1935 by K.B. Raper, *Dictyostelium discoideum* is a single celled organism (Raper, 1935), which naturally survives on forest floors in damp conditions, chemotaxing towards folate (secreted by bacteria) and feeding on bacteria through phagocytosis (Boeckeler and Williams, 2007; Cosson and Soldati, 2008). After exhaustion of its food source, *Dictyostelium* cells starve and undergo a complex multicellular phenomenon, known as development, where cells migrate towards one another, ultimately forming a multicellular fruiting body (**Figure 1.5)**. This process has one crucial role, sporulation, which is essential for survival of the organism (Williams et al., 2006a).

Upon starvation, *Dictyostelium* cells secrete the chemoattractant, cAMP, in pulses over a period of 5-6 hours, which mediates the coordination of

individual cells towards a central location by G-protein coupled receptor activation resulting in directed migration (McMains et al., 2008). Over this period, cells interact with one another to form streams until approximately 10^5 cells have migrated to a central aggregation centre called a mound (Williams et al., 2006a). At this point, differential gene expression determines alternate cell fate, where cells either express as pre-spore or pre-stalk cells in a respective 4:1 ratio (Williams et al., 2006a). After 10-16 hours, this cellular partitioning enables the formation of multicellular slugs, consisting of anterior pre-stalk and posterior pre-spore cells (MacWilliams and Bonner, 1979; Jang and Gomer, 2011).

Upon culmination, *Dictyostelium* stalk cells form a stalk, on top of which spore cells then form a spore head (Jang and Gomer, 2011). The final fruiting body structure measures approximately 1mm in height consisting of a basal disc, a stalk consisting of dead vacuolated stalk cells and a spore head containing approximately 80, 000 spore cells (Williams et al., 2006a).

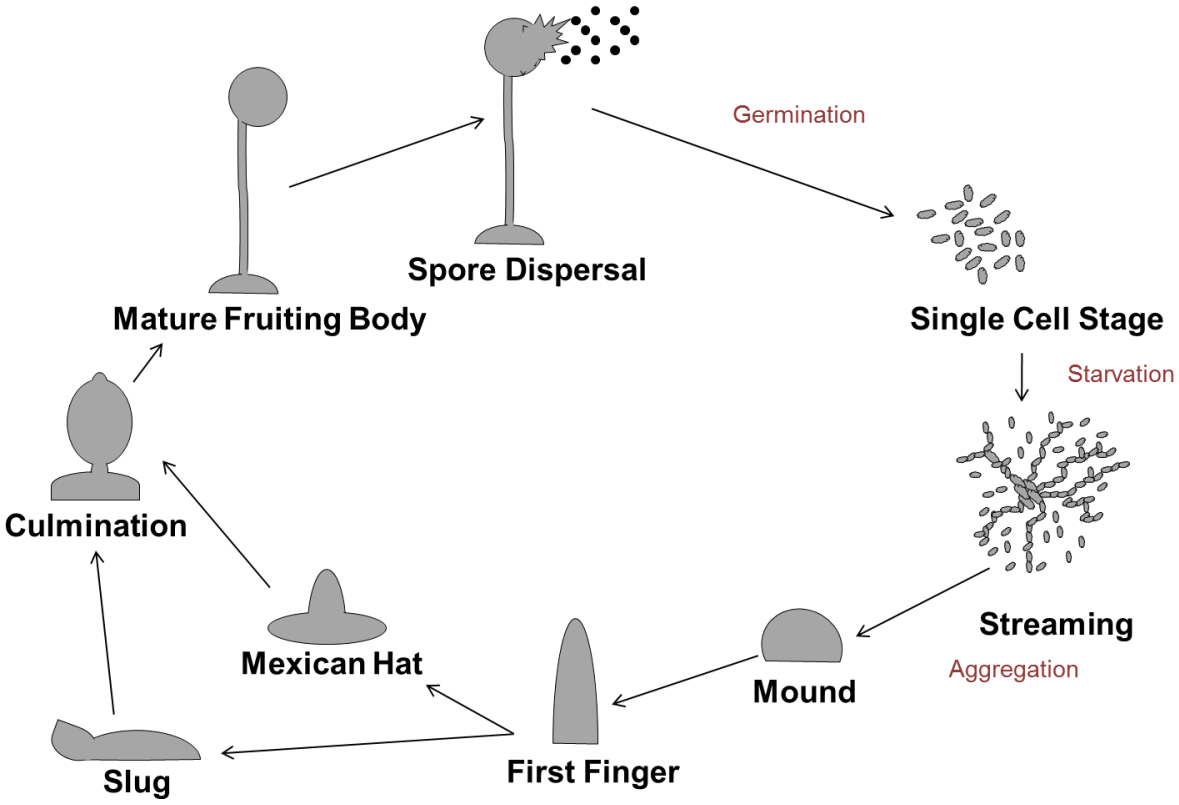

Figure 1.5. Life Cycle of *Dictyostelium discoideum*. Upon starvation, *Dictyostelium* cells secrete the chemoattractant, cAMP, initiating cellular migration towards a central aggregation point, where they form a mound. During this phase, cells differentiate to form anterior pre-stalk or posterior pre-spore cells, causing the mound to develop either into a migrating slug or a "Mexican hat"-shaped complex. Upon culmination, developed, vacuolated stalk cells ultimately form a stalk for spore cells to develop into a mature fruiting body, which then germinates to disperse spores and restart the life cycle.

1.7. *Dictyostelium* as a Biomedical Model

Since its discovery, *Dictyostelium* has been developed into a highly regarded biomedical model, where the cells have been transformed under laboratory conditions so they can easily be maintained at 22^{o}C and survive in liquid media, feeding on nutrients by macropinocytosis. Manipulation of the *Dictyostelium* genome has also resulted in cells showing resistance to antibiotics such as penicillin and streptomycin, which can contribute to the prevention of infection of axenic medium by airborne laboratory pathogens. Under laboratory conditions, *Dictyostelium* cells have a steady doubling time of approximately 8 hours and cells can be monitored at a number of stages during their developmental process, the most common stages being chemotaxis (in developmentally starved cells) and development.

Over time, the molecular mechanisms responsible for the life cycle of *Dictyostelium* have been revealed. The earliest substantial development of the organism as a biomedical model was the use of DNA-transformation techniques in *Dictyostelium* (Nellen et al., 1984). The full 34 Mb *Dictyostelium* genome spanning over 6 chromosomes has now been completed (Eichinger et al., 2005), allowing for the study of individual *Dictyostelium* genes as well as their comparison to the human genome. Sequencing of the *Dictyostelium* genome has identified 22% of *Dictyostelium* genes sharing homology with human genes, which has made the organism a useful model for human drug targets and intracellular pathways involved in human disease (Eichinger et al., 2005). Many genes and targets expressed in *Dictyostelium* are lacking in other biomedical models such as *Saccharomyces cerevisiae* and *Schizosaccharomyces pombe*, suggesting *Dictyostelium* may be a more advantageous non-sentient model (Eichinger et al., 2005).

Dictyostelium is now being increasingly used in biomedical research (Boeckeler and Williams, 2007; Williams et al., 2006b), where multiple methodologies exist. The effects of various compounds on cells can be monitored by using mutagenesis screens, gene manipulation, development assays and chemotaxis (Boeckeler and Williams, 2007). The organism has now been used as a model for various diseases which include the analysis of Schwachman-Diamond syndrome (Wong et al., 2011), mitochondrial disease (Francione et al., 2010), Alzheimer's disease signaling (McMains et al., 2010), as well as developing current understandings of microbial infection (Francione et al., 2009). *Dictyostelium* has also been used in the investigation of valproic acid and lithium effects in epilepsy and bi-polar research (King et al., 2009;

Terbach et al., 2011; Xu et al., 2007; Chang et al., 2012), and chemotherapy research (Boeckeler and Williams, 2007).

1.7.1. Channels and Receptors in *Dictyostelium*

The *Dictyostelium* genome contains a wide variety of channels and receptors, many of which share homology with those found in chordates. Examples include the P2X receptors (Burnstock and Verkhratsky, 2009), which are ATP-gated ion channels involved in osmoregulation (Baines et al., 2013) and calcium regulation (Ludlow et al., 2009), as well as polycystin-2 and mucolipin receptors, which are transient receptor potential (TRP) channels (Wilczynska et al., 2005). In addition, *Dictyostelium* contains a diverse range of seven-transmembrane receptors, which are the largest and most versatile family of receptors in eukaryotes (Eichinger et al., 2005; Pierce et al., 2002). These receptors are the target of many therapeutic drugs in humans, although receptor activation can result in emetic episodes **(Sections 1.4.1- 1.4.3)**.

In *Dictyostelium*, 55 G-protein coupled receptors exist, which can be subdivided into one family two (secretin), seventeen family three ($GABA_B$-like), twenty five family five (frizzled/smoothened) and twelve family six (cAMP) receptors (Prabhu and Eichinger, 2006). To date, a role for the secretin and the frizzled/smoothened receptors in *Dictyostelium*, have yet to be discovered.

1.7.2. $GABA_B$-like Receptors

The seventeen $GABA_B$-like receptors *in Dictyostelium*, GrlA-GrlR, resemble $GABA_B$ or metabotropic glutamate receptors, where the transmembrane domains in particular share weak homology with higher eukaryotic $GABA_B$ receptors (Prabhu and Eichinger, 2006). To date, few Grl-family receptors have been successfully characterised; of those that have, only GrlE (Anjard and Loomis, 2006) and GrlB (Wu and Janetopoulos, 2013) are responsive to GABA. Other partially characterised Grl-family receptors, GrlJ (Prabhu et al., 2007b) and GrlA (Prabhu et al., 2007a) do not appear to respond to GABA. Grl-family receptors may play differing roles throughout development, where GrlA (Prabhu et al., 2007a) and GrlJ (Prabhu et al., 2007b) are shown to be involved in post-aggregation development, GrlE is shown to induce sporulation (Anjard and Loomis, 2006), and GrlB is involved in pre-aggregation development (Wu and Janetopoulos, 2013). The remaining Grl-family receptors are yet to be characterised.

1.7.3. cAMP Receptors

Upon starvation, cAMP mediated chemotaxis towards a central aggregation point is driven by activation of cAR (cAMP) receptors, which belong to a family of 7-transmembrane serpentine GPCRs (Chung and Firtel, 2002). Located uniformly around the cell, 4 different types of cAR (cAR1-4) exist with varying affinities for cAMP (cAR1>cAR3>cAR2=cAR4) (McMains et al., 2008) and are shown to be involved in *Dictyostelium* development and differentiation (Verkerke-Van, I et al., 1998). In addition to the four cAR receptors, 7 Crl (cAMP like) receptors, CrlA-CrlG, exist, although these are unlikely to bind cAMP (Prabhu and Eichinger, 2006).

1.8. *Dictyostelium* movement

Cell movement occurs during both vegetative and starved states in *Dictyostelium*. Upon disappearance of available food sources, *Dictyostelium* undergoes a number of gene transcriptional changes, resulting in changes in cell motility (forming fast and slow cells) and a differentiation into pre-spore and pre-stalk cells as little as 30 minutes following starvation (Goury-Sistla et al., 2012). Upon starvation, cells begin to secrete and search for other sources of cAMP, undergoing random movement and migrating a zigzag manner (Li et al., 2008). *Dictyostelium* cells achieve this directionality by the forming pseudopods (a directional cellular protrusion), which split every fifteen seconds at an angle of approximately 60^{o} from the direction of the previous pseudopod (Bosgraaf and van Haastert, 2009). To initiate a change in direction, cells also produce *de novo* pseudopods, often far away from the existing pseudopod (Bosgraaf and van Haastert, 2009). This combination of cellular protrusions enhances the probability of detecting cAMP.

1.8.1. Detection of cAMP

In its starved state (also known as chemotactically competent), detection of cAMP by cAR receptors in *Dictyostelium* results in directional chemotaxis (King and Insall, 2009). Leading edge cell polarisation is a result of amplification of the external cue in *Dictyostelium*, allowing for an increased sensitivity to cAMP compared with the rest of the cell. This amplification process subsequently enables *Dictyostelium* cell migration to occur down a cAMP gradient between the front and back of the cell as low as 2% (Chung and Firtel, 2002; Jin et al., 2008).

Upon binding of cAMP to cAR, conformational changes are generated predominantly within intracellular loops 2 and 3 of the receptor, causing the dissociation and subsequent activation of bound heterotrimeric G-proteins (Prabhu and Eichinger, 2006). The *Dictyostelium* genome encodes 14 G_{α}-subunits whilst only encoding a single G_{β}- and one G_{γ}-subunit (although the G_{γ}-subunit is yet to be discovered) (Eichinger et al., 2005). Specifically, cAR activation results in dissociation by $G_{\alpha 2}$ and $G_{\beta\gamma}$ sub-units (Chung and Firtel, 2002), where both subunits play pivotal roles in cell polarisation (Chung and Firtel, 2002; Stephens et al., 2008). Dissociation of $G_{\beta\gamma}$ leads to activation of monomeric Ras-guanosine triphosphatases (GTPases), RasC and RasG, through binding to guanosine triphosphate (GTP) (Jin et al., 2008; Kae et al., 2007). GTPase binding to GTP is mediated by the Ras-guanine exchange factors (GEFs). Conversely, GTPases are deactivated by GTPase binding to guanosine diphosphate (GDP), which is mediated by Ras-guanine activating proteins (GAPs) catalysing hydrolysis of GTP to GDP. RasGEFs and RasGAPs therefore play key regulatory roles in Ras-GTPase signalling, particularly RasC and RasG, which in turn initiate downstream signalling events (Kae et al., 2007) **(Figure 1.6)**.

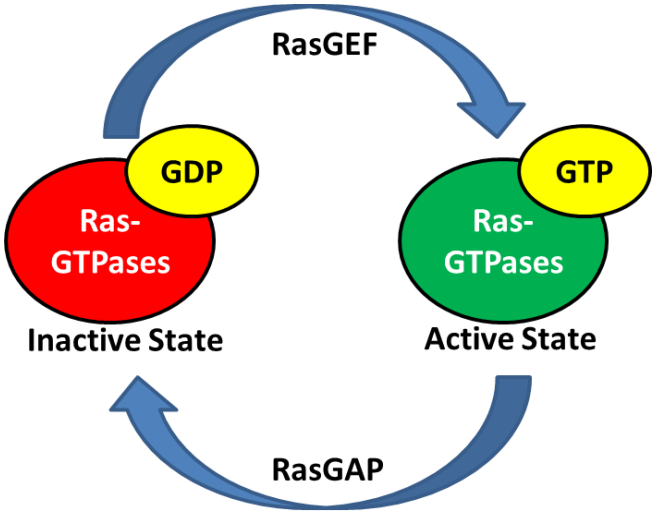

Figure 1.6. Ras activation in *Dictyostelium*. RasGTPases exists in their bound and unbound states, where it is bound to guanoside diphosphate (GDP) during in its inactive state. Ras guanine exchange factors (RasGEFs) mediate dissociation of GDP from RasGTPase facilitating a pocket for guanosine triphosphate (GTP) to bind. Binding of Ras-GTPase results in Ras activation and triggers downstream signalling events. Ras guanine activating proteins (RasGAP) hydrolyse GTP into GDP and thus cause Ras inactivation.

1.8.2. F-actin polymerisation

In order to generate motion, *Dictyostelium* cells contain an F-actin cytoskeleton, consisting of a branched network of F-actin filaments that extend pseudopods at the leading edge of the cell and retract uropods (trailing end of the cell) (Bagorda et al., 2006). During random cell movement, F-actin polymerisation occurs randomly and is not driven by an external cue. During chemotaxis, activation of Ras at the leading edge results in F-actin polymerisation, which can occur individually or in combination with various signal amplification processes (Kortholt et al., 2011) **(Figure 1.7)**.

F-actin polymerisation at the leading edge is also initiated by activation of Rho-GTPases, known as Rac. These Rho-GTPases are also regulated, in a similar way to Ras, by RacGAPs and RacGEFs. Recent research has identified a group of proteins, Elmo, that are involved in cAMP induced actin polymerisation,

which not only associate with G-protein subunits but also dock to RhoGTPases (Yan et al., 2012; Li et al., 2013; Xu and Jin, 2012).

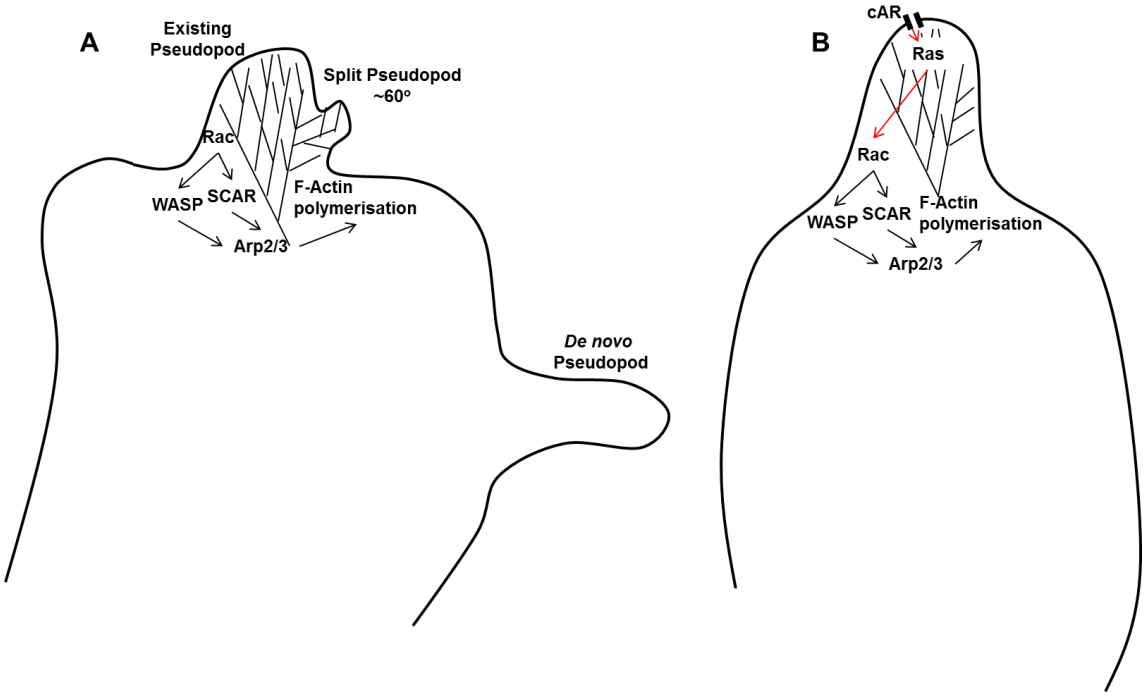

Figure 1.7. Pseudopod formation in *Dictyostelium.* **(A)** During random cell movement, F-actin polymerisation results in the formation of two different forms of pseudopod, split pseudopods and *de novo* pseudopods. Split pseudopods are those that extend from an existing pseudopod, whereas *de novo* pseudopods occur at a random location within the cell. Activation of Rac signalling results in WASP and/or SCAR mediated Arp2/3 activity, which binds to F-actin filaments and induces polymerisation. Rapid F-actin polymerisation results in forcing the cell membrane forward and creating a pseudopod. **(B)** Upon detection of cAMP by cAR, Ras activates Rac independently or by various signalling mechanisms. Rac activation then results in the polymerisation of F-actin, creating pseudopods directed towards the chemoattractant, cAMP.

Stimulation of Rac activates a complex known as suppressor of cAR (SCAR) (Veltman et al., 2012). SCAR then catalyses F-actin polymerisation through the Arp2/3 complex, which binds to the edges of existing F-actin filaments (Pollard and Borisy, 2003). Rapid formation of new F-actin filaments then drives the cell membrane forward, resulting in the formation of a pseudopod **(Figure 1.7)**. F-actin formation is controlled by ADF/cofilin proteins, which sever filaments and stabilise pseudopod production (Pollard and Borisy, 2003).

In addition to SCAR, Rac catalyses Wiskott-Aldrich syndrome protein (WASP), which also mediates F-actin polymerisation, although predominantly at clathrin-coated pits during movement of vesicles (Veltman et al., 2012). Despite playing a pivotal role in the generation of F-actin filaments, ablation of the *WASP/SCAR* genes do not inhibit chemotaxis, with only slight reductions in cell velocity observed (Bear et al., 1998; Ibarra et al., 2005), indicating WASP and SCAR are not essential to F-actin polymerisation and other signalling mechanisms are involved.

1.8.3. The Phosphatydylinositol-3-kinase Pathway

Activation of RasC and RasG, play crucial roles in the amplification of various chemotactic signals, including the phosphatydylinositol-3-kinase (PI3K) pathway (Bolourani et al., 2006). There are 6 types of PI3K in *Dictyostelium*: $PI3_{1\text{-}5}K$ all contain a Ras binding domain; $PI3_6K$ does not (Hoeller and Kay, 2007). Upon cAMP detection and subsequent activation by Ras, PI3Ks convert the phospholipid, phosphatidylinositol 4,5-bisphosphate (PIP_2) into phosphatidylinositol 3,4,5-triphosphate (PIP_3) at the leading edge (Huang et al., 2003). Waves of production of PIP_3 are followed by waves of F-actin polymerisation in a repeated fashion (Asano et al., 2008; Ueda and Shibata, 2007).

PIP_3 binds to myosin I at the leading cell edge, which is involved in recruitment of actin filaments (Chen and Iijima, 2012; Chen et al., 2012). In addition, PIP_3 also binds to plekstrin homology domain containing proteins PhdA (Funamoto et al., 2001), cytosolic regulator of adenylyl cyclase (CRAC) (Lilly and Devreotes, 1994) and protein kinase B (PkB/Akt) (Meili et al., 1999) **(Figure 1.8)**. Each protein plays a distinct role in the control of chemotactic

signalling. PhdA is a regulator of cell polarity, where it assists in the control of F-actin polymerisation at the leading edge of chemotaxing cells (Funamoto et al., 2001). PIP_3 mediated activation of CRAC and PKB/Akt are both involved in the activation of adenylyl cyclase A (a 12 transmembrane protein) at the rear edge of the cell membrane (Insall et al., 1994; Lilly and Devreotes, 1994). Adenylyl cyclase A is located throughout the cell membrane and activation facilitates extracellular cAMP release (Garcia and Parent, 2008a; Kae et al., 2007; McMains et al., 2008). Adenylyl cyclase A activity is predominantly regulated by activation of RasC rather than RasG (Kae et al., 2007).

PKB/Akt is also involved in the maintenance of cell polarity (Meili et al., 1999) and also activates p21 activated kinase A (PAKa) (Chung and Firtel, 2002). Once activated, PAKa relocates to the rear of the cell activating myosin heavy chain kinases, which regulate the formation of myosin II (Bagorda et al., 2006; Chung and Firtel, 2002). Myosin II assists chemotaxis by augmenting cell rigidity at the cell sides and rear, preventing pseudopod extension laterally, as well as enabling membrane retraction at the rear of the cell (Jin et al., 2008). Myosin II is removed from the leading edge of the cell by receptor activating protein 1 (Rap1), which is activated by a RhoGEF domain containing protein GbpD, in a similar way to other GTPases (Kortholt et al., 2010). Once activated, Rap1 then binds to a protein serine/threonine kinase (Phg2), which in turn regulates the breakdown of myosin II at the leading edge of the cell (Kortholt et al., 2010). Rap1 is also a regulator of PI3K activity by binding to the kinase, resulting in PIP_3 turnover (Kortholt et al., 2010).

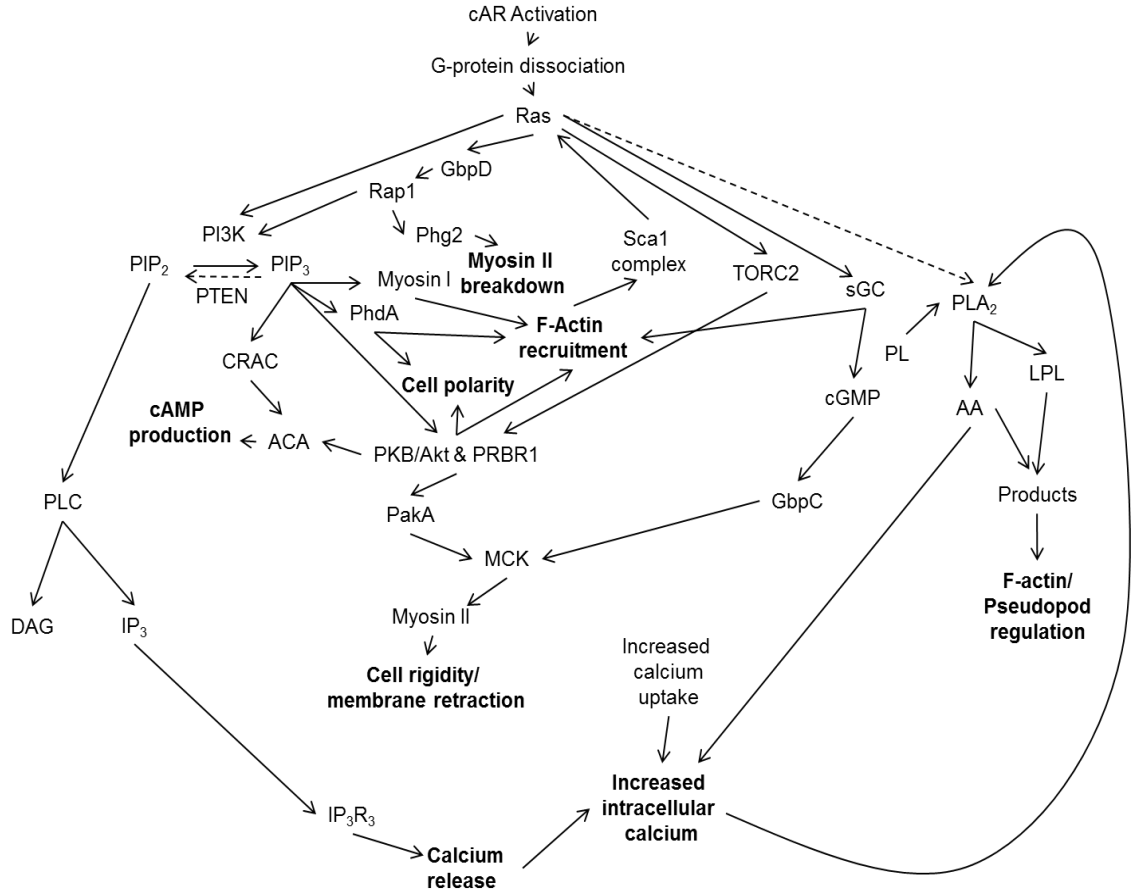

Figure 1.8. Summary of chemotactic movement in *Dictyostelium*. Detection of cAMP by cAR results in G-protein dissociation and activation of Ras. Activation of Ras mediates the activity of 4 distinct pathways. **1.** Ras activates PI3K, which subsequently converts PIP_2 to PIP_3. PI3K activity results in PIP_3 binding to myosin I, involved in F-actin recruitment; PhdA, involved in maintenance of cell polarity and F-actin recruitment; PKB/Akt, involved in adenylyl cylcase A (ACA) activation, cell polarity, F-actin recruitment and also PakA mediated myosin chain kinase (MCK) activation; and CRAC, involved in adenylyl cyclase activation. PI3K activity is also regulated by GbpD mediated activation of Rap1, which also regulates myosin II breakdown through Phg2 activity. PIP_3 is converted back to PIP_2 by PTEN activity, where PIP_2 is broken down into diacylglycerol (DAG) and inositol triphosphate (IP_3), which subsequently induces calcium release through the inositol triphosphate receptor (IP_3R_3). **2.** Ras activation is also regulated by the scaffold protein complex consisting of Sca1, aimless, RasGEFH and protein phosphatase 2A (Sca1 complex), which is formed upon F-actin recruitment. Ras activation then activates the TORC2 complex, which subsequently activates PKB/Akt and PKBR1 activity. **3.** Ras initiates soluble guanylyl cyclase (sGC) activity, which is involved in F-actin recruitment at the leading edge. In addition, soluble guanylyl cyclase produces a second messenger, cyclic guanosine monophosphate, which mediates myosin chain kinase and subsequent myosin II activity through the protein GbpC. **4.** Ras is presumed (indicated by the dotted line as this is yet to be proven) to activate phospholipase A_2, which converts phospholipids (PL) into arachadonic acid (AA) and lysophospholipids (LPL) resulting in F-actin and pseudopod regulation, although the molecular mechanisms are currently unclear. Phospholipase A_2 activity is regulated by intracellular calcium, which can be increased by three distinct mechanisms. Firstly, inositol triphosphate mediated release from calcium stores can increase intracellular calcium. Second, increased extracellular uptake of calcium will also increase intracellular calcium. Finally free fatty acids such as arachadonic acid can also influence calcium release, which subsequently results in increased phospholipase A_2 activity.

In addition to PI3K activation by Ras, PIP_3 production is also regulated by phosphatase and tension homologue (PTEN), which converts PIP_3 back to PIP_2 at the uropod (Iijima and Devreotes, 2002). Activation of PTEN assists in the temporal and spatial control of cell polarity, allowing surges of PIP_3 formation to occur at the leading edge only, which assists in the maintenance of chemotactic amplification and directionality (Iijima et al., 2002). PTEN is regulated by phospholipase C, another enzyme activated by G-protein dissociation, which breaks down PIP_2 diacylglycerol (DAG) and inositol triphosphate (IP_3) at the leading edge (Kortholt et al., 2007). As a result, phospholipase C activity results in translocation of PTEN to the rear of the cell (Kortholt et al., 2007).

During random cell movement, activation of Ras, PI3K and PTEN occurs independently of G-protein coupled receptor activation (Sasaki et al., 2007) where PI3K and Ras are shown to act in a positive feedback loop. This loop may act to control stochastic chances in the F-actin cytoskeleton and thus negatively regulate the formation of pseudopods (Sasaki et al., 2007). In the absence of PIP_3 gradients by ablation of all type I $PI3K_{1-5}$ and PTEN genes, *Dictyostelium* motility during random cell movement is substantially impaired, indicating a distinct role for the PI3K pathway, which may be directional sensing (Bosgraaf and van Haastert, 2009; Hoeller and Kay, 2007).

Chemotaxis in the absence of PIP_3 gradients, can still occur effectively in steep but not shallow cAMP gradients in *Dictyostelium* (Hoeller and Kay, 2007; van Haastert et al., 2007a). In addition, the PI3K pathway is shown to play a fundamental role in the mechanism of cell movement, however not its directionality (Andrew and Insall, 2007). In steep chemotactic gradients, PIP_3 production at the leading edge of the cell is abundant, indicating a significant

role for PI3K signalling in cell movement (King and Insall, 2009). In shallow chemotactic gradients however, PIP_3 localisation is comparatively weaker, where absence of PIP_3 gradients results in chemotactic defects (van Haastert et al., 2007a), indicating the phosphoinositide plays a comprehensive role in the general control of basic cell motility (King and Insall, 2009).

1.8.4. Target of Rapamycin complex 2

Dictyostelium chemotaxis is also regulated by the target of rapamycin complex 2 (TORC2), which consists of 3 proteins LST8, pianissimo and Rip3. TORC2 activation is regulated by RasC and mediates numerous downstream targets, including an overlapping role with PIP_3 in PKB/Akt regulation (King and Insall, 2008; Kamimura et al., 2008). Upon detection of cAMP gradients, F-actin initiates the recruitment of a scaffold protein complex, consisting of Sca1, aimless, RasGEFH and protein phosphate 2A, at the leading cell edge (Charest et al., 2010). This scaffold protein complex then activates RasC, which triggers TORC2 activity (Charest et al., 2010). Finally, TORC2 regulates PKB/Akt and its structurally-related homologue, PKBR1, to mediate F-actin formation, increased cAMP production through adenylyl cyclase and negative regulation of the Sca1 scaffold complex through phosphorylation (Charest et al., 2010) **(Figure 1.8)**. PKBR1 contains no plekstrin homology domains (Garcia and Parent, 2008b; Meili et al., 2000) and also targets two Ras-GEFs, a RacGAP and Talin B, which is a vital component for cellular adhesion in downstream signalling (King and Insall, 2008).

In addition to PKB/Akt providing a distinct role in both PI3K and TORC2 signalling, glycogen synthase kinase-A, a highly conserved homologue to human glycogen synthase kinase-3, is also involved in regulation of these

pathways (Teo et al., 2010). Ablation of the glycogen synthase kinase-A gene results disruption of both chemotaxis and cAMP signalling in *Dictyostelium* cells (Teo et al., 2010), mediated by both PIP_3 and TORC2 signalling, which resultantly blocks PKB/Akt and PKBR1phosphorylation.

1.8.5. The Phospholipase A_2 Pathway

Dictyostelium has a range independent and complex signalling pathways all involved in chemotactic signalling, one of which is the phospholipase A_2 pathway (Chen et al., 2007). The mechanism for activation of this pathway is currently unclear, however detection of cAMP (presumably via cAR) results in phospholipase A_2 activity, which converts phospholipids located on the cell membrane to lysophospholipids and arachadonic acid (King and Insall, 2009; Sasaki et al., 2007; van Haastert et al., 2007a). This process mediates rises in intracellular calcium levels, driving motility towards a chemoattractant (van Haastert et al., 2007b; King and Insall, 2009) **(Figure 1.8)**. Phospholipase A_2 activity is regulated by intracellular calcium, where increased levels result in activation of the pathway (van Haastert et al., 2007b). Intracellular calcium increases can be mediated by three distinct mechanisms, which include increased extracellular calcium uptake, IP_3R_3-mediated intracellular calcium release and increased fatty acid turnover (van Haastert et al., 2007b). Together, this indicates, *Dictyostelium* phospholipase A_2 activity can be influenced partially by either phospholipase A_2 itself (as this increases fatty acid turnover) or phospholipase C, which is responsible for conversion of PIP_2 into inositol triphosphate and subsequent activation of IP_3R_3 (van Haastert et al., 2007b).

The exact mechanisms by which phospholipase A_2 regulates *Dictyostelium* movement are currently unclear, however since the protein is cytosolic, it may induce pseudopods as well as regulate cell movement at the rear of the cell (Chen et al., 2007; Veltman et al., 2008). During random cell movement, phospholipase A_2 activity is involved in the splitting of existing pseudopods, forming the previously discussed zigzag walk (Bosgraaf and van Haastert, 2009). During shallow chemotactic gradients, ablation of the gene encoding phospholipase A_2 results in chemotactic defects, in a similar manner to removing PIP_3 gradients in *Dictyostelium* signalling, indicating both PI3K and phospholipase A_2 have parallel roles, which are crucial in the formation of pseudopods (van Haastert et al., 2007b). During steep gradients, as with PI3K, a role for phospholipase A_2 activity becomes less distinct, where cells can chemotax effectively in the absence of phospholipase A_2 (van Haastert et al., 2007a).

1.8.6. Alternative Amplification Pathways

The enzyme, soluble guanylyl cyclase is another mechanism for cell chemotaxis in response to cAMP, which can initiate chemotaxis in the absence of PI3K or phospholipase A_2 (Veltman and van Haastert, 2008). Soluble guanylyl cyclase is activated at the leading edge of cells and interacts with F-actin to drive the formation of pseudopods in chemotaxis (Veltman et al., 2008).

The second messenger product of soluble guanylyl cyclase, cyclic guanosine monophosphate is crucial at the rear of the cell during chemotaxis, where it suppresses pseudopod formation (Veltman et al., 2005). In addition, cyclic guanosine monophosphate also inhibits the formation of lateral pseudopods by regulating myosin at the sides and rear of the cell (Veltman et

al., 2008) **(Figure 1.8)**. Cyclic guanosine monophosphate activates an enzyme, GpbC, which interacts with myosin light- and heavy- chain kinases and also assists in the retraction of pseudopods through myosin II (Bosgraaf et al., 2002; Veltman and van Haastert, 2008; Wang et al., 2011). During random cell movement, cyclic guanosine monophosphate is involved in the formation of *de-novo* pseudopods in random cell movement (Bosgraaf and van Haastert, 2009).

Another explanation for a potential method for *Dictyostelium* cell migration is membrane blebbing at the leading edge of cells during cell migration (Yoshida and Soldati, 2006). This is a result of cell membrane and F-actin interaction disruptions (Fackler and Grosse, 2008). A change in hydrostatic pressure within the cell, in conjunction with myosin II contraction, causes a section of the cell membrane to project forming a bleb (Fackler and Grosse, 2008; King and Insall, 2009). When this occurs, F-actin polymerises at the centre of the bleb in order to counter and retract it. Membrane blebs occur in *Dictyostelium* and can assist cell migration (King and Insall, 2009).

A final possible kinase has been discovered known as Tsunami. This kinase is associated with microtubules and poor chemotaxis has been displayed in Tsunami null cells (Tang et al., 2008; Wang et al., 2011)**.** Very little is known about the protein or the roles it plays in chemotaxis, however it has been shown to have possible implications in the regulation of PIP_3.

Dictyostelium therefore contains a variety of signalling mechanisms controlling chemotaxis and random cell movement, where disruption of individual pathways does not inhibit chemotaxis. However, disruption of multiple pathways can severely impact upon chemotactic behaviour (Veltman et al., 2008). These multiple signalling pathways are comparable to those that

occur in leukocytes, making *Dictyostelium* an ideal model in the study of cell movement.

1.9. Aims of this work

This PhD thesis set out to investigate the potential for *Dictyostelium* to be used as an early screen in the prediction of emetic liability, which if successful may reduce the number of animals used in emetic research (Holmes et al., 2009). In order to do so, the effects of a number of emetic compounds were investigated for their acute effects on *Dictyostelium* chemotaxis towards cAMP. Compounds that affected *Dictyostelium* behaviour during motility were explored in further detail.

Emetic screening identified a number of bitter tastants, which blocked *Dictyostelium* motility. A mutagenesis screen was then performed using bitter tastants as a selection medium to identify a number of potential molecular targets. Some of these targets were selected and explored in further detail, where GrlJ was identified to show sensitivity to the bitter tastant phenylthiourea. *grlJ* was ablated in wild type Ax2 cells and the molecular mechanisms involved for phenylthiourea detection explored. Finally, in a search for proteins related to GrlJ, an uncharacterised human protein, sharing weak homology with GrlJ, was identified. This protein was cloned into *Dictyostelium* and its involvement in phenylthiourea detection explored.

Chapter 2

Materials and Methods

2.1. Materials

2.1.1. General reagents

2.1.1.1. Reagents purchased from Sigma-Aldrich Co. Ltd (Dorset, England)

2-Propanol, 5-fluorouracil, acrylamide (30% solution), actinomycin D, ammonium persulphate (APS), bacteriological agar, beta-mercaptoethanol, caffeine, calcium chloride, capsaicin, cisplatin, copper chloride, copper sulphate, curcumin, cyclic adenosine monophosphate, cycloheximide, denatonium benzoate, digoxin, fluoxetine, horse serum, lithium chloride, loperamide hydrochloride, Luria-Burtani (LB) broth tablets, magnesium chloride, metformin, methotrexate, N,N,N',N'-tetramethyl-etheline-1,2-diamine (TEMED), nicotine, PGF2α, phenylthiourea, potassium chloride, pyrogallol, quinine hydrochloride, resiniferatoxin, rolipram, sodium chloride, sodium dihydrogen phosphate, sodium dodecyl sulphate (SDS), sodium phosphate basic, streptozocin, sucrose, trichloroacetic acid, trisma base, triton-100, TWEEN20, veratridine, vincristine, zinc sulphate monohydrate.

2.1.1.2. Reagents purchased from other suppliers

Agarose, deoxynucleotide triphosphatases (dNTPs) (Bioline, London, England)

Ethdium bromide (Bio-Rad Laboratories, Hemel Hempsted, England)

6x Loading dye (Fermentas, Sunderland, England)

Axenic medium, SM medium (ForMedium, Norfolk, England)

Complete Mini Protease inhibitor cocktail, Complete Mini Phosphatase inhibitor cocktail (Roche, West Sussex, England)

Glycine, tris-borate-EDTA (TBE) 10x (ThermoFischer Scientific, Loughborough, England)

5-hydroxytryptamine, apomorphine hydrochloride, substance P (Tocris Bioscience Ltd, Bristol, England)

Acetic acid, acetone, bromophenol blue, chloroform, dimethylsulphoxide (DMSO), ethanol, glucose, glycerol, hydrochloric acid, isopropyl β-D-1-thiogalactopyranoside (IPTG), methanol, potassium dihydrogen phosphate, sodium hydroxide (VWR International Ltd, Leicestershire, England)

2.1.1.3. Antibiotics

Geneticin (Invitrogen Gröningen, Netherlands)

Blasticidin, penicillin/streptomycin solution 100x (PAA Laboratories Ltd, Somerset, England)

Ampicillin (Sigma-Aldrich Co. Ltd, Dorset, England)

2.1.1.4. Molecular weight standards

Generuler 100bp plus and 1kb DNA Ladder, PageRuler Plus prestained protein ladder (Fermentas, Sunderland, England)

2.1.1.5. Restriction enzymes

All restriction enzymes and corresponding buffers (Fermentas, Sunderland, England)

2.1.1.6. Other enzymes

BioTaq polymerase (Bioline, London, England)

Phusion Hot Start II, Proteinase K, T4 DNA ligase (Fermentas, Sunderland, England)

RNase A, DNase (Sigma-Aldrich Co. Ltd, Dorset, England)

2.1.1.7. Antibodies

IRDye800 Goat Anti-Mouse (Licor bioscience Ltd, Nebraska, USA)

M2 FLAG monoclonal antibody (Sigma-Aldrich Co.Ltd, Dorset, England)

2.1.1.8. Kits

DNAse treated with DNA-free kit (Ambion, England)

PIP_3 Mass ELISA Kit (Echeolon, USA)

First Strand cDNA Synthesis Kit (Fermentas, Sunderland, England)

Illustra MicroSpin S-400 HR columns (GE Healthcare, Buckinghamshire, UK)

Genome DNA Kit (MP Biomedicals, Illkirch, France)

QIAfilter Plasmid Maxi Kit and MinElute PCR Purification Kit (QIAgen Ltd, West Sussex, England)

High Pure RNA Isolation Kit (Roche, West Sussex, UK)

GeneEluteHP Plasmid Maxiprep kit (Sigma Aldrich Co. Ltd Dorset, England)

2.1.1.9. *Escherichia coli (E.coli)* strains

TOP10 chemically competent *E.coli*, chemically competent JM107 cells (Invitrogen, Gröningen, Netherlands)

XL10 Gold ultra-competent cells (Agilent, USA)

2.1.1.10. Primers

Primers were all purchased from VWR International Ltd. (Leicestershire, England)

2.1.1.11. Equipment

Bio-Rad gel casting system, Bio-Rad wide mini-sub cell electrophoresis system, GelDoc XR system, PowerPac 300 power supply, GenePulser Xcell electroporator (Bio-Rad Laboratories, Hemel Hempsted, England)

Neubauer improved haemocytometer, Dunn chamber (Hawksley, Sussex, England)

Centrifuge (Biofuge 13, Jencons)

Odyssey Infrared Imaging System (Li-Cor Biosciences, Nebraska, USA)

47mm black nitrocellulose filters (Millipore, Oxfordshire, England)

Olympus IX71 microscope (U-RFP-T laser, 482nm emission, QImaging RetegaExi Fast1394 digital camera (Olympus, Southend-on-sea, England)

PeqSTAR 2x thermocycler, PeqSTAR 96 universal thermocycler, 4mm electroporation cuvettes (PEQLAB Ltd, Portsmouth, England)

GeneFlash gel documentation system (Syngene Bio Imaging)

LabTek 8-well chambered coverglass (ThermoFisher Scientific, Loughborough, England)

2.2. Methods

2.2.1. *Dictyostelium* methods

2.2.1.1. Cell culture

Dictyostelium stocks were stored in freezing medium (7% DMSO, horse serum) at -80^{o}C. Every four weeks, frozen stocks were scraped onto SM agar plates, on which 300µL *Raoultella planticola* had been streaked. Colonies were allowed to form at 22^{o}C over 3-4 days, where cells from the growth zone of colonies were then transferred to liquid plates containing Ax medium and 100µg/mL penicillin/streptomycin. Liquid plates were washed three times per week and also maintained in log phase (1-4x10^{6} cells/mL) in shaking flasks (120rpm). Cell concentrations were determined using a Neubauer improved haemocytometer.

2.2.1.2. Growth curve assays

For proliferation assays in chapter 4, *Dictyostelium* cells were harvested and diluted in axenic medium to 1x10^{5} cells/mL. 10ml aliquots of cells were transferred to conical flasks containing consistent concentrations of solvent (DMSO) in addition to phenylthiourea or denatonium benzoate. Cells were then grown in shaking suspension (120rpm) and cell density calculated over seven days at 22^{o}C.

For proliferation assays in chapter 5, *Dictyostelium* cells were harvested and diluted in axenic medium to 3x10^{5} cells/mL and allowed to grow in shaking suspension until cells reached approximately 50% of maximal cell density.

10mL aliquots of cells were then transferred to conical flasks containing consistent concentrations of solvent (DMSO) and phenylthiourea. Cell density was calculated until stationary phase was reached under control conditions.

2.2.1.3. Colony formation assays

SM agar was heated and allowed to cool to approximately 50^{o}C before addition of desired quantities of DMSO (control) or phenylthiourea. Agar was then poured into Petri dishes allowed to set. Approximately 30 *Dictyostelium* cells were suspended in 300µL of *R. planticola*, spread onto the previously prepared SM agar plates and allowed to grow over four days at 22^{o}C.

2.2.1.4. Development assays

Approximately 1x10^{7} *Dictyostelium* cells were harvested from cells in shaking suspension, washed and resuspended in 1mL KK2 (16.2mM KH_2PO_4, 4mM K_2HPO_4). Cells were then evenly distributed onto 47mm black nitrocellulose filters that were soaked in KK2 or KK2 containing specific concentrations of a compound. Cells were then incubated at 22^{o}C over twenty four hours.

2.2.1.5. Spore shape

Following development of fruiting bodies after twenty four hours, *Dictyostelium* spores were harvested and suspended in 20µL KK2 before being transferred to coverslips. Images of spores were taken using light microscopy at 40x magnification.

2.2.1.6. Motility assays

Approximately 1x10^7 *Dictyostelium* cells were harvested from cells in shaking suspension, washed and resuspended in 6mL KK2. Cells were then pulsed for five hours with 30nM cAMP at 6 min intervals whilst shaking at 120rpm before being washed in phosphate buffer and resuspended in 1mL KK2. Cells were then transferred to a Dunn chamber as previously described (Zicha et al., 1991), with cells migrating towards 5µM cAMP. A stable chemotactic gradient was allowed to form over a thirty minute period, prior to recording cell behaviour using an Olympus IX71 microscope at 40x magnification with a QImaging RetigaExi Fast1394 digital camera. Cell images were recorded every six seconds over a fifteen minute period, with the initial five minutes period recorded prior to addition of test compounds. At five minutes, a 10µL aliquot of test compound, diluted in 5µM cAMP, was added to the outer well of the Dunn chamber and subsequent images recorded over the following ten min period for each compound. Solvent only controls were carried out for all experiments to ensure readouts were based upon compounds.

2.2.1.7. Random cell movement assays

Cells were harvested and pulsed as described above. After pulsing, *Dictyostelium* cells were washed and resuspended in 4 mL prior to a 10x dilution in KK2. 250µL cells were then transferred to 8-well chambered coverglass slides and allowed to adhere and begin random cell movement. Cell imaging was then recorded every eighteen seconds for the desired time period.

For assays assessing recovery to bitter tastants, cell behaviour was recorded for 35 minutes, where 250µL (double concentrated) tastant, suspended in KK2, was added after 288 seconds to give a desired

concentration. Cell behaviour was then monitored for a further fifteen frames, before replacement of all media from the chamber with KK2. Cell behaviour was then monitored for the remainder of the assay.

For assays assessing the response of a compound to a bitter tastant, cell behaviour was recorded for fifteen minutes, where 250µL (double concentrated) tastant, suspended in KK2, was added after 288 seconds to give a desired concentration. Cell behaviour was then monitored for the remainder of the assay. Finally for assessment of naringenin-mediated effects on *Dictyostelium* behaviour, cells were incubated in naringenin for one hour, prior to addition to the 8-well chambered coverglass. Cell behaviour was then monitored over five minutes.

2.2.1.8. Cell viability assays

Dictyostelium cells were pulsed as described above and resuspended in 4mL KK2, before exposure to each tastant for seven or twenty seven minutes. Cells were then stained with 0.4% trypan blue solution (final concentration 0.067%) for three minutes prior to counting using a Neubauer improved haemocytometer. Dead cells were identified as a distinctive blue colour since live cells did not change colour.

2.2.1.9. PH_{CRAC}GFP global stimulation experiments

Dictyostelium cells expressing PH_{CRAC}GFP were pulsed as previously described in random cell movement assays. 200µl cells were then added to 8-well chambered coverglass, suspended in KK2 or phenylthiourea. Cells were allowed to adhere for ten minutes and cell fluorescence was subsequently recorded at 60x magnification, using a GFP filter, with images being taken every

two seconds for two minutes. After 30 seconds, 50µl of 5µM cAMP was added to the cell suspension and changes in fluorescence monitored.

2.2.1.10. PIP_3 mass ELISA

$6x10^8$ *Dictyostelium* cells were harvested, washed and pulsed for five hours. Cell signalling was basalated with incubation of caffeine (3mM final concentration) for thirty minutes before being washed and resuspended in phosphate buffer at $4x10^7$ cells/ml with cells either incubated in phosphate buffer or phenylthiourea (3mM final concentration) for ten minutes. 2.5ml cells were added to a tube containing 250µl cAMP (1µM final concentration) and cell signalling was stopped by addition of 3ml trichloroacetic acid (0.5M), vortexed and incubated for five minutes on ice at time points 0, 5 and 20 seconds after cAMP addition. Samples were then spun and washed with 5% trichloroacetic acid before following the lipid extraction protocol for mass ELISA as described in the PIP_3 mass ELISA kit.

2.2.2. Molecular biology methods

2.2.2.1. Polymerase chain reaction

Amplification of DNA using polymerase chain reaction (PCR) was achieved under the following conditions for standard reactions: 2-5µL DNA, 2µL 2mM dNTPs, 2µL NH_4 BIOTAQ reaction buffer, 1µL $MgCl_2$, 0.2-0.5µL BIOTAQ DNA polymerase (5U μL^{-1}), 2µL 5' primer (10pmol), 2µL 3' primer (10pmol) and double distilled water up to 20µL (total volume). For PCR using a proof reading polymerase, the following conditions were used: 2-5µL DNA, 2µL dNTPs, 4µL Phusion HF buffer, 0.2µL Phusion Hot Start II Polymerase, 1µL 5' primer (10pmol), 1µL 3' primer (10pmol) and double distilled water up to 20µL (total volume).

The PCR was carried out using the following cyclical conditions for standard PCR reactions: initial denature, 10 minutes at 95^{o}C followed by 30 cycles as follows: denature 30 seconds, 95^{o}C, anneal 30 seconds, 50-60^{o}C (dependent on primer melting points), extension 4 minutes, 68^{o}C (or 1 minute 72^{o}C depending on the primer). The PCR was completed with a final extension of 10 minutes at 68^{o}C (or 72^{o}C). Samples were then stored at 4^{o}C. For Phusion Hot Start II polymerase reactions, PCR was carried out according to manufacturer's instructions.

2.2.2.2. Agarose gel electrophoresis

To separate and visualize DNA, 1% agarose gels containing ethidium bromide and 1x TBE buffer were used. 5-10µL DNA was added to 1-2µL 5xDNA loading dye. 100bp plus or 1kb DNA ladders (Fermentas) were used as molecular marker to determine DNA fragment size on the agarose gels. Gels were run in an electrophoresis tank for 40 minutes at 110V and visualized with UV light using a GeneFlash gel documentation system (Syngene Bio Imaging).

2.2.2.3. Transformation of competent *E.Coli*

Luria-Burtani (LB) plates were prepared by pouring LB agar media containing 1.0µL/mL ampicillin into 90mm Petri dishes. Chemically competent JM107 *E.coli* cells were thawed on ice and used for transformations. 10µL ligated DNA was added to 100µL competent cells, incubated on ice for 30 minutes before heat-shock treatment at 42^{o}C for 30 seconds. Cells were then rapidly stored on ice for 2 minutes, before addition of 250µL LB media and incubated in a shaking incubator at 37^{o}C for 1 hour. After incubation, cells were briefly spun down in a centrifuge, LB media aspirated and resuspended in

100µL fresh LB media, streaked onto LB agar plates (containing ampicillin) and incubated at 37^{o}C overnight.

For larger DNA cloning vectors, XL10 Gold chemically competent *E. coli* cells were used for transformations. This was achieved according to the manufacturer's instructions.

2.2.2.4. Plasmid preparation

Sigma GenElute Plasmid Miniprep Kits, Qiagen QIAfilter Plasmid Midi kits or Qiagen QIAfilter Plasmid Maxi kits columns were used to prepare plasmids for cloning and sequencing according to the manufacturer's instructions.

To verify positive transformants from *E.coli* without the use of commercial kits, 1.5mL culture was spun down for 2 minutes at 13 000rpm, supernatant aspirated and resuspended in 100µL P1 buffer (50mM Tris-Cl pH8.0, 10mM EDTA, 100µg/mL RNase A). Cells were lysed with 200µL P2 buffer (200mM NaOH, 1% SDS (W/V)) before incubation for 5 minutes at room temperature. The lysis mixture was then neutralized by addition of 150µL P3 buffer (3M potassium acetate pH5.5), mixed by inversion and spun down for 3 minutes at 13 000rpm. Supernatants were then transferred into fresh tubes, before DNA precipitation by addition of 1mL ethanol. The mixture was then vortexed, spun down for a further 3 minutes and supernatant. Residual ethanol was removed by a further spin and removal of supernatant before DNA was resuspended in 50µL double distilled water.

2.2.2.5. Restriction digests

All restriction digests were prepared according to the following conditions: 5µL DNA, 0.2-0.5µL each restriction enzyme (100µL^{-1}) (Fermentas), 1µL appropriate buffer (according the manufacturer's instructions) (Fermentas). Reactions were incubated at 37^{o}C for 20 minutes to 2 hours, depending on the type of restriction enzyme (FastDigest enzymes were used in shorter incubations).

2.2.2.6. Construction of knockout vectors

Two fragments of the open reading frame of the gene of interest, using Ax2 genomic DNA, were amplified using PCR. Primers were designed to contain restriction sites for cloning into the pLPBLP vector. PCR products were purified using GE Healthcare s400 MicroSpin columns or the GenElute PCR purification kit (Qiagen). The pLPBLP vector and gene fragments were double-digested with appropriate restriction enzymes, BamHI, PstI (for N-terminal fragments) and NcoI, KpnI (for C-terminal fragments). Gene fragments were then ligated into the pLPBLP vector backbone using 0.4µL T4DNA ligase (1U µL^{-1}) (Fermentas), 1µL T4DNA ligase buffer (Fermentas) at ratios of 1:10 and/or 1:100 insert: vector. Ligation mixtures were made up to 10µL using double distilled water and incubated at 16^{o}C overnight. Ligation mixtures were then heat inactivated at 70^{o}C for 15 minutes before being transformed into JM107 chemically competent *E.coli* cells. Colonies formed during overnight incubation were picked and grown in LB media containing 2-4µL/mL ampicillin before plasmid preparation. To test the insertion of a fragment of *Dictyostelium* genomic DNA, restriction digests were performed with previously used restriction enzymes. This process was repeated to insert the second gene

fragment into the pLPBLP vector backbone. Once both N and C terminal fragments had been inserted into the vector, the knockout construct was prepared using the QIAfilter Plasmid Maxi kit and electroporated into *Dictyostelium* cells.

2.2.2.7. Transformation of knockout constructs into *Dictyostelium*

Knockout constructs created using pLPBLP were excised from the vector backbone using restriction enzymes BamHI and KpnI. The digested knockout construct (20µg) was purified using isopropanol precipitation.

For electroporation, $1x10^7$ *Dictyostelium* cells were incubated on ice for 10 minutes before centrifugation at 1000xg for 3 minutes at 4^oC. Cells were then washed twice with phosphate buffer (KK2) at 4^oC prior to a further two washes with sterile filtered electroporation buffer (10mM sodium phosphate buffer pH 6.1, 50mM sucrose). Finally, the pellet was resuspended in 700µL electroporation buffer, transferred to a 0.4cm cuvette along with the previously digested and purified knockout construct (20µg) and incubated on ice for 10 minutes prior to electroporation. *Dictyostelium* cells were electroporated with a BIO-RAD GenePulser Xcell electroporator using 1 pulse, 850V and 25µF. Cells were incubated on ice for 10 minutes before addition of 8µL $CaCl_2$ (100mM) and 8µL $MgCl_2$ (100mM) followed by a further 15 minute incubation at room temperature. Cells were added to 10mL Ax medium containing penicillin/streptomycin (100x) and 100µL culture transferred to each well of a 96-well plate. After 24-hours, 100µL of double concentrated blasticidin (20µg/mL) in Ax media (containing penicillin/streptomycin) was added to each well of the 96-well plate.

2.2.2.8. Transformation of overexpression constructs by calcium chloride precipitation

Overexpression vectors containing a C-terminally fused GFP tag (pDEX27) or an N-terminally fused FLAG (PDM320) tag were obtained from www.dictybase.org. Full length cDNA was amplified by PCR using primers containing appropriate restriction sites. Overexpression constructs were double digested with restriction enzymes before ligation into the vector backbones. Overexpression constructs were prepared using QIAfilter Plasmid Maxi kits.

For calcium transformation, $1x10^7$ cells were harvested in Ax media and allowed to adhere to a 9cm Petri dish over 30 minutes. Ax media was replaced with 10mL filter sterilized MES-HL5 (0.6% (w/v) yeast extract, 22.2mM glucose, 1% (w/v) bacteriological peptone, 6.65mM MES; pH 7.1) and incubated at 22^{o}C for 1.5 hours. The DNA was prepared for transformation by adding 20µg DNA to 600µL double distilled water and 600µL 2x HBS (237mM NaCl, 9.65mM KCl, 1.6mM $Na_2H_2PO_4$, 41mM HEPES, 11.1mM D-glucose, pH 7.05) and precipitated using 76µL 2M $CaCl_2$. The solution was incubated for 25 minutes at 22^{o}C. After 1.5 hours, MES-HL5 medium used for incubation was replaced with 1.2mL DNA solution and incubated for 30 minutes. 10mL MES-HL5 was then added to cells and incubated for a further 3 hours at 22^{o}C before the medium was gently replaced with 2mL 15% glycerol stock (2.5mL 60% glycerol, 2.5mL double distilled water, 5mL 2x HBS). After 2 minutes, the glycerol stock was carefully removed, replaced with 10mL Ax media and allowed to recover overnight. Cells were then equally distributed onto 10 *Micrococcus luteus* lawns (geneticin resistant) on SM agar plates (containing 25µg/mL geneticin) and incubated at 22^{o}C.

2.2.2.9. Extraction of DNA from potential transformants

Surviving colonies growing in 96-well plates after transformation were allowed to reach confluence before removal of 200µL cells and centrifugation at 1000g for 3 minutes. The pellet was resuspended in 48µL of lysis buffer (50mM KCl, 10mM Tris pH 8.3, 2.5M $MgCl_2$, 0.45% Nonidet P 40, 0.45% TWEEN 20) and 2µL Proteinase K (822U/mL) before 5 minute incubation at room temperature. Samples were further incubated at 95^{o}C for 1 minute and the extracted DNA used in PCR reactions to screen for correctly transformed constructs.

2.2.2.10. Screening for correct mutants

Primers were designed to determine the whether transformed *Dictyostelium* cells contained the knock out construct with a correctly incorporated cassette encoding blasticidin resistance. Genomic DNA was extracted and used in PCR analysis based upon 3 different primer pairs to screen for the knockout construct: genomic, vector controls and an additional knockout diagnostic primer set. Genomic control primers were designed to flank 5' and 3' fragments cloned into the pLPBLP vector, which would confirm the presence of a non-deleted region of the gene. Vector control fragments were used to confirm the presence of the knockout cassette using primers flanking regions inside genomic DNA fragment and the cassette encoding blasticidin. The diagnostic knockout fragment was designed using the genomic control primer and the blasticidin resistance cassette primer. These primer pairs were created for both N and C terminal fragments of the knockout construct.

2.2.2.11. Sub-cloning of correct transformants

Once correct transformants had been confirmed by PCR, colonies were selected and plated onto sterile SM agar plates containing 200µL *Raoultella planticola*. The plates were incubated at 22^{o}C for 3-4 days to allow individual colonies to form, before the resulting cloned sub-colonies were screened again using the PCR primers previously described **(Section 2.2.2.10)**

2.2.2.12. RNA extraction

Dictyostelium cells were harvested and resuspended at 1x10^{7} cells/mL prior to washing with phosphate buffer (KK2) at 4^{o}C. RNA was extracted using the High Pure RNA isolation kit (Roche) according to the manufacturer's instructions.

2.2.2.13. Reverse transcription PCR

cDNA was synthesised using 1µg of extracted RNA using a First Strand cDNA synthesis kit (Fermentas). 2µL synthesized cDNA was then used in PCR reactions as previously described.

2.2.3. Proteomics

2.2.3.1. Western blot analysis

Sodium dodecyl sulphate polyacrylamide gels (SDS-PAGE) (12.5%) were prepared (Resolving gel – 2.215mL 30% acrylamide solution, 0.95mL Tris pH 8.8, 1.825mL water, 100µL 10% SDS, 50µL 10% ammonium persulphate, 5µL TEMED, stacking gel - 425µL 30% acrylamide solution, 157.5µL Tris pH 6.8, 1.875mL water, 25µL 10% SDS, 25µL 10% ammonium persulphate, 7.5µL TEMED) for electrophoresis. Protein samples were prepared by boiling at 95^{o}C in 5x loading buffer (0.8mL 2M Tris pH6.8, 3mL 80% glycerol, 5mL 10% SDS,

1.25mL β-mercaptoethanol, water to 10 mL, bromophenol blue) for 15 minutes. Protein samples and the molecular marker, PageRuler Plus Prestained Protein Ladder (Fermentas) were loaded into the stacking gel and the gel run at 200 volts for 60 minutes in 1x running buffer (10x – 30g Trisma base, 144g glycine, 100mL 10% SDS, made up to 1L). The separated protein was blotted onto a PVDF membrane (Immobilon-FL Transfer membrane), which was activated by saturation in methanol. Blotting paper (3mm), sponges and the activated membrane were soaked in transfer buffer containing 10% ETB buffer (10x 75g trisma base, 360g glycine, 25mL 10% SDS) and 10% methanol. The transfer blot was prepared and added to a tank containing ice cold transfer buffer and run at 400mA for 1 hour.

After blotting, the PVDF membrane was incubated using 5mL blocking buffer (Li-cor Biosciences) for 1 hour. The appropriate primary antibody was then added at a 1:1000 dilution and incubated at 4^{o}C overnight. Primary antibody was then washed away with 1xPBS (10x PBS – 14.4g Na_2HPO_4, 80g NaCl, 2gKCl, 2.4g KH_2PO_4 made up to 1L with double distilled water, pH 7.4) followed by 3x10 minute incubations with PBST (1x PBS with 1% TWEEN 20). The appropriate secondary antibody was then added at a 1:5000 dilution in blocking buffer and incubated at room temperature for 1 hour. Secondary antibody was them washed away with 1xPBS followed by 3x10 minute incubations with PBST. Images were then taken with Odyssey Infrared Imaging System (Li-cor Bioscienes).

2.3. Software

Microscopy and quantification of motility assays were analyzed using ImagePro Plus (Media Cybernetics). Random cell movement and global

stimulation microscopy experiments were quantified with Fiji, using the QuimP 11b software (Warwick University, Warwick, England) and MATLAB (Mathworks, Cambridge, England). Graphical and statistical analysis was performed using GraphPad Prism 5 (GraphPad Software Inc).

2.4. Websites

***Dictyostelium* gene and protein information**

www.dictybase.org

***Dictyostelium* gene expression information**

www.dictyexpress.biolab.sl

Basic Local Alignment Search Tool (BLAST) analysis

www.dictybase.org/tools/blast

www.ebi.ac.uk/tools/sss/psiblast

www.ncbi.nlm.nih.gov/BLAST

Protein sequence alignment

www.ebi.ac.uk/tools/msa/clustalw2

Protein domain analysis

www.smart.embl-heidelberg.de

www.pfam.sanger.ac.uk

Glycosylation analysis

http://www.cbs.dtu.dk/services/NetNGlyc/

Organismal gene and protein information

www.uniprot.org

Chapter 3

Dictyostelium as a model for screening emetic compounds

Emetic research employs a range of unpleasant experiments on multiple animal models, with a large variation in response to different compounds and doses in different models (Holmes et al. 2009). Sentient models range from those animals that vomit (e.g. dog, ferret, house musk shrew) to those that exhibit conditioned taste aversion/conditioned food avoidance and pica (e.g. rat) (Holmes et al. 2009). Development of a suitable screen to predict emetic liability of novel compounds, prior to performing *in vivo* experiments, could provide substantial preliminary data, which could in turn help to reduce the number of animals required at a later stage in drug development.

No studies have explored the utility for *Dictyostelium* as a high throughput screen for specific side-effects, such as emesis. In addition, whilst the various stages of *Dictyostelium* development have been extensively studied, relatively few have examined compound-specific or structure-activity related effects on motility. Compounds that affect *Dictyostelium* motility include transmethylation inhibitors (inhibitors that prevent methyl group transfers between structures) (van and van Haastert, 1984), formaldehyde (Waligorska et al., 2008), potassium permanganate (Waligorska et al., 2008), ammonia (Feit et al., 2001) and adenosine derivatives (Theibert and Devreotes, 1984). In addition, therapeutic compounds such as valproic acid (used in the treatment of epilepsy) (Xu et al., 2007), lithium (used in the treatment for bipolar disorder) (Williams et al., 2002; King et al., 2009), chlorpromazine (an antipsychotic) (Gayatri and Chatterjee, 1991), naringenin (a flavonoid with anti-cancer potential) (Misty et al., 2006) and nitric oxide (a vasodilator) (Tao et al., 1996) can block *Dictyostelium* motility.

Numerous methods for measuring *Dictyostelium* cell motility exist, including the Dunn chamber (Zicha et al., 1991), the Zigmond chamber (Zigmond, 1977), needle point assays (Gerisch and Keller, 1981) and under agarose assays (Nelson et al., 1975). Measuring motility using a Dunn or Zigmond chamber allows for the establishment of a stable linear chemotactic gradient enabling cell migration in a uniform environment (Postma and van Haastert, 2009).

In this chapter *Dictyostelium* motility was assessed using a range of structurally diverse emetic compounds to investigate the model as an early screen to predict emetic liability. A Dunn chamber motility assay was developed to quantify cell behaviour following exposure to compounds shown to be emetic in mammals.

3.2. Development of a Suitable Motility Assay

To monitor *Dictyostelium* chemotactic behaviour, cells were developed to chemotactic competency (King et al., 2009; Pakes et al., 2012b; Robery et al., 2011) and added to the Dunn chamber (**Chapter 2**) migrating towards cAMP (Zicha et al., 1991). To visualise *Dictyostelium* behaviour, phase contrast microscopy was used to record cell motility over a 15 minute period (**Figure 3.1)**.

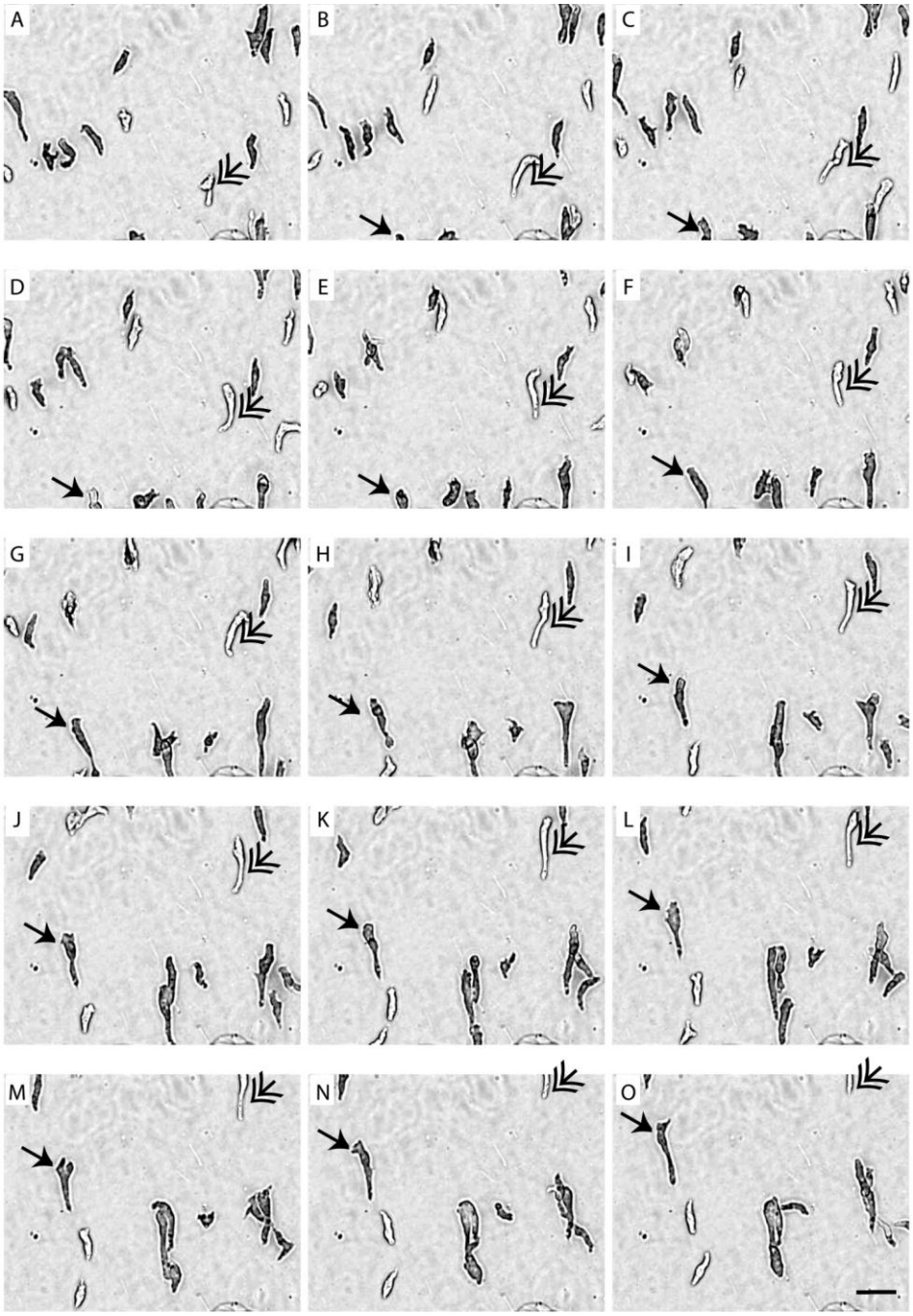

Figure 3.1. *Dictyostelium* cell migration over a 15 minute period. Phase contrast imaging was used to track cell migration over a 15 minute period during the assay. Under control conditions, cells migrated across the Dunn chamber. Each image is representative of 1 minute **(A-O)**. 2 separate cells have been highlighted by arrows to show individual cell migration towards cAMP. Bar = 10µm

To quantify *Dictyostelium* motility, ImagePro Plus was used to track the outlines of cells between individual frames **(Figure 3.2A)**. Outlines of individual cells throughout the 15 minute period were then used to determine the speed (velocity), cell shape (aspect), direction of migration (angle) and overall directionality across the assay (direction) **(Figure 3.2B)**. Velocity was defined as the distance travelled by the cell (measured from the centroid) between time

point 1 and time point 2 between each frame. Since individual cells migrated in slightly different directions, it is important to note the average velocity was actually a measurement for cell speed, because a single direction for all cells could not accurately be determined. Since ImagePro plus was used to calculate the velocity of individual cells, this measurement has been referred to as velocity throughout this thesis, when calculating the mean. The aspect of chemotaxing cells was described as the ratio of the lengths of the major and minor axes at each time point, where a value of 1 indicates a circle. The angle of cell movement was characterised by comparing the direction at which an individual cell was moving in comparison with the vertical axis. For this latter measurement, loss of movement would cause the value to deviate towards 0 as a direction would be indeterminable. As an additional, more illustrative way of describing cell behaviour, image overlays were produced, where outlines of a cell at every third time point were provided in a single image.

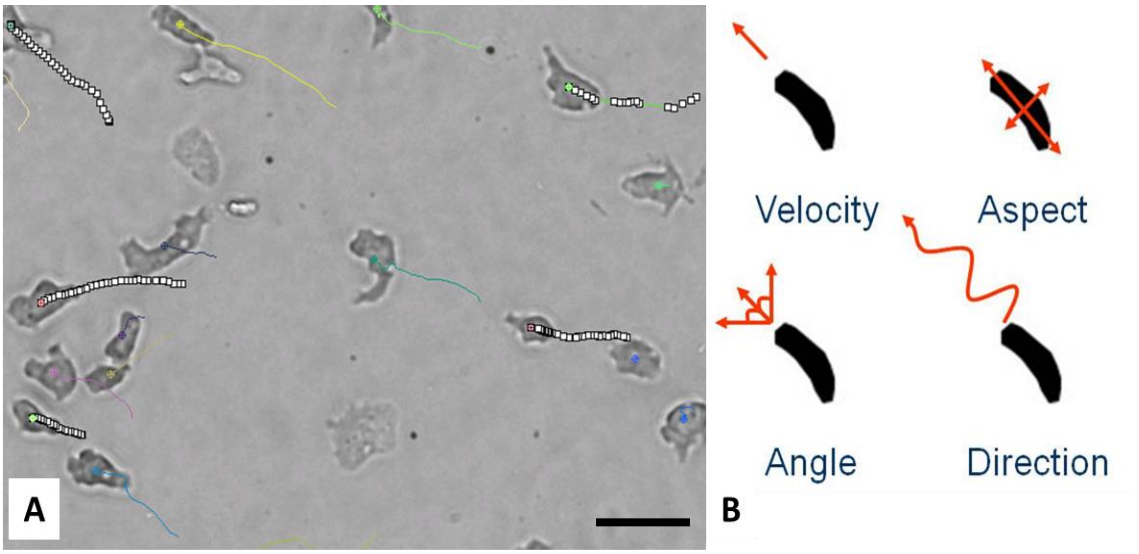

Figure 3.2. Analysis of *Dictyostelium* cell behaviour. **(A)** Cells moving under a chemotactic gradient were tracked using ImagePro Plus software **(B)** Measurements taken to determine cell behaviour were velocity (µm/sec); aspect (shape measured as a ratio between the length of cells across each axis); cell angle (degrees-where cell migration was measured in comparison to the y-axis); and cell direction (where still images were overlaid over one another to visually depict cell movement throughout the assay). Bar = 10µm.

To quantify cell behaviour, a sufficient number of cells were required to encompass cell movement throughout the assay. A minimum of 24 cells were tracked with mean velocity (speed) and aspect values at each time point and plotted onto a histogram **(Figure 3.3)**. To ensure data was distributed parametrically, a D'Agostino and Pearson omnibus normality test was performed. Each motility assay was also performed in at least triplicate to ensure cell behaviour was consistent and any changes in behaviour observed were genuine.

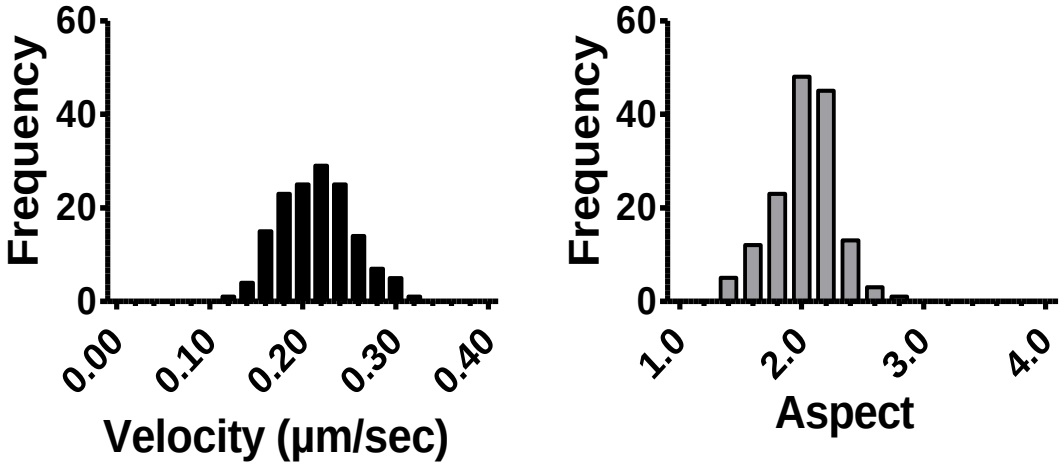

Figure 3.3. Histogram of *Dictyostelium* cell velocity and aspect. Mean cell velocity (speed) and aspect was recorded for 24 cells and the mean at each time point throughout the duration of the motility assay plotted. A D'Agostino and Pearson omnibus normality test showed data was normally distributed ($P<0.05$).

3.3. Control Conditions

To investigate any changes in *Dictyostelium* behaviour upon addition of a vehicle only control, experiments were performed by adding phosphate buffer (KK2) to the outer well of the chamber at 300 seconds **(Figure 3.4A-C)**. Two-tailed Student t-tests were performed between the first and final 300 seconds of the assay for cell velocity, aspect and angle to assess potential behavioural changes after the addition of a control vehicle. No significant changes in cell behaviour were observed during the assay. Illustrative examples of individual

cell behaviour are shown for four cells pre- and post-addition of vehicle-only control **(Figure 3.4D)**. In addition to phosphate buffer, these control experiments were all repeated using 1% DMSO, 0.9% ascorbic acid and 0.1% sodium hydroxide (all in phosphate buffer) as alternative solvents for compounds tested. These vehicles were all used in the presence of phosphate buffer in the attempt to neutralise any pH-specific effects that may be caused by the addition of compounds. None of these vehicles showed significant changes in cell behaviour comparing the 300 seconds pre-addition and 300-600 seconds post-addition based on the paired 2-tailed Student t-tests.

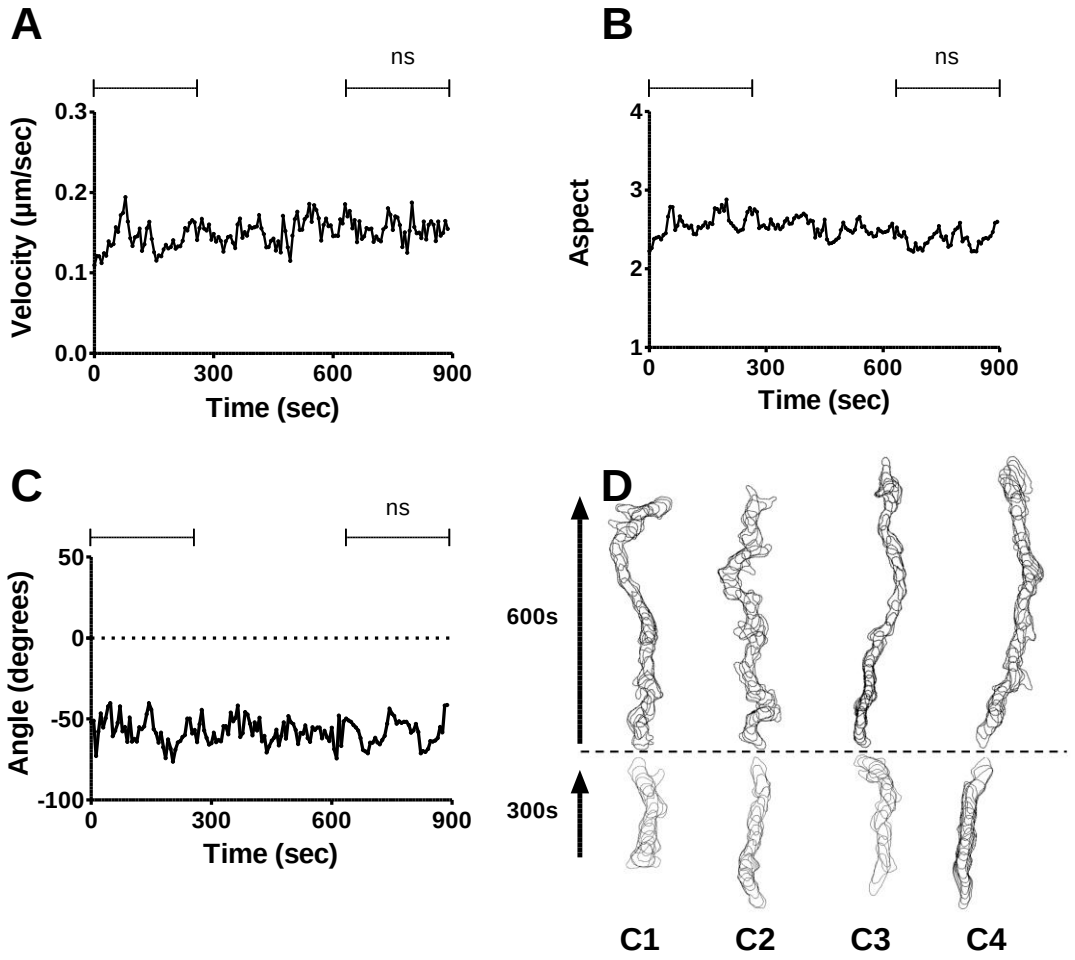

Figure 3.4. Analysis of *Dictyostelium* cell behaviour during motility under control conditions. Cell behaviour was measured under a stable chemotactic gradient in a Dunn chamber, with data from 85 cells quantified every 6 seconds over a 900 second period with the addition of vehicle only control (shown here for KK2) at 300 seconds. **(A)** Cell velocity; **(B) cell** aspect; **(C) cell** angular movement; **(D)** cell directionality. Cell outlines of 4 representative cells (C1-4) migrating under control conditions were overlaid and split into the first 300 and final 600 second intervals. Overlay images have been adjusted so that the chemotactic gradient is following the marked arrows. Cell behaviour showed no significant differences in velocity, aspect or angle observed between the first and final 300 seconds of the assay. Data from A-C is presented as mean of triplicate experiments analysing a minimum of 24 cells in each. Statistical analyses were performed using paired two-tailed Student t-tests comparing average values from T=0-300 and T=600-900 seconds as indicated. ns = not significant

Initial analysis of the assay for compounds showing chemotactic inhibition showed variability in chemotactic effects in the incubation period used. To investigate diffusion rates of compounds across the Dunn chamber, the time taken for 5x DNA loading dye (added to the outer well of the chamber) to completely diffuse was assessed. This experiment revealed a 3 minute delay in complete diffusion of the loading dye around the Dunn chamber **(Figure 3.5A-E).** Due to this diffusion delay, subsequent experiments were monitored in a defined region of the Dunn chamber to provide a consistent exposure to test compounds **(Figure 3.5F)**.

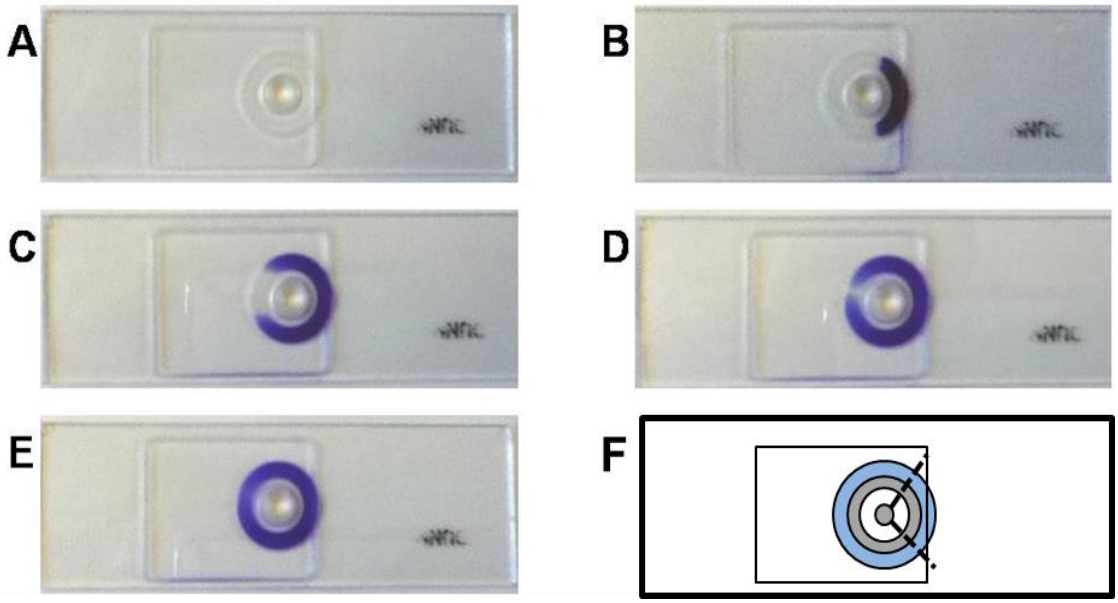

Figure 3.5. Diffusion of 5x loading dye around a Dunn Chamber. Loading dye was added to the outer well of a Dunn chamber containing KK2 and 5nM cAMP in order to simulate compound diffusion throughout the chamber. Images show conditions **(A)** prior to loading dye application, **(B)** upon addition and **(C)** 1 minute, **(D)** 2 minutes and **(E)** 3 minutes post-addition. **(F)** Schematic showing the region within the Dunn chamber used for imaging and subsequent quantification to ensure consistent exposure to test compounds.

3.4. Compounds and screening

A range of structurally diverse emetic and aversive compounds was used to assess the suitability of using *Dictyostelium* in a Dunn chamber for use in a high throughput motility screen to identify emetic compounds. The compounds chosen had a variety of primary pharmacological or molecular actions, which

may be responsible for emetic effects, summarised in **Table 3.1**. The mammalian species in which a compound has been shown to have emetic or related effects are also shown. The concentrations of compounds used in these tests were based upon emetic-inducing doses shown previously either *in vivo* (e.g. copper sulphate (Araya et al., 2001)), or in plasma concentrations (e.g. cisplatin (Percie du Sert et al., 2010)) or at concentrations shown to be active *in vitro* in mammalian tissue relevant to the emetic reflex (e.g. RTX on neurones (Smith et al., 2002), denatonium benzoate on intestinal epithelial cells (Chen et al., 2006)).

In all experiments, compounds were added to the outer well of the Dunn chamber after 300 seconds of recorded cell behaviour, providing an inbuilt control for each experiment. 29 compounds were screened, encompassing a wide range of targets and molecular mechanisms (**Table 3.1).** Six compounds, copper sulphate (1.6-5mM), copper chloride (1.6mM), denatonium benzoate (0.5-10mM), phenylthiourea (1-5mM), quinine hydrochloride (0.1-1mM) and capsaicin (0.05-0.3mM) showed a significant change in cell velocity and aspect comparing pre-compound addition and 300-600 seconds post-compound addition **(Table 3.1)**. The remaining 22 compounds were repeated at 10 to 200-fold higher concentrations to reduce the risk of obtaining false negative results. From this, rolipram was shown to inhibit *Dictyostelium* cell behaviour at an elevated concentration (0.7mM). Statistical analysis of cell behaviour was based on average velocity and aspect in the first and final five minutes of the assay used in a paired two-tailed Student t-test ($P \leq 0.05$). As cell velocity approached 0µm/sec and aspect approached 1, cell angle measurements became unreliable and statistical analysis was therefore not performed on this measurement.

Target Receptor/ Mechanism of Action	Common Name	Concentration	Effect on *Dictyostelium*	Species	Dose Range	Reference
5-HT Receptor Agonist	5-hydroxytryptamine	1µM, 100µM	N	S	4-10mg/kg	(Torii et al., 1991; Javid and Naylor, 2002; Fujiwara-Sawada et al., 2003)
CNS depressant	Lithium chloride	10mM	N	R,S,H	50-200mg/kg	(Karniol et al., 1978; Seeley et al., 2000; Yamamoto et al., 2004)
Cytotoxic	5-Fluorouracil	250µM	N	F,R,S,H	35-100mg/kg	(Matsuki et al., 1988; Pollera et al., 1989; Yamamoto et al., 2007)
	Actinomycin D	10µM	N	D,R	0.13-0.25mg/kg	(Eglen et al., 1993; Yamamoto et al., 2007)
	Cisplatin	50µM, 300µM	N	F,D,R,S, H	3-20mg/kg	(Andrews et al., 1990; Fukui et al., 1993a; Knox et al., 1993; Eglen et al., 1993; Kris et al., 1996; Andrews et al., 2000b; Nakayama et al., 2004; Horn et al., 2004; Parker et al., 2009; Percie du Sert et al., 2010)
	Cycloheximide	5mM	N	F,D	20mg/kg	(Andrews et al., 1990)
	Methotrexate	50µM, 250µM	N	S,H	80mg/kg	(Matsuki et al., 1988; Pollera et al., 1989)
	Streptozotocin	1µM	N	H	14-17mg/kg	(Borison and McCarthy, 1983; Seymour, 1993; Carter et al., 1981)
	Vincristine	1µM	N	R	0.1-1mg/kg	(Yamamoto et al., 2007)
Dopamine Receptor Agonist	Apomorphine HCl	10µM, 1mM	N	F,D,R,H	0.1-10mg/kg	(Andrews et al., 1990; Eglen et al., 1993; Knox et al., 1993; Andrews et al., 2001; Nakayama et al., 2004; Horn et al., 2009; Osinski et al., 2005)
Enteroendocrine Cell Stimulant	Metformin	500µM, 10mM	N	H*	1-30µM	(Cubeddu et al., 1992; Hoffmann et al., 2003)
Extracellular Enzyme Inhibitor	Digoxin	1µM	N	C,H	0.2-0.6mg/kg	(Gold et al., 1952; Parsons and Summers, 1971)
Free Radical Generator	Pyrogallol	500µM, 10mM	N	S	128mg/kg	(Torii et al., 1994; Andrews et al., 2000a)
Ligand Gated Ion Channel Activator	Veratridine HCl	30µM, 500µM	N	D, C	0.02-0.25mg/kg	(Borison and Fairbanks, 1952; Swiss, 1952; Bobkov, 1964)
Gastric mucosal irritant	Copper Sulphate	0.16- 5mM	Y	F,D,R,S, H	5-120mg/kg	(Torii et al., 1991; Andrews and Bhandari, 1993; Kan et al., 2002; Araya et al., 2003; Nakayama et al., 2004; Yamamoto et al., 2004)

	Copper Chloride	1.6mM	Y			Based on concentration of copper sulphate: (Torii et al., 1991; Andrews and Bhandari, 1993; Kan et al., 2002; Araya et al., 2003; Nakayama et al., 2004; Yamamoto et al., 2004)
	Zinc Sulphate	1.6mM	N	1%	H	(Cushny, 1918; Gaddum, 1961)
Neurokinin Receptor Agonist	Substance P	1µM	N	D	0.03-0.2mg/kg	(Andrews and Rudd, 2004)
Nicotinic Receptor Agonist	Nicotine	6µM, 100µM	N	F,D,R,S,H	1.5-20mg/kg	(Laffan and Borison, 1957; Torii et al., 1991; Jorenby et al., 1995; Andrews et al., 1996; Andrews et al., 2000b; Saito et al., 2003; Yamamoto et al., 2004; Parker et al., 2009)
Opioid Receptor Agonist	Loperamide HCl	1µM, 100µM	N	F	0.5mg/kg	(Bhandari et al., 1992; Andrews and Bhandari, 1993; Nakayama et al., 2004)
PDEIV Inhibitor	Rolipram	10µM, 700µM	Y	F,D,R,S	0.5-10mg/kg	(Heaslip and Evans, 1995; Aoki et al., 2001; Hirose et al., 2007; Davis et al., 2009)
Prostaglandin	PGF2α	1µM, 100µM	N	F,S	1-13.5mg/kg	(Kan et al., 2002; Kan et al., 2003)
SSRI/Transmitter Uptake Inhibitor	Fluoxetine	6.5µM	N	S	60mg/kg	(Fujiwara-Sawada et al., 2003)
T2R Receptor ligand	Denatonium Benzoate	0.05-10mM	Y	R*, H*	0.01-10mM	(Sibert and Frude, 1991; Chen et al., 2006; Tordoff et al., 2008; Glendinning et al., 2008)
	Phenylthiourea	0.05-5mM	Y	H*	2-5mM	(Chen et al., 2006)
	Quinine HCl	0.05-1mM	Y	R*	0.0082-250mM	(Scott and Giza, 1987; Tordoff et al., 2008)
	Xanthohumol	0.05-0.15mM	N	NA	NA	(Miranda et al., 1999; Intelmann et al., 2009)
TRPV1 Receptor Agonist	Capsaicin	0.01-0.3mM	Y	S	0.04-0.4mg/kg	(Rudd and Wai, 2001; Smith et al., 2002)
	Resiniferatoxin	1µM, 10µM	N	S	0.1-1000µg/kg	(Andrews and Bhandari, 1993; Andrews et al., 1996; Andrews et al., 2000b; Cheng et al., 2005)

Table 3.1. Emetic or taste aversive compounds assessed for effects on *Dictyostelium* behaviour during motility. Compounds were grouped by target receptor/mechanism of action. Compound concentrations, used to test for acute effects on *Dictyostelium* motility, were derived from experiments in other species: F = Ferret; D = Dog; R = Rat; S = *Suncus murinus* [House musk shrew]; C = Cat; H = Human. N/A =Not applicable. Note that for *in vivo* experiments in the rat, the table refers to the dose at which pica was observed, for all other species it refers to the emetic dose. A significant effect on motility (defined as a significant change in cell velocity following acute treatment (see Figure 2-5)) is represented by Y (Yes), with no effect denoted N (No). * Caused conditioned taste aversion responses in the rat or data derived from *in vitro* studies.

3.4.1. Gastric mucosal irritants

Copper is a gastric irritant shown to cause emesis or conditioned taste aversion in the ferret, dog, rat, shrew, and nausea in humans at high concentrations (Torii et al., 1991; Andrews and Bhandari, 1993; Kan et al., 2003; Araya et al., 2003; Nakayama et al., 2004; Yamamoto et al., 2004). Zinc is another gastric mucosal irritant, shown to cause emesis in humans (Cushny, 1918; Gaddum, 1961). *Dictyostelium* cell motility was significantly decreased by the copper based salts copper sulphate and chloride but not zinc. In these assays, cell behaviour was constant over the first 5 minutes, where addition of copper salts caused a decrease in velocity and induced cell rounding. This is summarised in a series of phase contrast time lapse frames **(Figure 3.6)**.

Three independent repeats of this experiment, where cells were tracked and behaviour quantified illustrated a significant decrease in cell velocity, from 0.18±0.01µm/sec to 0.05±0.01µm/sec ($P<0.01$), and aspect, from 2.6±0.2 to 1.7±0.1 ($P<0.05$), upon addition of 5mM copper sulphate (**Figure 3.7A, B).** A loss of cell behaviour also correlated with a deviation in angularity towards zero **(Figure 3.7C)**. This rapid block in cell directionality and distance travelled caused by copper sulphate when compared *Dictyostelium* cells migrating under control conditions is represented in a cell image overlay plot (**Figure 3.7D)**.

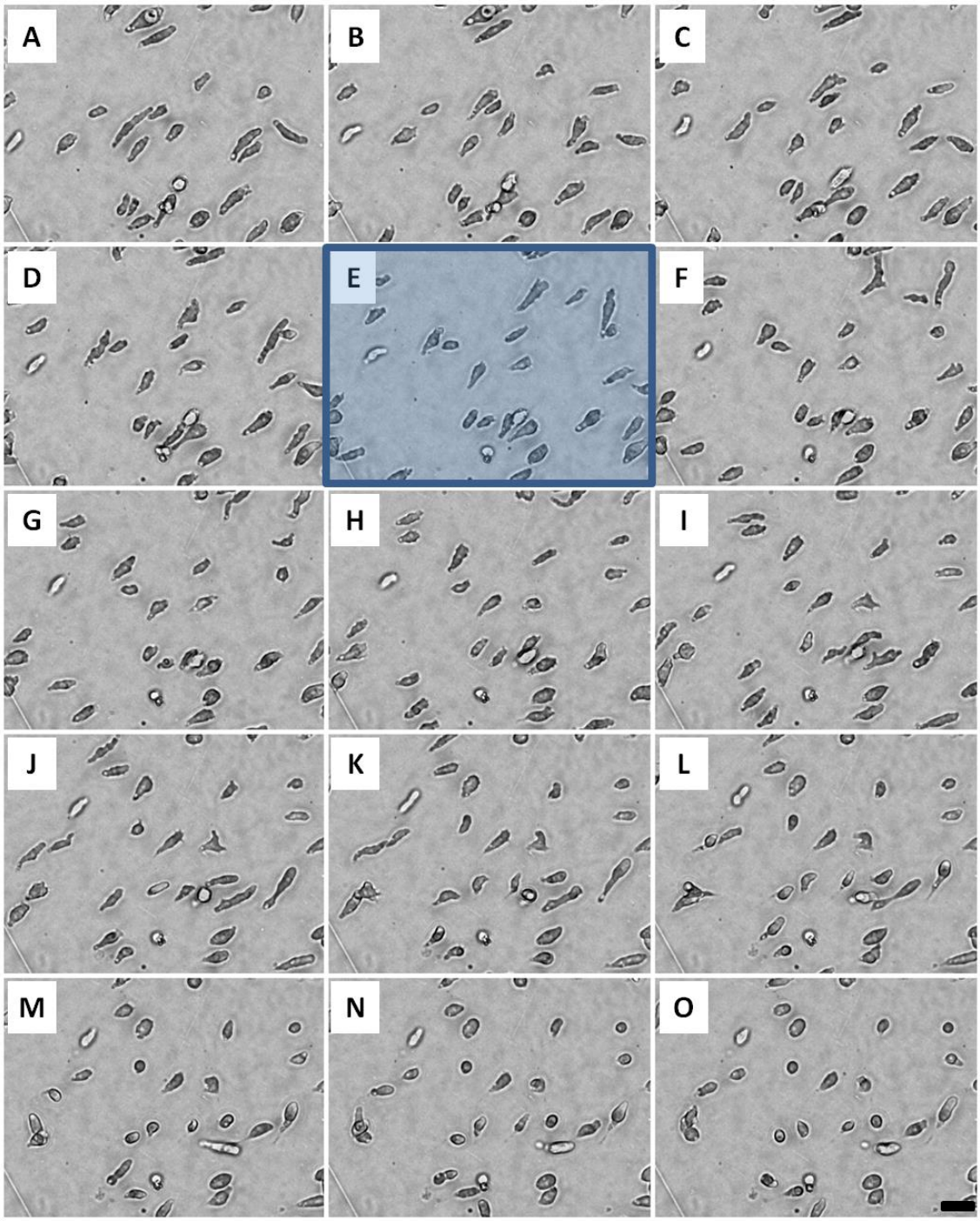

Figure 3.6. *Dictyostelium* cell motility with addition of 5mM copper sulphate after 300 seconds. Phase contrast images shown at 60 second intervals over 15 minutes under control conditions (**A-D).** After 300 seconds (**E),** (highlighted) 5mM copper sulphate was added to the outer well of the Dunn chamber and cell behaviour recorded over the remainder of the assay (**F-O**). Addition of copper sulphate caused a reduction in cell migration and a loss of cell shape. Each image represents images taken at 1 minute intervals. Bar = 20µm

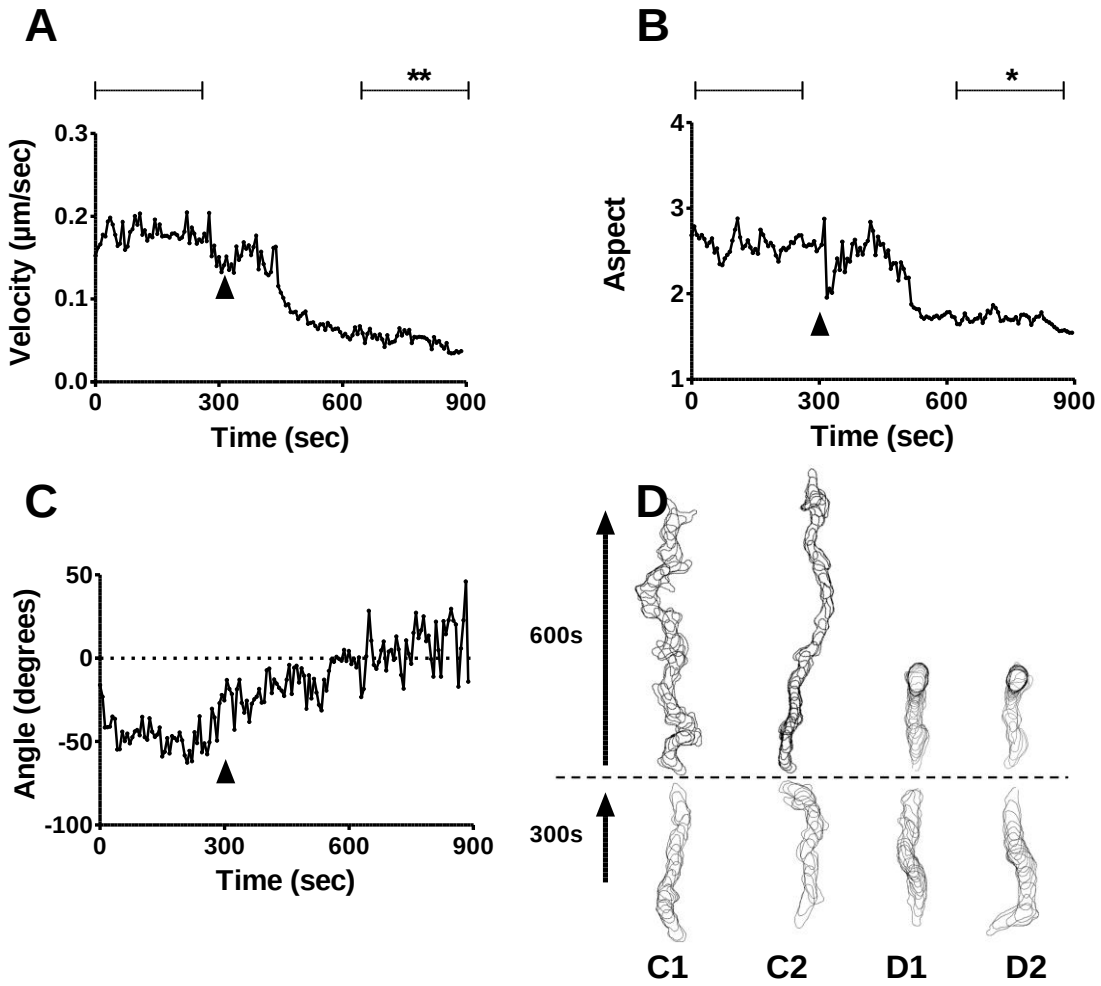

Figure 3.7. Analysis of *Dictyostelium* cell behaviour following active exposure to 5mM copper sulphate. Cell behaviour was measured under a stable chemotactic gradient in a Dunn chamber, with data from 124 cells quantified every 6 seconds over a 900 second period with the addition of 5mM copper sulphate at 300 seconds. **(A)** Cell velocity; **(B)** cell aspect; **(C)** cell angular movement; **(D)** cell directionality. Cell outlines of 2 representative cells from (C1-2) control experiments and (D1-2) copper sulphate were overlaid and split into the first 300 and final 600 second intervals. Overlay images have been adjusted so that the chemotactic gradient is following the marked arrows. Cell behaviour showed significant differences in velocity (P=0.0051) and aspect (P=0.0179) observed between the first and final 300 seconds of the assay. Data from A-C is presented as mean of triplicate experiments analysing a minimum of 30 cells in each. Statistical analyses were performed using paired two-tailed Student t-tests comparing average values from T=0-300 and T=600-900 seconds as indicated by the horizontal bars in panels A and B. * P<0.05, ** P<0.01.

To investigate concentration-related responses to copper sulphate, these experiments were repeated with a range of concentrations from 0.16-5mM. A significant inhibition of cell velocity was observed at 1.6mM and above; and 2.4mM and above for velocity and aspect respectively **(Table 3.2)**.

Compound	Concentration (mM)	Velocity (pre) (µm/sec)	Velocity (post) (µm/sec)	P-value (Velocity)	Aspect (pre)	Aspect (post)	P-Value (Aspect)
Copper Sulphate	0.16	0.22±0.03	0.21±0.02	ns	2.5±0.1	2.5±0.3	ns
	0.8	0.21±0.02	0.16±0.00	ns	3.2±0.2	2.9±0.3	ns
	1.2	0.17±0.01	0.14±0.04	ns	2.7±0.2	2.6±0.3	ns
	1.6	0.19±0.04	0.08±0.02	0.0319	2.5±0.0	1.9±0.3	ns
	2.4	0.17±0.02	0.03±0.01	0.0284	3.0±0.1	1.5±0.1	0.0111
	3.4	0.15±0.01	0.04±0.01	0.0069	3.1±0.2	1.8±0.5	ns
	5.0	0.18±0.01	0.05±0.01	0.0051	2.6±0.2	1.7±0.1	0.0179
Copper Chloride	1.6	0.24±0.03	0.08±0.03	0.0450	2.6±0.1	2.0±0.1	0.0163

Table 3.2. Copper-dependent effect of *Dictyostelium* cell behaviour (velocity and aspect). Concentration range of copper sulphate and copper chloride, showing a significant acute effect on *Dictyostelium* cell velocity and aspect between the first 300 (pre) and final 300 (post) seconds of the assay. Statistical analyses were performed using 2-tailed paired Student t-tests, where a minimum of 30 cells were measured in each of three replicates. ns = not significant.

In order to investigate the specificity for the inhibition of *Dictyostelium* motility for the metal cation copper, rather than sulphate, cells were also exposed to 1.6mM copper chloride. At this concentration, copper chloride caused a significant decrease in velocity, from 0.24±0.03µm/sec to 0.08±0.03µm/sec ($P<0.05$), and aspect, from 2.6±0.1 to 2.0±0.1 ($P<0.05$) **(Figure 3.8, Table 3.2)**.

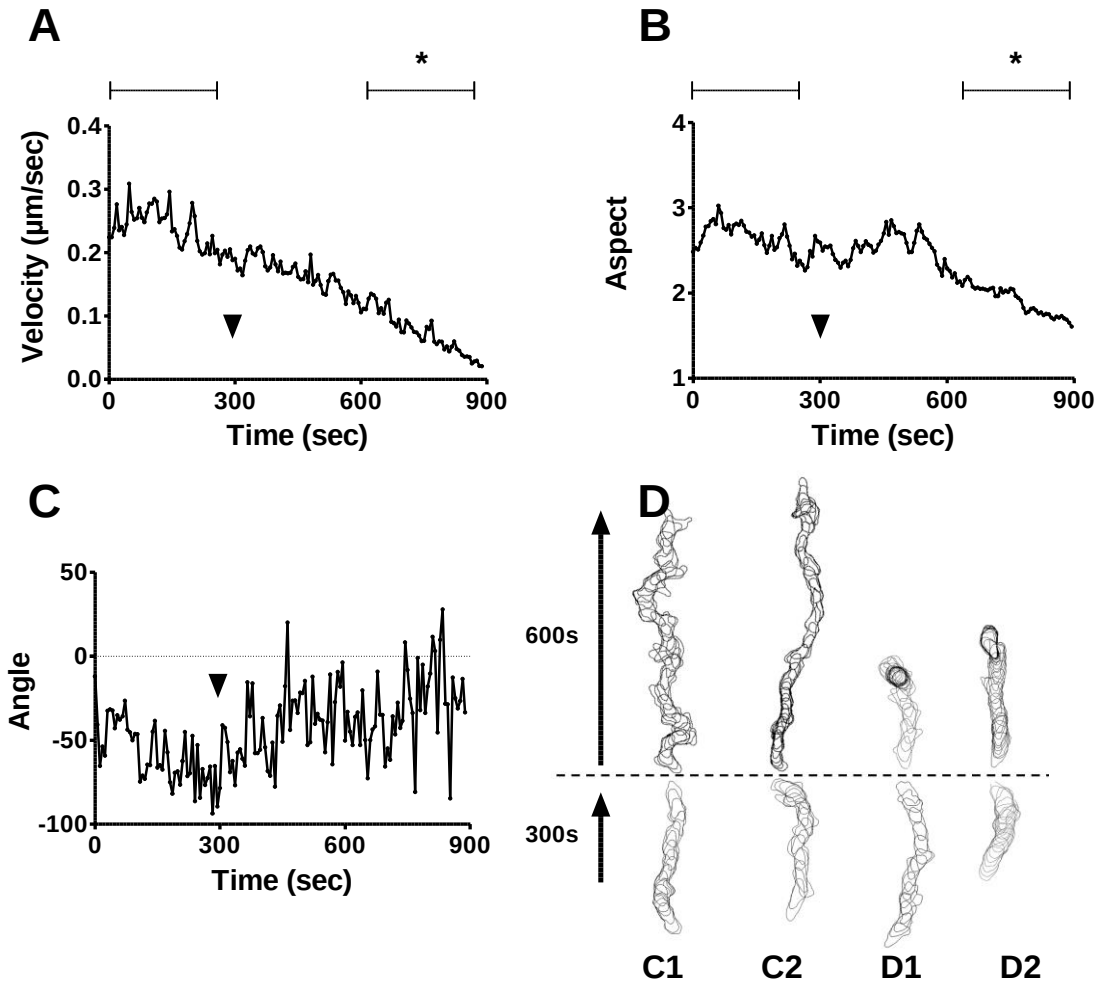

Figure 3.8. Analysis of *Dictyostelium* cell behaviour following active exposure to 1.6mM copper chloride. Cell behaviour was measured under a stable chemotactic gradient in a Dunn chamber, with data from 49 cells quantified every 6 seconds over a 900 second period with the addition of 5mM copper sulphate at 300 seconds. **(A)** cell velocity; **(B)** cell aspect; **(C)** cell angular movement; **(D)** cell directionality. Cell outlines of 2 representative cells from (C1-2) control experiments and (D1-2) copper sulphate were overlaid and split into the first 300 and final 600 second intervals. Overlay images have been adjusted so that the chemotactic gradient is following the marked arrows. Cell behaviour showed significant differences in velocity (P=0.0450) and aspect (P=0.0163) observed between the first and final 300 seconds of the assay. Data from A-C is presented as mean of triplicate experiments analysing a minimum of 15 cells in each. Statistical analyses were performed using paired two-tailed Student t-tests comparing average values from T=0-300 and T=600-900 seconds as indicated by the horizontal bars in panels A and B. * P<0.05

The dose dependency of copper on *Dictyostelium* chemotactic behaviour shown in **Table 3.2** was then analysed by plotting the total reduction in velocity when compared to initial control conditions. This was used to construct a concentration-response curve to measure the potency of *Dictyostelium* motility inhibition. It was shown that the inhibition of migration was concentration-dependent on copper sulphate concentration, with an IC_{50} value of 1433±3µM, R^2=0.54 based on a three parameter non-linear regression calculated in GraphPad prism (Materials and Methods) **(Figure 3.9).**

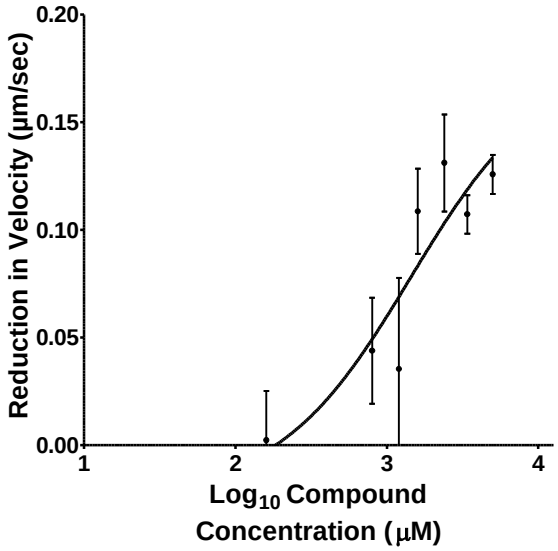

Figure 3.9. Concentration-dependent reduction of cell velocity for copper sulphate. Reduction in cell velocity compared to control conditions was plotted against log_{10} copper sulphate concentration (0.16-5mM). All data is presented as a mean ± S.E.M of triplicate experiments, comparing mean cell velocity during the first 5 minutes and final 5 minutes with increasing concentration.

3.4.2. TRPV1 Receptor Agonists

Capsaicin and its ultra-potent analogue resiniferatoxin were both analysed for their acute effects on *Dictyostelium* motility (**Table 3.1)**. Both capsaicin and resiniferatoxin are vanilloid compounds shown to cause emesis in *Suncus murinus* (Rudd and Wai, 2001; Smith et al., 2002; Andrews et al., 1996; Andrews et al., 2000b; Cheng et al., 2005). Capsaicin, the constituent responsible for the pungency in chillies, was shown to be a potent inhibitor of motility. At 300µM, capsaicin caused a rapid and strong reduction in cell velocity, from 0.16±0.01µm/sec to 0.03±0.00µm/sec ($P<0.01$), and aspect, from 2.4±0.1 to 1.7±0.1 ($P<0.05$) **(Figure 3.10A-B)**. In addition, angularity deviated towards 0 degrees and cell directionality was substantially reduced upon capsaicin exposure when compared to control conditions **(Figure 3.10C-D)**. Resiniferatoxin, did not cause any significant ($P<0.05$) changes in cell migration at 1µM or 10µM (higher concentrations could not be used due to a lack of solubility).

Dictyostelium behaviour was then recorded upon exposure to multiple concentrations of capsaicin, ranging from 10-300µM **(Table 3.3)**. In these experiments capsaicin evoked significant reductions in velocity and aspect above 50µM and 100µM respectively.

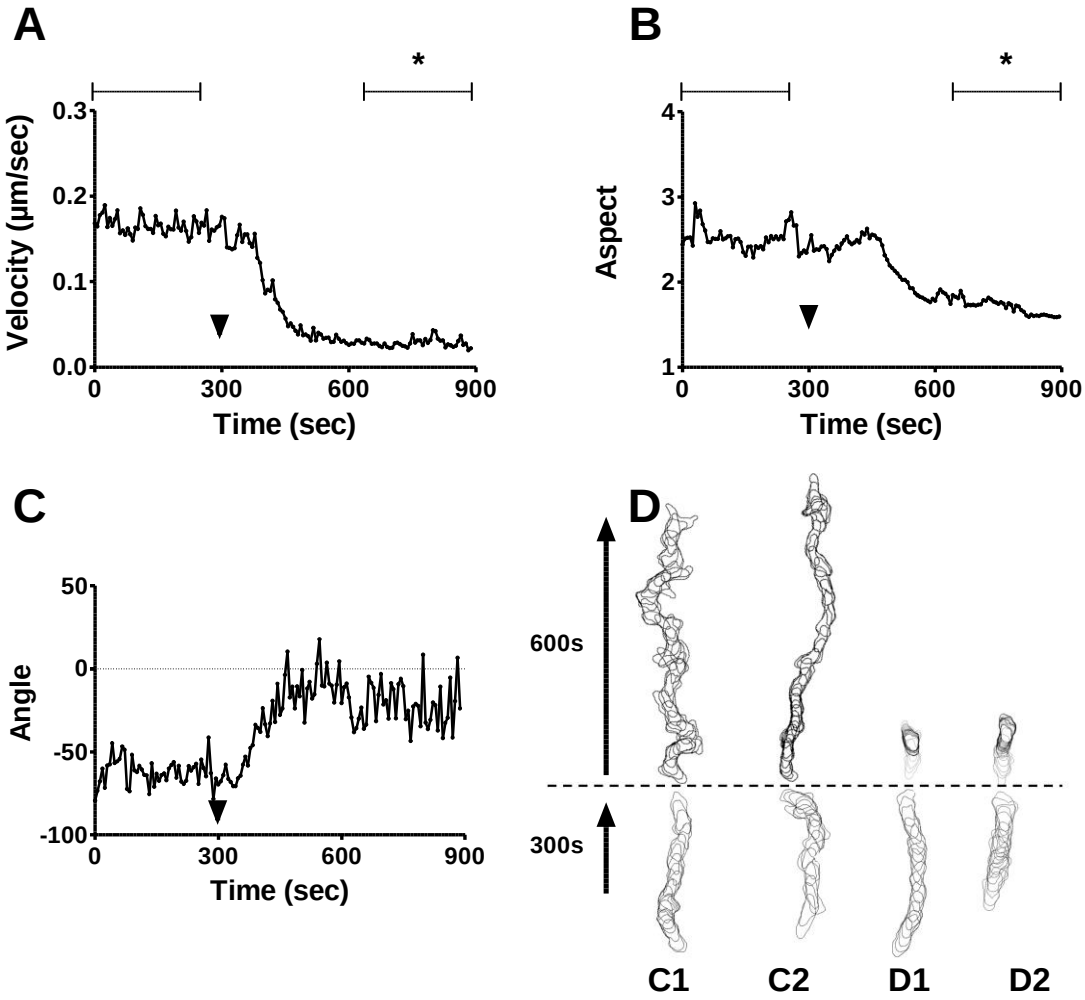

Figure 3.10. Analysis of *Dictyostelium* cell behaviour following active exposure to 300µM capsaicin. Cell behaviour was measured under a stable chemotactic gradient in a Dunn chamber, with data from 113 cells quantified every 6 seconds over a 900 second period with the addition of 5mM copper sulphate at 300 seconds. **(A)** Cell velocity; **(B)** cell aspect; **(C)** cell angular movement; **(D)** cell directionality. Cell outlines of 2 representative cells from (C1-2) control experiments and (D1-2) capsaicin were overlaid and split into the first 300 and final 600 second intervals. Overlay images have been adjusted so that the chemotactic gradient is following the marked arrows. Cell behaviour showed significant differences in velocity (P=0.0056) and aspect (P=0.0.0401) observed between the first and final 300 seconds of the assay. Data from A-C is presented as mean of triplicate experiments analysing approximately a minimum of 30 cells in each. Statistical analyses were performed using paired two-tailed Student t-tests comparing average values from T=0-300 and T=600-900 seconds as indicated by the horizontal bars in panels A and B. * P<0.05

Compound	Concentration (mM)	Velocity (pre) (µm/sec)	Velocity (post) (µm/sec)	P-value (Velocity)	Aspect (pre)	Aspect (post)	P-Value (Aspect)
Capsaicin	0.01	0.15±0.04	0.07±0.05	ns	2.4±0.1	2.3±0.1	ns
	0.05	0.20±0.01	0.10±0.01	0.0247	2.5±0.1	2.3±0.1	ns
	0.1	0.12±0.03	0.01±0.00	0.0407	2.5±0.2	1.8 ±0.1	0.0313
	0.2	0.18±0.00	0.04±0.00	0.0005	2.6±0.1	1.8±0.0	0.0321
	0.3	0.16±0.01	0.03±0.00	0.0056	2.4±0.1	1.7±0.1	0.0401

Table 3.3: Capsaicin-dependent effect of *Dictyostelium* cell behaviour (velocity and aspect). Concentration range of capsaicin showing a significant acute effect on *Dictyostelium* cell velocity and aspect between the first 300 (pre) and final 300 (post) seconds of the assay. Statistical analyses were performed using 2-tailed paired Student t-tests, where a minimum of 30 cells were measured in each of three replicates. ns = not significant.

The rate at which *Dictyostelium* cell velocity dropped was then assessed for the effect of capsaicin on cell behaviour to establish a concentration-response relationship. Capsaicin caused a concentration-dependent response, where increasing concentrations of capsaicin evoked decreases in cell velocity **(Figure 3.11).** Capsaicin was a potent inhibitor of *Dictyostelium* motility (IC_{50}=11.9±4.0µM, R^2=0.78).

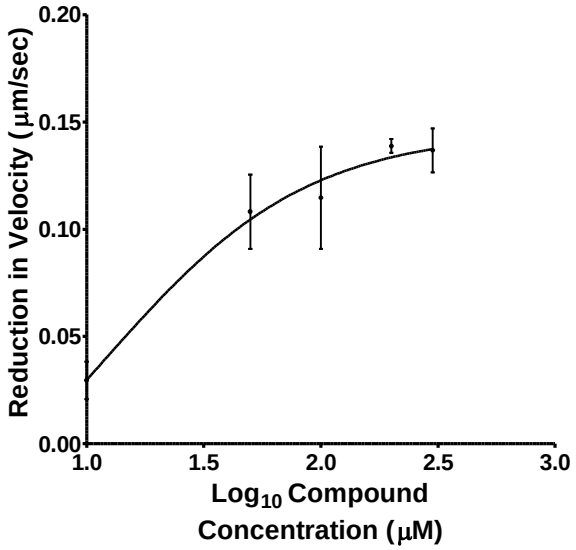

Figure 3.11. Concentration-dependent reduction of cell velocity for capsaicin. Reduction in cell velocity compared to control conditions was plotted against log_{10} capsaicin concentration (0.01-0.3mM). All data is presented as a mean ± S.E.M of triplicate experiments, comparing mean cell velocity during the first 5 minutes and final 5 minutes with increasing concentration.

3.4.3. T2R Receptor Agonists

Chemotaxing *Dictyostelium* cells were exposed to four compounds commonly used as examples of bitter tastants. These compounds cause taste aversion in rats as well as emetic episodes in humans at high concentrations, activating T2R receptors (Scott and Giza, 1987; Sibert and Frude, 1991; Chen et al., 2006; Tordoff et al., 2008; Glendinning et al., 2008). Denatonium benzoate, phenylthiourea and quinine hydrochloride all affected cell behaviour, causing significant reductions in cell velocity and aspect as well as reducing cell directionality at multiple concentrations. A final bitter tastant, xanthohumol had no effect on *Dictyostelium* motility. It is important to note, that whilst phenylthiourea, quinine hydrochloride and denatonium benzoate all contain nitrogenous and potentially alkaline structures, the presence of phosphate buffer should have neutralised any potential pH-specific effects that may occur as a result of tastant exposure to *Dictyostelium* cells.

Denatonium benzoate is a synthetic bitter tastant known to activate multiple mammalian T2R receptors (Meyerhof et al., 2010). Analysis of denatonium benzoate effects on *Dictyostelium* chemotactic behaviour showed that 5mM caused a sharp, significant reduction in cell velocity, from 0.15±0.01μm/sec to 0.05±0.01μm/sec ($P<0.05$), and aspect, from 3.2±0.2 to 1.9±0.1 ($P<0.01$) **(Figure 3.12A-B)**. Angularity also rapidly deviated towards 0 degrees and the overall reduction in cell movement is represented by the steep reduction cell directionality when compared to control conditions **(Figure 3.12C-D)**.

A second naturally occurring bitter tastant, phenylthiourea, is commonly known to activate the TAS2R38 receptor in humans, where polymorphisms in

the responsible gene have been shown to cause varying levels of sensitivity to the bitterness of the compound (Pronin et al., 2004; Bufe et al., 2005; Meyerhof et al., 2010). At a 5mM, phenylthiourea also caused significant, acute reductions in cell velocity, from 0.17±0.02µm/sec to 0.06±0.02µm/sec ($P<0.05$), and aspect, from 3.1±0.1 to 2.1±0.1 ($P<0.01$) **(Figure 3.13A-B)**. In addition, cell angularity deviated towards 0 and cell directionality was also reduced post exposure **(Figure 3.13C-D)**.

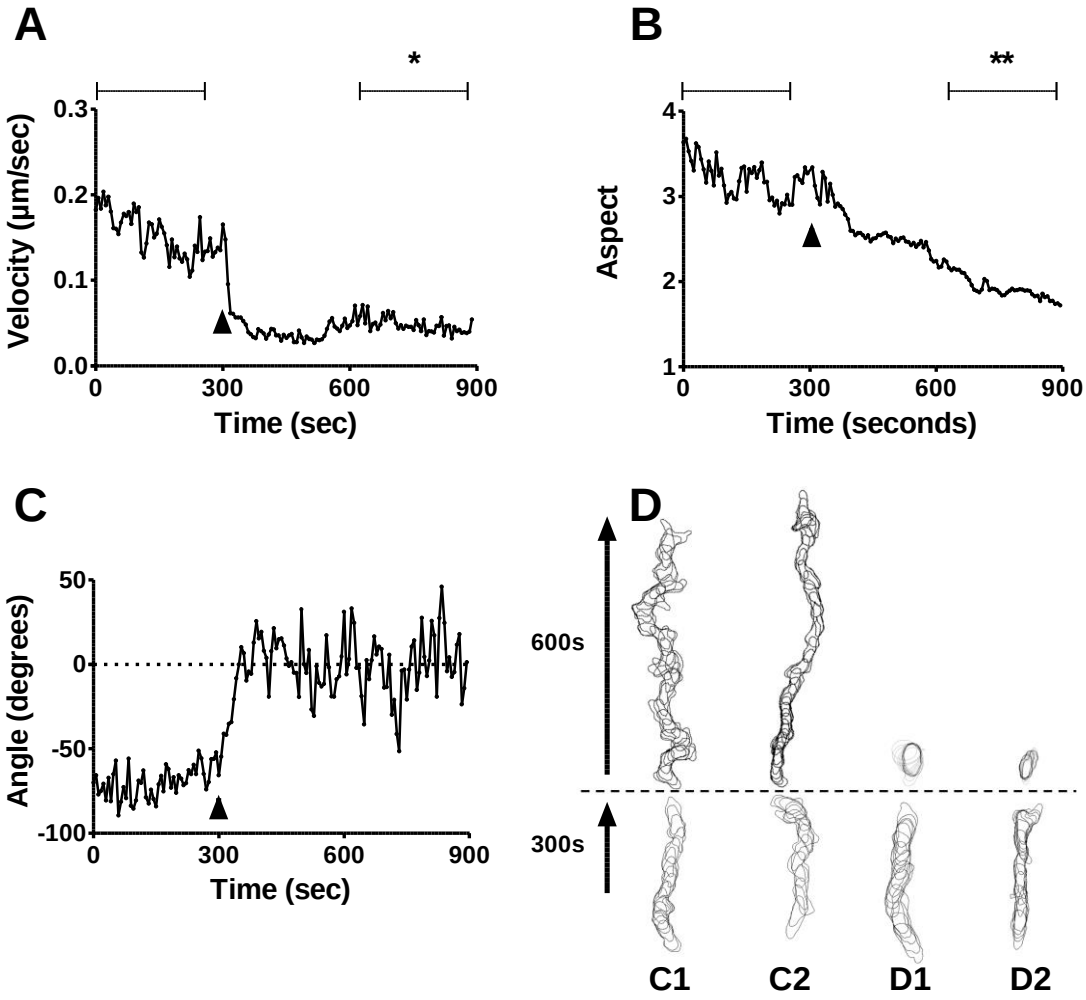

Figure 3.12. Analysis of *Dictyostelium* cell behaviour following active exposure to 5mM denatonium benzoate. Cell behaviour was measured under a stable chemotactic gradient in a Dunn chamber, with data from 89 cells quantified every 6 seconds over a 900 second period with the addition of 5mM denatonium benzoate at 300 seconds. **(A)** Cell velocity; **(B)** cell aspect; **(C)** cell angular movement; **(D)** cell directionality. Cell outlines of 2 representative cells from (C1-2) control experiments and (D1-2) denatonium benzoate were overlaid and split into the first 300 and final 600 second intervals. Overlay images have been adjusted so that the chemotactic gradient is following the marked arrows. Cell behaviour showed significant differences in velocity (P=0.0212) and aspect (P=0.0095) observed between the first and final 300 seconds of the assay. Data from A-C is presented as mean of triplicate experiments analysing a minimum of 25 cells in each. Statistical analyses were performed using paired two-tailed Student t-tests comparing average values from T=0-300 and T=600-900 seconds as indicated by the horizontal bars in panels A and B. * P<0.05, ** P<0.01.

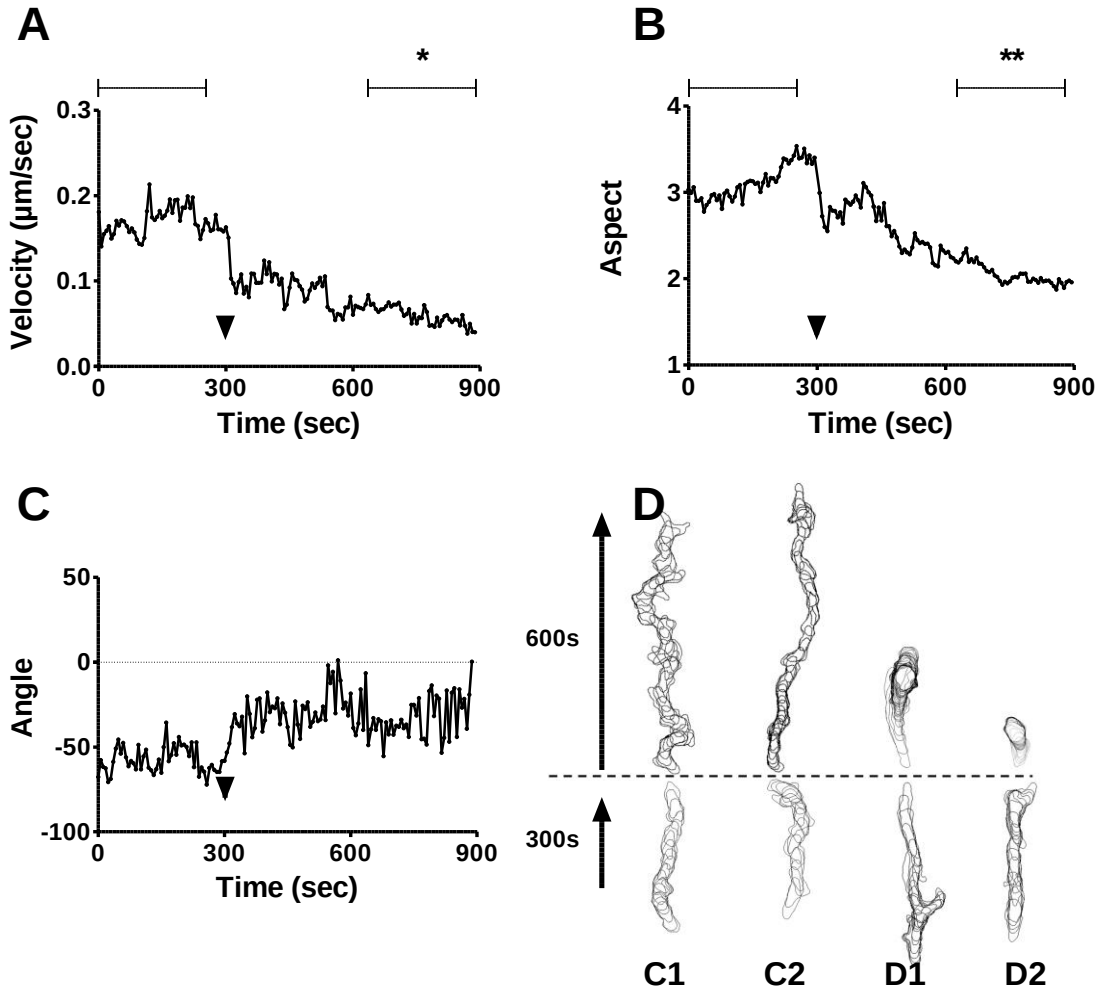

Figure 3.13. Analysis of *Dictyostelium* cell behaviour following active exposure to 5mM phenylthiourea. Cell behaviour was measured under a stable chemotactic gradient in a Dunn chamber, with data from 59 cells quantified every 6 seconds over a 900 second period with the addition of 5mM phenylthiourea at 300 seconds. **(A)** Cell velocity; **(B)** cell aspect; **(C)** cell angular movement; **(D)** cell directionality. Cell outlines of 2 representative cells from (C1-2) control experiments and (D1-2) copper sulphate were overlaid and split into the first 300 and final 600 second intervals. Overlay images have been adjusted so that the chemotactic gradient is following the marked arrows. Cell behaviour showed significant differences in velocity (P=0.0402) and aspect (P=0.0037) observed between the first and final 300 seconds of the assay. Data from A-C is presented as mean of triplicate experiments analysing a minimum of 19 cells in each. Statistical analyses were performed using paired two-tailed Student t-tests comparing average values from T=0-300 and T=600-900 seconds as indicated by the horizontal bars in panels A and B. * P<0.05, ** P<0.01

Quinine hydrochloride is another naturally occurring bitter tastant responsible for activating multiple T2R receptors (Meyerhof et al., 2010). At 0.5mM, quinine hydrochloride caused a significant decrease in *Dictyostelium* cell velocity, from 0.15±0.02µm/sec to 0.08±0.00µm/sec ($P<0.05$) **(Figure 3.14A)**. Interestingly, aspect was not affected, whilst cell angularity deviated towards 0 and cell directionality was predominantly reduced **(Figure 3.14B-D)**.

Since all three bitter tastants were shown to acutely block *Dictyostelium* motility, each compound was assayed at a range of concentrations to compare activities. Of the three T2R receptor ligands, quinine hydrochloride appeared to evoke the most potent response in *Dictyostelium* motility requiring just 0.1mM to cause a significant reduction in velocity **(Table 3.4)**. Interestingly, quinine hydrochloride did not appear to cause significant rounding of cells at any concentration within the range used in this report.

Denatonium benzoate was also a strong inhibitor of *Dictyostelium* motility where exposure to of 0.5mM and above caused significant reductions in both velocity and aspect **(Table 3.4)**. Finally, phenylthiourea was shown to be the weakest of the three bitter tastants at inhibiting *Dictyostelium* motility as a concentration of 1mM and above was required to significantly affect cell velocity and aspect.

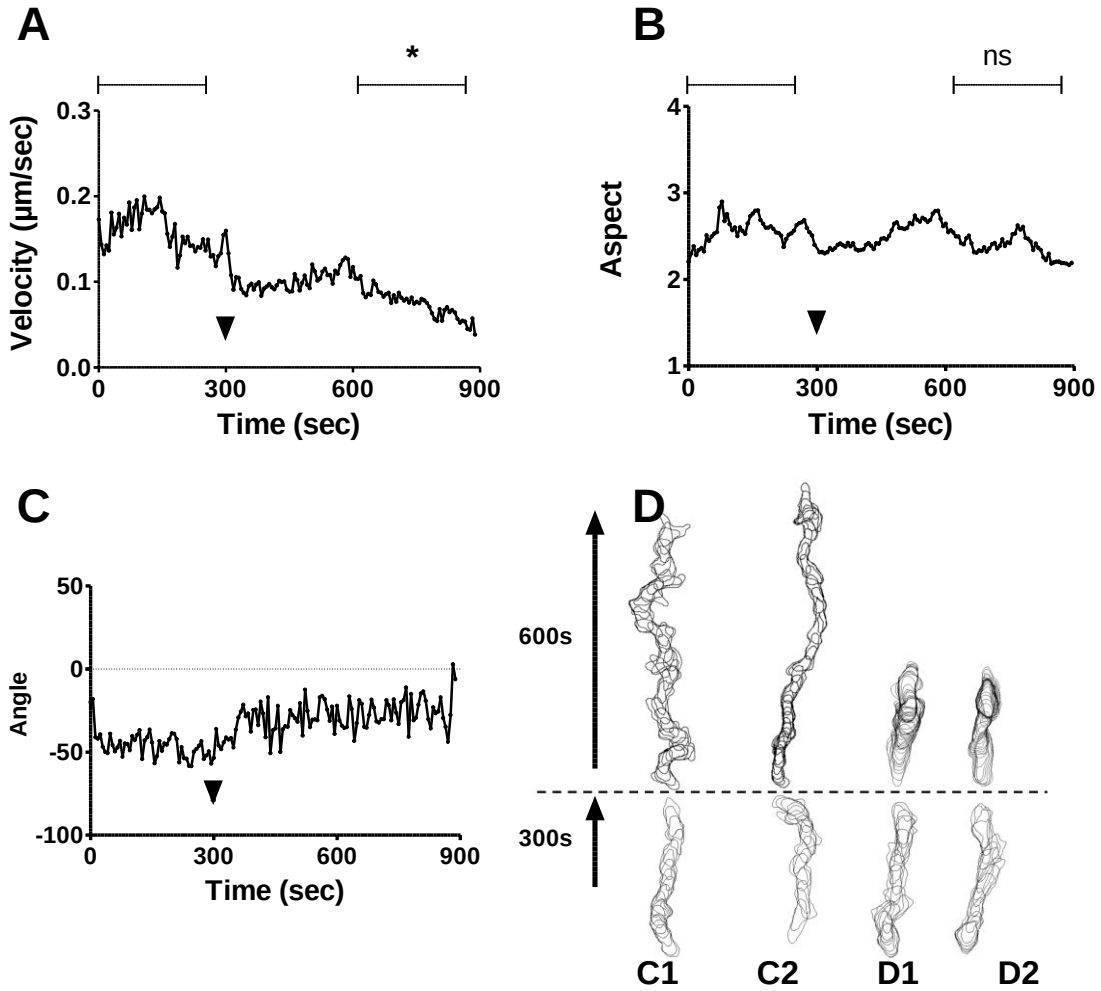

Figure 3.14. Analysis of *Dictyostelium* cell behaviour following active exposure to 0.5mM quinine hydrochloride. Cell behaviour was measured under a stable chemotactic gradient in a Dunn chamber, with data from 81 cells quantified every 6 seconds over a 900 second period with the addition of 0.5mM quinine hydrochloride at 300 seconds. **(A)** Cell velocity; **(B)** cell aspect; **(C)** cell angular movement; **(D)** cell directionality. Cell outlines of 2 representative cells from (C1-2) control experiments and (D1-2) quinine hydrochloride were overlaid and split into the first 300 and final 600 second intervals. Overlay images have been adjusted so that the chemotactic gradient is following the marked arrows. Cell behaviour showed a significant difference in velocity (P=0.0286) observed between the first and final 300 seconds of the assay. Data from A-C is presented as mean of triplicate experiments analysing a minimum of 25 cells in each. Statistical analyses were performed using paired two-tailed Student t-tests comparing average values from T=0-300 and T=600-900 seconds as indicated by the horizontal bars in panels A and B. ns = not significant, * P<0.05.

Compound	Concentration (mM)	Velocity (pre) (µm/sec)	Velocity (post) (µm/sec)	P-value (Velocity)	Aspect (pre)	Aspect (post)	P-Value (Aspect)
Denatonium Benzoate	0.05	0.21±0.02	0.19±0.02	ns	2.4±0.1	2.3±0.2	ns
	0.5	0.16±0.01	0.06±0.01	0.0151	3.1±0.2	2.1±0.2	0.0108
	1.0	0.17±0.03	0.04±0.00	0.0369	2.6±0.1	1.4±0.1	0.0185
	5.0	0.15±0.01	0.05±0.01	0.0212	3.2±0.2	1.9±0.1	0.0095
	10	0.22±0.00	0.07±0.01	0.0060	2.5±0.0	1.2±0.1	0.0040
Phenylthiourea	0.05	0.17±0.03	0.13±0.02	ns	3.1±.02	2. ±0.3	ns
	0.2	0.11±0.02	0.11±0.03	ns	2.5±0.2	2.5±0.4	ns
	0.5	0.18±0.02	0.15±0.01	ns	3.3±0.1	3.0±0.2	ns
	1.0	0.16±0.01	0.07±0.02	0.0239	3.4±0.3	2.4±0.1	0.0126
	2.0	0.15±0.00	0.08±0.01	0.0108	3.1±0.2	1.7±0.1	0.0142
	5.0	0.17±0.02	0.06±0.02	0.0402	3.1±0.1	2.1±0.1	0.0037
Quinine Hydrochloride	0.05	0.19±0.01	0.19±0.02	ns	2.9±0.4	2.7±0.3	ns
	0.1	0.10±0.01	0.06±0.01	0.0491	2.4±0.1	2.2±0.3	ns
	0.2	0.13±0.02	0.06±0.00	0.0332	2.6±0.3	2.2±0.1	ns
	0.5	0.15±0.02	0.08±0.00	0.0286	2.6±0.2	2.3±0.1	ns
	1.0	0.20±0.00	0.11±0.01	0.0353	2.5±0.1	2.1±0.2	ns

Table 3.4. Bitter tastant-dependent effect of *Dictyostelium* cell behaviour (velocity and aspect). Concentration range of denatonium benzoate, phenylthiourea and quinine hydrochloride showing a significant acute effect on *Dictyostelium* cell velocity and aspect between the first 300 (pre) and final 300 (post) seconds of the assay. Statistical analyses were performed using 2-tailed paired Student t-tests, where a minimum of 25 cells were measured in each of three replicates. Ns = not significant.

All three compounds were further analysed for their potency to inhibit *Dictyostelium* motility, where they showed a concentration-dependent relationship (**Figure 3.15)**. Subsequent IC_{50} calculations indicate the potency of inhibition was quinine hydrochloride (IC_{50}=44.3±6.8µM, R^2=0.61) > denatonium benzoate (IC_{50}=129±4µM, R^2=0.65) > phenylthiourea (IC_{50}=366±6µM, R^2=0.50).

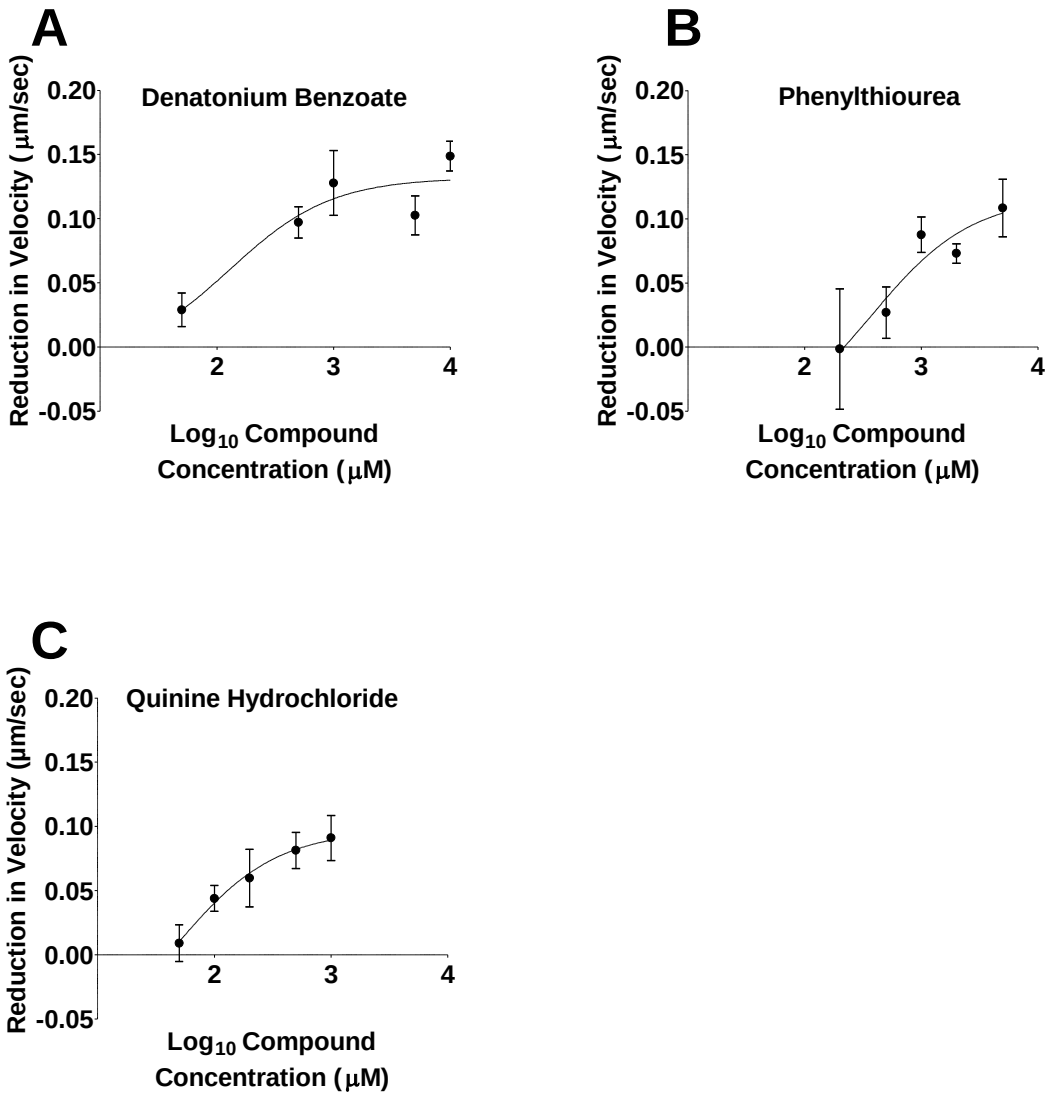

Figure 3.15. Concentration-dependent reduction of cell velocity for bitter tastants. Reduction in cell velocity compared to control conditions was plotted against log_{10} denatonium benzoate (0.05-10mM), phenylthiourea (0.2-5mM) and quinine hydrochloride (0.05-1mM) respectively. All data is presented as a mean ± S.E.M of triplicate experiments, comparing mean cell velocity during the first 5 minutes and final 5 minutes with increasing concentration.

3.4.4. Phosphodiesterase IV Inhibitors

Rolipram is a phosphodiesterase IV inhibitor, an anti-inflammatory agent used in the treatment of airway disorders such as asthma. The therapeutic compound has also been associated with emetic episodes in the ferret, dog, rat and *Suncus murinus* (Heaslip and Evans, 1995; Aoki et al., 2001; Hirose et al., 2007; Davis et al., 2009). *Dictyostelium* motility assays were performed at a concentration of 0.01mM and 0.7mM. No significant effects ($P>0.05$) were observed in any measurements between the first 5 minutes and final 5 minutes at 0.01mM concentration. However upon increasing the concentration, 0.7mM, rolipram evoked a significant reduction in cell velocity, from 0.16±0.01µm/sec to 0.02±0.01µm/sec, and aspect, from 2.5±0.2 to 1.7±0.2, as well as reducing cell directionality **(Figure 3.16)**.

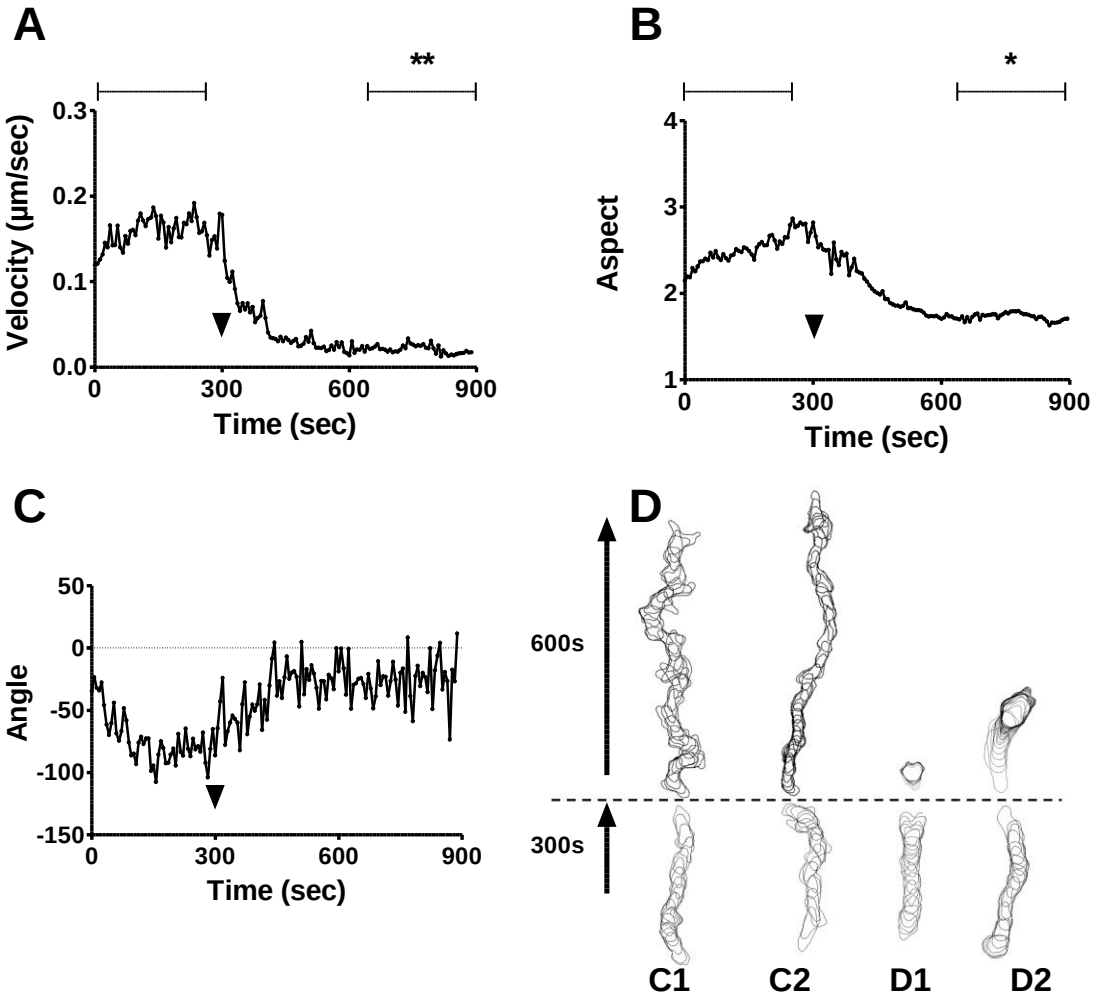

Figure 3.16. Analysis of *Dictyostelium* cell behaviour following active exposure to 0.7mM rolipram. Cell behaviour was measured under a stable chemotactic gradient in a Dunn chamber, with data from 82 cells quantified every 6 seconds over a 900 second period with the addition of 0.7mM rolipram at 300 seconds. **(A)** Cell velocity; **(B)** cell aspect; **(C)** cell angular movement; **(D)** cell directionality. Cell outlines of 2 representative cells from (C1-2) control experiments and (D1-2) rolipram were overlaid and split into the first 300 and final 600 second intervals. Overlay images have been adjusted so that the chemotactic gradient is following the marked arrows. Cell behaviour showed significant differences in velocity (P=0.0069) and aspect (P=0.0195) observed between the first and final 300 seconds of the assay. Data from A-C is presented as mean of triplicate experiments analysing a minimum of 25 cells in each. Statistical analyses were performed using paired two-tailed Student t-tests comparing average values from T=0-300 and T=600-900 seconds as indicated by the horizontal bars in panels A and B. * P<0.05, ** P<0.01.

3.4.5. Cytotoxic Compounds

Seven different cytotoxic compounds, 5-fluorouracil (250µM), actinomycin D (10µM, 700µM), cisplatin (50µM, 300µM), cycloheximide (5mM), methotrexate (50µM, 250µM), streptozotocin (1µM) and vincristine (1µM) were tested for acute effects on *Dictyostelium* behaviour during motility **(Table 3.1, Appendix 1)**. None of these compounds evoked any significant reductions in *Dictyostelium* cell velocity or aspect, or altered cell directionality in the incubation period used.

3.4.6. Receptor Agonists

Various receptor agonists were screened for their effects on *Dictyostelium* motility **(Table 3.1, Appendix 1)**. Apart from those previously identified (T2R receptor ligands and the TRPV1 receptor agonist, capsaicin) receptor agonists, 5-hydroxytryptamine (1µM, 100µM), apomorphine hydrochloride (10µM, 1mM), substance P (1µM), nicotine (6µM, 100µM), loperamide hydrochloride (1µM, 100µM); and the sodium channel activator veratridine hydrochloride (30µM, 500µM), did not cause any significant reductions in *Dictyostelium* cell velocity, aspect or angle of movement in the incubation period used.

3.4.7. Inhibitors

Apart from the significant behavioural effects observed with a high concentration of the phosphodiesterase inhibitor, rolipram; no other therapeutic targets affected *Dictyostelium* motility in the incubation period used **(Table 3.1, Appendix 1)**. These were the selective serotonin reuptake inhibitor (SSRI), fluoxetine (6.5µM), as well as the extracellular enzyme inhibitor, digoxin (1µM).

3.4.8. Free Radical Generator

Pyrogallol (500µM, 10mM), a generator of harmful free radicals did not affect *Dictyostelium* cell motility, where no significant changes to cell velocity, aspect or angle of movement occurred **(Table 3.1, Appendix 1)**.

3.4.9. Other compounds

The remaining three compounds reported in **Table 3.1** were the central nervous system depressant, lithium chloride (10mM); the enteroendocrine cell stimulant, metformin (500µM, 10mM) and the prostaglandin $PGF_{2\alpha}$ (1µM, 100µM) **(Appendix 1)**. All three compounds did not elicit any significant changes in *Dictyostelium* cell behaviour in the Dunn chamber motility assay.

3.5. Cell viability

An acute block in *Dictyostelium* motility caused by compounds could be due to a variety of mechanisms including cell toxicity or death. To determine whether the effect chemotactic inhibition of cells was caused by death, cell viability was assessed by using trypan blue staining (Materials and methods) after acute (10 minute) and prolonged (30 minute) exposure **(Table 3.5)**. Chemotactically-competent cells were treated with denatonium benzoate, phenylthiourea, quinine hydrochloride and capsaicin chosen at around at $8xIC_{50}$ concentrations, where a minimal increase in cell response was shown at increasing concentrations (i.e. maximum response) **(Figures 3.9, 3.11, 3.15)**.

Analysis of survival rates following bitter and hot tastant exposure showed some treatments reduced survival. All compounds apart from capsaicin caused a <5% drop in cell survival cells after 10 and 30 minute exposures. Capsaicin (100µM) caused a significant drop of approximately 50% in cell survival after 30 minutes.

Cell viability assays with capsaicin were repeated (50µM) producing only a 2% drop in cell survival.

Compound/ Exposure Time (Min)	Cell Count (alive)	S.E.M	Cell Count (dead)	S.E.M	Cell Total	Cell Viability (%Survival)	Significance
Control							
10	135	2.2	1	0.6	136	**99**	NA
30	135	4.3	0	0	135	**100**	NA
1mM DB							
10	181	16.5	7	0	188	**96**	ns
30	183	5.9	16	3.2	199	**92**	ns
350µM QHCl							
10	139	12.1	1	1	140	**99**	ns
30	146	2.59	3	1.2	150	**97**	ns
3mM PTU							
10	128	8.7	0	0	128	**100**	ns
30	119	7.1	4	0.9	123	**97**	ns
100µM Capsaicin							
10	87	1.5	83	7.7	170	**51**	*
30	74	4.1	57	1.8	131	**57**	**
50µM Capsaicin							
10	174	1.3	3	1.5	177	**98**	ns
30	150	8.9	3	0.8	153	**98**	ns

Table 3.5. *Dictyostelium* cell viability upon acute exposure to hot and bitter tastants. Chemotactically competent cells were treated with 1% DMSO in KK2 (control), 1mM denatonium benzoate (DB), 350µM quinine hydrochloride (QHCl), 3mM phenylthiourea (PTU), 100µM capsaicin or 50µM capsaicin and exposed for 10 and 30 minutes. Initial 10 minute exposures revealed a no significant decrease in live cells when compared to control conditions. After 30 minutes exposure, a significant decrease in live cells had occurred in 100µM capsaicin (difference in rank sum = 15.00) when compared to control conditions. Compound concentrations were based on 8x previously determined IC_{50} calculations. All experiments were performed in triplicate and statistical analyses performed were Kruskal-Wallis tests with a *Post-hoc* Dunns multiple comparison test. Kruskal-Wallis statistics were 15.32 (P=0.0091) and 14.91 (P=0.0108) for 10 minute and 30 minute measurements respectively. NA = not applicable, ns = not significant, * P<0.05, ** P<0.01.

3.6 Reversibility of Inhibition of Cell Movement

To investigate further the effects of bitter and hot tastants on *Dictyostelium* behaviour, an assay was developed to determine whether tastant-induced effects could be reversed upon aspiration of each compound. This was not possible using the Dunn chamber assay since the compound-containing medium could not be removed without severely affecting the cAMP gradient across the chamber. To overcome this, random cell movement of chemotactically competent cells was recorded in the absence of a cAMP gradient during random movement. Cell velocity was used to measure initial control conditions for 4.5 minutes. Cells were then exposed to each tastant at 8x IC_{50} concentration (as described previously) for 4.5 minutes, before the media was aspirated and replaced with fresh KK2. Cells were monitored for the remainder of the assay **(Figure 3.17)**.

Dictyostelium cells were capable of recovering following bitter and hot tastant exposure. Upon addition of each tastant, a significant ($P<0.05$) reduction in cell velocity was observed during random cell movement. After tastant aspiration and replacement with phosphate buffer, *Dictyostelium* cell behaviour recovered in all conditions. This assay also demonstrated that cell motility was affected in random cell movement in addition to cAMP-orientated motility.

Finally, to examine long-term exposure to tastants, *Dictyostelium* behaviour was monitored in development assays. In these experiments, cells were developed on a nitrocellulose membrane in the absence and presence of each tastant over 24 hours and fruiting body formation was observed at the concentrations used previously **(Figure 3.18)**.

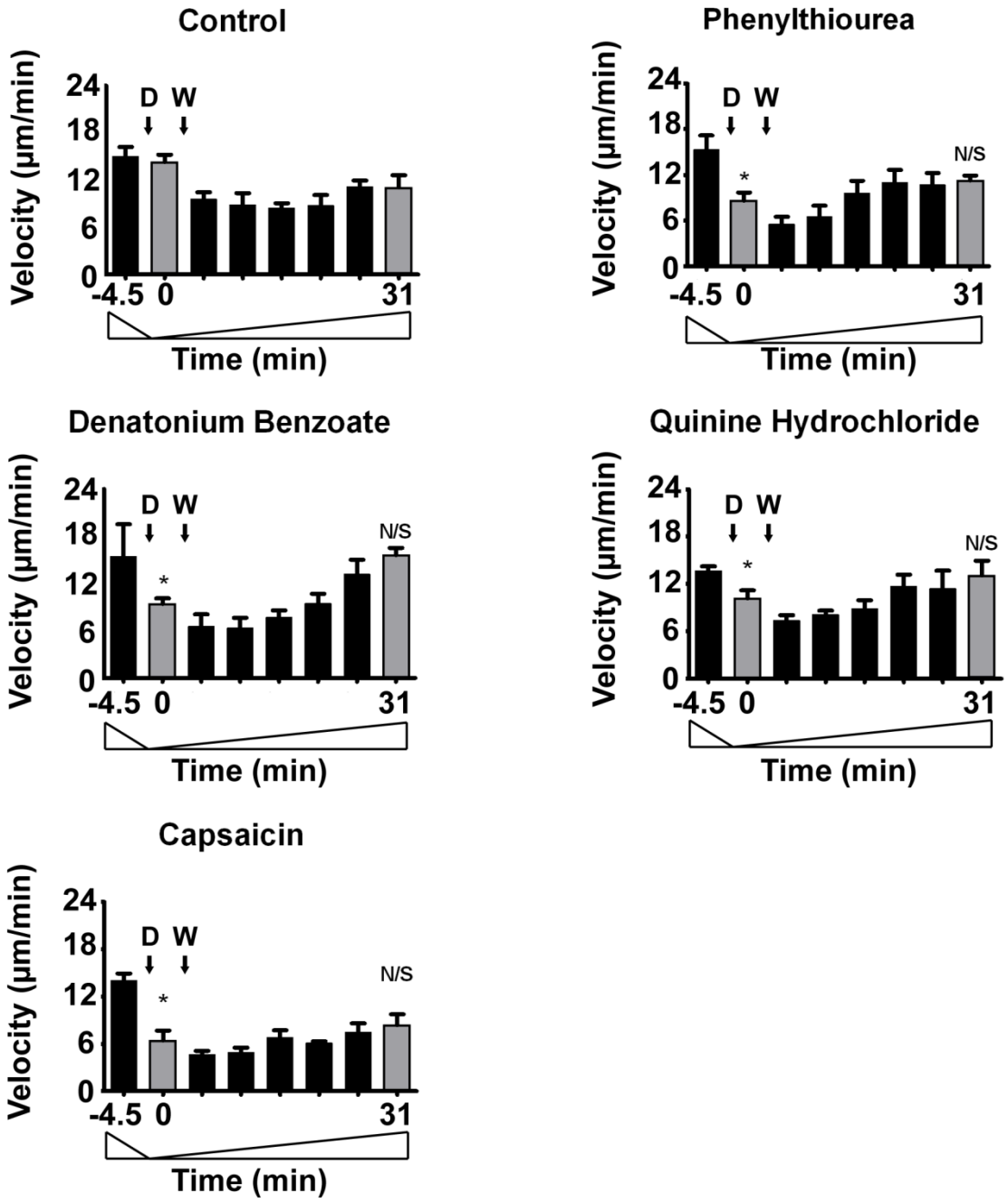

Figure 3.17. *Dictyostelium* cell behaviour reversibility following bitter and hot tastant exposure. Mean cell velocity during random cell movement over a 35 min period. Control conditions were established for an initial 4.5 minutes prior to addition of tastants (-4.5-0 minutes) and either phenylthiourea (3mM), denatonium benzoate (1mM), quinine hydrochloride (350µM) or capsaicin (50µM) added to the cells and monitored for a further 4.5 minutes (0-4.5 minutes) **(D)**. Media was then aspirated **(W)** and replaced with KK2 whereby cell behaviour was then monitored for a further 26 minutes. Initial cell velocity (-4.5min) was then compared to drug exposure (0) and the final time point (31) (highlighted by the grey bars). In all conditions, cell velocity was significantly reduced upon addition of tastants ($P<0.05$) and recovered by the end of the assay as there was no significant difference in cell velocity under control conditions and the final time point measured. Data is presented as a mean ± S.E.M for each 4.5 min period, with triplicate experiments analysing approximately 30 cells in each. N/S = not significant, * = $P<0.05$.

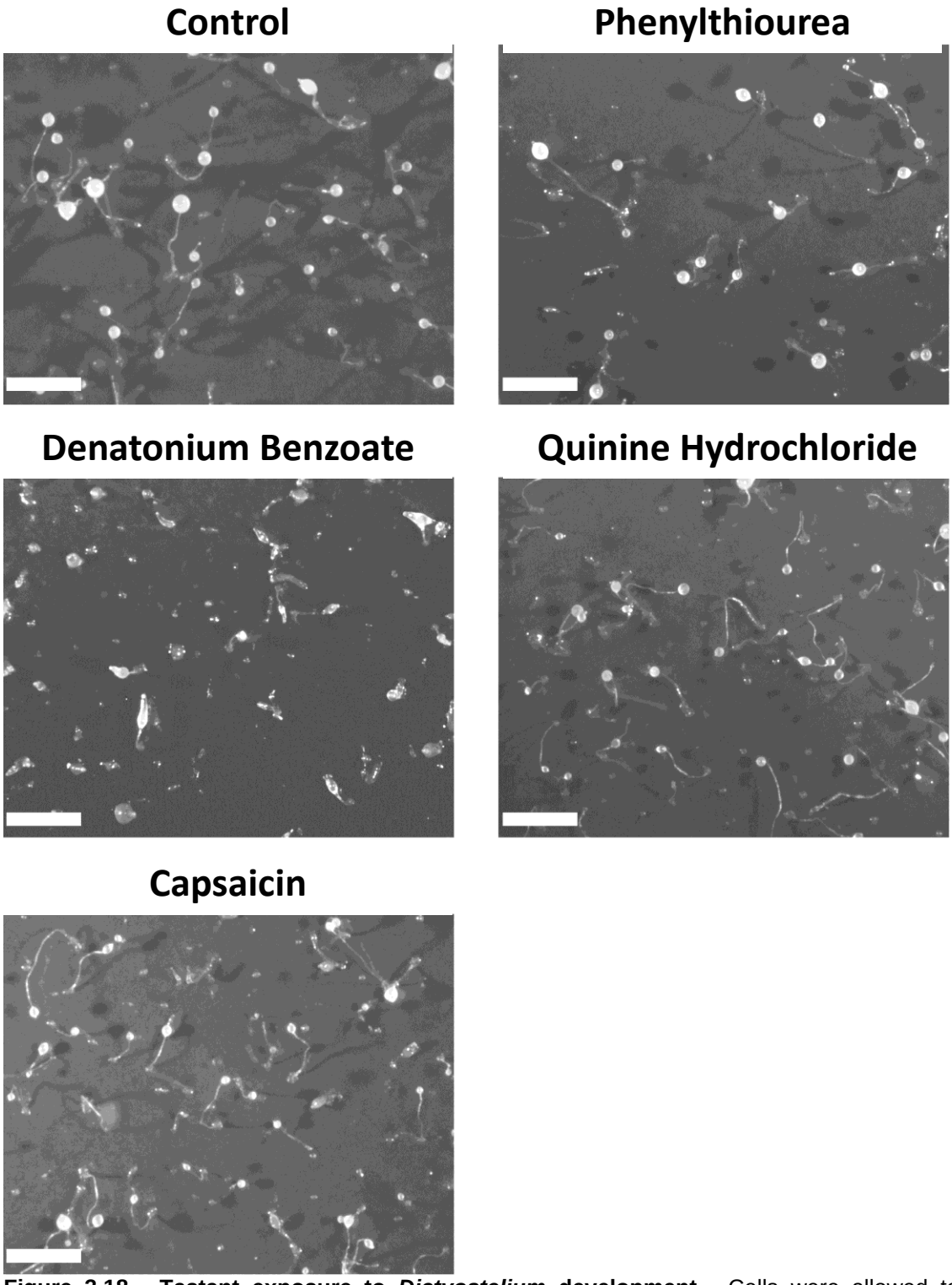

Figure 3.18. Tastant exposure to *Dictyostelium* development. Cells were allowed to develop over 24 hours on a nitrocellulose membrane in the presence of control conditions, phenylthiourea (3mM), denatonium benzoate (1mM), quinine hydrochloride (350µM) and capsaicin (100µM). *Dictyostelium* development was observed under all conditions, however when compared to control conditions, fruiting bodies appeared slightly smaller in size at concentrations exposed to quinine hydrochloride. Under denatonium benzoate conditions, development only appeared to reach the mound and culmination phases. All images are representative of triplicate experiments indicating cell survival after 24-hours exposure to each compound. Scale bar represents 1mm.

Exposure of developing *Dictyostelium* cells to bitter and hot tastants at concentrations shown to block behaviour did not grossly affect development. Development assays indicated that 24-hour exposure to each compound allowed for maturation to occur where the stalk and fruiting body structures remained intact. In addition, abnormal development was observed under denatonium benzoate conditions, where immature fruiting bodies were shown. 48-hour exposure to denatonium benzoate allowed the development of normal fruiting bodies when compared to control conditions. These results suggest that denatonium benzoate may interfere with *Dictyostelium* development by delaying the rate of development; however no long term toxicity occurred as fruiting bodies developed normally after 48 hours.

3.7. Discussion

To assess the suitability of using *Dictyostelium* in acute exposure experiments for predicting emetic liability, 29 emetic or taste aversive compounds were examined. Compounds were selected from each major class of emesis-inducing chemical group. Each compound was screened for any acute effects on *Dictyostelium* behaviour over a ten minute period. Of the 29 compounds screened, seven blocked *Dictyostelium* motility by reducing cell velocity and inducing cell rounding. These seven compounds could be divided into four distinct categories, which included copper containing compounds **(Figures 3.7, 3.8)**, a TRPV1 receptor agonist (capsaicin) **(Figure 3.10)**, three T2R receptor ligands (denatonium benzoate **(Figure 3.12)**, phenylthiourea **(Figure 3.13)** and quinine **(Figure 3.14)**, as well as the phosphodiesterase IV inhibitor, rolipram **(Figure 3.16)**. Compounds were also shown to function in a concentration-dependent manner, enabling IC_{50} values to be approximated

(Figures 3.9, 3.11, 3.15). The potency of the compounds was ranked capsaicin (IC_{50}=11.9±4.0μM) > quinine hydrochloride (IC_{50}=44.3±6.8μM) > denatonium benzoate (IC_{50}=129±4μM) > phenylthiourea (IC_{50}=366±5μM) > copper sulphate (IC_{50}=1433±3μM). The low R^2 values for these calculations were derived from a three-parameter non-linear regression, suggesting that the IC_{50} values are not entirely accurate and should be used for approximation only. The concentration-dependent inhibition of *Dictyostelium* cell behaviour does however suggest a possible role for direct activation or inhibition of cell surface receptors, which would allow for greater inhibition of cell movement with higher compound concentration.

3.7.2. Compounds and screening

The concentrations of emetic or aversive compounds used in this study were based upon previous *in vivo* and *in vitro* experiments **(Table 3.1)**. Compound concentrations shown to block *Dictyostelium* motility fall within these previously reported ranges in other biomedical models, indicating this amoeboid assay may be as sensitive as others at detecting targets. For example, mouse STC-1 cells have been shown to respond to 1-20mM denatonium benzoate, which falls well within the 0.1-10mM concentration range used in this study (Masuho et al. 2005; Chen et al, 2006). The tastant capsaicin has also been used in human based taste experiments at a concentration of 300μM, at which *Dictyostelium* motility is strongly inhibited (Green and Hayes, 2003).

3.7.3. Gastric Mucosal Irritants

In humans, copper containing compounds are responsible for gastrointestinal upsets, including nausea and vomiting at higher concentrations (Araya et al., 2001; Araya et al., 2003). This has led to the formation of guidelines to the concentration of copper found in drinking water of 4mg/L (Araya et al., 2001; Kayashima et al., 1978b; Kayashima et al., 1978a; Niijima et al., 1987; Makale and King, 1992; Araya et al., 2003). The chloride and sulphate salts of copper caused a significant concentration-dependent block in *Dictyostelium* behaviour suggesting copper and not its salts inhibit motility **(Figure 3.7, 3.8, 3.9)**.

In mammalian systems, research at the beginning of the 20th century suggested the gastro-duodenal luminal concentration of copper was a vital inducing factor in emesis (Cushny, 1918); however the specific molecular mechanisms underlying copper-induced emesis in mammalian systems remains unclear. Gastric perfusion studies have shown that copper may trigger a gut-mucosal emetic response by stimulating vagal afferents neurones (Niijima et al., 1987).

The mechanism of action behind the copper-mediated block in *Dictyostelium* motility remains unknown; however, the amoeba has been shown to express a degree of resistance to copper due to high cellular export (Burlando et al. 2002). The molecular mechanism behind this may be the potential inhibition of ATP ion currents, controlled by cell surface cation P2X receptors, which subsequently affect calcium influx (Burlando et al., 2002; Bavan et al., 2009; Ludlow et al., 2009). The concentration-dependent effects of copper may provide a useful indicator for the identification of high copper

concentrations in polluted water (Araya et al., 2003; Blaise et al., 2008). The sensitivity of *Dictyostelium* to copper would however not be sufficient to determine a raised copper level in drinking water based upon a 4mg/L (0.062mM) threshold concentration (Araya et al., 2001).

The closely related metal, zinc, which has also been associated with emesis, did not affect *Dictyostelium* motility (Cushny, 1918, Gadum 1961). Zinc sulphate was however only studied at one concentration in this thesis so it remains to be determined whether zinc would affect *Dictyostelium* motility at higher concentrations.

3.7.4. TRPV1 Receptor Agonists

Capsaicin is the active compound associated with the burning sensation found in chillies and other spicy foods. This vanilloid is shown to be an agonist for the transient potential receptor vanilloid 1 (TRPV1) receptor, responsible for burning sensations associated with taste and pain (Szolcsanyi, 2004). Activation of this receptor has also been shown to cause emesis through the release of endogenous substance P (Smith et al., 2002). In addition, capsaicin and some of its related vanilloids evoke a bitter sensation when in contact with the taste buds on the tongue (Green and Hayes, 2003). Addition of capsaicin to the Dunn chamber in *Dictyostelium* motility screens caused a strong and potent concentration dependent block in cell behaviour **(Figure 3.10, 3.11)**.

In *Suncus murinus*, capsaicin induces emesis at concentrations as low as 10nM when injected intracerebroventricuarly, where it has been suggested to act via the nucleus tractus solitarius (Andrews et al., 2000b; Rudd and Wai, 2001). Mammalian sensitivity to capsaicin within the brain is therefore 5000-fold more sensitive than concentrations reported to block *Dictyostelium*

behaviour in these studies. Concentrations used in these studies have however been applied directly at the site of action, and therefore may not be representative of an emetic threshold for conventional methods of capsaicin administration in humans.

TRPV1 channels belong to the transient receptor potential (TRP) superfamily of receptors, a group of calcium permeable channels located both on the cell membrane as well as within a cell (Dong et al., 2010). These receptors are located throughout the body (Pingle et al., 2007) and are conserved across mammalian species such as *Suncus murinus* (Andrews and Bhandari, 1993; Andrews et al., 2000b) as well as in *Caenorhabditis elegans.* Homology searches of the *Dictyostelium* proteome however did not identify any human homologues (Ezak et al., 2010) of the TRPV1-6 proteins nor the *C. elegans* candidates (OSM-9, OCR-2) **(Appendix 2)**.

Five other sub-families of TRP receptor also exist in mammalian systems: canonical, melastatin, mucolipin, polycystin and ankryin receptors. The *Dictyostelium* genome encodes a Polycystin-2 and a mucolipin channel (Wilczynska et al., 2005), although these channels have not been shown to be affected by capsaicin. This suggests an alternative molecular target for capsaicin in *Dictyostelium* may be responsible for the block in cell motility. Identification of this mechanism may provide further insight into the action of emetic and pain responses as well describing the sensory pathway for pungent compounds.

Other structurally related vanilloid compounds piperine and olvanil were also tested in the motility assay. Piperine is used at concentrations ranging from 0.1mM in HEK293 cell lines showing intracellular calcium release (Correa

et al., 2010), to 70mM in human taste sensation studies (Green and Hayes, 2003). Olvanil has potential anti-emetic effects at concentrations ranging from 0.05mg/kg to 5mg/kg in the ferret (Chu et al., 2010a; Chu et al., 2010b). *Dictyostelium motility* assays using Dunn chamber was also performed with application of olvanil and piperine, however due to the highly insoluble nature of these compounds, the assay was only performed at low concentrations (100µM olvanil, 500µM piperine), which were not sufficient to elicit any responses.

Surprisingly, the emetic and the ultra-potent analogue of capsaicin, resiniferatoxin, did not affect *Dictyostelium* motility at 1-10µM. Like capsaicin, resiniferatoxin is also an agonist of the TRPV1 receptor, containing a homovanillic acid group, which has been proposed to be a key structure in the activation of the TRPV1 channel (Szallasi, 1994). Whilst resiniferatoxin is substantially more potent at causing TRPV1 desensitization than capsaicin, it causes substantially less irritation than capsaicin at therapeutic concentrations (Kissin and Szallasi, 2011). A differential response to the two vanilloids could therefore be explained by the irritability caused by capsaicin that is not caused by resiniferatoxin, or by a non-TRPV1 target, regulated by capsaicin and not resiniferatoxin. Structure activity relationship studies have also shown that resiniferatoxin, capsaicin and their analogues can have varying effects on different types of TRPV1 receptor (Tomohiro et al., 2013; Czikora et al., 2012). This suggests a possible alternative theory, where a TRPV1 receptor of low amino acid homology to known receptors, is sensitive to variations in structures between capsaicin and resiniferatoxin.

3.7.5. T2R Receptor Agonists

Most bitter tasting compounds are ligands of the human taste type 2 (T2R) receptor, a family of G-protein coupled receptors shown to exist in humans since a pre-Neanderthal age, as a mechanism for identifying potentially toxic substances (Hilliard et al., 2004; Shi and Zhang, 2006; McBride et al., 2007; Oike et al., 2007; Tordoff et al., 2008; Lalueza-Fox et al., 2009b; Ezak et al., 2010; Isono and Morita, 2010). In humans, 25 of these T2R receptors have been identified where different bitter tastants can bind to one or a combination of receptors (Meyerhof et al., 2010). In addition to mammals, many organisms also avoid or show aversive behaviour towards bitter tasting compounds, ranging from fish (Oike et al., 2007), to the fruit fly *Drosophila* (McBride et al., 2007) and the nematode worm *C. elegans* (Hilliard et al., 2004). Three bitter tasting T2R receptor agonists, denatonium benzoate, quinine hydrochloride and phenylthiourea, all caused significant blocks in *Dictyostelium* motility **(Figures 3.12, 3.13, 3.14)**. In addition, the concentration-dependent block in *Dictyostelium* motility observed for the three reported compounds suggests a mechanism for detection of bitter compounds **(Figure 3.15)**.

In humans, it has been proposed that a key T2R receptor, human TAS2R38 is predominantly responsible for how and what humans perceive as bitter tasting (Kim et al., 2003). Single nucleotide polymorphisms in the *TAS2R38* gene results in different phenotypic responses to certain bitter tasting compounds such as phenylthiourea (also known as phenylthiocarbamide) and its structurally related analogue, propylthiouracil, resulting in supertaster, taster and non-taster status (Kim et al., 2003; Hayes et al., 2008; Bufe et al., 2005). Another receptor ligand of the TAS2R38 receptor also includes denatonium benzoate, suggesting a potentially parallel mechanism of action for these two

tastants (Meyerhof et al. 2010). In addition, quinine hydrochloride, which blocked *Dictyostelium* motility but did not induce cell rounding, does not activate this receptor (Meyerhof et al. 2010).

Of the 25 different genes encoding T2R receptor ligands in humans, no homologues were found within the *Dictyostelium* proteome suggesting an alternative mechanism of action for the recognition of bitter tasting compounds. In addition, no homologues were found for bitter-sensing receptors that exist in either the mammal (e.g. TA2R102); zebra fish, *Danio rerio* (e.g. T2R200.1), or the fly, *D. melanogaster* (GR47A), or the nematode worm, *C. elegans* (QUI-1) were found **(Appendix 3)**. Identifying the molecular targets for these compounds may therefore provide a novel signalling mechanism for the detection of bitter tasting compounds. Significantly, the multiple organisms described above have developed their own receptors responsible for bitter tastant detection and therefore *Dictyostelium* may also have its own. Subsequent downstream signalling pathways resulting from receptor activation may however be conserved across some species, which may provide valuable insight into molecular signalling pathways involved in bitter tastant detection.

In humans, T2R receptor signalling is also regulated by a receptor belonging to TRP superfamily, TRPM5, suggesting that both bitter and pungent compounds may share a common signalling pathway (Liman, 2007; Talavera et al., 2008). Analysis of the *Dictyostelium* proteome again did not identify any potential homologues **(Appendix 4)**. Since neither T2R, nor TRPM5 receptor homologues can be found in *Dictyostelium*, it is likely that other molecular targets are responsible for the effect of these compounds.

Another interesting observation was that the bitter tastant, xanthohumol (Tabata et al., 1997; Miranda et al., 1999) did not generate a significant block in *Dictyostelium* motility **(Table 3.1)**. In addition, the cytotoxic compound, cycloheximide, which is also a T2R receptor ligand, did not inhibit *Dictyostelium* motility **(Table 3.1).** Interestingly, the nematode worm, *C. Elegans* will migrate in the presence of cycloheximide, but not quinine hydrochloride (Tajima et al., 2001), which has also been confirmed in the *Dictyostelium* motility assay reported in this study**.**

A final group of compounds not reported here are the bitter tastant curcumin and its derivatives, which are not believed to be T2R receptor agonists (Meyerhof et al. 2010). Upon addition to randomly migrating *Dictyostelium* cells, curcumin also caused an acute block in cell behaviour **(Appendix 5)**. In addition, a colleague within the laboratory screened a number of curcumin derivatives, where *Dictyostelium* correctly distinguished between a highly emetic and a non-emetic analogue based upon the inhibition of cell movement (James Snyder, Emory University, personal communication). This data therefore identifies the potential utility for using *Dictyostelium* in structure-activity relationship and translational studies.

3.7.6. Phosphodiesterase IV Inhibitors

Rolipram, a phosphodiesterase IV inhibitor, is an anti-inflammatory agent that causes nausea and vomiting as a side effect (Aoki et al., 2001). At a low concentration (10µM), rolipram did not exert an effect on *Dictyostelium* cells, but blocked cell movement at higher concentrations (700µM) **(Figure 3.16)**.

In *Dictyostelium*, phosphodiesterases have three distinct roles in the dephosphorylation of cyclic nucleotides, which include extra- and intracellular

cAMP during aggregation and development respectively; as well as intracellular cGMP, which is involved in motility (Bader et al., 2007). Each cyclic nucleotide is degraded by one of seven phosphodiesterases in *Dictyostelium*, which can be divided into two main classes: Class I (to which three enzymes belong) and Class II (to which four enzymes belong). There is one candidate phosphodiesterase IV homologue in *Dictyostelium*, which shares a 33-35% homology with the four isoforms (A-D) found in mammals. Inhibition of *Dictyostelium* phosphodiesterases would therefore be expected to elevate extracellular cAMP (and potentially intracellular cAMP and cGMP) levels. Subsequent expected saturation of cAMP receptors in *Dictyostelium* would therefore lead to the observed inhibition of cell behaviour shown in the assay. The high concentration required for this effect may thus reflect a potential non-specific action of rolipram on non-mammalian phosphodiesterases such as those found in *Dictyostelium*.

3.7.7. Other Compounds

A range of emetic and aversive compounds did not have a significant effect on *Dictyostelium* cell behaviour. These compounds included cytotoxic agents, receptor agonist, inhibitors, a free radical generator, a CNS depressant, an enteroendocrine cell stimulant and a prostaglandin. Many of these compounds have known molecular targets, such as apomorphine, which is known to activate the dopamine D_2 receptor, inducing emesis at concentrations ranging from 0.1-10mg/kg in a range of sentient models (Andrews et al., 1990; Eglen et al., 1993; Knox et al., 1993; Andrews et al., 2001; Nakayama et al., 2004; Horn et al., 2009; Osinski et al., 2005). The lack of efficacy for these compounds in *Dictyostelium* at equivalent concentrations could be due to either the absence of the target protein, a non-essential role for the protein in acute

motility experiments, or structural differences in the proteins altering the activity of the compound.

Alternatively, another explanation for a lack of acute effect is the short term nature (ten minutes) of the experiment in comparison to previous reports that employ longer incubation periods of 1-24 hours. This provides an important limitation in this assay since the acute nature of the assay may not expose the chronic or delayed effects of compounds. For example, cytotoxic agents such as cisplatin used in anti-cancer treatments, did not block *Dictyostelium* motility within the ten minute response time recorded. However cisplatin is previously shown to cause a chronic block in development following twenty four hour exposure (Li et al., 2000).

3.7.8 Cell Viability

The mechanism of action for inhibition of *Dictyostelium* motility by five different tastants is currently unknown. Acute motility inhibition could occur through a range of mechanisms, such as interaction with cell surface receptors, downstream molecular targets or alternatively by cell death. To determine whether the tastants involved in *Dictyostelium* motility inhibition were toxic and causing cell death, a cell viability assay was performed and the 10 and 30 minute exposures to each tastant showed no tastants decreased cell viability apart from capsaicin; where a high concentration (100µM) produced a significant loss in cell survival after ten and thirty minutes **(Table 3.5)**. However reduced concentrations (50µM) showed that cells were viable after 10 and 30 minute exposures. It is likely that the cell death of approximately 50% observed in 100µM capsaicin after 10 minutes was one that was maximal, as cell death did not increase substantially further after 30 minutes. Upon halving the

capsaicin concentration, 98% cells were viable after both exposure times. These results suggest that cells predominantly survive short term (up to 30 minute) exposure to each compound.

3.7.9 Reversibility of Inhibition of Cell Movement

Despite cells having been shown to be viable after 30 minutes, the reversibility of the effects on *Dictyostelium* cell behaviour with each compound was unknown. Using a separate cell movement assay, the block in *Dictyostelium* behaviour was shown to be reversible upon removal of each tastant **(Figure 3.17)**. This data, combined with the cell viability assay, showed clearly cells were displaying no toxicological effects upon short term exposure to bitter and hot tastants. In addition, the acute and reversible nature of the inhibition of *Dictyostelium* behaviour strongly suggests the involvement of compounds binding to cell surface receptors.

To assess long-term exposure to each compound, *Dictyostelium* cells were allowed to develop over 24 hours in the presence of each tastant **(Figure 3.18)**. In all cases *Dictyostelium* cells developed fully, although the developmental process was delayed in the presence of denatonium benzoate, where cells had only reached culmination phase after 24 hour exposure **(Figure 3.18)**.

Long term exposure to bitter and hot tastants allowed for the development of fruiting bodies after 24 hours indicating cells had overcome the inhibitory effects of each tastant. This could be due to a possible internalisation of cell surface receptors or a possible change in gene expression of cells which subsequently allowed development in the presence each tastant. In addition, the compound effects observed cannot have been sustained for a prolonged

period of time as fruiting bodies were fully developed, apart from those developing in the presence of denatonium benzoate. The delayed effects on *Dictyostelium* development in the presence of denatonium benzoate could possibly be due to a high concentration (which may have been observed at higher concentrations for other tastants), or alternatively, the inhibition of multiple cell signalling mechanisms producing a delayed developmental effect.

3.9. Summary

A broad range of emetic and taste aversive compounds were tested for their acute effects of *Dictyostelium* cell behaviour during motility using the Dunn chamber. Of these compounds, seven caused significant ($P<0.05$) reductions in cell velocity and/or aspect as well as a decrease in cell directionality. These compounds could be sub-divided into four chemically distinct groups, which were copper salts, T2R receptor ligands, a TRPV1 receptor agonist and a phosphodiesterase IV inhibitor. It was found that copper, bitter and hot tastants blocked *Dictyostelium* motility in a concentration-dependent manner, where an order of potency was established to be capsaicin >quinine hydrochloride > denatonium benzoate > phenylthiourea > copper sulphate. Upon further analysis of the bitter and hot tastants, it was shown that these compounds do not block *Dictyostelium* cell migration by induction of cell death or by an irreversible mechanism. Finally the unknown mechanisms of action for bitter and hot tastants in *Dictyostelium* may provide novel receptors or targets for use bitter and hot tastant action.

Chapter 4

Identification of molecular mechanisms involved in bitter tastant detection in *Dictyostelium*

Motility assays using a Dunn chamber were used to screen a range of structurally diverse emetic and aversive compounds for acute effects on *Dictyostelium* cell behaviour. This screening process identified seven out of twenty nine compounds that caused a rapid and concentration-dependent block in cell movement with effects shown to be reversible and non-toxic **(Chapter 3)**. Since bitter tastants were shown to block *Dictyostelium* behaviour, these compounds were selected for further investigation.

In this chapter, the potency of phenylthiourea and denatonium benzoate for inhibiting *Dictyostelium* cell growth in shaking suspension was established, enabling a restriction enzyme-mediated integration (REMI) mutagenesis screen to identify proteins controlling bitter tastant function. From this screen an extended list of mutants was then chosen, and screened for acute resistance to tastants during motility using a Dunn chamber, as previously described **(Chapter 3)**.

4.2. Tastant potency analysis

Since previous experiments examining the effects of bitter tastants on *Dictyostelium* focused on monitoring cell movement, viability and development (Robery et al., 2011), it was necessary to characterise the effects of these compounds on cell growth. The inhibitory effects (IC_{50}) of two bitter tastants, phenylthiourea and denatonium benzoate was determined on *Dictyostelium* growth in shaking suspension. These compounds were selected based upon binding affinities to different mammalian T2R receptors (Meyerhof et al., 2010).

In the analysis of bitter tastant potency, *Dictyostelium* cells were grown in shaking suspension following exposure to a range of concentrations of denatonium benzoate (0-10mM) or phenylthiourea (0-5mM) for a 168 hour (7

day) period until proliferating cells under control conditions reached stationary phase **(Figure 4.1)**. Concentrations were chosen to provide a range of effects from no effect to a complete block in cell growth based upon data obtained in motility assays. Data derived from these experiments were also used to produce secondary plots where *Dictyostelium* cell division during growth phase was used to estimate the potency (IC_{50}) value of 1.46mM for denatonium benzoate and 1.95mM for phenylthiourea **(Figure 4.1)**. Additional analysis of the block in *Dictyostelium* growth showed significant reductions ($P<0.05$) at 1mM and 2mM during phenylthiourea growth. At higher concentrations, denatonium benzoate (5mM, 10mM) and phenylthiourea (5mM) caused cell death. In an independent but parallel study, cells were also grown in axenic media in the presence of a range of concentrations for two bitter, non-T2R receptor agonists, naringenin (Meyerhof et al., 2010) and valproic acid (Johannessen and Henriksen, 1979) by colleagues within the laboratory. Based upon these values, a REMI mutant screen was carried out at 1mM for both denatonium benzoate and phenylthiourea. In these experiments, a library of REMI mutants was formed by random integration of a cassette encoding blasticidin resistance throughout the *Dictyostelium* genome. Mutants were then grown in the presence of each tastant for 21 days and surviving colonies used to determine potential loci controlling molecular mechanisms for bitter tastants. The REMI screen was also performed in the presence of naringenin and valproic acid.

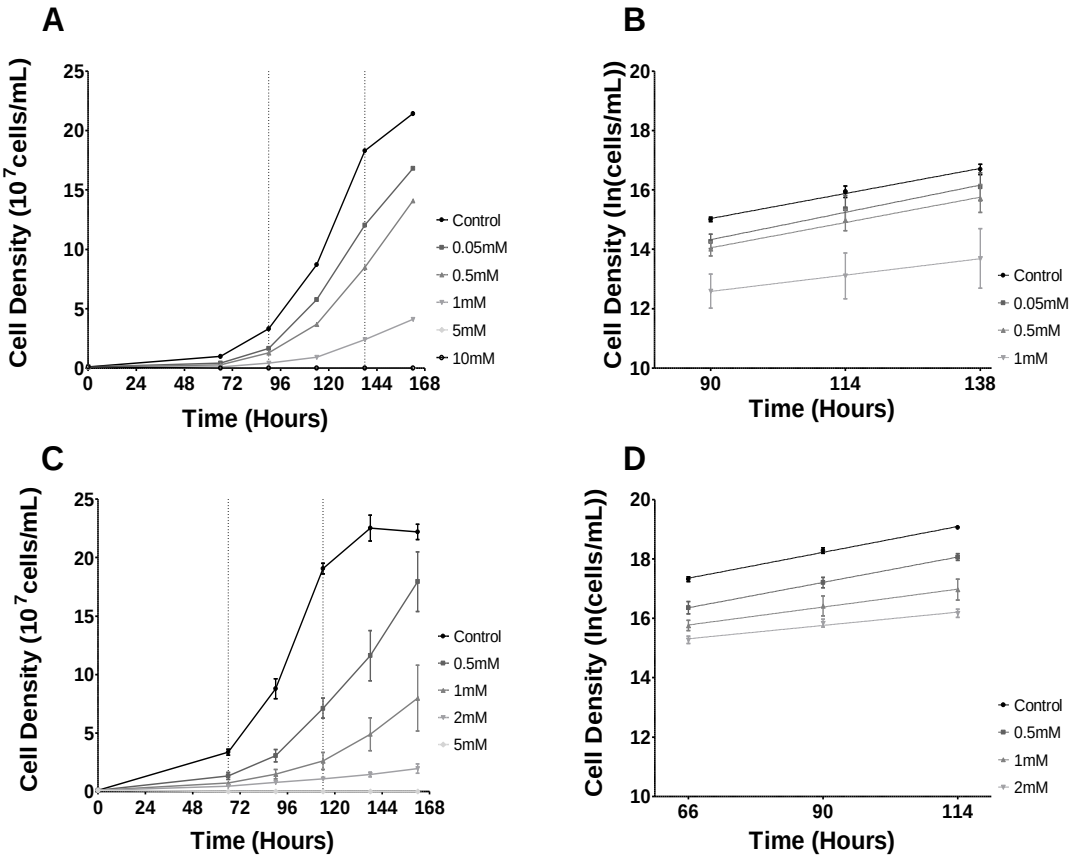

Figure 4.1. *Dictyostelium* proliferation in varying concentrations of denatonium benzoate and phenylthiourea. *Dictyostelium* cells were grown in axenic media over 168 hours in shaking suspension in the presence of denatonium benzoate and phenylthiourea. **(A)** Denatonium benzoate concentrations from 0.05-10mM provided a range of inhibitory effects on cell growth, where it was found that 5 and 10mM concentrations caused cell death. **(B)** A secondary plot during log growth phase (90-138 hours) for control-1mM denatonium benzoate showing the change in cell density at each concentration was produced to determine a potency of inhibition (IC_{50}) of 1.46±1.37mM. **(C)** Phenylthiourea concentrations from 0.5-5mM provided a range of inhibitory effects on cell growth, where it was found that 5mM caused cell death. **(D)** A secondary plot during log growth phase (66-114 hours) for control-2mM phenylthiourea showing the change in cell density at each concentration was produced to determine a potency of inhibition (IC_{50}) of 1.95±0.57mM. In addition, a significant (P=0.05) decrease in cell growth was observed for 1mM and 2mM 5mM phenylthiourea based upon a Mann-Whitney test. Data from A-D is presented as a mean of triplicate experiments with vertical bars representing standard errors of the mean (SEM).

4.3. Initial characterisation of REMI mutants

Preliminary analysis of REMI mutants surviving the growth screens suggested the involvement of 187 loci controlling resistance to one or multiple of the bitter tastants denatonium benzoate, phenylthiourea, naringenin and valproic acid **(Appendix 6)**. In some mutants, the inserted resistance cassette was found in intergenic regions between two genes so it was unclear which of the two genes may be responsible for compound resistance.

REMI mutants showing resistance to bitter tastants in cell growth were shown to involve a number of proteins controlling a variety of functions, from receptors to enzymes involved in DNA replication **(Appendix 6)**. Since the compounds were shown to cause an acute inhibition of cell movement (Robery et al., 2011), a shortlist of twenty mutants was constructed based upon gene ontology (GO). Molecular functions, biological processes and cellular components for proteins of interest were those that could generate an acute response to bitter tastants found previously **(Chapter 3)**. These included receptor activity, cell membrane localisation, G-protein coupled receptor subunits, involvement in vesicle function, second messengers (e.g. small GTPase activity), enzyme activity (phosphorylation, transferase, acyltransferase or ATPase), or involvement in actin organisation, ion transport or cell motility **(Table 4.1 & 4.2)**. As a first step in the analysis of these mutants, any available cells lines with ablated genes identified in the screen were then tested for resistance to selected bitter compounds.

Compound	Gene Name	Gene Product	Function
D	*agpB*	Acyltransferase	Enzyme activity
D, V	*agpC*	Acyltransferase	Enzyme activity
D, N, P, P, V	*DDB_G0267590*	GRAM domain containing protein	Phagocytic vesicles
D, N, V, V, V	*DDB_G0269760*	BTB/POZ domain-containing protein	Potassium channel
D, N, V	*DDB_G0284149*	Orthologue of yeast VID24	VID vesicles
D	*DDB_G0284605*	P-type-, Calcium ATPase	Enzyme activity
D	*DDB_G0288003*	EGF-like domain-containing protein	Macropinocytosis
D	*DDB_G0291203*	Transmembrane protein	Transmembrane
D	*forJ*	Formin domain-containing protein	Actin binding
D, D, D, D	*Fuk*	Fucokinase	Enzyme activity
D	*gpaC*	G-protein subunit alpha 3	Second messenger
P	*gpaI*	G-protein subunit alpha 9	Second messenger
D, P	*gpaK*	G-protein subunit alpha 11	Second messenger
P	*grlJ*	$GABA_B$-like family protein	Receptor
D, N, V	*gxcI*	RhoGEF domain-containing protein I	Small GTPase
V, V	*gxcP*	PH domain-containing protein P	Small GTPase
D	*memo1*	Orthologue of *Homo sapiens* MEMO1	Cell motility
D, D, N, P, V	*pkd2*	Polycystin-2-like protein	Calcium channel
D, D	*rvb2*	ATPase domain-containing protein	Macropinocytosis
D	*ublcp1-2*	Ubiquitin-like CTD phosphatase 1	Enzyme activity

Table 4.1. Shortlist of bitter tastant resistant mutants identified in the REMI mutant screen. A shortlist of 20 mutants was constructed for further analysis based on their resistance in growth to one or multiple bitter tastants denatonium benzoate (D), phenylthiourea (P), naringenin (N), valproic acid (V). In each case, the number of occasions each gene was recovered in the screen (represented by multiple listing of a compound), the gene name, a brief description of each gene product and the protein function is described (obtained from www.dictybase.org).

Compound	Gene of Interest	Protein description								
		Receptor	Cell Membrane	Sub-unit	Actin Organisation	Vesicles	Transport	GAP/GEF	Enzyme Activity	Cell Motility
D	*agpB*								X	
D, V	*agpC*								X	
D, N, P, V	*DDB_G0267590*		X			X				
D, N, V	*DDB_G0269760*	X	X				X			
D, N, V	*DDB_G0284149*					X				
D	*DDB_G0284605*		X				X			
D	*DDB_G0288003*		X							
D	*DDB_G0291203*		X							
D	*forJ*				X					
D	*Fuk*								X	
D	*gpaC*		X	X						
P	*gpaI*		X	X						
D, P	*gpaK*		X	X						
P	*grlJ*	X	X							
D, N, V	*gxcI*							X		
V	*gxcP*							X		
D	*memo1*									X
D, N, P, V	*pkd2*	X	X				X			
D	*rvb2*								X	
D	*ublcp1-2*									X

Table 4.2. Shortlist of bitter tastant resistant mutants identified in REMI mutant screen. A shortlist of 20 mutants was constructed for further analysis based on ability to grow in the presence of one or multiple of the bitter tastants denatonium benzoate (D), phenylthiourea (P), naringenin (N), or valproic acid (V). In each case, the predicted/inferred protein function for identified mutated genes in the REMI mutant screen is shown based upon gene ontology (obtained from www.dictybase.org).

4.4. Initial screening of available mutants

A research-community based bank of cell lines is available through Dictybase (www.dictybase.org), which facilitated initial screening of shortlisted mutants, where motility assays were used to determine the effects of bitter tastants. Mutants were initially screened against the bitter tastants to which they showed resistance in the REMI mutant screen. Four of ten screened mutants showed resistance to denatonium benzoate (1mM), phenylthiourea (2mM) and/or naringenin (0.2mM). Where a mutant displayed resistance to a single tastant, a second motility assay using a different compound was performed to determine whether cells showed specificity to a single tastant or showed a broader resistance. These experiments identified *grlJ*$^{-}$ showing resistance to phenylthiourea; *gxcP*$^{-}$ and *gxcKK*$^{-}$ showing resistance to denatonium benzoate; and *pkd2*$^{-}$ showing resistance to naringenin. In addition to the selected REMI mutants, additional cell lines with ablated homologous genes or with functions associated with the protein products identified in the screen were also examined.

4.4.1. *grlJ*$^{-}$

Since the REMI mutant screen identified the *grlJ*$^{-}$ mutant as resistant to phenylthiourea, the effect of this tastant on *Dictyostelium* motility was analysed using a Dunn chamber in both wild type and *grlJ*$^{-}$ cells. Since previously reported reductions in cell movement resulted in a deviation of cell angle towards zero degrees **(Chapter 3)**, this measurement was no longer used. To ensure that no false (non-compound related) chemotactic behaviour was observed, mean velocity and aspect from the initial 300 seconds of the assay was used to normalise all measurements taken throughout the assay and

subsequent experiments. Without normalisation, a REMI mutant may have appeared to show resistance to bitter tastants due to an inherent defect in motility, which is shown in numerous mutants (Hoeller and Kay, 2007; Tang et al., 2008; Teo et al., 2010; Garcia et al., 2013).

Addition of phenylthiourea (2mM) to wild type cells during motility caused a rapid and significant reduction in velocity, from 0.99±0.01 to 0.52±0.01 ($P<0.01$), and aspect, from 1.00±0.01 to 0.57±0.00 ($P<0.01$) **(Figure 4.2A-B)**. Under the same conditions, *grlJ*$^{-}$ cells showed partial resistance. Whilst a significant reduction in velocity, from 1.00±0.02 to 0.69±0.01 ($P<0.01$) was shown in *grlJ*$^{-}$, cells maintained the ability to migrate towards cAMP **(Figure 4.2A, C)**. In addition, no significant change in aspect was observed after phenylthiourea exposure (1.00±0.01 to 0.86±0.01), which was contrasting to effects shown wild type cells **(Figure 4.2B)**. *grlJ*$^{-}$ cells were also exposed to another bitter tastant, denatonium benzoate (1mM), where cells did not show any resistance to the compound, resulting in a block in cell behaviour similar to wild type cells.

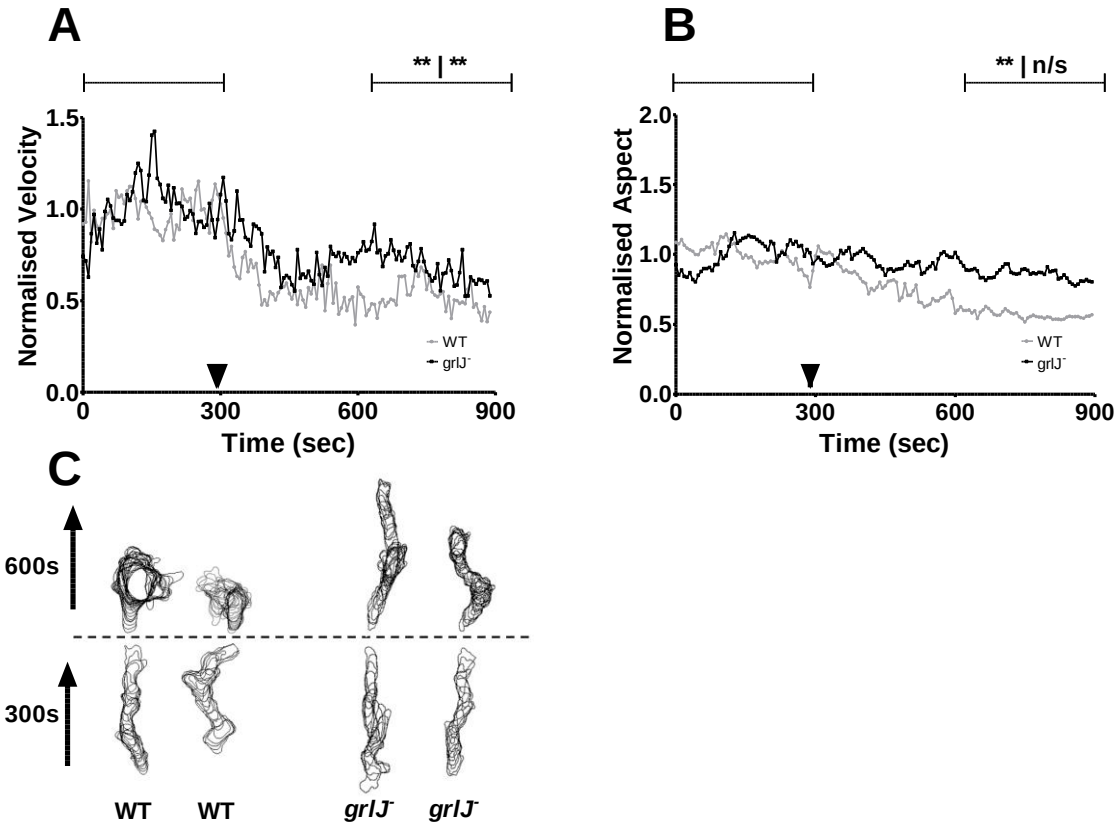

Figure 4.2. Analysis of *Dictyostelium* wild-type and *grlJ*⁻ cells during motility following acute exposure to 2mM phenylthiourea. Cell behaviour (velocity and aspect) was measured under a stable chemotactic gradient in a Dunn chamber, where data from a total of 48 wild type and 87 *grlJ*⁻ cells was quantified every 6 seconds over a 900 second period with the addition of 2mM phenylthiourea at 300 seconds. Velocity and aspect were normalised to the mean of the measurements from first 300 seconds before phenylthiourea addition for each individual replicate. **(A)** Normalised cell velocity; **(B)** Normalised cell aspect; **(C) C**ell directionality. Cell outlines of 2 representative cells from wild-type (WT) control and *grlJ*⁻ mutant cells were overlaid and split into the first 300 and final 600 second intervals. Overlay images have been adjusted so that the chemotactic gradient is following the marked arrows. Cell behaviour showed significant decreases in wild type (p = 0.0093) and *grlJ*⁻ (p = 0.0066) velocity; as well as a significant decrease in wild-type (p = 0.0065) but not *grlJ*⁻ aspect observed between the first and final 300 seconds of the assay. Data from A-B is presented as mean of triplicate experiments. Statistical analyses were performed using paired two-tailed Student t-tests comparing average values from T=0-300 and T=600-900 seconds as previously described. The significance of statistical analysis between the two time points in each cell line are illustrated on the graphs (|) in wild type, followed by *grlJ*⁻ cells. n/s = not significant, ** P<0.01.

GrlJ belongs to a group of seventeen Family 3 GPCRs (grlA-R) present in *Dictyostelium* (Prabhu et al., 2007b). To determine whether the other members of the Grl family of receptors controlled resistance to phenylthiourea, a second mutant, *grlE*⁻ (Fountain, 2010), was also screened in motility assays using phenylthiourea (2mM) and denatonium benzoate (1mM). In each case, *grlE*⁻ cells did not show resistance to either tastant, with treatment causing a significant decrease in cell behaviour similar to wild-type cells. These data

suggest that *grlJ*$^{-}$ cells may be partially resistant to phenylthiourea (but not denatonium benzoate), exhibiting a phenotype not shared by at least one other *Dictyostelium grl*$^{-}$ mutant.

4.4.2. Guanine exchange factors for Rac (RacGEF)

The REMI mutant screen also identified GxcP and GxcI, two RacGEFs that may be involved in controlling resistance to denatonium benzoate, naringenin and/or valproic acid during cell growth. Analysis of the available mutant, *gxcP*$^{-}$, in motility assays showed no significant change in normalised velocity (from 0.91±0.02 to 0.78±0.02) or aspect (from 1.00±0.02 to 0.92±0.01) upon the addition of denatonium benzoate (1mM), and cells continued to migrate down a cAMP gradient, in contrast to wild-type cells (where normalised velocity changed from 1.00±0.01 to 0.22±0.01 and aspect changed from 1.00±0.01 to 0.54±0.00), which did not **(Figure 4.3)**. To measure the behaviour of *gxcP*$^{-}$ cells in the presence of a second bitter tastant, the mutant was also exposed to phenylthiourea (2mM) during motility, where cells were not resistant, showing a reduction in cell behaviour similar to wild type cells. These results suggest that GxcP is likely to be involved in denatonium benzoate but not phenylthiourea-mediated inhibition of cell movement.

Since ablation of the gene encoding GxcP provides resistance to denatonium benzoate, other related proteins were also investigated for a similar role. *Dictyostelium* contains an extensive family of RacGEFs, of which 42 contain the RhoGEF domain present in GxcP (Vlahou and Rivero, 2006). Two cell lines with a gene ablated sharing homology with *gxcP*, *gxcB*$^{-}$ (Strehle et al., 2006) and *gxcKK*$^{-}$, were also tested for resistance to denatonium benzoate (1mM) in motility assays. Whilst *gxcB*$^{-}$ cells showed no resistance to the

tastant, *gxcKK*$^{-}$ cells were unaffected by the addition of denatonium benzoate (1mM) **(Figure 4.4)**. In order to measure specificity to denatonium benzoate, *gxcKK*$^{-}$ cells were also exposed to phenylthiourea (2mM) during motility assays, where the mutant showed a significant reduction in cell behaviour comparable to wild-type cells. This data suggests the involvement of GxcP and GxcKK in the detection of denatonium benzoate.

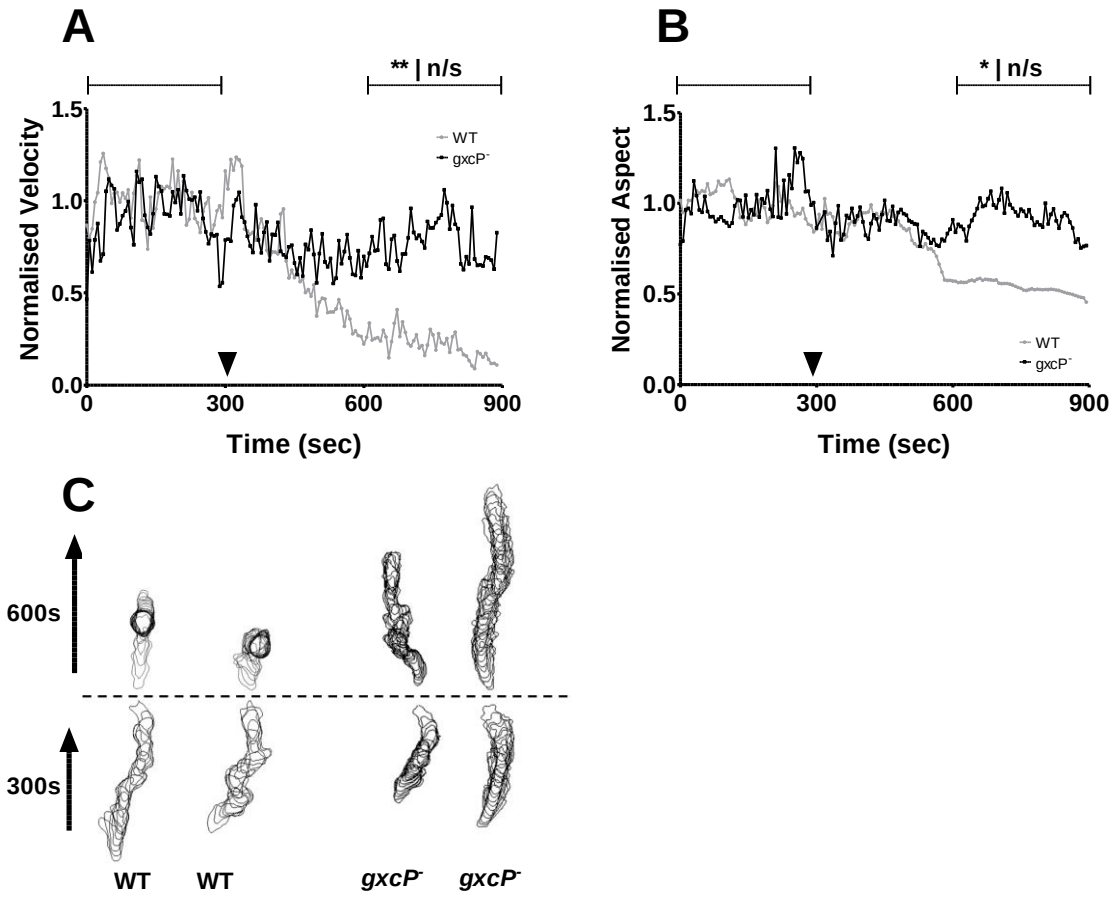

Figure 4.3. Analysis of *Dictyostelium* wild-type and *gxcP*$^-$ cells during motility following acute exposure to 1mM denatonium benzoate. Cell behaviour (velocity and aspect) was measured under a stable chemotactic gradient in a Dunn chamber, where data from a total of 40 wild-type and 91 *gxcP*$^-$ cells was quantified every 6 seconds over a 900 second period with the addition of 1mM denatonium benzoate at 300 seconds. Velocity and aspect were normalised to the mean of the measurements from first 300 seconds before denatonium benzoate addition for each individual replicate. **(A)** Normalised cell velocity; **(B)** Normalised cell aspect; **(C)** Cell directionality. Outlines of 2 representative cells from WT and *gxcP*$^-$ were overlaid and split into the first 300 and final 600 second intervals. Overlay images have been adjusted so that the chemotactic gradient is following the marked arrows. Cell behaviour showed significant decreases in wild-type but not *gxcP*$^-$ for velocity (p = 0.0012) and aspect (p = 0.0135) observed between the first and final 300 seconds of the assay. Data from A-B is presented as mean of triplicate experiments. Statistical analyses were performed using paired two-tailed Student t-tests comparing average values from T=0-300 and T=600-900 seconds as previously described. The significance of statistical analysis between the two time points in each cell line are illustrated on the graphs (|) in wild type, followed by *gxcP*$^-$ cells. n/s = not significant, * P<0.05, **P<0.01.

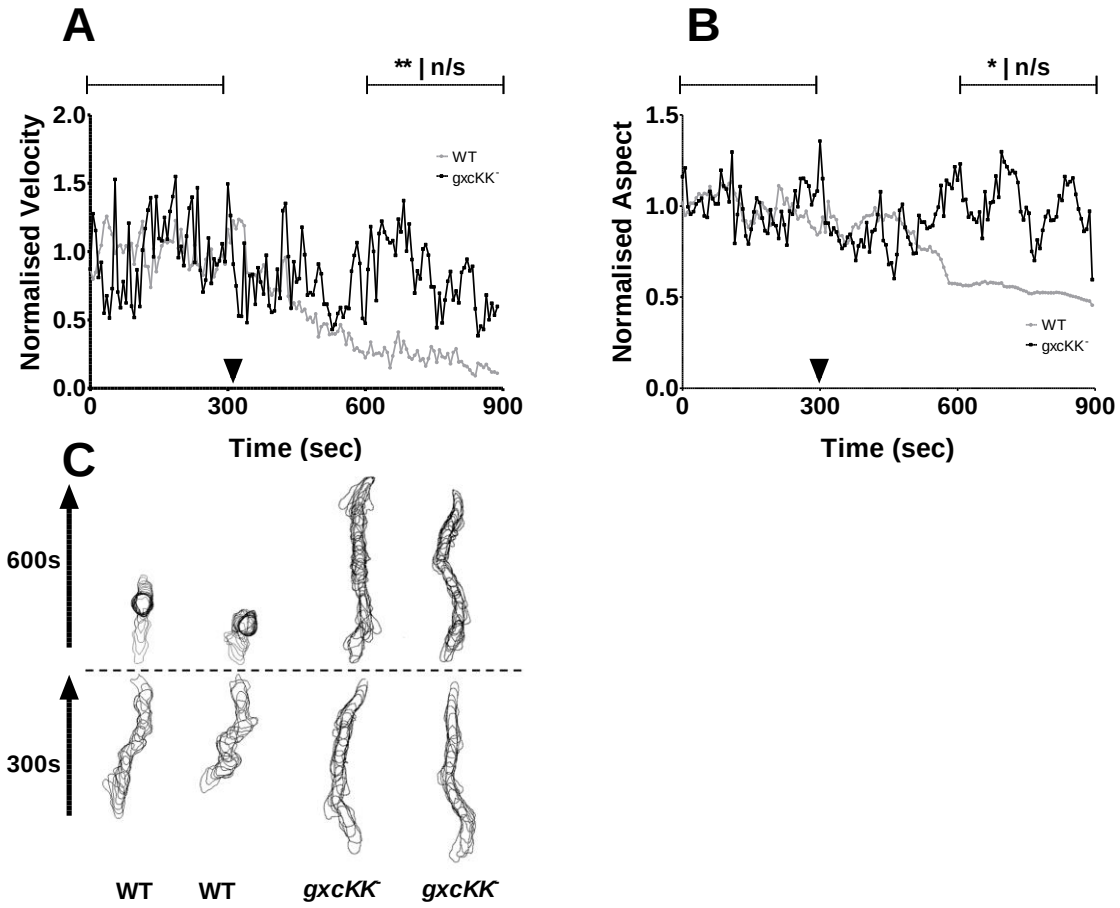

Figure 4.4. Analysis of *Dictyostelium* wild wild-type and *gxcKK*⁻ cells during motility following acute exposure to 1mM denatonium benzoate. Cell behaviour (velocity and aspect) was measured under a stable chemotactic gradient in a Dunn chamber, where data from a total of 40 wild-type and 39 *gxcKK*⁻ cells was quantified every 6 seconds over a 900 second period with the addition of 1mM denatonium benzoate at 300 seconds. Velocity and aspect were normalised to the mean of the measurements from first 300 seconds before phenylthiourea addition for each individual replicate. **(A)** Normalised cell velocity; **(B)** Normalised cell aspect; **(C)** Cell directionality. Outlines of 2 representative cells from WT and *gxcKK*⁻ were overlaid and split into the first 300 and final 600 second intervals. Overlay images have been adjusted so that the chemotactic gradient is following the marked arrows. Cell behaviour showed significant decreases in wild-type but not *gxcKK*⁻ for velocity (p = 0.0012) and aspect (p = 0.0135) observed between the first and final 300 seconds of the assay. Data from A-B is presented as mean of triplicate experiments. Statistical analyses were performed using paired two-tailed Student t-tests comparing average values from T=0-300 and T=600-900 seconds as previously described. The significance of statistical analysis between the two time points in each cell line are illustrated on the graphs (|) in wild type, followed by *gxcKK*⁻ cells. n/s = not significant, * P<0.05, **P<0.01.

4.4.3. *pkd2*$^{-}$

The *pkd2* gene was identified in the REMI mutant screen as showing putative resistance to denatonium benzoate, phenylthiourea, naringenin and valproic acid **(Table 1 and 2)**. To investigate this, a *pkd2*$^{-}$ mutant was obtained and screened in separate motility assays with exposure to denatonium benzoate (1mM) and phenylthiourea (2mM), where in both cases cells showed no resistance to either tastant. This data indicated the Pkd2 channel is not involved the response to phenylthiourea or denatonium benzoate.

Pkd2 is one of several calcium channels that exist in *Dictyostelium.* In order to investigate the role of another calcium channel, IplA (Wilczynska et al., 2005), motility assays were also performed using an *iplA*$^{-}$ mutant exposed to denatonium benzoate (1mM), where cells displayed no resistance. The TRP channel mutants, *pkd2*$^{-}$, and *iplA*$^{-}$ were also both screened against capsaicin (0.1mM) due to this compound's binding affinity for a related channel, TRPV1 (Pingle et al., 2007). Neither cell line was found to display any resistance to the capsaicin.

In a parallel experiment, to those described here, a REMI mutant screen using the bitter tastant naringenin also identified *pkd2*$^{-}$. To examine this, the acute effects of naringenin (0.2mM) on *Dictyostelium* cell behaviour were monitored using a Dunn chamber motility assay. Naringenin (0.2mM) had no effect on wild-type *Dictyostelium* cell behaviour following acute (ten minute) exposure. Prolonged one hour exposure to naringenin (0.2mM) has previously been shown to cause a near complete block in *Dictyostelium* motility (Misty et al., 2006). A new assay was therefore developed by modifying the random cell movement assay used previously **(Chapter 3)**. Following a one-hour incubation

of cells in naringenin (0.2mM), *Dictyostelium* cell behaviour was recorded for five minutes and analysed using QuimP software, which was used to quantify cell displacement, circularity, protrusion formation and motility (defined as the magnitude of all membrane protrusions and retractions summed up over time). Wild-type *Dictyostelium* random cell movement was strongly inhibited following incubation with naringenin (0.2mM), showing a significant near-complete block in displacement (11.13±1.5µm solvent control, 1.79±0.24µm naringenin exposure) protrusion formation (5.42±0.05 solvent control, 0.061±0.01 naringenin) and motility (0.47±0.03 solvent control, 0.04±0.01 naringenin), as well as significant cell rounding (0.75±0.00 solvent control, 0.94±0.00 naringenin) when compared to control (solvent only) conditions **(Figure 4.5)**. Under the same conditions, *pkd2*$^{-}$ cells displayed resistance to naringenin (0.2mM), where no significant change was observed in comparison to control *pkd2*$^{-}$ conditions in displacement (8.83±1.2µm solvent control, 7.77±1.1µm naringenin), circularity (0.74±0.00 solvent control, 0.72±0.01 naringenin), number of protrusions (5.57±0.05 solvent control, 3.34±0.05 naringenin), or cell motility (0.45±0.03 solvent control, 0.37±0.03 naringenin) **(Figure 4.5)**. In addition, a significant difference between wild-type and *pkd2*$^{-}$ cells was observed after naringenin (0.2mM) incubation for displacement ($P<0.01$), circularity ($P<0.001$), protrusion formation ($P<0.05$) and motility ($P<0.01$). This data indicated that the Pkd2 receptor may be involved in naringenin detection **(Figure 4.5)**.

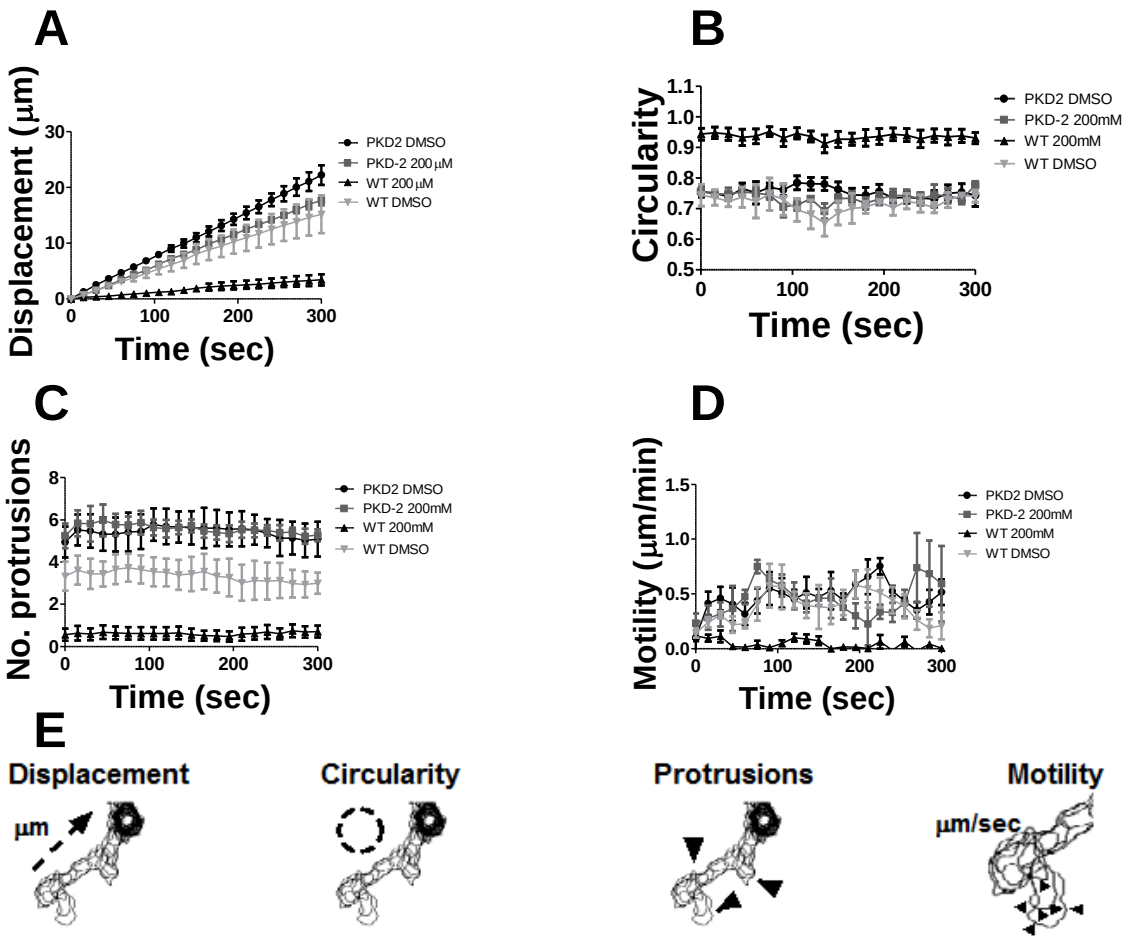

Figure 4.5. Analysis of *Dictyostelium* wild-type and *pkd2*$^-$ cells during random cell movement after one hour incubation with 200μM naringenin. Cell behaviour (displacement, circularity, number of protrusions and motility) was measured during random cell movement following one hour incubation, with data representing 30 cells per experimental condition quantified every 15 seconds over a 300 second period. **(A)** Cell displacement; **(B)** Cell circularity; **(C)** Number of cellular protrusions formed in a 10 frame window; **(D)** Cell motility. A one-way analysis identified a significant difference in displacement ($F=25.62$, $p < 0.0001$), circularity ($F=26.04$, $p < 0.0001$), number of protrusions formed ($F=19.12$, $p = 0.0001$), and motility ($F=14.96$, $p = 0.0003$) with a *post-hoc* Tukey's multiple comparison test showing a significant decrease in wild-type but not *pkd2*$^-$ displacement ($p < 0.01$), circularity ($p < 0.001$), number of protrusions formed ($p < 0.05$) and cell motility ($p < 0.01$). **(E)** Image overlays of WT cells showing quantification of measurements taken over the course of the assay. Data from A-D is presented as mean of triplicate experiments with vertical bars representing SEM.

4.5. Discussion

Previous experiments reported here have demonstrated that bitter tastants inhibit *Dictyostelium* cell movement **(Chapter 3)**. To date, the molecular mechanisms for detection of these tastants are unknown in *Dictyostelium*. In order to identify potential molecular mechanisms for these tastants, a REMI mutant library was screened to identify mutants resistant to the effect of denatonium benzoate (Meyerhof et al., 2010), phenylthiourea (Meyerhof et al., 2010), naringenin (Meyerhof et al., 2010) and valproic acid (Johannessen and Henriksen, 1979). This chapter described the characterisation of the potency for two standard bitter compounds, phenylthiourea and denatonium benzoate. These results facilitated screening of a mutant library for denatonium benzoate and phenylthiourea resistance followed by the initial characterisation of mutants.

4.5.1. Tastant potency analysis

In order to perform a REMI screen, the potency of phenylthiourea was estimated through the inhibition of cell proliferation in shaking cultures. A range of phenylthiourea concentrations up to 5mM were used over seven days and the log-phase growth rate (Wang and Bushman, 2006) was used to estimate an IC_{50} of 1.95mM **(Figure 4.1)**. Previous studies had identified an IC_{50} for inhibition of cell movement in *Dictyostelium* of 0.37mM, which is approximately five-fold lower than the concentration required here to inhibit proliferation **(Chapter 3)**. This may be due to the presence of rich growth medium or conversely, chemotactic cells may be more sensitive to phenylthiourea than growing cells due to the multiple changes in gene expression that occur during starvation.

In humans, the threshold for phenylthiourea taste detection is at concentrations ranging from 3.28μM to 1.3mM depending on genetic polymorphisms (Bufe et al., 2005). Aside from bitter tastant activation, phenylthiourea is a toxic compound that can cause pulmonary oedema (Scott et al., 1990), decrease survival in mouse embryo cells (Smith and Crespi, 2002) and inhibit melanin production (Criton and Le Mellay-Hamon, 2008) at concentrations ranging from 10μM to 100μM. In contrast to mammalian models, high (10mM) phenylthiourea concentrations have no toxic effects in insect cell lines (Rivers et al., 2009). A phenylthiourea IC_{50} of 1.95mM in *Dictyostelium* cell proliferation is therefore high in comparison to mammalian cell lines but falls within the range of concentrations used in *in vitro* assays in insect cell lines.

To perform a REMI mutagenesis screen in denatonium benzoate, the cell proliferation assay was repeated using concentrations up to 10mM. Seven day incubation of *Dictyostelium* cells in shaking suspension with denatonium benzoate identified the potency for inhibition (IC_{50}) as 1.5mM **(Figure 4.1)**. Previous experiments have shown an IC_{50} for inhibition of *Dictyostelium* cell movement by denatonium benzoate of 0.13mM, which is approximately 10-fold lower than the concentration that inhibited proliferation in this study **(Chapter 3)**. This variation in IC_{50} could be also explained by the presence of axenic media as described for phenylthiourea or through different levels of target proteins present in the two conditions.

Denatonium benzoate in rodent models causes aversion in the rat at 0.1mM (Tordoff et al., 2008) and in hamsters at 3mM (Frank et al., 2004), showing different potencies in closely related mammalian species. In addition,

human T2R receptors demonstrate variation in sensitivity to denatonium benzoate, where concentrations ranging from 100nM to 1mM causes receptor activation (Meyerhof et al., 2010). Denatonium benzoate is a compound with low toxicity (Hansen et al., 1993) since, for example, studies have shown that children can comfortably ingest up to 10g without displaying any major side effects (Sibert and Frude, 1991). High denatonium benzoate concentrations up to 10mM also have effects on gastric distension in the rat when infused directly into the gastrointestinal tract of the rat (Horn et al., 2011). The IC_{50} derived in this study for denatonium benzoate effects on cell proliferation in *Dictyostelium* is therefore consistent with the concentration ranges studied in other systems.

4.5.2. Initial characterisation of REMI mutants

A range 187 mutants were identified in the REMI screen, which potentially control resistance to one or a combination of bitter tastants **(Appendix 6)**. The number of mutants potentially involved in controlling phenylthiourea sensitivity suggests the involvement of multiple mechanisms of action. As a result, prolonged phenylthiourea exposure as used in the REMI screen, may identify *Dictyostelium* proteins involved in an acute or a delayed response. In addition, more than one mutation, which could collectively cause resistance to phenylthiourea, may also occur in a single mutant as a result of the mutagenesis screen. Finally, prolonged exposure to phenylthiourea may induce tolerance in some mutant strains causing in a false-positive mutant result. Since the phenylthiourea response to cell motility was one that occurred within minutes of exposure, a shortlist comprising twenty REMI mutants based on protein functions likely to target cell movement was used to narrow down potential targets involved in acute inhibition of cell movement **(Table 4.1 and 4.2)**.

Previous research has suggested a poor correlation between REMI mutant resistance in cell survival (i.e. growth) and a phenotypic resistance in motility to a particular compound (Terbach et al., 2011). Since bitter tastant detection in *Dictyostelium* initially involved motility using a Dunn chamber, this approach was chosen to screen available REMI mutants identified. Mutants were exposed to denatonium benzoate and/or phenylthiourea in an acute ten minute baseline time period **(Table 4.3)**. Four of the ten mutants screened, *grlJ*$^-$ **(Figure 4.2)**, *gxcP*$^-$ **(Figure 4.3)**, *gxcKK*$^-$ **(Figure 4.4)** and *pkd2*$^-$ **(Figure 4.5)**, showed resistance to bitter tastants in velocity and/or aspect when compared to the wild-type strain. No mutants showed resistance to more than one bitter tastant, nor did any individual compound lack an effect on cell behaviour in a range of mutants **(Table 4.3)**. These data have identified three different tastants acting via separate mechanisms in *Dictyostelium*, which include a seven transmembrane domain $GABA_B$-like protein involved in acute phenylthiourea recognition; two small GTPases involved in acute signalling in response to denatonium benzoate; and a calcium channel involved in naringenin detection upon prolonged exposure.

Gene	Category Protein	Compound	Resistant
agpB	Acyltransferase	D	N
DDB_G0284605	P-type-, Calcium ATPase	D	N
grlJ	$GABA_B$-like receptor	P, D	Y, N
grlE	$GABA_B$-like receptor	P, D	N, N
gxcP	Pleckstrin homology domain-containing protein P	D, P	Y, N
gxcB	Pleckstrin homology domain-containing protein B	D	N
gxcKK	Pleckstrin homology domain-containing protein KK	D	Y, N
iplA	inositol 1,4,5-trisphosphate receptor-like protein	D, C	N, N
pkd2	polycystin-2-like protein	D, N, P, C	N,Y,N, N
rvb2	ATPase domain-containing protein	D	N

Table 4.3: Summary of REMI mutants screened for resistance to bitter tastants in motility using a Dunn chamber. *Dictyostelium* mutants were screened as previously described with 1mM denatonium benzoate (D), 2mM phenylthiourea (P), 0.1mM capsaicin (C) and/or 0.2mM naringenin (N). Resistance of motility to a specific compound (defined as a non-significant change in cell velocity and/or aspect following acute treatment) is represented by Y (Yes), with no effect denoted N (No). **N.B.** *Dictyostelium* naringenin experiments were performed using random cell movement (i.e. in the absence of a cAMP gradient) rather than motility.

4.5.3. *grlJ*⁻

The G-protein coupled receptor mutant, *grlJ*⁻, showed partial resistance to the block in cell behaviour caused by phenylthiourea (2mM) **(Figure 4.2)**, but did not show resistance to denatonium benzoate (1mM) under the same conditions. These data suggest a role for GrlJ in the detection of phenylthiourea.

In *Dictyostelium*, GrlJ plays a role in post aggregation development, so that *grlJ*⁻ cells form broken slugs and have a malformed spore shape (Prabhu et al., 2007b). GrlJ shares a structure similar to $GABA_B$ receptors in mammalian systems, particularly in the transmembrane domains (Prabhu and Eichinger, 2006). It is currently unclear if these conserved regions in GrlJ function as ligand binding domains as shown in human T2R receptors, where transmembrane regions act as ligand binding pockets in bitter tastant detection (Sakurai et al., 2010).

In addition to T2R receptors, previous studies have demonstrated the involvement of alternative receptors in bitter tastant detection. In humans cell lines, this includes the calcium-sensing receptor, which responds to denatonium benzoate (Rogachevskaja et al., 2011). Cell lines in frogs are also shown to detect bitter tastants through melatonin and adrenergic receptors (Zubare-Samuelov et al., 2003). Model systems naturally lacking T2R receptors such as fish (Ishimaru et al., 2005), fly (Isono and Morita, 2010) and nematode (Hilliard et al., 2004) have more than one GPCR responsible for bitter tastant detection. These studies show non-T2R receptors may function as bitter tastant receptors, which supports a possible role of GrlJ in phenylthiourea detection. To determine whether GrlJ is the only Grl-family receptor responsible for bitter tastant detection, *grlE*$^{-}$ was also screened for phenylthiourea resistance in motility assays, where cells were shown to be sensitive **(Table 4.3)**. This suggests there may be ligand receptor specificity for phenylthiourea towards GrlJ, although other Grl-family receptors cannot be discounted. This will be analysed further in **Chapter 5** and **Chapter 6** by ablating *grlJ* in the wild type cell line used throughout this thesis.

4.5.4. RacGEFs

The RacGEF mutant, *gxcP*$^{-}$, showed resistance to the denatonium benzoate-mediated block in cell movement found in wild type cells **(Figure 4.3)**. Of two related RacGEF mutants, only *gxcKK*$^{-}$ (not *gxcB*$^{-}$) showed resistance to the tastant **(Figure 4.4, Table 4.3)**. RacGEFs such as GxcP, GxcKK and GxcB all contain RhoGEF domains, which activate molecular switches by converting GDP to GTP (Vlahou and Rivero, 2006). These are regulated by pleckstrin homology domains, also present within the protein, which serve as an anchor at the cell membrane allowing molecular interactions (Vlahou and Rivero, 2006).

RacGEFs have important roles in motility, cell morphology as well as actin organisation (Pakes et al., 2012a; Knetsch et al., 2001). Little is known about the function of GxcP and GxcKK, however inhibition of these RacGEFs by denatonium benzoate could result in the block in cell movement observed. In addition, two different RacGEF mutants showing resistance to denatonium benzoate suggests GxcP and GxcKK may play parallel roles in controlling the response to or detection of denatonium benzoate.

GxcB is contains a triple array of calponin domains, which interact with F-actin and bundle actin filaments (Strehle et al., 2006; Friedberg and Rivero, 2010). The calponin domains found in GxcB but not GxcP and GxcKK may therefore provide an indication to the mechanism of action for denatonium benzoate detection in *Dictyostelium*, where actin binding of GxcB does not affect cell movement (**Figure 4.6)**.

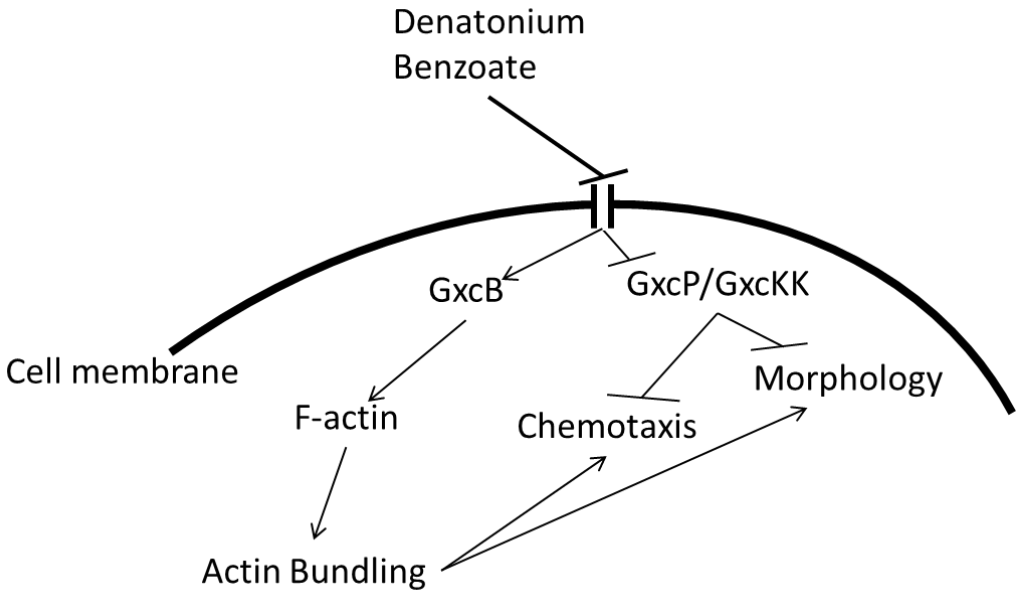

Figure 4.6: Possible differing mechanisms of action for denatonium benzoate detection between RacGEFs. GxcB binds to F-actin and bundles actin, which may be independent of the inhibition of cell movement caused by denatonium benzoate. GxcKK and GxcP may be directly affected by a denatonium benzoate-mediated inhibition of cell movement.

4.5.5 pkd2^{-}

The calcium channel mutant, *pkd2*$^{-}$, was identified in phenylthiourea, denatonium benzoate, naringenin and valproic acid growth screens **(Table 4.1 & 4.2)**. No acute resistance was observed in denatonium benzoate (1mM) and phenylthiourea (1mM) motility assays **(Table 4.3)**. Since no acute effect of naringenin was observed using motility assays in wild type cells, prolonged (one hour) exposure to naringenin (0.2mM) identified a distinct resistance in *pkd2*$^{-}$ cells compared to wild-type cells in random cell movement **(Figure 4.5)**.

Naringenin is a naturally occurring bitter tasting flavonoid that does not activate mammalian T2R receptors (Meyerhof et al., 2010). The mechanism of action for naringenin detection in taste perception is currently unknown. Naringenin has a range of therapeutic benefits including as an anti-microbial treatment (Yin et al., 2012), as well as possible anti-angiogenic and anti-metastatic properties (Weng and Yen, 2012). Naringenin induces apoptosis in cancer cell lines at concentrations ranging from 50µM to 200µM (Arul and Subramanian, 2013), as well as inhibiting adhesion of *Salmonella enterica* to gastrointestinal epithelial cells at 735µM (Yin et al., 2012). Arising from the data reported in this thesis, naringenin has also been shown to inhibit the formation of polycystic cysts in mammalian kidney cell lines at concentrations relevant to *Dictyostelium* inhibition of cell movement (Mark Carew, Kingston University, personal communication). Together these data indicate that the inhibition of *Dictyostelium* cell movement observed at 200µM naringenin is within a concentration relevant to mammalian cell lines.

4.6. Summary

Four mutants screened in motility assays showed resistance to bitter tastants, with *grlJ*$^{-}$ cells showing partial resistance to phenylthiourea, *gxcP*$^{-}$ and *gxcKK*$^{-}$ showing resistance to denatonium benzoate, and *pkd2*$^{-}$ showing resistance to naringenin. GrlJ is a novel GPCR-like protein belonging to a receptor family of which little is known about in *Dictyostelium*. Partial resistance to phenylthiourea showing specificity for GrlJ suggests there may be ligand receptor specificity for the tastant. This will be analysed further in subsequent chapters. Since *gxcP*$^{-}$ and *gxcKK*$^{-}$ both show resistance to denatonium benzoate, these results suggest multiple RacGEFs may function in the same or parallel pathways. These parallel pathways may be directly affected by denatonium benzoate in RacGEFs that do not contain a calponin domain. Finally, *pkd2*$^{-}$ cells did not show resistance to either denatonium benzoate or phenylthiourea, although cells were resistant to naringenin in random cell movement following one hour exposure. Since naringenin required prolonged exposure to block cell behaviour, this bitter compound may function through different mechanisms to denatonium benzoate and phenylthiourea.

Chapter 5

Ablation of *grlJ*

Phenylthiourea is a standard bitter compound thought to activate a single receptor, TAS2R38 (Bufe et al., 2005). Different genetic polymorphisms in the *TAS2R38* gene, result in a variation in taste sensitivity depending on an individual's super taster, taster or non-taster status (Bufe et al., 2005). This variation between taster status and sensitivity to phenylthiourea is however not fully explained by *TAS2R38* single nucleotide polymorphisms, which has led to the suggestion that alternative mechanisms may be involved in detection of these receptor ligands (Hayes et al., 2008).

Previous chapters in this thesis identified a number of bitter tastants to block *Dictyostelium* behaviour in both motility and random cell movement. In addition, a REMI mutagenesis screen identified a number of *Dictyostelium* mutants showing resistance in growth to denatonium benzoate, phenylthiourea, naringenin and valproic acid using motility assays in a Dunn chamber **(Chapter 4)**. Four out of ten REMI mutants were identified as showing selective resistance to a single bitter tastant in cell movement, where *grlJ*$^{-}$ cells showed partial resistance to phenylthiourea.

In this chapter, the role of the poorly characterised protein, GrlJ, is analysed as a potential receptor for phenylthiourea detection in *Dictyostelium*. *grlJ* was ablated from wild type strains and subsequent phenotypic responses to phenylthiourea investigated. The gene was then recapitulated to confirm rescue of the wild type phenotypes.

5.1. Creating a *grlJ*⁻ knockout strain

To test the involvement of the REMI mutant, *grlJ*⁻, in resistance to phenylthiourea as mutant specific and not secondary mutations caused in the REMI mutagenesis process or due to differences in the background strain, *grlJ* was ablated in wild type Ax2 cells. This was achieved by integration of a knockout cassette, containing the *grlJ* gene, where a central region of the gene (encoding part of the N-terminus and the first four transmembrane domains) was replaced by a gene encoding a protein that gives resistance to blasticidin, into *Dictyostelium* cells. Following homologous integration of the knockout cassette into the *Dictyostelium* genome, the expression of *grlJ* encoding a G-protein coupled receptor, is effectively blocked.

5' and 3' fragments of *grlJ* were cloned into the pLPBLP vector (Faix et al., 2004) flanking the cassette encoding blasticidin resistance **(Figure 5.1A-B)**. Digestion of the knockout vector with individual restriction enzymes confirmed the presence of restriction sites within the pLPBLP vector, where double digests identified vector backbone in addition to insertion of 5' (729bp) and 3' (545bp) fragments of *grlJ*. A double digest with BamHI and KpnI also excised the knockout cassette (2846bp) from the vector, where only a single band could be identified since the vector backbone (2898bp) was not distinguishable by gel electrophoresis. **(Figure 5.1C)**. The linearised vector was then transformed into wild type Ax2 *Dictyostelium* cells by electroporation and potential knockout mutants isolated by selection with blasticidin. Surviving colonies, potentially containing the knockout cassette, were then screened by PCR to determine whether the knockout cassette had homologously integrated into the *grlJ* gene and thus created a knockout cell line **(Figure 5.1C)**.

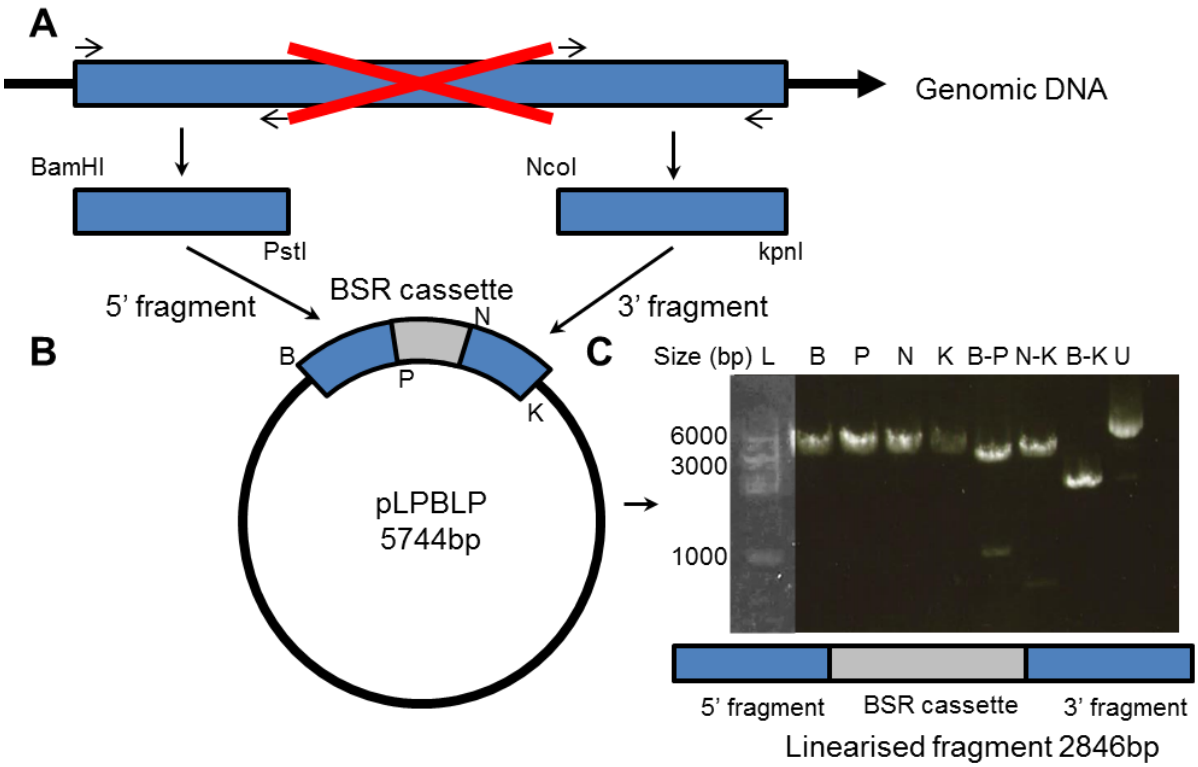

Figure 5.1. Creation of a *grlJ*⁻ knockout construct. **(A)** 5' and 3' fragments of *grlJ* genomic DNA were amplified using primers containing BamHI, PstI, NcoI and KpnI cut sites by PCR. **(B)** Fragments were cloned into either side of the cassette encoding blasticidin (BSR) of pLPBLP. **(C)** A series of restriction digests were used to confirm incorporation of 5' and 3' *grlJ* DNA fragments into the vector. All restriction digests were run on a 1% agarose gel by electrophoresis using a 1kb DNA ladder (L), where single digests BamHI (B), PstI (P), NcoI (N) and KpnI (K); as well as double digests BamHI-PstI (B-P), which produced the 5' fragment (729bp), NcoI-KpnI (N-K) produced the 3' fragment (545bp) and BamHI-KpnI (B-K) produced the linearised knockout fragment (2846bp) for use in electroporation. Uncut vector containing the knockout fragment was also used as a control (U).

5.1.1. PCR screening and identification of *grlJ*⁻ knockouts

Identification of homologously integrated cells was determined by screening for blasticidin resistant colonies using PCR (Terbach et al., 2011). Primers were designed to amplify genomic and vector control fragments, as well as a diagnostic knockout fragment in PCR screening. Genomic control primers were designed to flank 5' and 3' fragments cloned into the pLPBLP vector, which would confirm the presence of a non-deleted region of *grlJ* **(Figure 5.2A)**. Vector control fragments used to confirm the presence of the knockout cassette were amplified, using PCR primers designed complementary to regions inside the genomic DNA fragment and the cassette encoding blasticidin **(Figure 5.2A)**. Finally a diagnostic knockout

fragment using a 5' or 3' primer located outside of the gene and the blasticidin resistance cassette primer confirmed homologous integration of the resistance cassette **(Figure 5.2A)**. Screening for a homologously integrated knockout cassette **(Figure 5.2B)**, identified two out of several hundred blasticidin-resistant clones showing correct homologous integration events on both the 5' and 3' sides **(Figure 5.2C)**. In order to derive isogenic cell lines from a single cell, these two positive transformants were then sub-cloned and grown on *Raoultella* plates.

Since the presence of the blasticidin resistance gene may influence cell behaviour, this gene was removed by CRE recombinase (Kimmel and Faix, 2006) **(Figure 5.2D)**. Isogenic *grlJ*$^{-}$ mutants were electroporated with pDEX-NLS-CRE and placed under G418 selection or blasticidin selection. Colonies that survived under G418 (contained within the shuttle vector), but not blasticidin, were harvested and complementary DNA (cDNA) synthesised by reverse-transcription (RT) PCR. To confirm loss of the blasticidin resistance gene, PCR primers were designed to flank a deleted region of the gene, which showed a band in wild type but not *grlJ* cDNA after gel electrophoresis. In addition, to confirm deletion of part of the *grlJ* gene, a second set of primers were designed to flank across the deleted region of the gene, which identified a band that was smaller (428bp) in *grlJ*$^{-}$ cDNA in comparison to wild type cDNA **(Figure 5.2E)**. Upon confirmation of blasticidin cassette excision, *Dictyostelium* cells were grown in axenic media, under no selection, where the shuttle vector encoding G418 resistance was lost.

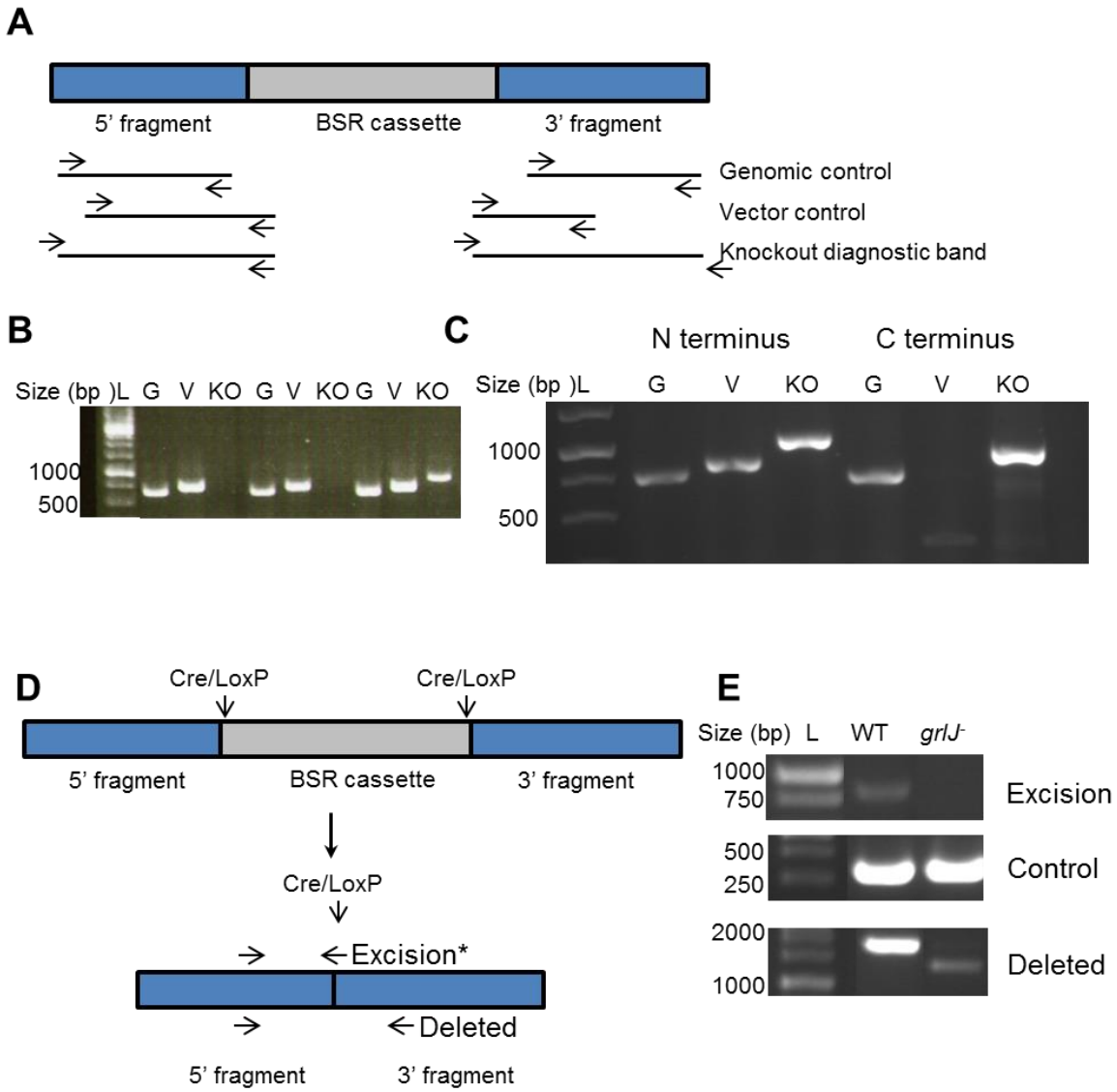

Figure 5.2. PCR Screening for homologous integrants of *grlJ*⁻. Genomic DNA of transformed mutants showing resistance to blasticidin was extracted and screened using PCR. **(A)** Genomic, vector and diagnostic knockout primers were designed to screen for homologous integration. **(B)** Electrophoresis of PCR products would identify non-homologous integrants showing bands in genomic (G) and vector (V) but not diagnostic knockout (KO) PCR products, where homologous integrants showed bands in all three PCR products. **(C)** Homologous integration was then confirmed on both N and C terminal regions of the gene. **(D)** *Dictyostelium grlJ*⁻ mutants were electroporated with pDEX-NLS-CRE for excision of the cassette encoding blasticidin resistance. **(E)** To identify mutants showing excision of the cassette encoding blasticidin resistance, RT-PCR analysis wild type (WT) and *grlJ*⁻ mutants was performed using primers designed within the deleted region of *grlJ*⁻ (Excision), which showed a band in WT but not *grlJ*⁻ cDNA. Expression of an unrelated control gene (*IG7*) was used to ensure equal cDNA was present in each sample (Control). Finally, primers were designed to flank either side of the deleted region in *grlJ* (Deleted), which confirmed deletion of part of *grlJ* (428bp) in *grlJ*⁻ compared to WT cDNA. *3' primer designed to confirm loss of the gene encoding blasticidin was designed within the deleted region of the *grlJ* gene.

5.2. Assessment of *grlJ*$^{-}$ phenotypic behaviour

Creation of a *grlJ*$^{-}$ cell line using the wild type Ax2 background strain enabled the comparison of previously identified phenotypes associated with *grlJ*$^{-}$ cells. These include the production of malformed spores during development and an increased proliferation rate when compared to wild type cells (Prabhu et al., 2007b).

5.2.1. Analysis of spore shape in *grlJ*$^{-}$ cells

To test previously identified malformations in spore shape, wild type and *grlJ*$^{-}$ cells were developed over twenty four hours, to allow the formation of fruiting bodies. Spores fruiting bodies were harvested and visualised using light microscopy. Spore shape, determined by the ratio between length and breadth of spores (aspect), of 214 spores was determined from triplicate experiments in each cell line, showing a significant (P=0.0110) difference between *grlJ*$^{-}$ spores (mean aspect of 2.0±0.03) **(Figure 5.2B, D)** compared to wild type spores (mean aspect of 1.9±0.02) **(Figure 5.3A, C)**. This data confirmed *grlJ*$^{-}$ knockouts developed in the Ax2 background supports a previously identified phenotype during development using a similar Ax2 parent strain (Prabhu et al., 2007b).

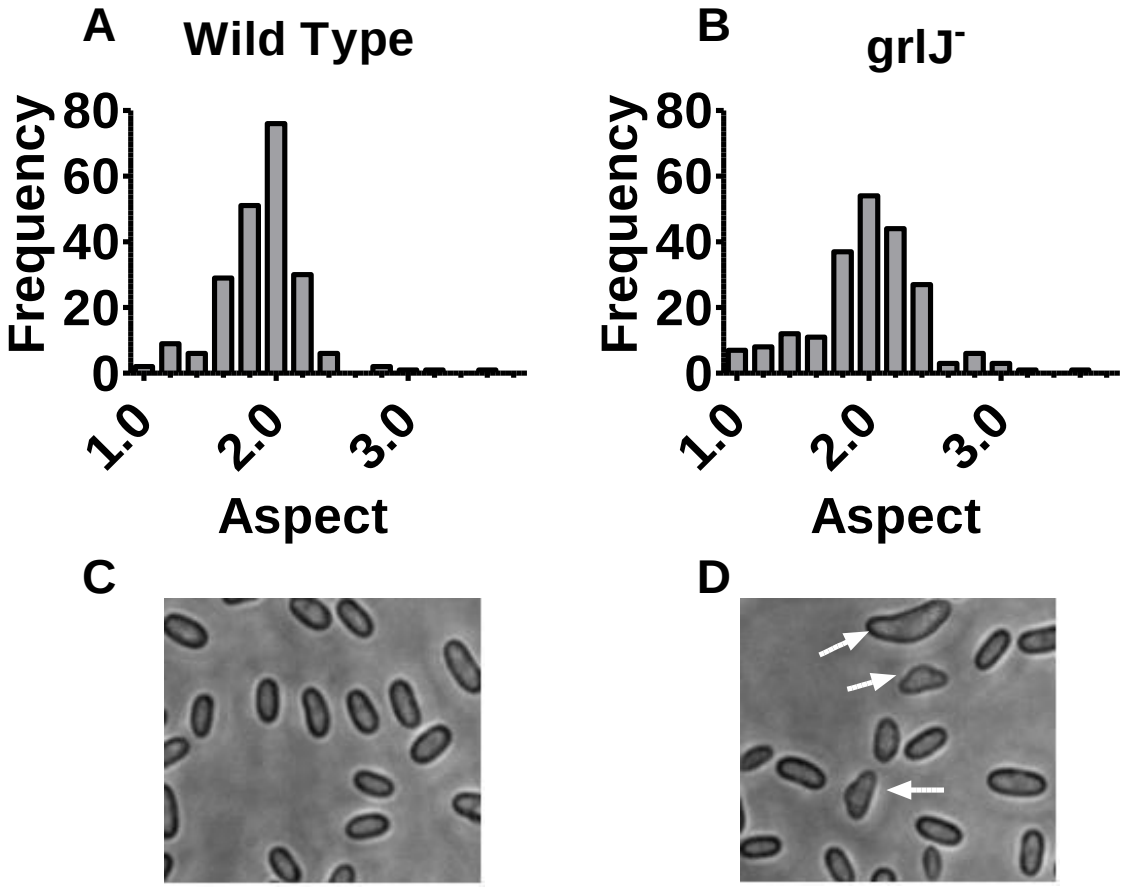

Figure 5.3. Quantification of spore shape during *Dictyostelium* wild type and *grlJ*⁻ development. Dictyostelium cells were allowed to develop over 24 hours before spores were suspended in phosphate buffer and placed onto a coverslip. Phase contrast imaging of 214 spores in wild type and *grlJ*⁻ spores were quantified for aspect using ImagePro Plus. **(A)** Frequency distribution quantifying wild type spore aspect. **(B)** Frequency distribution quantifying spore *grlJ*⁻ spore aspect identified a significant difference (P=0.0110) in shape when compared to wild type strains. **(C)** Normal spore shape shown in wild type spores. **(D)** Malformed spores developed in *grlJ*⁻ strains showing an increased variability in shape. Malformed spores are highlighted by the white arrows. Statistical analysis was performed using two-way ANOVA comparing spore aspect between wild type and *grlJ*⁻ strains.

5.2.2. Analysis of *grlJ*$^{-}$ cell growth in the presence of phenylthiourea

Proliferation of wild-type *Dictyostelium* cells was inhibited over a range of phenylthiourea concentrations, with previous work estimating an IC_{50} of 1.95mM **(Chapter 4)**. In the analysis of bitter tastant potency, wild type and *grlJ*$^{-}$ cells were diluted to $3x10^5$ cells grown in shaking suspension under control conditions for 144 hours until cells reached stationary phase **(Figure 5.4A)**. Using the same starting cell density, wild type and *grlJ*$^{-}$ cells were then grown in shaking suspension for 96 hours under control conditions, until cells reached a density of approximately 50% of stationary phase (~$1.8x10^7$ cells/mL). Each cell line was then exposed to a range of phenylthiourea concentrations (1µM-10mM) for a further 48 hours and cell density determined. In comparison to control conditions during the first 24 hours, wild type and *grlJ*$^{-}$ cells showed significant ($P<0.05$) decreases in proliferation at 1mM and 3mM phenylthiourea respectively **(Figure 5.4B-C)**. Wild type and *grlJ*$^{-}$ cell proliferation after 24 hours post-phenylthiourea exposure was then expressed as a percentage of control (solvent only) conditions, where a 2-way ANOVA identified a significant difference between each strain with increasing phenylthiourea concentration ($P<0.0001$) **(Figure 5.4D)**. This data identified a partial resistance in cell growth to phenylthiourea in *grlJ*$^{-}$ cells when compared to wild type cells.

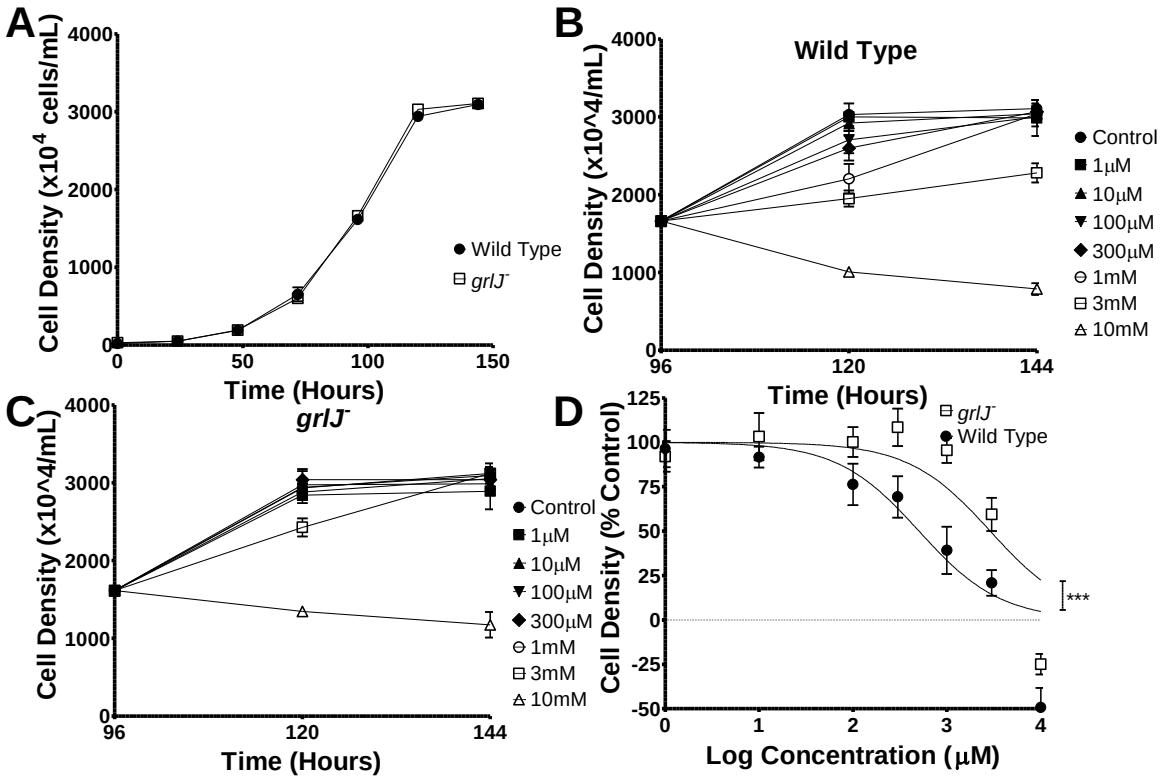

Figure 5.4. *Dictyostelium* Wild type and *grlJ*⁻ proliferation in shaking suspension in the absence and presence of phenylthiourea. (A) *Dictyostelium* wild type and *grlJ*⁻ cells were grown under control conditions until cells reached stationary phase. **(B)** wild type cells were then for 96 hours under control conditions until cells reached approximately 50% of stationary phase, before exposure to 10μM, 100μM, 300μM, 1mM, 3mM and 10mM concentrations of phenylthiourea. A significant decrease in cell density was reached at 1mM phenylthiourea ($P<0.05$) in comparison to control conditions after 24 hours exposure. **(C)** Under the same conditions, *grlJ*⁻ cells showed resistance to phenylthiourea, where a significant decrease in cell density was reached at 3mM ($P<0.05$). **(D)** Cell density 24 hours after exposure to phenylthiourea was then plotted as a percentage of control growth, where a 2-way ANOVA identified a significant difference in cell density as the concentration increased between wild type and *grlJ*⁻ cells ($P<0.0001$).

Dictyostelium growth can be recorded in either shaking suspension, consuming media by macropinocytosis, or on bacterial plates, consuming bacteria by phagocytosis. To assess the effect of phenylthiourea on wild type and *grlJ*$^{-}$ cells during growth on a bacterial lawn, cells were allowed to grow over four days in the presence of *R. planticola*. *Dictyostelium* cell survival rate (determined by the number of colonies formed) and the rate of cell growth (determined by the size of colonies formed) were used to compare wild type and *grlJ*$^{-}$ *Dictyostelium* cells under control and phenylthiourea (3mM) conditions **(Figure 5.5A)**. Addition of phenylthiourea (3mM) to wild type cells caused a significant reduction ($P<0.0001$) in colony number from 107±8.5 to 35.2±4.7 **(Figure 5.5B)**, and in *grlJ*$^{-}$ cells ($P<0.0001$) from 120.2±4.6 to 51.6±2.5 **(Figure 5.5C)** as assessed by a Mann-Whitney test. In addition, phenylthiourea also caused a significant reduction in colony size formed by wild type cells ($P<0.0001$), from 0.38±0.01cm to 0.14±0.01cm, and *grlJ*$^{-}$ cells ($P<0.0001$), from 0.44±0.01cm to 0.22±0.01cm. Upon comparison of colony number between wild type *grlJ*$^{-}$ cells, significantly more colonies were formed in the *grlJ*$^{-}$ strain during phenylthiourea incubation ($P=0.0159$). Furthermore, colonies produced by *grlJ*$^{-}$ cells in the presence of phenylthiourea were also significantly larger than those produced by wild type cells ($P=0.0079$). Together this data suggested *grlJ*$^{-}$ cells showed resistance to phenylthiourea in both growth and survival.

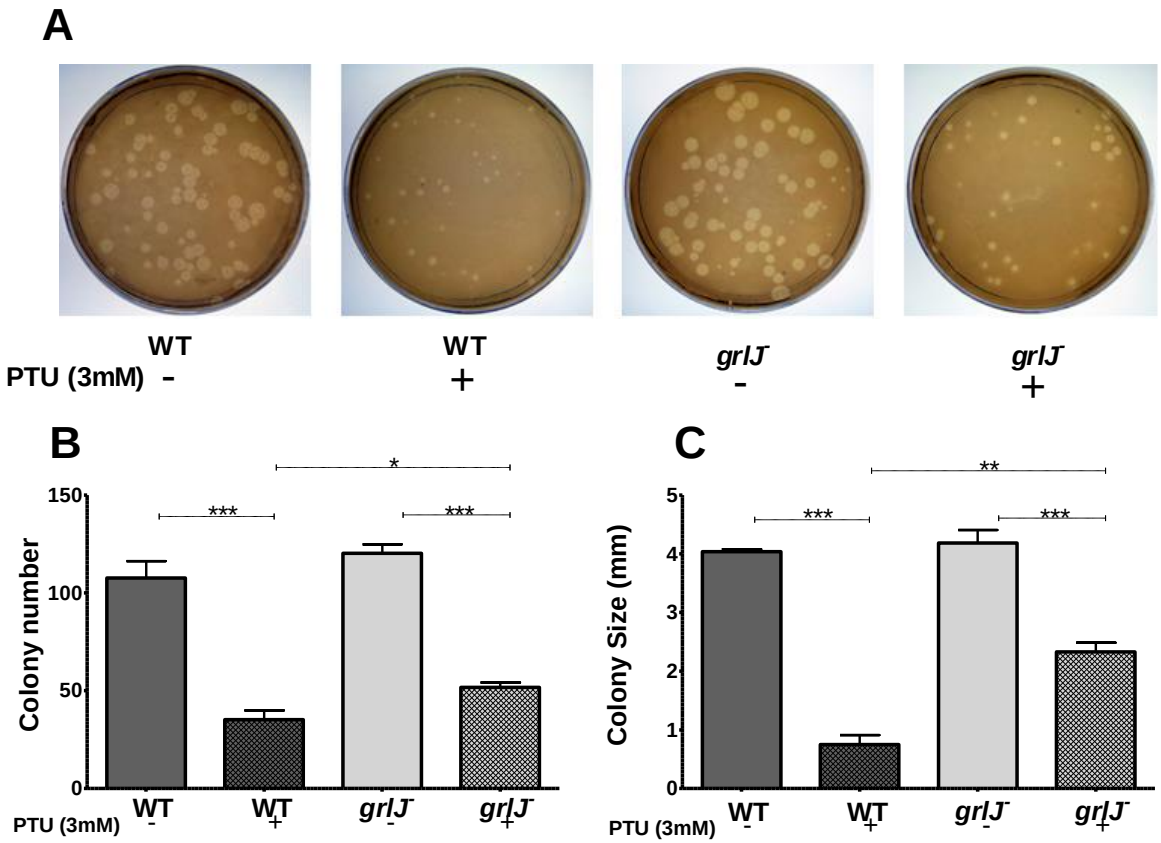

Figure 5.5. *Dictyostelium* wild type and *grlJ-* growth on bacterial lawns in the absence and presence of phenylthiourea (3mM). Wild type and *grlJ-* cells were grown on bacterial lawns in the absence or presence of 3mM phenylthiourea. **(A)** Photographs of bacterial plates under each condition. **(B)** A significant decrease in the number of colonies formed for both wild type (P<0.0001) and *grlJ-* (P<0.0001) strains was observed when grown in the presence of phenylthiourea. In addition, significantly (P=0.0159) more *grlJ-* colonies were formed in the presence of phenylthiourea when compared wild type. **(C)** A significant decrease in colony size for both wild type (P<0.0001) and *grlJ-* (P<0.0001) strains was observed when grown in the presence of phenylthiourea. A significant difference in colony size between wild type and *grlJ-* strains was also identified post-phenylthiourea exposure (P=0.0059). Data from B-C is representative of quintuplicate independent experiments with vertical bars representing standard error of the mean. Statistical analysis was performed using a Mann-Whitney test. *P<0.05, ** P<0.01, ***P<0.001

5.2.3. Analysis of random cell movement in *grlJ-* cells

Previous motility experiments identified *grlJ-* cells to show partial resistance to changes in velocity caused by phenylthiourea (2mM) and resistance to changes in cell shape **(Chapter 4)**. In order to quantify cell behaviour, specifically cell shape, in more detail, random cell movement assays were adapted from conditions described previously **(Chapter 3)**. Chemotactically competent cell behaviour was monitored in the absence of a cAMP gradient using time lapse microscopy, where an image was taken every eighteen seconds. During random cell movement, a control period of

288 seconds was established to enable comparison of wild type and *grlJ*$^{-}$ cell behaviour, where no differences were observed. Phenylthiourea was then added to cells to give a final concentration of 3mM, and cell behaviour monitored for a further 612 seconds. Quantification of cell behaviour was used to determine changes in displacement, circularity, protrusion formation and average cell motility (magnitude of all membrane protrusions and retractions summed over time). Addition of phenylthiourea (3mM) at 288 seconds resulted in a near complete block in cell behaviour in wild type cells, where displacement changed from 22.1±1.9µm at 288 seconds to 28.0±4.8µm at 900 seconds. In addition, phenylthiourea exposure caused an increase in cell circularity, from an average of 0.67±0.01 during the first 288 seconds to 0.91±0.01 during the final 288 seconds (P=0.0017), a decrease in protrusion formation, from 4.3±1.1 to 0.6±0.1 (P=0.0441), as well as a decrease in motility, from 14.4±3.8nm/sec to 0.08±0.04nm/sec (P=0.0294). Under the same conditions, *grlJ*$^{-}$ cells showed partial resistance to phenylthiourea, where cell displacement at 288 seconds significantly increased by 900 seconds from 26.4±2.7µm to 51.4±10.1µm (P=0.0225). In addition, *grlJ*$^{-}$ cells showed a reduced but significant increase in cell circularity, from 0.64±0.02 during the first 288 seconds to 0.77±0.01 during the final 288 seconds (P=0.0011) as well as a significant change in motility, from 18.3±4.1nm/sec to 8.8±1.3nm/sec (P=0.0134). Comparison of protrusion formation between the first and final 288 seconds of the assay did not identify any significant changes in *grlJ*$^{-}$ cells, from 5.0±1.2 to 4.2±0.3. Furthermore, statistical comparison of wild type and *grlJ*$^{-}$ behaviour in response to phenylthiourea identified a significant difference in displacement (P=0.0288), circularity (P=0.0085), protrusion formation (P=0.0101) and motility (P=0.0146) during the final 288 seconds

of the assay **(Figure 5.6)**. These results suggest a partial resistance of *grlJ*$^{-}$ cells to phenylthiourea in comparison to wild type cells.

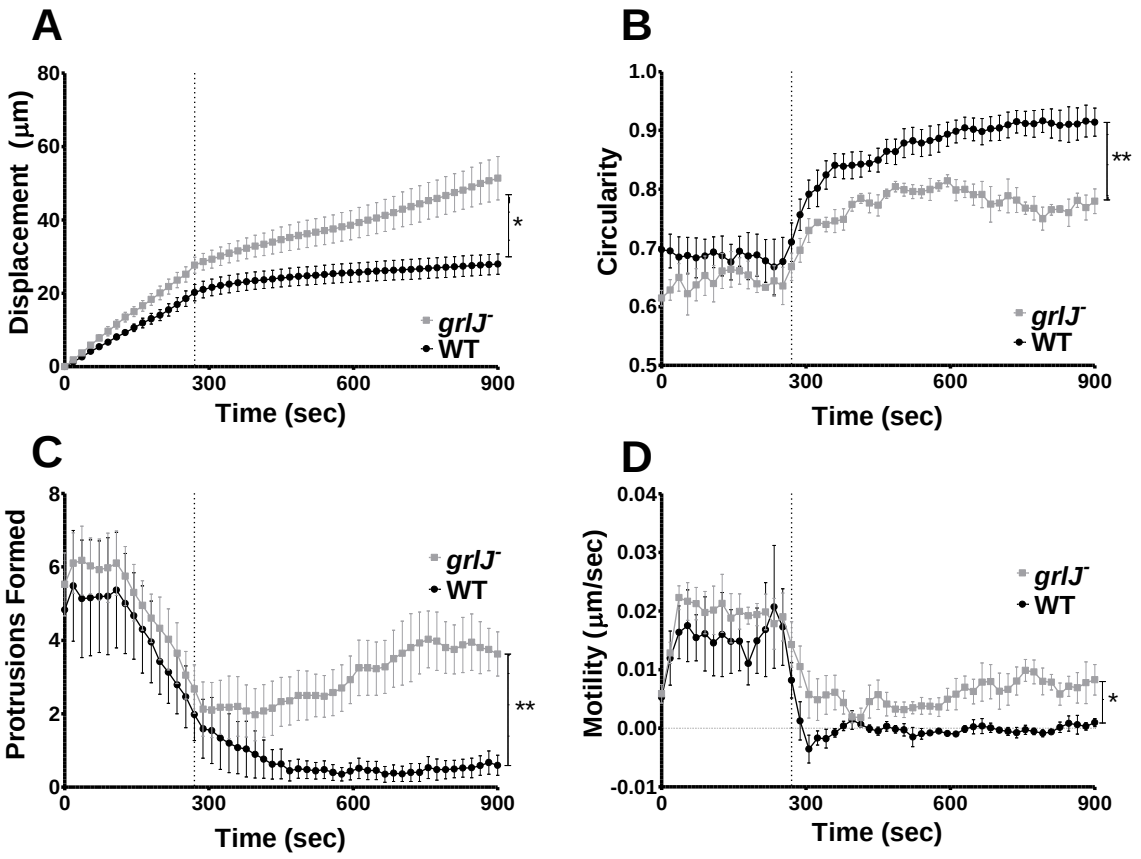

E

Compound/Concentration	Mean Measurements (612-900sec)			
	Displacement (µm)	Circularity	Protrusions	Motility (nm/sec)
3mM Phenylthiourea (WT)	28.0±4.8	0.90±0.001	0.48±0.02	-0.08±0.14
3mM Phenylthiourea (*GrlJ* $^{-}$)	59.4±10.2	0.78±0.014	3.68±0.07	7.48±0.28
Significant Difference	*	**	*	*

Figure 5.6. *Dictyostelium* WT and *GrlJ*$^{-}$ random cell movement following exposure to phenylthiourea (3mM) after 288 seconds. Random movement of *Dictyostelium* cells was monitored under control conditions for 288 seconds before the addition of double concentrated phenylthiourea (3mM final concentration), where cell behaviour was monitored for the remainder of the assay. **(A)** Displacement. A significant (P=0.0228) difference in displacement at the final cumulative time point was observed between WT and *grlJ*$^{-}$ cells. **(B)** Circularity. WT cells were found to show significantly (P<0.0085) increased circularity compared to *GrlJ*$^{-}$ cells during the final 612-900 seconds. **(C)** Number of Protrusions within a 10 frame window. Significantly (P=0.0101) fewer protrusions were formed in WT cells than *GrlJ*$^{-}$ cells during the final 612-900 seconds. **(D)** Motility. WT cells were found to be significantly (P=0.0146) less active than *GrlJ*$^{-}$ cells during the final 612-900 seconds. **(E)** Data quantification showing mean measurements taken during the final 612-900 seconds of the assay for displacement, circularity, number of protrusions and motility. In all measurements, no significant difference was observed between WT and *GrlJ*$^{-}$ cells under control conditions (0-288 seconds). Measurements were derived from an average of 40 cells measured from quadruplicate experiments. Statistical analysis was performed using an unpaired two-tailed t-test. Vertical bars represent the standard error of the mean, *p < 0.05, **p < 0.01.

5.3. Complementation of *grlJ*$^{-}$ cells with *grlJ*

In order to determine whether the phenotypic responses observed in *grlJ*$^{-}$ cells was due to ablation of the gene, cells were complemented with *grlJ* overexpression construct, tagged with a C-terminal GFP. Full length *grlJ* cDNA containing EcoRI restriction sites at both 5' and 3' ends, was amplified and cloned into a pDEX_27 vector (Muller-Taubenberger, 2006) **(Figure 5.7A)**. To determine correct orientation of the construct, restriction digest using BglII was performed, identifying a small fragment in correctly orientated overexpression constructs **(Figure 5.7B)**. Overexpression constructs were then transformed into wild type and *grlJ*$^{-}$ cells to create *grlJ*$^{-/+}$ and WT/*grlJ*$^{+}$ cell lines. Expression of *grlJ* was then confirmed by RT-PCR using a primer located within the deleted region of the gene **(Figure 5.7C)**. Finally, fluorescence microscopy was used to confirm protein localisation on the membrane as previously described (Prabhu et al., 2007b) **(5.7D, E)**.

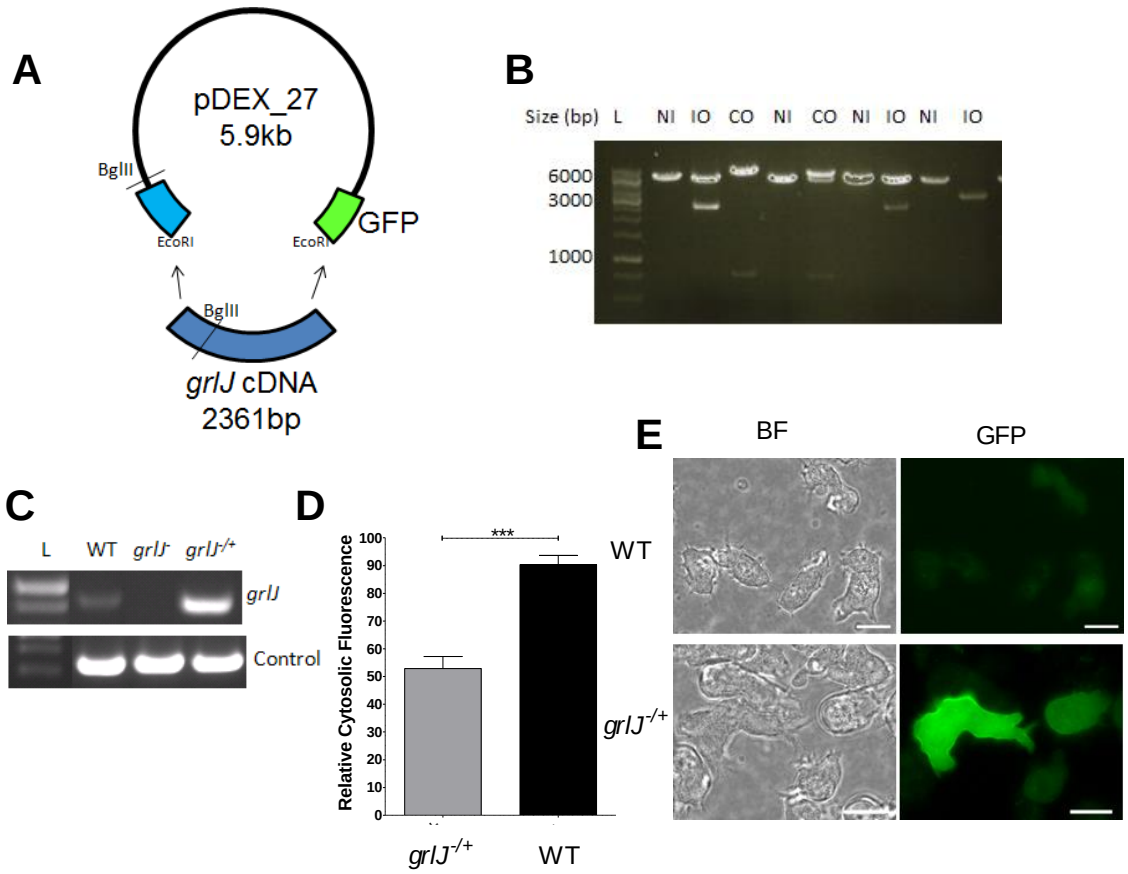

Figure 5.7. Overexpression of *grlJ* in wild type and *grlJ*$^{-}$ cell lines. **(A)** Schematic of an overexpression construct created using pDEX_27; using EcoRI restriction sites to insert *grlJ*. Both pDEX_27 and *grlJ* contained a BglII restriction site, which was used to determine correct orientation of the *grlJ* insert. **(B)** Restriction digests using BglII on candidate *grlJ*$^{-/+}$ constructs identified constructs containing either no insert (NI), large inserts with the incorrect orientation (IO) and small inserts containing inserts with correct orientation (CO). Correctly orientated constructs were used for transformation into *grlJ*$^{-}$ cells which produced the *grlJ*$^{-/+}$ cell line. **(C)** RT-PCR showing *grlJ* gene expression in both WT and *grlJ*$^{-/+}$ but not *grlJ*$^{-}$ cell lines. Control bands represent constitutively active gene, *IG7*. **(D)** *grlJ*$^{-/+}$ cells showed membrane bound GFP fluorescence when compared to WT cells containing an empty GFP vector. **(E)** Quantification of membrane fluorescence showed significantly less ($P<0.0001$) fluorescence was observed in the cytosol in grlJ$^{-/+}$ cells using a Mann-Whitney test based upon quantification of 10 cells.

5.3.1. Analysis cell behaviour in *grlJ*$^{-/+}$ cells

To test that the phenotypes observed in the *grlJ*$^{-}$ cell line was due to gene loss, the *grlJ*$^{-/+}$ cell line was analysed for spore shape and cell behaviour. In the analysis of spore shape, wild type spores were identified to have a mean aspect of 1.9±0.02, *grlJ*$^{-}$ showed a mean aspect of 2.0±0.03, and *grlJ*$^{-/+}$ cells had a mean aspect of 1.9±0.03. A 1-way analysis of variance, identified a significant difference ($P<0.05$) between wild type and *grlJ*$^{-}$ as well as *grlJ*$^{-}$ and *grlJ*$^{-/+}$ strains **(Figure 5.8)**.

This data indicated the normal spore shape observed in wild type cells that was altered in *grlJ*$^{-}$ cells, was restored upon recapitulation of the *grlJ* gene in *grlJ*$^{-/+}$ cell lines.

To determine whether resistance to phenylthiourea in random cell movement shown in the *grlJ*$^{-}$ mutant was reversed by recapitulation of *grlJ*, *grlJ*$^{-/+}$ cells were exposed to phenylthiourea (3mM) cells as described previously. Addition of phenylthiourea resulted an inhibition in *grlJ-/+* cell behaviour where no significant changes in displacement, from 12.0±2.8µm at 288 seconds to 22.3±3.6µm at 900 seconds. In addition, *grlJ-/+* cells showed significant changes in circularity, from 0.72±0.002 to 0.81±0.001 (P=0.0198), protrusion formation, from 3.21±0.1 to 4.7±0.02 (P=0.0139) but not motility, from 4.3±0.5nm/sec to 0.04±0.01nm/sec. Further statistical analysis using a one-way analysis of variance identified a significant difference in displacement between wild type and *grlJ*$^{-}$ ($P<0.05$), as well as *grlJ*$^{-}$ and *grlJ*$^{-/+}$ ($P<0.01$); protrusion formation between WT and *grlJ*$^{-}$ ($P<0.01$) as well as *grlJ*$^{-}$ and *grlJ*$^{-/+}$ ($P<0.01$) cell lines; and motility between WT and *grlJ*$^{-}$ ($P<0.05$) as well as *grlJ*$^{-}$ and *grlJ*$^{-/+}$ ($P<0.05$) **(Figure 5.8)**. These results indicate the wild type phenotypic response to phenylthiourea (3mM) in random cell movement lost in the *grlJ*$^{-}$ mutant, was restored in *grlJ*$^{-/+}$ cells, thus confirming a role for GrlJ in the involvement of phenylthiourea detection in *Dictyostelium*.

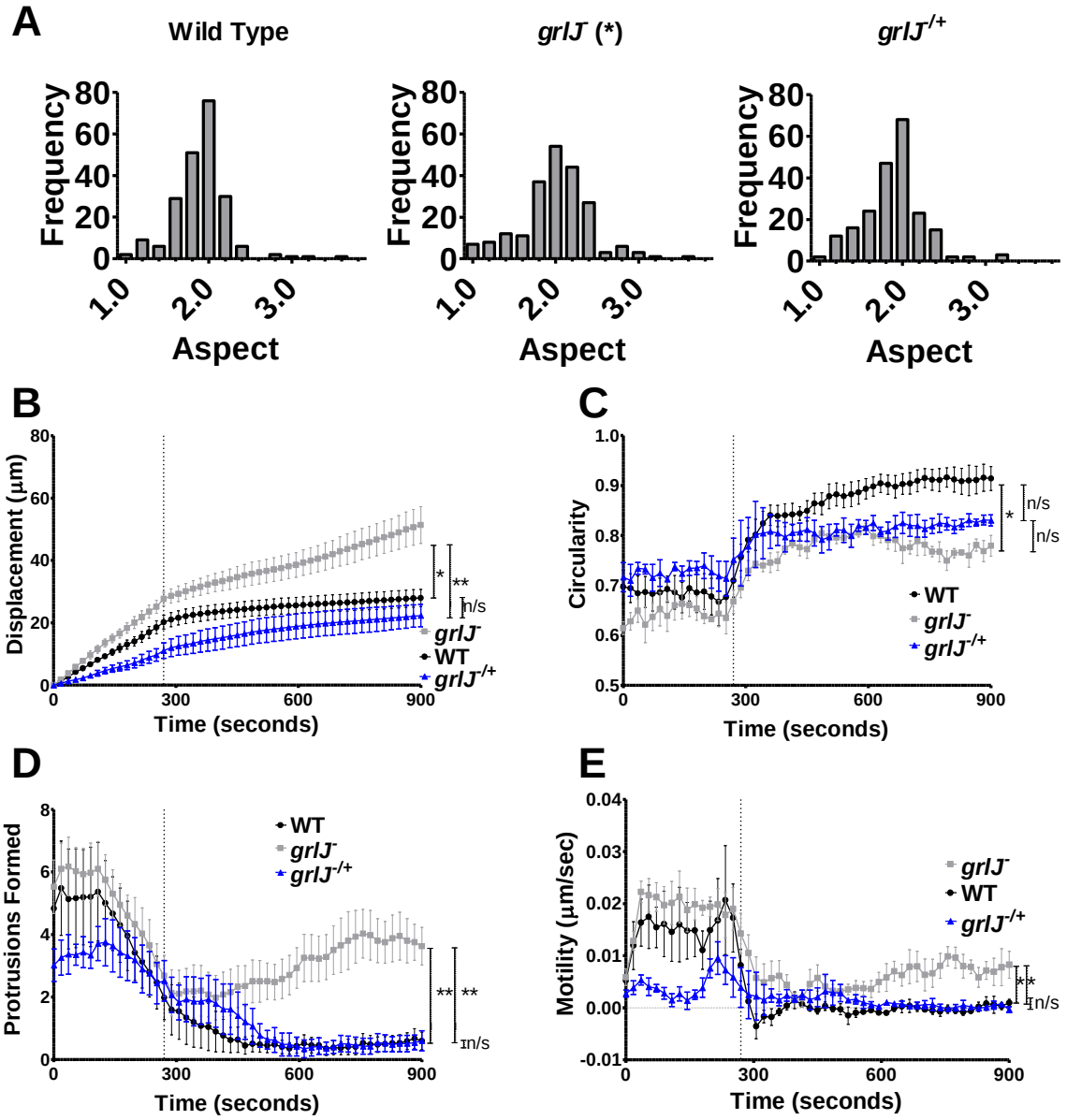

Figure 5.8. Confirmation of *grlJ*$^{-/+}$ phenotypes. **(A)** Spores from wild type, *grlJ*$^{-}$ and *grlJ*$^{-/+}$ were isolated and imaged using phase contrast microscopy. Spore aspect was determined and a 1-way ANOVA revealing a significant difference spore shape between wild type and *grlJ*$^{-}$ ($P<0.05$) as well as *grlJ*$^{-}$ and *grlJ*$^{-/+}$ ($P<0.05$) cell lines. During random cell movement, 3mM phenylthiourea was added to cells after 288 seconds and changes in cell behaviour monitored. A one-way ANOVA with subsequent *post-hoc* Tukey's test was performed for **(B)** Displacement. A significant difference was observed at the final cumulative time point of the assay between WT and *grlJ*$^{-}$ ($P<0.05$) as well as *grlJ*$^{-}$ and *grlJ*$^{-/+}$ ($P<0.01$) cell lines. **(C)** Circularity. A significant difference was observed between wild type and *grlJ*$^{-}$ cell circularity ($P<0.05$) during the final 612-900 seconds. **(D)** Number of Protrusions within a 10 frame window. Significantly fewer protrusions were produced in wild type and *grlJ*$^{-/+}$ cells compared to *grlJ*$^{-}$ cells during the final 612-900 seconds. **(E)** Motility. A significant difference was identified showing WT and *grlJ*$^{-/+}$ cells to be ($P<0.05$) less active than *grlJ*$^{-}$ cells during the final 612-900 seconds. In all measurements, no significant difference was observed between WT, *grlJ*$^{-}$ and *grlJ*$^{-/+}$ cells under control conditions (0-288 seconds). Measurements were derived from 30 cells measured from a minimum of triplicate experiments. Vertical bars represent the standard error of the mean, n/s not significant, *$p < 0.05$, **$p < 0.01$.

5.4. Discussion

As previously described **(Chapter 4)**, a REMI mutagenesis screen identified a G-protein coupled receptor-like protein, GrlJ, to be involved in the detection of the bitter tastant, phenylthiourea. In order to test the partial resistant nature of the *grlJ*$^{-}$ REMI mutant was mutant specific, *grlJ* was ablated in wild type cells of an Ax2 cells background **(Figure 5.1, 5.2)**. To test previously identified malformations in spore shape produced by *grlJ*$^{-}$ cells (Prabhu et al., 2007b), wild type and *grlJ*$^{-}$ cells were developed over twenty four hours and spores compared, identifying a significant difference in spore shape between the two cell lines **(Figure 5.3)**. *grlJ*$^{-}$ cells were then assessed for their response to phenylthiourea on cell growth in shaking suspension **(Figure 5.4)**, growth on bacteria **(Figure 5.5)** and in random cell movement **(Figure 5.6)**, where significant differences were observed in all assays between wild type and *grlJ*$^{-}$ cells. To test the effects observed in the mutant cell line were due to gene ablation, *grlJ*, linked to a GFP from a highly active promoter was overexpressed in *grlJ*$^{-}$ cells, forming *grlJ*$^{-/+}$, which showed previously reported membrane fluorescence (Prabhu et al., 2007b) **(Figure 5.7)**. Re-introduction of GrlJ restored sensitivity to phenylthiourea in random cell movement assays, thus confirming the partial resistance observed in *grlJ*$^{-}$ cells was due to gene ablation **(Figure 5.8)**.

5.4.1. Assessment of *grlJ*$^{-}$ phenotypes

Previous research has identified *grlJ*$^{-}$ strains as showing aberrant spore shape in comparison to wild type cells (Prabhu et al., 2007b). To assess this phenotype in wild type cell lines, spore shape was analysed, where *grlJ*$^{-}$ cells showed significantly increased variation in spore aspect ratio in comparison to wild type spores **(Figure 5.3)**. Expression of *grlJ* occurs throughout *Dictyostelium*

development, however it is elevated after aggregation (Prabhu et al., 2007b). Since *grlJ* may be a negative regulator of *Dictyostelium* development (Prabhu et al., 2007b), ablation of *grlJ* may have affected fruiting body maturation, leading to the production of malformed spores.

To assess *grlJ*$^-$ response to phenylthiourea during prolonged exposure, cells were used in proliferation assays described previously in this thesis **(Chapter 4)**. *grlJ*$^-$ cells have been reported to show a higher proliferation rate in comparison to wild type cells (Prabhu et al., 2007b), which was not consistent with data reported here **(Chapter 4)**. These differences in cell growth rate may be due to specific differences in the parent strain, which can result in different phenotypes in mutants. For example, previous research has shown distinct differences in developmental morphology upon ablation of the gene, *gskA*, using two different *Dictyostelium* parent strains (Schilde et al., 2004). Alternatively, differences in the methodology for constructing growth curves may also have resulted in different growth rates to those reported in this thesis.

A range of phenylthiourea concentrations up to 10mM were used in cell proliferation assays using both wild type *grlJ*$^-$ cells, where the mutant cell line showed partial resistance to the tastant **(Figure 5.4)**. *grlJ*$^-$ cells also showed resistance to phenylthiourea in growth on bacterial lawns in comparison to wild type cells **(Figure 5.5).** In comparison to growth in shaking suspension, phenylthiourea showed a much stronger effect in growth on bacterial lawns, which may be related to differences between macropinocytosis and phagocytosis. Previous research has shown *grlJ* to be transcribed during bacterial growth, which has led to suggestions that the receptor may play a role in actin reshaping during phagocytosis (Sillo et al., 2008). In addition, the related protein, GrlB, has also been shown to be involved in

bacterial phagocytosis (Wu and Janetopoulos, 2013). If GrlJ was also involved in phagocytosis, a significant difference in cell survival rate between wild type and *grlJ*$^{-}$ strains could therefore be related inhibition of phagocytosis, which would inhibit the ability for *Dictyostelium* to consume bacteria.

Despite random cell movement in wild type and *grlJ*$^{-}$ cell lines being reduced upon addition of phenylthiourea, *grlJ*$^{-}$ cells showed partial resistance in comparison to wild type cells **(Figure 5.6)**. Cell growth and movement is also inhibited by compounds such as naringenin (Misty et al., 2006), and epigallocatechin gallate (a green tea catechin) (McQuade et al., 2013), both of which induce cell rounding, showing a similar effect to that produced by phenylthiourea in *Dictyostelium*. Since deactivation of G-protein coupled receptors, using *gβ*$^{-}$ cells, results in impaired phagocytosis and cell movement due to disruption of F-actin remodelling (Peracino et al., 1998), compounds such as phenylthiourea may be acting through G-protein coupled receptors. This is supported by GrlJ being a seven-transmembrane spanning protein, likely to be a G-protein coupled receptor (Prabhu and Eichinger, 2006). GrlJ and its role as a G-protein coupled receptor will be analysed in the next chapter.

5.4.2. Complementation of *grlJ*$^{-}$ cells with *grlJ*

To date, few Grl-family proteins have been characterised. Of those that have, GrlA (Prabhu et al., 2007a), GrlB (Wu and Janetopoulos, 2013), GrlE (Anjard and Loomis, 2006) and GrlJ (Prabhu et al., 2007b) all show protein localisation at the cell cortex. Complementation of the *grlJ*$^{-}$ cell line with *grlJ* tagged with GFP also suggested protein localisation at the cell cortex **(Figure 5.7)**. Overexpression of *grlJ* restored the wild type phenotypic responses to spore shape previously identified

(Figure 5.8). In addition, *grlJ*$^{-/+}$ also restored the wild type response to phenylthiourea during random cell movement **(Figure 5.8)**. Together, this data therefore confirms a function for GrlJ in the detection of phenylthiourea.

5.5. Summary

Identification of a REMI mutant, *grlJ*$^{-}$, showed partial resistance to phenylthiourea during motility in comparison to wild type cells. To test the role for GrlJ in phenylthiourea detection, the gene was successfully ablated, creating a new isogenic cell line, *grlJ*$^{-}$. Using *grlJ*$^{-}$ cells, a previously reported phenotype of malformed spores in comparison to wild type cells was confirmed (Prabhu et al., 2007b). In determining the response of *grlJ*$^{-}$ to phenylthiourea, the mutant showed partial resistance to cell proliferation in shaking suspension, growth on bacterial lawns and random cell movement. To test these effects were due to gene ablation, *grlJ*, tagged with a C-terminal GFP tag, was overexpressed in *grlJ*$^{-}$ cells, creating the strain, *grlJ*$^{-/+}$. Recapitulation of the *grlJ* gene restored GrlJ function, resulting in normal spore shape as well as restoring sensitivity to phenylthiourea in random cell movement. A mechanism of action for GrlJ-mediated phenylthiourea detection will be explored in the following chapter.

Chapter 6

Identification of signalling mechanisms involved in GrlJ activation

Phenylthiourea is a bitter tastant, shown to activate the TAS2R38 receptor in humans (Bufe et al., 2005). Five different single nucleotide polymorphisms within the *TAS2R38* gene give rise to three different phenotypic responses in humans, super-taster, taster and non-taster, where supertasters perceive phenylthiourea as extremely bitter and non-tasters cannot taste phenylthiourea (Bufe et al., 2005). Previous research has shown these polymorphisms do not fully explain the variability in phenylthiourea taste-perception, leading to suggestions that other unidentified receptors may be involved in detection of the tastant (Hayes et al., 2008).

Previous chapters in this thesis describe the identification of a $GABA_B$-like receptor, GrlJ, shown to play a role in phenylthiourea detection in *Dictyostelium*. Generation of the *grlJ*$^-$ strain in wild type Ax2 background showed partial resistance to phenylthiourea in both growth (in shaking suspension and on bacterial lawns) and cell movement. Complementation of the mutant with the wild-type *grlJ* gene (to create a *grlJ*$^{-/+}$ strain) restored wild-type sensitivity to phenylthiourea (3mM). Addition of the tastant to chemotactically competent cells undergoing random cell movement resulted in significant reductions in displacement, protrusion formation and motility, in addition to inducing cell rounding **(Chapter 5)**. These data therefore suggest the identification of a putative G-protein coupled receptor involved in phenylthiourea detection in *Dictyostelium*.

In the chapter described here, the role of a protein that is poorly characterised in function, GrlJ, is analysed as a potential receptor involved in phenylthiourea detection. To date, nothing is known about the molecular signalling that occurs upon GrlJ activation in *Dictyostelium*, and therefore, potential downstream targets will be explored.

6.1. Cell Stress

Previous studies have shown hyperosmotic stress results in rapid actin reorganisation resulting in cell rounding in *Dictyostelium* (Aizawa et al., 1999), a response previously shown to occur in the presence of bitter tastants **(Chapter 3)**. Hyperosmotic stress is shown to cause upregulation of three genes, *yakA*, *gapA* and *rtoA* after a 30 minute incubation (Pakes et al., 2011). To identify whether phenylthiourea induced stress in *Dictyostelium* cells, chemotactically-competent wild-type cells were incubated for 30 minutes in phenylthiourea (3mM) or the hyperosmotic stressor sorbitol (200mM). *Dictyostelium* cells were then lysed before extraction of RNA, which was then purified and analysed by RT-PCR for expression of *yakA*, *gapA* and *rtoA*. Semi-quantitative analysis for changes in gene expression and a repeated-measures two-way ANOVA identified a significant ($P<0.01$) 72±27% increase in *rtoA* expression during sorbitol incubation in comparison to control conditions **(Figure 6.1)**. No significant changes in gene expression were observed in *yakA* or *gapA* in the presence of sorbitol or phenylthiourea. Together, these data suggest sorbitol but not phenylthiourea caused increased *rtoA* expression following thirty minute incubation in wild type cells.

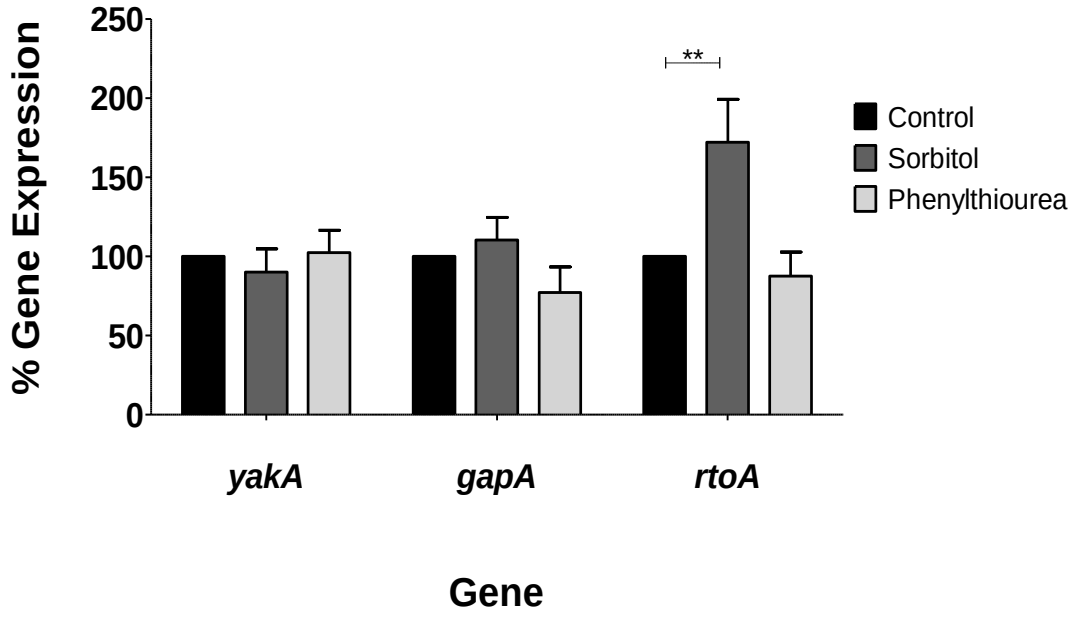

Figure 6.1. Expression of wild-type *Dictyostelium* stress-related genes upon incubation with sorbitol (200mM) or phenylthiourea (3mM). Gene expression of *yakA, gapA and rtoA* was monitored by RT-PCR, following 30 minute exposure to sorbitol (200mM) or phenylthiourea (3mM). A repeated measures 2-way ANOVA identified a significant difference between gene expression and compound treatments ($P<0.001$), where a *post-hoc* Bonferroni tests showed a significant ($P<0.01$) increase in *rtoA* expression in response to sorbitol incubation. Results of quadruplicate experiments are shown as a percentage gene expression compared to control conditions (100%) where cells were incubated in phosphate buffer. Constitutively expressed *IG-7* was used as an expression control for normalisation of gene expression levels. Vertical bars represent standard error of the mean, ** = $P<0.01$.

6.2. G-protein coupled receptor signaling in phenylthiourea detection

Dictyostelium contains a single β-subunit, gβ, that couples to all heterotrimeric G-protein coupled receptors, which upon ablation deactivates all G-protein coupled receptor -mediated signalling (Lilly et al., 1993). To investigate the role of GrlJ responding to phenylthiourea in a G-protein coupled receptor-mediated manner, chemotactically-competent *gβ*$^{-}$ cells were used in random cell movement assays as previously described **(Chapter 5)**. Application of phenylthiourea (3mM) to *gβ*$^{-}$ cells during random cell movement resulted in a significant increase in displacement (P=0.0465), from 13.1±2.0μm to 71.0±24.7μm from 288 seconds to 900 seconds. Furthermore no changes in cell behaviour, defined by circularity, protrusion formation and motility when comparing the first and final 288 seconds of the assay were observed. Direct comparison of cell behaviour between *gβ*$^{-}$ and wild type cells identified significant differences in displacement (P=0.0417), circularity (P=0.0066), protrusion formation (P=0.0220) and motility (P=0.0029) during the final 288 seconds of the assay **(Figure 6.2)**. This evidence supports a role for GrlJ as a G-protein coupled receptor activated in response to phenylthiourea detection.

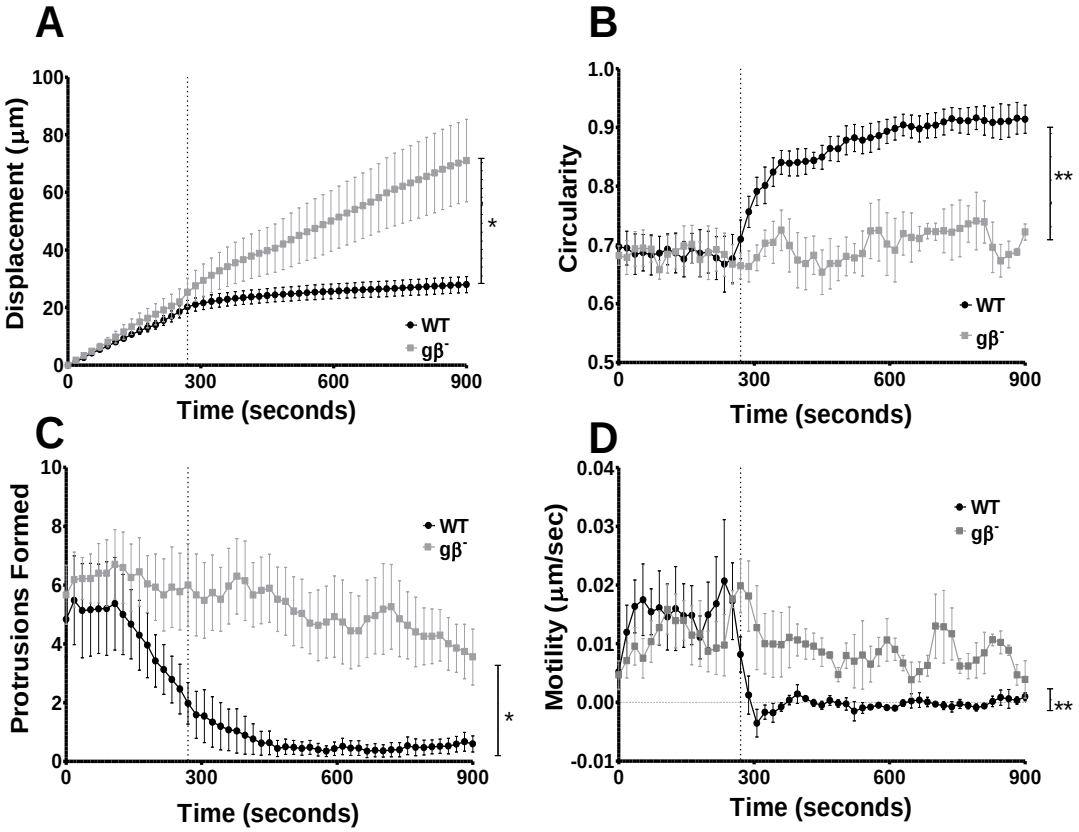

E	Mean Measurements (612-900sec)			
Compound/Concentration	**Displacement (µm)**	**Circularity**	**Protrusions**	**Motility (nm/sec)**
3mM Phenylthiourea (WT)	28.0±4.8	0.90±0.001	0.48±0.02	-0.08±0.14
3mM Phenylthiourea (*gβ*$^-$)	71.0±24.7	0.71±0.00	4.46±0.01	7.94±0.72
Significant Difference	*	**	*	**

Figure 6.2. *Dictyostelium* WT and *gβ*$^-$ random cell movement following exposure to phenylthiourea (3mM) after 288 seconds. Random movement of *Dictyostelium* cells was monitored under control conditions for 288 seconds before the addition of phenylthiourea (3mM final concentration), and cell behaviour was monitored for the remaining 612 seconds of the assay. **(A)** Displacement. A significant difference in displacement at the final time point was observed between WT and *gβ*$^-$ cells (P=0.0417). **(B)** Circularity. WT cells showed significantly (P=0.0066) increased circularity compared to *gβ*$^-$ cells during the final 612-900 seconds. **(C)** Number of protrusions within a 10 frame window. Significantly fewer protrusions were formed in WT cells than *gβ*$^-$ cells during the final 612-900 seconds (P=0.0220). **(D)** Motility. WT cells were found to be significantly less active than *gβ*$^-$ cells during the final 612-900 seconds (P=0.0029). **(E)** Data quantification showing mean measurements taken during the final 612-900 seconds of the assay for displacement, circularity, number of protrusions and motility. In all measurements, no significant difference was observed between WT and *gβ*$^-$ cells under control conditions (0-288 seconds). Measurements were derived from an average of 30 cells measured from triplicate experiments. Statistical analysis was performed using unpaired two-tailed Student t-tests. Vertical bars represent the standard error of the mean, *p < 0.05, **p < 0.01, ***p < 0.001.

6.3. Involvement of the PI3K pathway in phenylthiourea detection

Resistance of *gβ*$^{-}$ cells to phenylthiourea strongly supports a role for GrlJ in G-protein coupled receptor-mediated inhibition of cell movement. In *Dictyostelium*, G-protein coupled receptor activation causes dissociation of heterotrimeric G-proteins, resulting in multiple downstream signalling pathways, including cell polarity (Manahan et al., 2004). One of the key amplification pathways involved in the generation of *Dictyostelium* cell polarity is the PI3K pathway, responsible for the production of phosphatidylinositols (Jin et al., 2009). Since phenylthiourea is shown to block *Dictyostelium* motility and random cell movement through G-protein coupled receptors signalling in chemotactically competent cells, the PI3K pathway was investigated.

To investigate a possible role for the PI3K pathway in phenylthiourea detection, a *PI3K*$^{-}$*/PTEN*$^{-}$ cell line that lacks all five type 1 PI3-kinases as well as the phosphatase and tensin homologue (PTEN) (Hoeller and Kay, 2007) was used. Application of phenylthiourea (3mM) to *PI3K*$^{-}$*/PTEN*$^{-}$ cells during random cell movement resulted in a significant increase in displacement (P=0.0053), from 5.7±0.89µm to 39.2±7.0µm from 288 seconds to 900 seconds. In addition, cell behaviour, as defined by circularity, protrusion formation and motility when comparing the first and final 288 seconds of the assay was not affected. Furthermore, direct comparison of cell behaviour between *PI3K*$^{-}$*/PTEN*$^{-}$ and wild type cells identified significant differences in circularity (P=0.0374), protrusion formation (P=0.0009) and motility (P=0.0004) during the final 288 seconds of the assay **(Figure 6.2)**. This evidence supports a role for GrlJ as a G-protein coupled receptor activated in response to phenylthiourea detection, which results in the inhibition of the PI3K pathway and subsequent loss of cell behaviour.

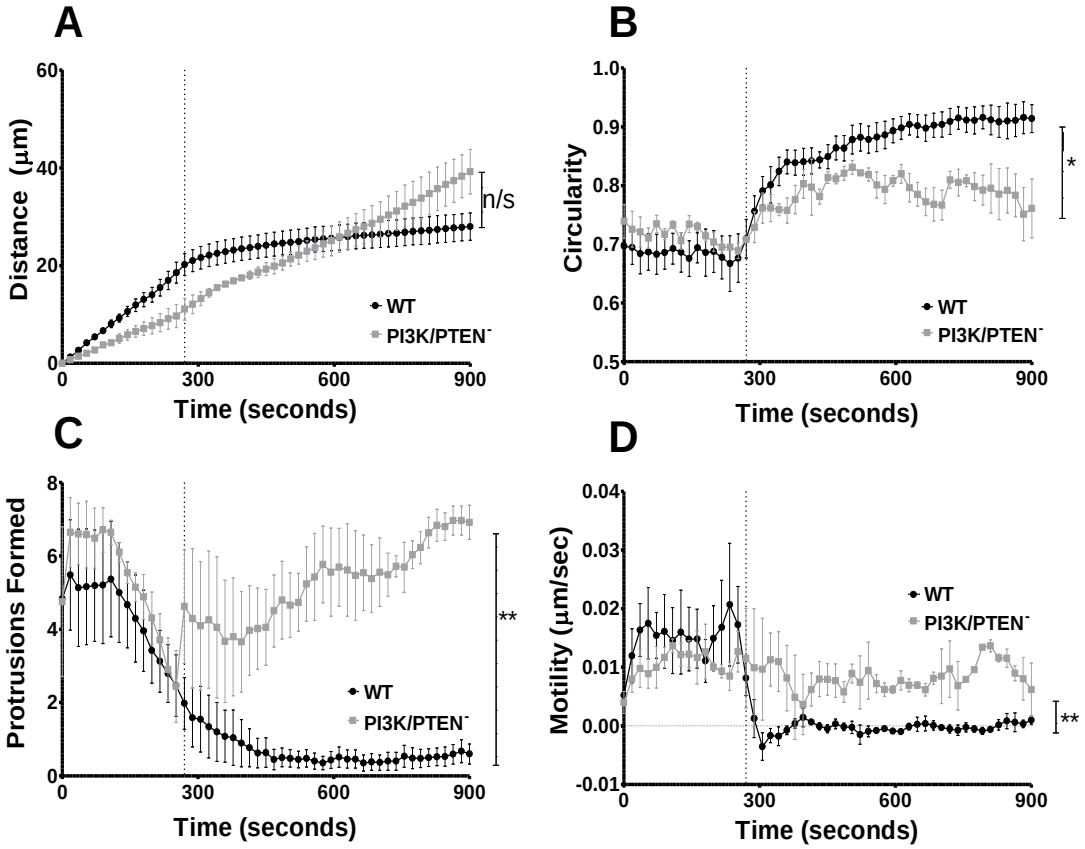

E

	Mean Measurements (612-900sec)			
Compound/Concentration	**Displacement (µm)**	**Circularity**	**Protrusions**	**Motility (nm/sec)**
3mM Phenylthiourea (WT)	28.0±4.8	0.90±0.001	0.48±0.02	-0.08±0.14
3mM Phenylthiourea (PI3K¯)	39.2±7.0	0.79±0.61	6.09±0.15	8.92±0.57
Significant Difference	n/s	*	***	***

Figure 6.3. *Dictyostelium* WT and *PI3K⁻/PTEN⁻* random cell movement upon exposure to phenylthiourea (3mM) after 288 seconds. Random movement of *Dictyostelium* cells was monitored under control conditions for 288 seconds before the addition of phenylthiourea (3mM final concentration), where cell behaviour was monitored for the remaining 612 seconds of the assay. **(A)** Displacement. No significant difference in displacement at the final time point was observed between WT and *PI3K⁻/PTEN⁻* cells. **(B)** Circularity. WT cells were found to show significantly increased circularity compared to *PI3K⁻/PTEN⁻* cells during the final 612-900 seconds (P=0.0374). **(C)** Number of Protrusions within a 10 frame window. Significantly fewer protrusions were formed in WT cells than *PI3K⁻/PTEN⁻* cells during the final 612-900 seconds (P=0.0009). **(D)** Motility. WT cells were found to be significantly less active than *PI3K⁻/PTEN⁻* cells during the final 612-900 seconds (P=0.0004) . **(E)** Data quantification showing mean measurements taken during the final 612-900 seconds of the assay for displacement, circularity, number of protrusions and motility. In all measurements, no significant difference was observed between WT and *PI3K⁻/PTEN⁻* cells under control conditions (0-288 seconds). Measurements were derived from an average of 30 cells measured from triplicate experiments. Statistical analysis was performed using unpaired two-tailed Student t-tests. Vertical bars represent the standard error of the mean, *p < 0.05, **p < 0.01, n/s not significant.

To monitor dynamic cAMP-induced changes in PIP_3 production following exposure to phenylthiourea, *Dictyostelium* wild type and *grlJ*$^-$ cells were electroporated with *PH$_{CRAC}$GFP* (Dormann et al., 2002), a molecular target for PIP_3 binding, composed of GFP fused to the PH domain of cytosolic activator of adenylyl cyclase (CRAC). Electroporated cells were then placed under G418 selection and surviving cells screened for GFP localisation using fluorescence microscopy, creating the strains *WT/PH$_{crac}$GFP* and *grlJ*$^-$*/PH$_{crac}$GFP*.

Chemotactically-competent *WT/PH$_{CRAC}$GFP* and *grlJ*$^-$*/PH$_{CRAC}$GFP* cells were then incubated in control phosphate buffer alone or supplemented with phenylthiourea (3mM) for ten minutes in glass-bottomed chambers. Cells were visualised by fluorescence microscopy under control conditions for 30 seconds before addition of cAMP (1µM final concentration). This global cAMP stimulation caused a temporary increase in fluorescence at the membrane, providing a quantifiable real-time readout for the transient production of PIP_3 at the cell membrane. Approximately ten seconds following the addition of cAMP, significant increases in membrane fluorescence were identified in *WT/PH$_{CRAC}$GFP*, from 1.15±0.06 to 1.46±0.09 (P=0.0017) and *grlJ*$^-$*/PH$_{CRAC}$GFP* from 1.17±0.08 to 1.31±0.08 (P=0.0016) **(Figure 6.4)**. Pre-treatment with phenylthiourea (3mM) blocked the transient increase in membrane fluorescence observed in *WT/PH$_{CRAC}$GFP* cells, but not in *grlJ*$^-$*/PH$_{CRAC}$GFP* cells, where a significant (P=0.0012) increase was identified, from 1.01±0.05 to 1.18±0.04 approximately ten seconds following addition of cAMP **(Figure 6.4)**. This data identified phenylthiourea detection by GrlJ causes inhibition of CRAC translocation to the cell membrane during global stimulation with cAMP.

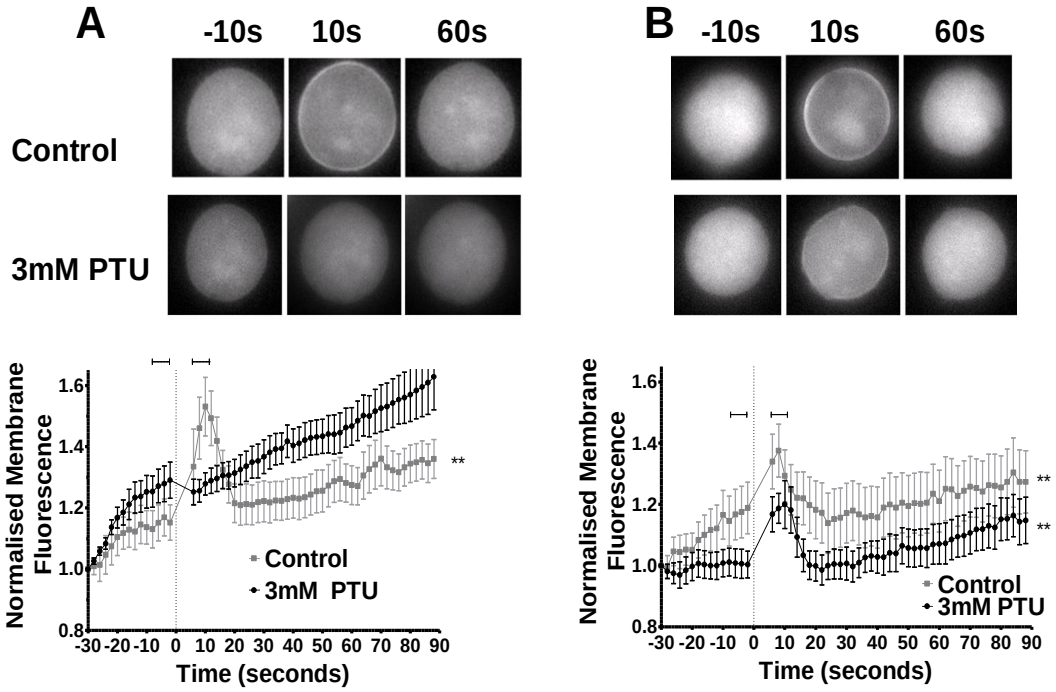

Figure 6.4. PH_{CRAC} membrane fluorescence during global cAMP stimulation in wild type and *grlJ*⁻ cells following incubation in phosphate buffer or phenylthiourea (3mM). *WT/PH_{CRAC}GFP* and *grlJ⁻/PH_{CRAC}GFP* were stimulated with 1µM cAMP after an initial 30 second control period. **(A)** Relative *WT/PH_{CRAC}GFP* fluorescence of cells during control conditions and after 10 minute incubation with phenylthiourea (3mM). WT cells showed a significant (P=0.0017) increase in membrane fluorescence upon cAMP stimulation under control conditions after approximately 10 seconds. Upon pre-treatment with 3mM phenylthiourea, cells showed no significant changes in membrane fluorescence after cAMP stimulation, where membrane fluorescence had been inhibited. **(B)** *grlJ⁻/PH_{CRAC}GFP* cells showed significant (P=0.0016 and P=0.0012) increases in membrane fluorescence upon cAMP stimulation for both control and phenylthiourea conditions respectively. Figures are representative of 5 independent experiments measuring a minimum total of ten cells. 2-tailed Student t-tests were used for statistical comparisons. Error bars represent standard error of the mean (SEM). ** P<0.01.

To test PIP_3 production was inhibited by GrlJ-mediated phenylthiourea detection, phospholipids were extracted from cells during global stimulation and quantified using mass ELISA. Chemotactically-competent wild-type, *grlJ⁻* and *grlJ$^{-/+}$* cells were incubated in control medium or phenylthiourea (3mM) for ten minutes before the cells were incubated in trichloroacetic acid at 0, 5 and 20 seconds after global stimulation with cAMP (1µM). Lipids were then extracted and PIP_3 levels quantified. Under control conditions, PIP_3 production rose from 4.8±3.9pmol to 13.8±1.2pmol after 5 seconds post-cAMP stimulation in wild type cells. In addition,

PIP_3 production rose from 2.1±0.05pmol to 10.3±3.4pmol after 5 seconds post-cAMP stimulation in *grlJ*$^{-}$ cells and from 2.7±1.3pmol to 11.0±4.5pmol in *grlJ*$^{-/+}$ cells. A two-way ANOVA identified significant increases in PIP_3 production 5 seconds post-cAMP addition in wild type (P<0.05), *grlJ*$^{-}$ (P<0.05) and *grlJ*$^{-/+}$ (P<0.05) **(Figure 6.5A)**. Ten minutes pre-incubation with phenylthiourea (3mM) blocked PIP3 production in wild type and *grlJ*$^{-/+}$ cells but not *grlJ*- cells, where PIP_3 levels rose from 1.3±0.4pmol to 6.6±2.6pmol 5 seconds post-cAMP stimulation. Subsequent statistical analysis identified a significant increase in PIP_3 production 5 seconds post-cAMP addition in *grlJ*$^{-}$ cells (P<0.01) only **(Figure 6.5B)**. This evidence further supports a role for phenylthiourea causing inhibition of the PI3K pathway upon detection by GrlJ.

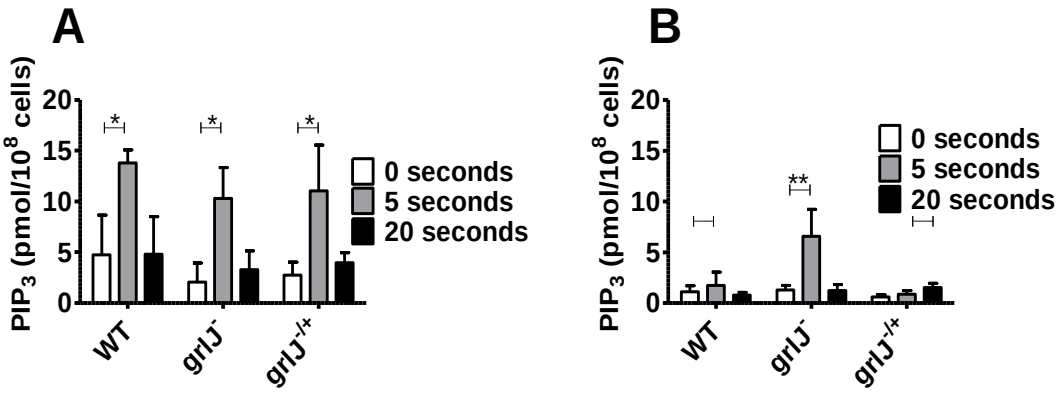

Figure 6.5. PIP_3 production during global stimulation with cAMP in wild type, *grlJ*$^{-}$ and *grlJ*$^{-/+}$ cells following ten minute incubation with phosphate buffer or phenylthiourea (3mM). Mass ELISA was used to quantify PIP_3 production 0, 5 and 20 seconds post stimulation with 1µM cAMP. **(A)** Under control conditions, significant changes (P=0.0003) in PIP_3 production at each time point was observed, where a *post-hoc* Bonferroni test identified a significant increase in PIP_3 production at 5 seconds following global stimulation in wild type (P<0.05), *grlJ*$^{-}$ (P<0.05) and *grlJ*$^{-/+}$ (P<0.05) cells. **(B)** Incubation with phenylthiourea (3mM). Significant changes (P=0.0202) in PIP_3 production at each time points was observed, where a *post-hoc* Bonferroni test identified a significant increase in PIP_3 production at 5 seconds following global stimulation in *grlJ*$^{-}$ (P<0.05) but not wild-type or grlJ$^{-/+}$ cell lines. Figures are representative of triplicate experiments using a 2-way ANOVA for statistical comparisons. Error bars represent standard error of the mean (SEM). * P<0.05 ** P<0.01.

6.4. Discussion

Generation of the *Dictyostelium grlJ*$^{-}$ and *grlJ*$^{-/+}$ mutants in the Ax2 background strain, used previously to screen for responses to emetic and aversive compounds **(Chapter 3)**, enabled a comparison of phenylthiourea detection between these cell lines. GrlJ was previously shown to be partially responsible for a reduction in *Dictyostelium* growth and cell movement in the presence of phenylthiourea **(Chapter 5)**. To establish the molecular mechanism of the GrlJ-mediated response to phenylthiourea, responses to cell stress **(Figure 6.1)**, through G-protein coupled receptor involvement **(Figure 6.2)** and the PI3K pathway **(Figure 6.3, 6.4, 6.5)** were explored. These experiments confirmed that phenylthiourea detection occurs through G-protein coupled receptor involvement and identified inhibition of the PI3K pathway to be involved in cell behavioural responses to phenylthiourea.

6.4.1. Cell Stress

Hyperosmotic stress results in cell rounding and a subsequent loss of cell shape in *Dictyostelium* (Aizawa et al., 1999). Exposure of wild type cells to hyperosmotic stress conditions using sorbitol (0.2mM) caused significant upregulation of *rtoA* but not *yakA* or *gapA*, which had previously also shown increased expression under these conditions (Pakes et al., 2011) **(Figure 6.1)**. Conflicting evidence has also suggested that YakA does not play a role in the response to osmotic shock (Taminato et al., 2002), which is supported by the results of the cell stress experiments in this chapter.

Osmotic stress initiates the activation of STATc signalling in *Dictyostelium*, which subsequently affects regulation of *gapA* and *rtoA* (Na et al., 2007; Kawata, 2011). STATc activation is regulated by intracellular cyclic guanosine

monophosphate and calcium levels (Araki et al., 2010). Although currently unknown, it is likely detection of hyperosmotic stress is mediated by G-protein coupled receptor activation, due to activation of the monomeric G-protein, Rap1 (Kang et al., 2002). Initiation of osmotic stress in *Dictyostelium* increases actin phosphorylation and produces major cytoskeletal changes (Zischka et al., 1999), resulting in increased cell rounding (Rivero et al., 1996), which is consistent with the acute cellular response to phenylthiourea observed.

Since expression of *yakA*, *gapA* or *rtoA* was unaffected by phenylthiourea, it is likely the tastant does not block *Dictyostelium* behaviour by the induction of osmotic stress or via increased STATc activity. In addition, osmotically-stressed cells also maintain their ability to migrate towards cAMP, albeit at a reduced rate (Kuwayama and van Haastert, 1998; Rivero et al., 1996), which is inconsistent with the phenylthiourea-mediated block in *Dictyostelium* behaviour previously shown in Dunn chamber motility (Robery et al., 2011). Together, this evidence demonstrates that hyperosmotic stress or its components in signalling are unlikely to be involved in the phenylthiourea-mediated inhibition of cell behaviour in *Dictyostelium*.

6.4.2. G-protein coupled receptor signalling in phenylthiourea detection

Cell rounding in *Dictyostelium* can be mediated by both G-protein coupled receptor dependent and independent targets. For example, the membrane permeable compound, latrunculin, commonly used in *Dictyostelium*, induces cell rounding by inhibition of actin polymerisation and the destabilisation of existing filaments (Langridge and Kay, 2007; Xu et al., 2007). Conversely, G-protein coupled receptor binding compounds such as derivatives of cAMP (van Haastert et al., 1982)

or high concentrations of cAMP can also initiate cell rounding (Langridge and Kay, 2006; Varnum and Soll, 1984). To test a role for GrlJ as a G-protein coupled receptor involved in phenylthiourea detection, random cell movement assays were performed using the *gβ*$^{-}$ mutant. *Dictyostelium* contains a single Gβ subunit (Lilly et al., 1993), which is essential for all G-protein coupled receptor mediated signalling. *gβ*$^{-}$ cells showed no change in behaviour in random movement upon exposure to phenylthiourea (3mM), whereas significant differences in all movement parameters were observed for wild-type cells **(Figure 6.2)**. This data suggested that phenylthiourea detection was occurring through heterotrimeric G-proteins, which further supports a role for the through G-protein coupled receptor involvement GrlJ as the receptor responsible.

Dictyostelium contains 55 monomeric and heterotrimeric G-protein coupled receptors, which includes four cAMP receptors, eight cAMP-like receptors, one secretin receptor, seventeen Grl-family receptors and twenty five frizzled receptors (Prabhu and Eichinger, 2006). Heterotrimeric G-protein signalling is crucial to the developmental cycle in *Dictyostelium*, since *gβ*$^{-}$ cells cannot aggregate upon starvation (Lilly et al., 1993) due to an inability to amplify external chemical gradients, such as in the case of cAMP (Wang et al., 2011). This is consistent with studies of neutrophil chemotaxis, where subunit inhibition results in the disruption of motility through effects on PI3K pathway (Lehmann et al., 2008). In addition, studies have shown *Dictyostelium* cells lacking the Gβ-subunit cannot regulate actin polymerisation efficiently (Peracino et al., 1998). Since the phenylthiourea-mediated block in cell behaviour did not occur in cells lacking heterotrimeric G-protein assembly, the block in *Dictyostelium* behaviour is likely to be G-protein coupled receptor mediated.

Phenylthiourea detection also occurs through G-protein coupled receptor activation in mammalian cells (Bufe et al., 2005), resulting in dissociation of Gα-gustducin from heterotrimeric T2R receptors (Caicedo et al., 2003; Clapp et al., 2008). Gα-gustducin dissociation results in phosphodiesterase-mediated reduction in intracellular cAMP concentration, which subsequently results in the inhibitory regulation of calcium signalling (Clapp et al., 2008). In *Dictyostelium*, cAMP production is regulated by PKB/Akt and CRAC-mediated activation of adenylyl cyclase A (Garcia and Parent, 2008a; Kae et al., 2007; McMains et al., 2008). Therefore, the signalling mechanisms responsible for the regulation of intracellular cAMP differ between human taste cells and *Dictyostelium*. However, inhibition of *Dictyostelium* cell behaviour through G-protein coupled receptor activation could result in decreased cAMP levels through inhibition of signalling pathways involved in chemotaxis such as PI3K or TORC2 (Kamimura et al., 2008; Charest et al., 2010)

In human taste cells, regulation of cAMP and subsequent calcium signalling by Gα-gustducin may not be crucial to bitter tastant detection since the G-protein is not expressed in all taste receptor cells (Caicedo et al., 2003). The Gα-subunit, Gαi2, is also expressed in most bitter taste receptor cells, although its role in bitter taste transduction is currently unknown (Caicedo et al., 2003; Ueda et al., 2003; Kusakabe et al., 2000). Dissociation of Gαi2 from CXR4 receptors in leukocytes results in PI3K activity and subsequently initiates chemotactic behaviour in leukocytes (Ngai et al., 2009). Therefore, dissociation of Gαi2 in taste cells upon bitter tastant detection may regulate PI3K activity. Since *Dictyostelium* and leukocytes share many common signalling pathways (Jin et al., 2009), G-protein dissociation upon G-protein coupled receptor-mediated detection of bitter tastants may inhibit PI3K activity.

T2R receptor activation also results in the dissociation of Gβ3 and Gɣ13 subunits in mammalian taste cells, which activate phospholipase C to degrade PIP_2 into diacylglycerol and inositol triphosphate (Rossler et al., 2000; Rossler et al., 1998). In *Dictyostelium*, PIP_2 formation, regulated by PTEN, also activates phospholipase C to produce diacylglycerol and inositol triphosphate (Kortholt et al., 2007). Phospholipase C activation is shown to regulate PIP_3 mediated chemotaxis (Kortholt et al., 2007; Suire et al., 2012), disruption of which by phenylthiourea, could therefore interfere with the maintenance of cell polarity and correctly orientated migration.

In chemotactically-competent *Dictyostelium* cells, G-protein coupled receptor-mediated migration is driven through four key signalling pathways, which include the PI3K (Huang et al., 2003), phospholipase A_2 (although a receptor responsible is yet to be discovered) (Chen et al., 2007), soluble guanylyl cyclase (Veltman et al., 2008) and TORC2 complex (Kamimura et al., 2008). This research has identified phenylthiourea-mediated GrlJ activation alone to be responsible for inhibiting at least one of these key signalling pathways in *Dictyostelium* since *grlJ*$^-$ cells show partial resistance to the bitter tastant.

6.4.3. Involvement of the PI3K pathway

Phosphoinositide signalling is one of the four key signalling mechanisms initiated upon cAR activation (Veltman et al., 2008). Cells lacking the ability to activate the PI3K pathway, both pharmacologically and upon gene ablation, maintain their ability to migrate towards a steep but not shallow chemotactic gradients (Hoeller and Kay, 2007; Loovers et al., 2006). In shallow gradients and in random cell movement, cells lacking the ability to generate PIP_3 gradients are rounded and form

unstable protrusions (Loovers et al., 2006; Hoeller and Kay, 2007). The PI3K pathway is therefore critical in migration during shallow chemotactic gradients, playing a comprehensive role in the general control of basic cell motility (King and Insall, 2009; van Haastert et al., 2007a). During random cell movement, the PI3K pathway is thought to negatively regulate the formation of pseudopods and control stochastic changes in the actin cytoskeleton in a process independent of G-protein signalling (Sasaki et al., 2007). PI3K activity therefore occurs both dependent and independent of G-protein coupled receptor activation, where inhibition during random cell movement or chemotaxis in a shallow gradient could have detrimental effects on cell behaviour.

To determine whether the PI3K pathway was involved in phenylthiourea-mediated inhibition of cell movement, a mutant lacking all PI3K activity, *PI31-5K/PTEN*$^{-}$ was used in random cell movement assays. Addition of phenylthiourea showed that the *PI31-5K/PTEN*$^{-}$ mutant is partially resistant to the block in *Dictyostelium* behaviour observed in wild-type cells **(Figure 6.3)**. Inhibition of signalling through the PI3K pathway results in the loss of spatial and temporal control in *Dictyostelium* chemotaxis (Huang et al., 2003). This effect is shown throughout this thesis in both random cell movement and chemotaxis in a steep gradient of cAMP, where phenylthiourea causes cells to round up and stop moving **(Chapters 3-5)**. Since *Dictyostelium* behaviour was inhibited under both of these conditions, signalling mechanisms other than the PI3K pathway are likely also to be inhibited upon phenylthiourea detection.

To examine a role for PI3K-dependent signalling through GrlJ in phenylthiourea detection, the transient stimulation of PIP_3 was assessed. In these experiments, wild-type and *grlJ*$^{-}$ cells expressing PH_{CRAC}GFP were incubated with

latrunculin in a control buffer or phenylthiourea (3mM) before global stimulation with cAMP. Treatment of cells with latrunculin results in a loss of cell polarity and disruption of the actin cytoskeleton, resulting in PIP_3 accumulation across the whole cell membrane upon global stimulation (Janetopoulos et al., 2004). Under control conditions, using latrunculin-treated cells, global stimulation resulted in a surge in PH_{CRAC}GFP fluorescence at the cell membrane in both wild-type and *grlJ*$^-$ cells, which is consistent with previous findings (Huang et al., 2003; Xu et al., 2007) **(Figure 6.4)**. PH_{CRAC}GFP is a marker for PIP_3 synthesis since the phosphoinositide binds to the pleckstrin homology domain within CRAC (Dormann et al., 2002). Under physiological conditions (in the absence of latrunculin), PIP_3 also enables the recruitment of myosin-I to the cell membrane, where it induces actin polymerisation and subsequent formation of pseudopods in the direction of the cAMP gradient (Chen and Iijima, 2012).

Upon global stimulation of transformed cells (with PH_{CRAC}GFP) pre-incubated with phenylthiourea (3mM), only *grlJ*$^-$ cells showed translocation of fluorescence to the membrane, where polarisation in wild type cells was inhibited **(Figure 6.4)**. This evidence identified GrlJ as a receptor that blocks the translocation of CRAC to the cell membrane. To test the GrlJ-mediated detection of phenylthiourea resulted in inhibition of PIP_3 and not CRAC, quantification of the phosphoinositide by mass ELISA identified a block in PIP_3 production in wild type and *grlJ*$^{-/+}$ but not *grlJ*$^-$ cells upon global stimulation **(Figure 6.5)**. These data together therefore indicated detection of phenylthiourea through GrlJ caused a block in PIP_3 production. Synthesis of PIP_3 can be blocked by a number of mechanisms, such as increased PTEN activity for example, which is shown to act as a negative regulator of cell

polarity, by converting PIP_3 back into PIP_2 (Iijima et al., 2004; Huang et al., 2003; Iijima and Devreotes, 2002).

PTEN is previously shown to act as a global inhibitor of PIP_3 production at the cytoplasmic face of the membrane (Gerisch et al., 2012). Global stimulation with cAMP initiates negative fluctuations in PTEN resulting in a subset of the membrane lacking PTEN and allowing for the synthesis of PIP_3 synthesis, resulting in specifically orientated polarisation (Gerisch et al., 2012). These spatially orientated patches of PIP_3 subsequently allow for the formation of pseudopods (Asano et al., 2008; Postma et al., 2004). Increased PTEN activity could therefore decrease spatially orientated patches of PIP_3 in addition to enhancing PIP_3 degradation at the membrane upon global stimulation.

Another mechanism for a decrease in PIP_3 production mediated by GrlJ could be a reduction in total phosphoinositides. Previous research has shown an anti-epileptic drug, valproic acid, blocks chemotactic migration of *Dictyostelium* cells towards cAMP by reducing the production of phosphoinositides (Xu et al., 2007; Chang et al., 2012). In *Dictyostelium*, phosphoinositides are constantly recycled, where inositol triphosphate (a product of phospholipase C mediated PIP_2 degradation) is converted into inositol and subsequently into phosphatidylinositol (PIP), before conversion to PIP_2 (Chang et al., 2012). In addition, *de novo* synthesis of phosphoinositides is also regulated by myo-inositol-3P-synthase (INO1) mediated breakdown of glucose-6-phosphate (a product of respiration) into inositol monophosphate; as well as propyloligopeptidase, which regulates the conversion of higher order inositol phosphates to inositol triphosphate (Chang et al., 2012). Although valproic acid is taken into cells by solute carrier proteins (Terbach et al., 2011), activation of GrlJ by phenylthiourea could provide an inhibitory effect on

phosphoinositide levels by inhibiting enzymes involved in recycling or *de novo* synthesis. Alternatively, as with valproic acid, phosphoinositol levels could also be reduced by a mechanism, independent of inositol recycling (Chang et al., 2012).

In addition to potential targets downstream from G-protein coupled receptor signalling, such as increased PTEN activity or decreased phosphoinositol levels, GrlJ activation by phenylthiourea may inhibit proteins upstream of PI3K activity. For example, the myosin, MyoG, is required for *Dictyostelium* polarisation and chemotaxis in response to cAMP stimulation (Breshears et al., 2010). Ablation of this protein in *Dictyostelium* results in rounded cells that are unable to polarise or migrate in random movement or chemotactically towards cAMP (Breshears et al., 2010). GrlJ activation by phenylthiourea could therefore inhibit MyoG, preventing *Dictyostelium* PI3K activity and causing subsequent inhibition of random cell movement and motility.

GrlJ-mediated inhibition of PI3K signalling by phenylthiourea may also be inhibited by monomeric G-protein signalling. *Dictyostelium* chemotactic signalling occurs primarily as a result of heterotrimeric G-protein dissociation from cAR in response to cAMP, leading to the activation of monomeric G-proteins, particularly RasC and RasG (Bolourani et al., 2006). These activated GTPases then target activation of a number of signalling cascades, which includes the PI3K pathway (Kortholt et al., 2011). In addition, another RasGTPase, Rap1, is shown to regulate PIP_3 formation by direct interaction with the PI3K pathway (Kortholt et al., 2010). Finally, RasGTPase activation also has a distinct role in basal chemotactic motility, which is independent of signal amplification pathways (Kortholt et al., 2011). Since phenylthiourea results in a complete block in *Dictyostelium* behaviour, GrlJ activation could therefore potentially block Ras signalling, which could result in both an

inhibition in cell movement as well as inhibition of signal amplification targets such as PI3K.

In *Dictyostelium*, Ras signalling is regulated by both RasGEFs and RasGAPs, which activate and deactivate the monomeric G-protein respectively. Disruption of RasGAP activity, such as Nf1, results in severe chemotactic defects, where cells are unable to deactivate GTPase activity (Zhang et al., 2008). This results in prolonged PI3K activity and an inability for surges in PIP_3 to be negatively regulated in directional sensing (Zhang et al., 2008). Conversely, disruption of RasGEFs, such as RasGEFA and RasGEFR, results in reduced activation of RasC and RasG, respectively (Kae et al., 2007). Disruption of RasC and RasG results in decreased PI3K activity, inhibiting adenylyl cyclase and PKB/Akt activity respectively, (Bolourani et al., 2006), both of which are involved in the PI3K pathway (Lilly and Devreotes, 1994; Funamoto et al., 2001; Meili et al., 1999). Therefore phenylthiourea-mediated activation of GrlJ could induce decreased RasGEF or potentially increased RasGAP activity, which would result in the disruption of PI3K-mediated signalling, amongst other chemotactic signalling pathways.

Monomeric G-protein activation of Ras may also be inhibited by regulators further upstream, such as disruption of guanine exchange factors for heterotrimeric Gα-proteins. For example, previous research has identified disruption of the guanine exchange factor, Ric8, responsible for the dissociation of Gα2 in response to chemotactic signalling, results in dramatic reductions of motility down shallow cAMP gradients (Kataria et al., 2013). In addition, G-protein coupled receptor-mediated activation of Ras and subsequent PI3K signalling is also shown to be regulated by phospholipase Cβ2/β3 signalling in neutrophils, inhibition of which could therefore also result in reduced PIP_3 formation (Suire et al., 2012).

In mammals, TAS2R38 activation by phenylthiourea produces a phosphodiesterase cascade, resulting in a reduction of intracellular cAMP, as well as phospholipase Cβ2-mediated cleavage of PIP_2 into IP_3 and DAG (Bufe et al., 2005; Kinnamon, 2011). Therefore, whilst phospholipid signalling is central to T2R receptor signalling events, the PI3K pathway has not been investigated in bitter taste transduction. Interestingly, previous research has shown binding of odorants, such as the bittersweet compound, citral, activates PI3K in mouse and rat olfactory receptor neurones (Ukhanov et al., 2013; Ukhanov et al., 2011; Brunert et al., 2010). Binding of odorants such as citral to olfactory receptors is believed to cause a stabilising effect, which mediates PI3K activity to inhibit downstream cell excitation (Ukhanov et al., 2011; Ukhanov et al., 2013). In *Dictyostelium*, phenylthiourea causes partial inhibition of cell behaviour by inhibiting PI3K activity **(Figure 6.3)**. Therefore, whilst olfactory receptor (in mammals) and GrlJ (in Dictyostelium) activation causes opposing PI3K activity, both mechanisms mediate an inhibitory cellular response.

Activation of the PI3K pathway is also mediated by the heterotrimeric G-protein, Gαi2, which is also found in many bitter taste receptor cells (Ngai et al., 2009; Ueda et al., 2003; Kusakabe et al., 2000; Caicedo et al., 2003). Since a mechanism for signal transduction by the G-protein response to bitter tastants remains unknown, compounds such as phenylthiourea may cause Gαi2 activation, which may result in an inhibitory regulatory role for cell excitability in taste cells.

6.5. Summary

Ablation of *grlJ* in *Dictyostelium* cells resulted in partial resistance to phenylthiourea in motility and random cell movement assays, where the wild-type response was restored upon gene complementation. Upon analysis of the molecular mechanisms behind GrlJ-mediated detection of phenylthiourea, inhibition in cell behaviour was caused by G-protein coupled receptor activation. Further analysis into the signalling pathways downstream from GrlJ activation, identified inhibition of the PI3K pathway to be involved in the phenylthiourea mediated block in random cell movement and motility.

Finally, the currently accepted mechanism of action for phenylthiourea detection in humans is regarded as insufficient (Hayes et al., 2008), and hence alternative pathways and/or receptors may exist. GrlJ is a $GABA_B$-like protein that shares sequence homology with other GABAB receptors, and it possible that this similarity may extend beyond structure to potential mechanisms of action for phenylthiourea detection. This hypothesis will be explored in chapter 7.

Chapter 7

Identification of an uncharacterised human protein involved in phenylthiourea detection

In mammalian taste receptor cells, bitter taste transduction occurs through T2R receptor activation, where cleavage of PIP_2 to release inositol triphosphate results in calcium release and cell excitation (Kinnamon, 2011). Phenylthiourea and its related compound, propylthiouracil, are unique bitter tastants that activate the TAS2R38 receptor only (Bufe et al., 2005). Sensitivity to TAS2R38 receptor agonists in human taste cells varies depending on single nucleotide polymorphisms in the *TAS2R38* gene, resulting in five different haplotypes and three different taster statuses: supertaster, taster and non-taster (Bufe et al., 2005). Previous research has however shown high concentrations of the TAS2R38 agonist, propylthiouracil, causes identical bitter sensation in both taster and non-taster status individuals (Hayes et al., 2008). This research has provided convincing evidence that other, yet to be identified receptors, must be involved in perception of TAS2R38 agonists such as phenylthiourea and propylthiouracil (Hayes et al., 2008; Genick et al., 2011).

Previous chapters in this thesis describe the inhibition of cell movement in *Dictyostelium* by phenylthiourea involves G-protein coupled receptor-mediated signalling, partially through GrlJ. Phenylthiourea-mediated activation of GrlJ results the inhibition of transient PIP_3 production upon global stimulation with cAMP in chemotactically-competent cells **(Chapter 6)**.

In this chapter, an uncharacterised human protein was identified by homology to GrlJ, and a role for this protein in *Dictyostelium* phenylthiourea perception was examined.

7.1. Identification of an uncharacterised human protein

To determine whether any other organisms contained a protein related to GrlJ and thus may detect phenylthiourea, a database search to identify proteins homologous at a protein level (BLAST analysis) was performed using GrlJ. This identified fourteen of the seventeen members of the Grl-family of receptors in *Dictyostelium* and a number of proteins from various multicellular organisms and bacteria **(Table 7.1)**. Interestingly, the first protein belonging to a chordate was an uncharacterised human protein, Q8NHA5, sharing weak homology with GrlJ, showing 26% identity and 48% similarity, with a BLASTP probability of $2e^{-20}$. To investigate the structure of Q8NHA5, the protein sequence was analysed using hydrophobicity analysis (Kyte and Doolittle, 1982), which confirmed the protein contained a seven transmembrane domain. This was also confirmed using the Pfam 27.0 database (Punta et al., 2012).

To compare the *Dictyostelium* GrlJ and the human Q8NHA5 proteins directly, protein sequences were aligned using Clustal Omega multiple sequence alignment tool (Sievers et al., 2011) **(Figure 7.1.)**. Based upon these alignments GrlJ and Q8NHA5 shared limited amino acid similarity in the N and C terminal regions, although some sequence conservation occurred within the transmembrane domains. Since all G-protein coupled receptors have seven transmembrane domains, GrlJ was also aligned with the unrelated proteins, human TAS2R38 **(Appendix 7)** and *Dictyostelium* cAR1 receptor **(Appendix 8)**, where substantially less sequence homology was observed throughout these regions. This suggested transmembrane sequence homology between Q8NHA5 and GrlJ specifically, rather than a common sequence found in all G-protein coupled receptors.

Since *grlJ* encodes a $GABA_B$-like receptor (Prabhu et al., 2007b), the human Q8NHA5 protein sequence was compared with other human $GABA_B$ receptors, where Q8NHA5 shared high sequence homology with $GABA_B$ receptor subunit 1 isoform 1B showing 93% identity and 94% similarity; 1A showing 90% identity and 91% similarity; and 1C showing 90% identity and 91% similarity. Subsequent alignment of Q8NHA5, $GABA_{BR1B}$, $GABA_{BR1C}$ and $GABA_{BR1A}$ showed most sequence similarity within the transmembrane regions of the protein **(Figure 7.2.)**. Since GrlJ encodes a $GABA_B$-like receptor and Q8NHA5 shared substantial sequence homology with $GABA_{BR1}$ isoforms, it is likely that the uncharacterised Q8NHA5 protein is a $GABA_B$ subunit 1 receptor.

BLAST hit/ Protein Name	Organism	Receptor	Amino Acid Length	BLASTP probability	Identity (%)	Similarity (%)
GRLJ_DICDI	*Dictyostelium discoideum*	Metabotrophic glutamate receptor B like	783	0	100	100
GRLF_DICDI	*Dictyostelium discoideum*	Metabotrophic glutamate receptor B like	770	0	60	74
GRLB_DICDI	*Dictyostelium discoideum*	Metabotrophic glutamate receptor B like	755	0	58	74
GRLA_DICDI	*Dictyostelium discoideum*	Metabotrophic glutamate receptor B like	798	0	55	73
GRLO_DICDI	*Dictyostelium discoideum*	Metabotrophic glutamate receptor B like	819	1.00E-164	41	58
GRLC_DICDI	*Dictyostelium discoideum*	Metabotrophic glutamate receptor B like	800	1.00E-102	28	51
GRLH_DICDI	*Dictyostelium discoideum*	Metabotrophic glutamate receptor B like	764	5.00E-99	31	52
GRLG_DICDI	*Dictyostelium discoideum*	Metabotrophic glutamate receptor B like	772	8.00E-97	30	52
GRLM_DICDI	*Dictyostelium discoideum*	Metabotrophic glutamate receptor B like	749	7.00E-92	30	51
GRLD_DICDI	*Dictyostelium discoideum*	Metabotrophic glutamate receptor B like	791	2.00E-90	29	49
GRLK_DICDI	*Dictyostelium discoideum*	Metabotrophic glutamate receptor B like	704	3.00E-87	30	52
GRLL_DICDI	*Dictyostelium discoideum*	Metabotrophic glutamate receptor B like	708	8.00E-70	27	48

GRLN_DICDI	*Dictyostelium discoideum*	Metabotrophic glutamate receptor B like	891	2.00E-58	28	47
C3Y433_BRAFL	*Branchiostoma floridae*	Putative uncharacterized protein	1104	2.00E-26	26	47
C3YEC0_BRAFL	*Branchiostoma floridae*	Putative uncharacterized protein	631	1.00E-22	28	52
B3RUR6_TRIAD	*Trichoplax adhaerens*	Putative uncharacterized protein	729	1.00E-21	27	47
A7RHX2_NEMVE	*Nematostella vectensis*	Predicted protein (Fragment)	719	2.00E-21	25	50
Q6FFI9_ACIAD	*Acinetobacter sp.*	Putative uncharacterized protein	393	4.00E-21	26	46
B3RTG5_TRIAD	*Trichoplax adhaerens*	Putative uncharacterized protein	837	7.00E-21	26	46
GRLE_DICDI	*Dictyostelium discoideum*	Metabotrophic glutamate receptor B like	816	2.00E-20	23	44
Q8NHA5_HUMAN	*Homo sapien*	Uncharacterized protein	866	3.00E-20	26	48

Table 7.1. Database search (BLAST analysis) for proteins sharing homology with GrlJ. A basic local alignment search tool analysis was performed using the protein sequence of GrlJ identifying fourteen of seventeen *Dictyostelium* Grl-family proteins (highlighted by in grey), two uncharacterised *Branciostoma floridae* (lancelet) proteins, two uncharacterised *Trichoplax adhaerens* (placozoa) proteins, one predicted *Nematostella vectensis* (sea anemone) protein, one uncharacterised *Acinetobacter sp.*(bacteria) protein and one uncharacterised *Homo sapien* protein (highlighted in dark grey). In addition, *Dictyostelium* GrlJ also shared protein sequence homology with ten G-protein coupled receptors belonging to the slime mould *Polysphondylium palladium*. Since *Dictyostelium* and *Polysphondylium* are closely related, these results have been omitted for simplicity.

```
grlJ          -------------------------------------------------MKILLYIAIILS 12
Q8NHA5        MGPGAPFARVGWPLPLLVVMAAGVAPVWASHSPHLPRPHSRVPPHPSSERRAVYIGALFP 60
                                                              :  :**. ::.

grlJ          FFSLITISSECKIAVLLSGSPNDLGYNYLMNEARVKAESELKLDFSIYYENLEESMEEAE 72
Q8NHA5        MSGGWPGGQACQPAVEMALEDVNSRRDILPDYELKLIHHDSKVALDMGCDPGQATKYLYE 120
              : .  . .. *: ** :: .  :   : * :      . : *: :.:  :  : :    *

grlJ          KAFQDALHKG------------ANLIVVGSFVHVGLGLKYAALTKDQDIYWIIRGNKRPN 120
Q8NHA5        LLYNDPIKIILMPGCSSVSTLVAEAARMWNLIVLSYGSSSPALSNRQRFPTFFRTHPSAT 180
                ::*.::             *:   : .:: :. * . .**:: * :  ::* :  ..

grlJ          PDLP------------HVVILNFNSFELHYLLGYFSGLMTKTGIVG------FVAPGPDV 162
Q8NHA5        LHNPTRVKLFEKWGWKKIATIQQTTEVFTSTLDDLEERVKEAGIEITFRQSFFSDPAVPV 240
               . *            ::. :: .:  :   *. :.  :.::**        *  *.  *

grlJ          NTISTDNSFYLGAKYARPNITFLNVYVQSWYNPNVSYSAAKMLIKNG----ADLIGMSQD 218
Q8NHA5        KNLKVYKERLFGKKYVWFLIGWYADNWFKIYDPSINCTVDEMTEAVEGHITTEIVMLNPA 300
              :.:.. :.  :* **.   * :      . *:*.:. :. :*         :::: :.

grlJ          DMSCQKAMMDSGLIGIGATGYPTHLLFGGNVGVSYITNWTNLYVKYAQHVLNDDWPDYSS 278
Q8NHA5        NTRSISNMTSQEFVEKLTKRLKRHPEETGGFQEAPLAYDAIWALALALNKTSGGGGRSGV 360
              :  . . * .. ::   :.    *    *..  : ::  :   :  * :  ...    .

grlJ          YFTNLSREDSIFIDDYSYKVPIDIQNLVNDEIQRLKNTSYIPYRSDPYLAQLGIPFDSKG 338
Q8NHA5        RLEDFNYNNQTITDQIYRAMNSSSFEGVSGHVVFDASGSRMAWTLIEQLQGG----SYKK 416
               : ::. ::. : *:    :  .  : *...:    . * :.:     *       . *

grlJ          LLVEDQFRANKKLLKGDSISKVIDFGQYSIPIEFIDYP-NSLKYGVTIVSGVCIFICLVC 397
Q8NHA5        IGYYDSTKDDLSWSKTDKWIGGSPPADQTLVIKTFRFLSQKLFISVSVLSSLGIVLAVVC 476
              :   *. : : .  * *.       .: :: *: : :  :.*  .*:::*.: *.:.:**

grlJ          MTLVVVFKKARVIKSSSPAFLLLILLGCCIIFAACILFAQS-------PTNQTCSARIWL 450
Q8NHA5        LSFNIYNSHVRYIQNSQPNLNNLTAVGCSLALAAVFPLGLDGYHIGRNQFPFVCQARLWL 536
              ::: :  .:.* *:.*.* :  *  :**.: :** : :. .           .*.**:**
```

```
grlJ            LSLGYTLFLGNLLVKNWRIWLLFDNPKLKK---RAITNWKLYPWVFAILAIDVMILAIWQ 507
Q8NHA5          LGLGFSLGYGSMFTKIWWVHTVFTKKEEKKEWRKTLEPWKLYATVGLLVGMDVLTLAIWQ 596
                *.**::*  *.::.* * :  :* : : **   :::  ****. *  ::.:**: *****

grlJ            GLGNINAESRIGYDSLTQYQYKNVCSSDDQGSIALYLLLVFHGLVLLVACFISFKIKVVD 567
Q8NHA5          IVDPLHRTIEVPLERR-CYGQENEQGSVAIRALGLCIFYGYKGLLLLLGIFLAYETKSVS 655
                 :. ::   .:  :    *  :*  .*    ::.* ::  ::**:**:. *:::: * *.

grlJ            IEEFNESKPITTSVY-IITFCLFIVIPLMVSPQSLTSQTTIICVCAIVTTLISMLLLFGS 626
Q8NHA5          TEKINDHRAVGMAIYNVAVLCLITAPVTMILSSQQDAAFAFASLAIVFSSYITLVVLFVP 715
                 *::*: :.:  ::* : .:**: .   *: ...  :  :: .:. :.:: *::::** .

grlJ            KFYKMATQGLAINETFATSTKSSSKSSKSSYGKDNPNPNAINFGEDDTSDETSEEKHKSP 686
Q8NHA5          KMRRLITRGEWQSEAQDTMKTGSSTNNNEEEKSRLLEKENRELEKIIAEKEERVSELRHQ 775
                *: :: *:*   .*:  * ...**...:..  .   : :  :: :  :..*   .: :

grlJ            KQKSVNFSNKSNSHLAVFTSDEETSKTSKLSIDFENSSKDISIDQLQQQKQQPINTNGDL 746
Q8NHA5          LQSRQQLRSRRHPPTPPEPSGGLPRGPPEPPDRLSCDGSRVHLLYKVNPQHCPGNGSVRD 835
                 *.  :: .: :.  .  .*.  .  ..: .  :. ... : :    : :: * * .

grlJ            ENKSNDKIDDDNDNSSVLSKRISNQQNGETEIDSNNV 783
Q8NHA5          KDEAERHNQDEDTGNSHLDLIVGGVFTGESN------ 866
                ::::: : :*:: ..* *.  :..  .**::
```

Figure 7.1. GrlJ and Q8NHA5 sequence alignment. Amino acid sequences of GrlJ and Q8NHA5 were aligned using Clustal Omega low sequence homology, where most sequence homology was seen in the transmembrane domains (highlighted in grey). " * " Amino acid positions containing a single fully conserved residue. " **: "** Amino acid positions containing strongly similar properties scoring >0.5 in the Gonnet PAM 250 matrix. " **.** " Amino acid positions containing weakly similar properties scoring <0.5 in the Gonnet PAM 250 matrix.

```
Q8NHA5      ------------------------------------------------------------
GABAB_1B    ------------------------------------------------------------
GABAB_1A    MLLLLLLAPLFLRPPGAGGAQTPNATSEGCQIIHPPWEGGIRYRGLTRDQVKAINFLPVD
GABAB_1C    MLLLLLLAPLFLRPPGAGGAQTPNATSEGCQIIHPPWEGGIRYRGLTRDQVKAINFLPVD

Q8NHA5      ----------------------------------------------MGPGAPF-------
GABAB_1B    ----------------------------------------------MGPGAPF-------
GABAB_1A    YEIEYVCRGEREVVGPKVRKCLANGSWTDMDTPSRCVRICSKSYLTLENGKVFLTGGDLP
GABAB_1C    YEIEYVCRGEREVVGPKVRKCLANGSWTDMDTPSRCV-----------------------

Q8NHA5      ----ARVGWPLPLLVVMAAGVAPVWASHSPHLPRPHSRVPPHPSSERRAVYIGALFPMSG
GABAB_1B    ----ARVGWPLPLLVVMAAGVAPVWASHSPHLPRPHSRVPPHPSSERRAVYIGALFPMSG
GABAB_1A    ALDGARVDFRCDPDFHLVGSSRSICSQGQWSTPKPHCQVNRTPHSERRAVYIGALFPMSG
GABAB_1C    ---------------------------------------NRTPHSERRAVYIGALFPMSG
                                                    * ****************

Q8NHA5      GWPGGQACQPAVEMALEDVNSRRDILPDYELKLIHHDSKVALDMGCDPGQATKYLYELLY
GABAB_1B    GWPGGQACQPAVEMALEDVNSRRDILPDYELKLIHHDS------KCDPGQATKYLYELLY
GABAB_1A    GWPGGQACQPAVEMALEDVNSRRDILPDYELKLIHHDS------KCDPGQATKYLYELLY
GABAB_1C    GWPGGQACQPAVEMALEDVNSRRDILPDYELKLIHHDS------KCDPGQATKYLYELLY
            ************************************       ***************

Q8NHA5      NDPIKIILMPGCSSVSTLVAEAARMWNLIVLSYGSSSPALSNRQRFPTFFRTHPSATLHN
GABAB_1B    NDPIKIILMPGCSSVSTLVAEAARMWNLIVLSYGSSSPALSNRQRFPTFFRTHPSATLHN
GABAB_1A    NDPIKIILMPGCSSVSTLVAEAARMWNLIVLSYGSSSPALSNRQRFPTFFRTHPSATLHN
GABAB_1C    NDPIKIILMPGCSSVSTLVAEAARMWNLIVLSYGSSSPALSNRQRFPTFFRTHPSATLHN
            ************************************************************

Q8NHA5      PTRVKLFEKWGWKKIATIQQTTEVFTSTLDDLEERVKEAGIEITFRQSFFSDPAVPVKNL
GABAB_1B    PTRVKLFEKWGWKKIATIQQTTEVFTSTLDDLEERVKEAGIEITFRQSFFSDPAVPVKNL
GABAB_1A    PTRVKLFEKWGWKKIATIQQTTEVFTSTLDDLEERVKEAGIEITFRQSFFSDPAVPVKNL
GABAB_1C    PTRVKLFEKWGWKKIATIQQTTEVFTSTLDDLEERVKEAGIEITFRQSFFSDPAVPVKNL
            ************************************************************

Q8NHA5      K----------------------VYKERLFGKKYVWFLIGWYADNWFKIYDPSINCTVDE
GABAB_1B    KRQDARIIVGLFYETEARKVFCEVYKERLFGKKYVWFLIGWYADNWFKIYDPSINCTVDE
```

```
GABAB_1A      KRQDARIIVGLFYETEARKVFCEVYKERLFGKKYVWFLIGWYADNWFKIYDPSINCTVDE
GABAB_1C      KRQDARIIVGLFYETEARKVFCEVYKERLFGKKYVWFLIGWYADNWFKIYDPSINCTVDE
              *                     ************************************

Q8NHA5        MTEAVEGHITTEIVMLNPANTRSISNMTSQEFVEKLTKRLKRHPEETGGFQEAPLAYDAI
GABAB_1B      MTEAVEGHITTEIVMLNPANTRSISNMTSQEFVEKLTKRLKRHPEETGGFQEAPLAYDAI
GABAB_1A      MTEAVEGHITTEIVMLNPANTRSISNMTSQEFVEKLTKRLKRHPEETGGFQEAPLAYDAI
GABAB_1C      MTEAVEGHITTEIVMLNPANTRSISNMTSQEFVEKLTKRLKRHPEETGGFQEAPLAYDAI
              ************************************************************

Q8NHA5        WALALALNKTSGGGGRSGVRLEDFNYNNQTITDQIYRAMNSSSFEGVSGHVVFDASGSRM
GABAB_1B      WALALALNKTSGGGGRSGVRLEDFNYNNQTITDQIYRAMNSSSFEGVSGHVVFDASGSRM
GABAB_1A      WALALALNKTSGGGGRSGVRLEDFNYNNQTITDQIYRAMNSSSFEGVSGHVVFDASGSRM
GABAB_1C      WALALALNKTSGGGGRSGVRLEDFNYNNQTITDQIYRAMNSSSFEGVSGHVVFDASGSRM
              ************************************************************

Q8NHA5        AWTLIEQLQGGSYKKIGYYDSTKDDLSWSKTDKWIGGSPPADQTLVIKTFRFLSQKLFIS
GABAB_1B      AWTLIEQLQGGSYKKIGYYDSTKDDLSWSKTDKWIGGSPPADQTLVIKTFRFLSQKLFIS
GABAB_1A      AWTLIEQLQGGSYKKIGYYDSTKDDLSWSKTDKWIGGSPPADQTLVIKTFRFLSQKLFIS
GABAB_1C      AWTLIEQLQGGSYKKIGYYDSTKDDLSWSKTDKWIGGSPPADQTLVIKTFRFLSQKLFIS
              ************************************************************

Q8NHA5        VSVLSSLGIVLAVVCLSFNIYNSHVRYIQNSQPNLNNLTAVGCSLALAAVFPLGLDGYHI
GABAB_1B      VSVLSSLGIVLAVVCLSFNIYNSHVRYIQNSQPNLNNLTAVGCSLALAAVFPLGLDGYHI
GABAB_1A      VSVLSSLGIVLAVVCLSFNIYNSHVRYIQNSQPNLNNLTAVGCSLALAAVFPLGLDGYHI
GABAB_1C      VSVLSSLGIVLAVVCLSFNIYNSHVRYIQNSQPNLNNLTAVGCSLALAAVFPLGLDGYHI
              ************************************************************

Q8NHA5        GRNQFPFVCQARLWLLGLGFSLGYGSMFTKIWWVHTVFTKKEEKKEWRKTLEPWKLYATV
GABAB_1B      GRNQFPFVCQARLWLLGLGFSLGYGSMFTKIWWVHTVFTKKEEKKEWRKTLEPWKLYATV
GABAB_1A      GRNQFPFVCQARLWLLGLGFSLGYGSMFTKIWWVHTVFTKKEEKKEWRKTLEPWKLYATV
GABAB_1C      GRNQFPFVCQARLWLLGLGFSLGYGSMFTKIWWVHTVFTKKEEKKEWRKTLEPWKLYATV
              ************************************************************

Q8NHA5        GLLVGMDVLTLAIWQIVDPLHRTIEVPLERRCYGQE-------NEQGSVAIRALGLCIFY
GABAB_1B      GLLVGMDVLTLAIWQIVDPLHRTIETFAKEEPKEDIDVSILPQLEHCSSRKMNTWLGIFY
GABAB_1A      GLLVGMDVLTLAIWQIVDPLHRTIETFAKEEPKEDIDVSILPQLEHCSSRKMNTWLGIFY
GABAB_1C      GLLVGMDVLTLAIWQIVDPLHRTIETFAKEEPKEDIDVSILPQLEHCSSRKMNTWLGIFY
```

```
                ************************.  :..   :        *: *       * ***

Q8NHA5          GYKGLLLLLGIFLAYETKSVSTEKINDHRAVGMAIYNVAVLCLITAPVTMILSSQQDAAF
GABAB_1B        GYKGLLLLLGIFLAYETKSVSTEKINDHRAVGMAIYNVAVLCLITAPVTMILSSQQDAAF
GABAB_1A        GYKGLLLLLGIFLAYETKSVSTEKINDHRAVGMAIYNVAVLCLITAPVTMILSSQQDAAF
GABAB_1C        GYKGLLLLLGIFLAYETKSVSTEKINDHRAVGMAIYNVAVLCLITAPVTMILSSQQDAAF
                ************************************************************

Q8NHA5          AFASLAIVFSSYITLVVLFVPKMRRLITRGEWQSEAQDTMKTGSSTNNNEEEKSRLLEKE
GABAB_1B        AFASLAIVFSSYITLVVLFVPKMRRLITRGEWQSEAQDTMKTGSSTNNNEEEKSRLLEKE
GABAB_1A        AFASLAIVFSSYITLVVLFVPKMRRLITRGEWQSEAQDTMKTGSSTNNNEEEKSRLLEKE
GABAB_1C        AFASLAIVFSSYITLVVLFVPKMRRLITRGEWQSEAQDTMKTGSSTNNNEEEKSRLLEKE
                ************************************************************

Q8NHA5          NRELEKIIAEKEERVSELRHQLQSRQQLRSRRHPPTPPEPSGGLPRGPPEPPDRLSCDGS
GABAB_1B        NRELEKIIAEKEERVSELRHQLQSRQQLRSRRHPPTPPEPSGGLPRGPPEPPDRLSCDGS
GABAB_1A        NRELEKIIAEKEERVSELRHQLQSRQQLRSRRHPPTPPEPSGGLPRGPPEPPDRLSCDGS
GABAB_1C        NRELEKIIAEKEERVSELRHQLQSRQQLRSRRHPPTPPEPSGGLPRGPPEPPDRLSCDGS
                ************************************************************

Q8NHA5          RVHLLYKVNPQHCPGNGSVRDKDEAERHNQDEDTGNSHLDLIVGGVFTGESN
GABAB_1B        RVHLLYK-----------------------------------------------
GABAB_1A        RVHLLYK-----------------------------------------------
GABAB_1C        RVHLLYK-----------------------------------------------
                *******
```

Figure 7.2. Q8NHA5 and $GABA_B$ receptor subunit 1 isoform sequence alignments. Amino acid sequences of Q8NHA5 $GABA_B$ receptor subunit 1B, 1C and 1A were aligned using Clustal Omega showing high sequence homology. " ***** " Amino acid positions containing a single fully conserved residue. " **:** " Amino acid positions containing strongly similar properties scoring >0.5 in the Gonnet PAM 250 matrix. " **.** **"** Amino acid positions containing weakly similar properties scoring <0.5 in the Gonnet PAM 250 matrix.

Maturation and localisation of $GABA_B$ receptors involves addition of N-linked glycosylation sites to the N-terminus of the protein (White et al., 1998). In addition, research has also identified the involvement of N-linked glycosylation sites the maturation of T2R receptors (Reichling et al., 2008). To examine GrlJ and Q8NHA5 for potential glycosylation sites, the N-terminal protein sequence of GrlJ, Q8NHA5 and $GABA_{BR1B}$ were analysed using NetNGlyc 1.0 Server. Interestingly, five putative sites were found in GrlJ, six were found in Q8NHA5 and seven were found in the $GABA_{BR1B}$ N-terminal regions. Furthermore, all three receptors contained an N-glycosylation site at around the same regions between the 175-200th amino acid; between the 250-300th amino acid and between the 300-350th amino acid in the N-terminus of the protein **(Figure 7.3)**. These common sites support a conserved role for the proteins.

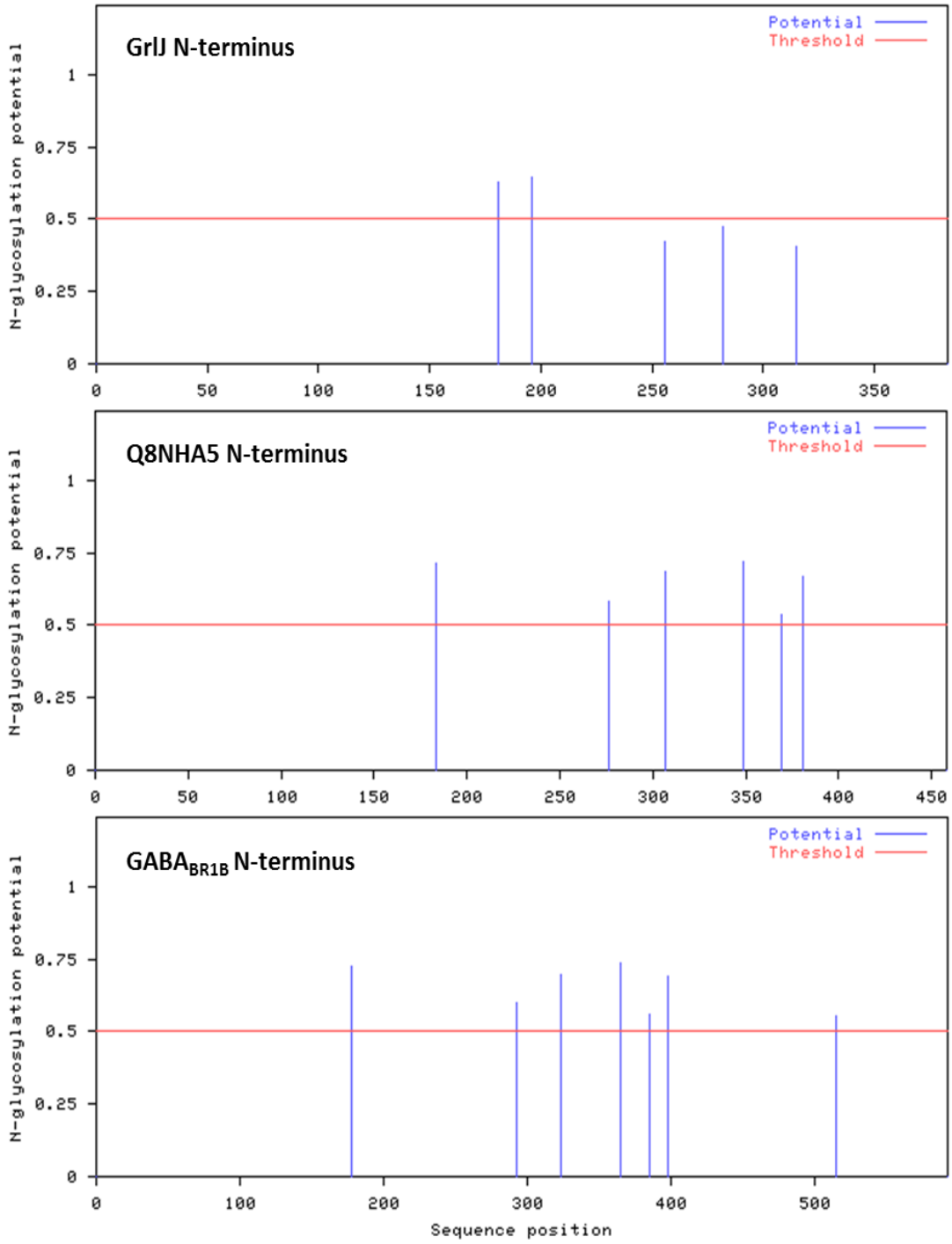

Figure 7.3 Predicted N-glycosylation sites in GrlJ, Q8NHA5 and GABA$_{BR1B}$ N-termini. Protein sequence analysis of N-terminal regions using NetNGlyc1.0 server identified five potential N-glycosylation sites GrlJ, six potential sites in Q8NHA5 and seven potential sites in GABA$_{BR1}$.

7.2. Expression of *Q8NHA5* in *Dictyostelium*

Since Q8NHA5 shared structural similarity to GrlJ **(Figure 7.4A)** a role for Q8NHA5 in phenylthiourea detection was examined by expression of the human gene in *Dictyostelium* in wild type and *grlJ*$^{-}$ cell lines. Full length cDNA was synthesised using a reading frame corrected for *Dictyostelium* codon bias and restriction sites for BglII and SpeI added to the 5' and 3' ends respectively **(Figure 7.4B)**. This was then cloned into the vector, PDM320, which contained an N-terminal FLAG tag under the control of an actin 15 promoter (Veltman et al., 2009). Wild type and *grlJ*$^{-}$ cells were then transformed with the overexpression construct to create *WT/Q8NHA5*$^{+}$ and *grlJ*$^{-}$*/Q8NHA5*$^{+}$ cell lines. Transformants were then placed under G418 selection, where RT-PCR of surviving colonies confirmed gene expression using primers specific to *Q8NHA5* **(Figure 7.4C)**. The protein levels of Q8NHA5 could however not be confirmed by Western blot. **(Figure 7.4D)**.

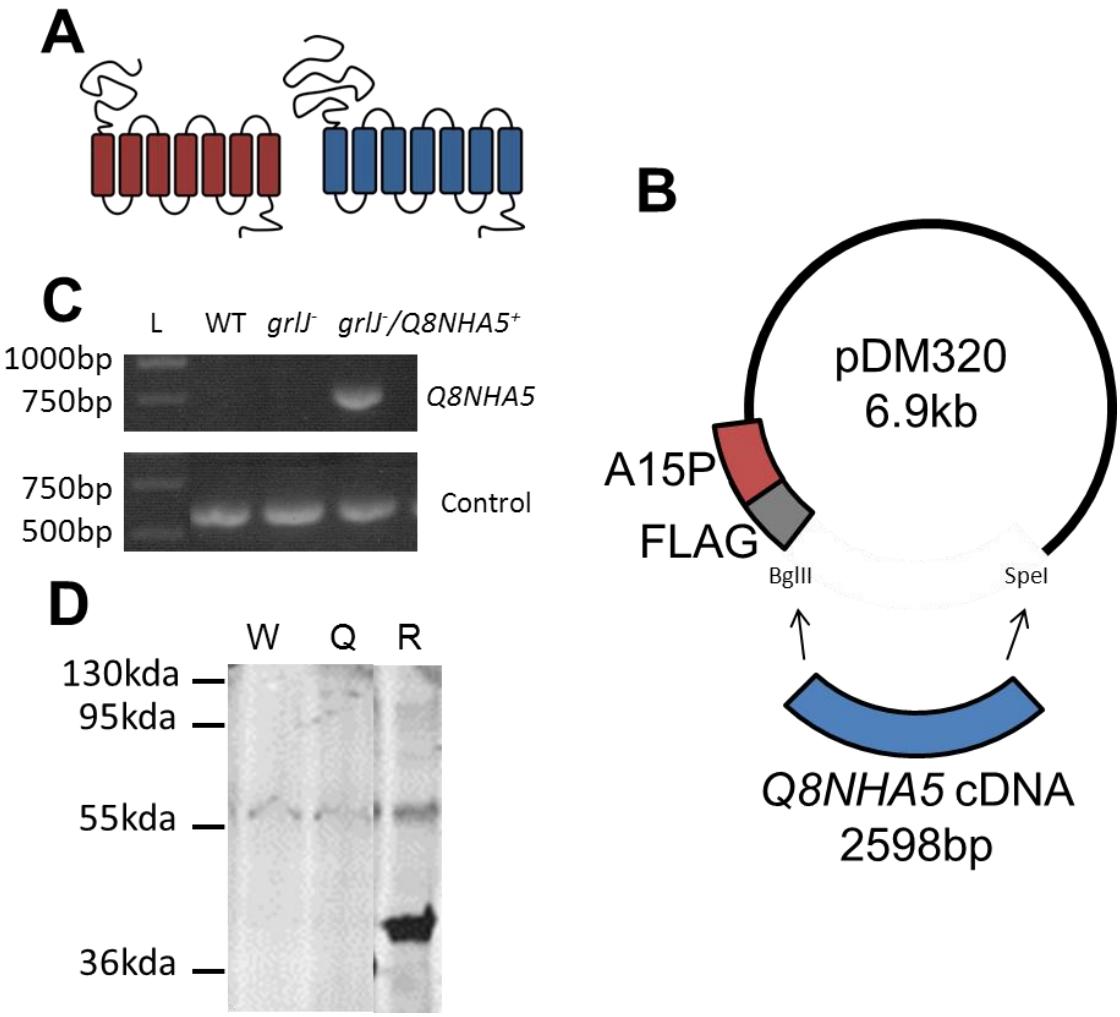

Figure 7.4. Overexpression of *Q8NHA5* in *grlJ*⁻ cells. (A) Predicted tertiary structure of GrlJ and Q8NHA5 suggest both proteins show similar overall structure of seven transmembrane regions (coloured) with large N- and small C-terminal regions. **(B)** Schematic of an overexpression construct created using pDM320; using BglII and SpeI restriction sites to insert *Q8NHA5*. **(C)** RT-PCR showing expression of the human gene in *grlJ*⁻/*Q8NHA5*⁺ but not wild type or *grlJ*⁻ cell lines. Control bands represent constitutively active gene, *IG7*. **(D)** Western blot showing wild type (W), *grlJ*⁻/*Q8NHA5*⁺ (Q) and a control rat brain (R) lysate. A band for Q8NHA5, of approximately 97kDa could not be identified. Control band in rat brain lysate was approximately 48kDa.

7.3. Spore shape analysis of *grlJ*$^{-}$ complemented with *Q8NHA5*

In order to determine whether expression of *Q8NHA5* could recapitulate wild type phenotypic traits that were present in *grlJ*$^{-}$ cells **(Chapter 5)**, *grlJ*$^{-}$*/Q8NHA5*$^{+}$ spores were isolated and their shape was analysed as described previously **(Chapter 5)**. Wild type and *grlJ*$^{-}$ cells showed a significant (P<0.05) change in spore shape (mean aspect of 1.9±0.02 and 2.0±0.03 respectively). Surprisingly, *grlJ*$^{-}$*/Q8NHA5*$^{+}$ restored wild type spore shape (1.9±0.03) **(Figure 7.5)**. A one-way analysis of variance identified a significant difference between wild type and *grlJ*$^{-}$ spore shape (P<0.05) but not wild type and *grlJ*$^{-}$*/Q8NHA5*. In addition, *grlJ*$^{-}$ and *grlJ*$^{-}$*/Q8NHA5* spore shape also showed no significant difference, suggesting a partial but not complete restoration of spore shape identified in wild type cells.

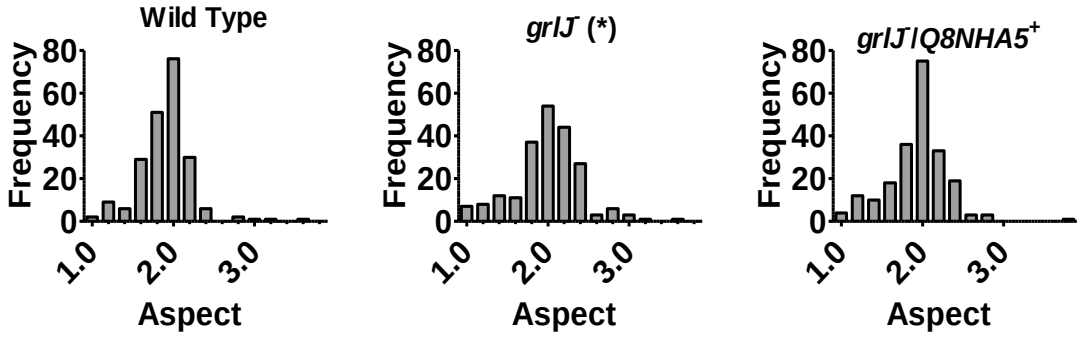

Figure 7.5. Determination of spore shape in wild type, *grlJ*$^{-}$ and *grlJ*$^{-}$*/Q8NHA5*$^{+}$ strains. A total of 214 Spores from each wild type, *grlJ*$^{-}$ and *grlJ*$^{+}$*/Q8NHA5*$^{+}$ were isolated and imaged using phase contrast microscopy. Spore aspect was determined and a 1-way ANOVA with *post-hoc* Tukey's multiple comparison test revealed a significant difference (P<0.05) in spore shape between wild type and *grlJ*$^{-}$ (P<0.05) cell lines.

7.4. Random cell movement analysis of *grlJ*$^{-}$ complemented with *Q8NHA5*

Since *grlJ*$^{-}$ cells showed significant resistance to phenylthiourea (3mM) in random cell movement when compared to wild type cells, chemotactically-competent *grlJ*$^{-}$*/Q8NHA5*$^{+}$ cells were used in random cell movement assays as described previously **(Chapters 5 and 6)**. Addition of phenylthiourea (3mM) after 288 seconds resulted in loss in behaviour in *grlJ*$^{-}$*/Q8NHA5*$^{+}$ cells, where comparison of mean cell behaviour between the first and final 288 seconds identified a significant increase in circularity (P=0.0195) from 0.77±0.01 to 0.86±0.00, a significant decrease in the number of protrusions formed (P=0.0084) from 2.6±0.1 to 1.0±0.03, and a significant decrease in motility (P=0.0065), from 4.6±0.4nm/sec to 1.3±0.2nm/sec. Interestingly, a significant change in displacement was also identified (P=0.0078), where average cell displacement from 13.1±1.4µm at 288 seconds changed to 25.1±5.5µm at the end of the assay. A one-way analysis of variance identified significant differences in displacement, circularity, protrusion formation and motility between wild type and *grlJ*$^{-}$ as well as between *grlJ*$^{-}$ and *grlJ*$^{-}$*/Q8NHA5*$^{+}$ cell lines, and no significant differences in any measurements between wild type and *grlJ*$^{-}$*/Q8NHA5*$^{+}$ cells **(Figure 7.6)**. These results suggest that the uncharacterised human protein, Q8NHA5, may be involved in the detection of phenylthiourea.

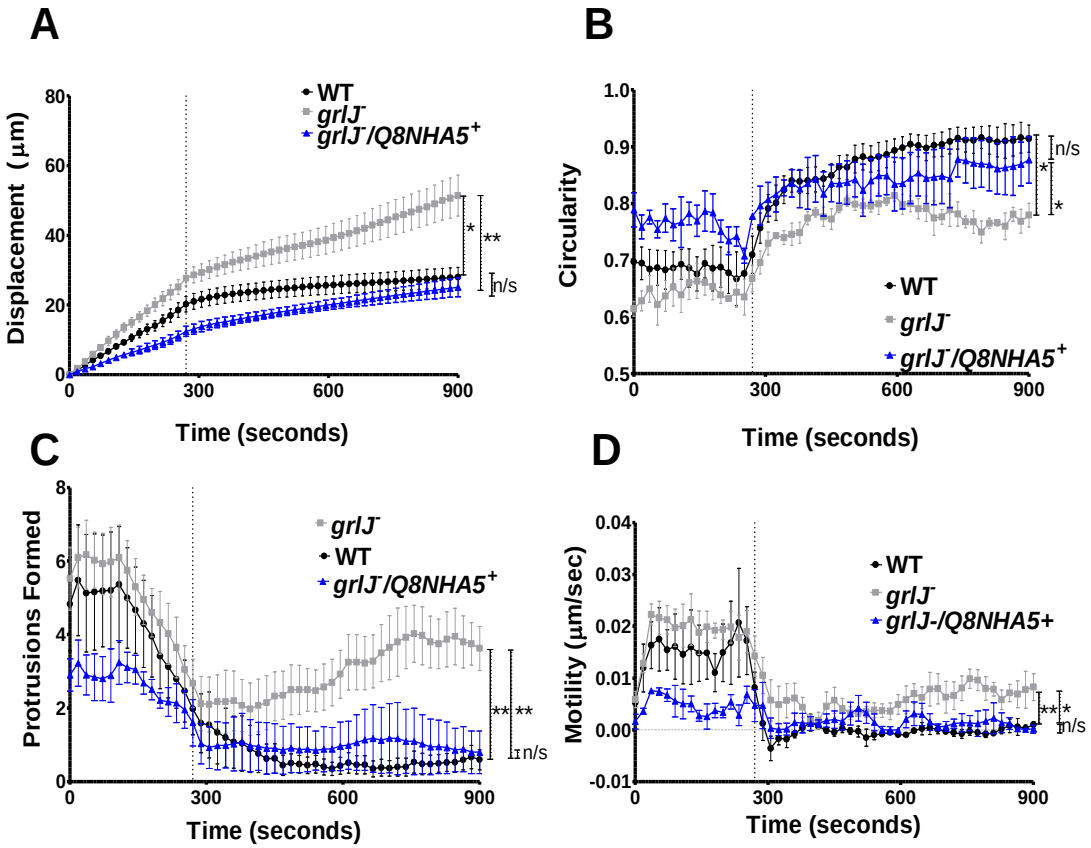

Figure 7.6. *Dictyostelium* wild type, *grlJ*$^{-}$ and *grlJ*$^{-}$*/Q8NHA5*$^{+}$ random cell movement following exposure to phenylthiourea (3mM) after 288 seconds. During random cell movement, 3mM phenylthiourea was added to *grlJ*$^{-}$*/Q8NHA5*$^{+}$ cells after 288 seconds and changes in cell behaviour monitored. A one-way ANOVA with subsequent *post-hoc* Tukey's test was performed for **(A)** Displacement. A significant difference was observed at the final cumulative time point of the assay between WT and *grlJ*$^{-}$ (P<0.05) as well as *grlJ*$^{-}$ and *grlJ*$^{-}$ */Q8NHA5*$^{+}$ (P<0.01) cell lines. **(B)** Circularity. A significant difference was observed during the final 288 seconds of the assay between WT and *grlJ*$^{-}$ (P<0.05) as well as *grlJ*$^{-}$ and *grlJ*$^{-}$ */Q8NHA5*$^{+}$ (P<0.05) cell lines. **(C)** Number of protrusions within a 10 frame window. Significant differences between cell lines was shown with both WT and *grlJ*$^{-/+}$ (P<0.01) cell lines producing significantly fewer protrusions compared to *grlJ*$^{-}$ cells during the final 612-900 seconds. **(D)** Motility. A significant difference was observed between WT and *grlJ*$^{-/+}$ cells to be significantly (P<0.01 and P<0.05 respectively) less active than *grlJ*$^{-}$ cells during the final 612-900 seconds. In all measurements, no significant difference was observed between WT, *grlJ*$^{-}$ and *grlJ*$^{-}$ */Q8NHA5*$^{+}$ cells under control conditions (0-288 seconds). Measurements were derived from 30 cells measured from a minimum of triplicate experiments. Vertical bars represent the standard error of the mean, *p < 0.05, **p < 0.01, n/s not significant.

7.5. Involvement of the PI3K pathway

To investigate whether the Q8NHA5-mediated inhibition of *Dictyostelium* cell behaviour was through dysregulation of the PI3K pathway, global cAMP stimulation experiments were performed as described previously by extracting PIP_3 **(Chapter 6).** Chemotactically-competent *grlJ*$^-$/*Q8NHA5*$^+$ cells were incubated in phosphate buffer or phenylthiourea (3mM) for ten minutes prior to cAMP global stimulation and lipids extracted at 0, 5 and 20 seconds post stimulation. Under control conditions, PIP_3 levels rose from 3.8±2.4pmol to 10.6±5.8pmol after five seconds and dropped to 5.5±2.1pmol after twenty seconds post cAMP addition **(Figure 7.7)**. Ten minute incubation with phenylthiourea (3mM) resulted in a change in PIP_3 levels from 1.3±0.9pmol to 1.7±0.7pmol after five seconds to 1.3±0.7pmol after twenty seconds cAMP stimulation **(Figure 7.7)**. A two-way ANOVA identified a significant difference in in PIP_3 production 5 seconds post-cAMP addition under control conditions ($P<0.05$), but not after phenylthiourea incubation. This evidence suggests a role for the uncharacterized human protein, Q8NHA5, in detection phenylthiourea through inhibiting production of PIP_3 in *Dictyostelium*.

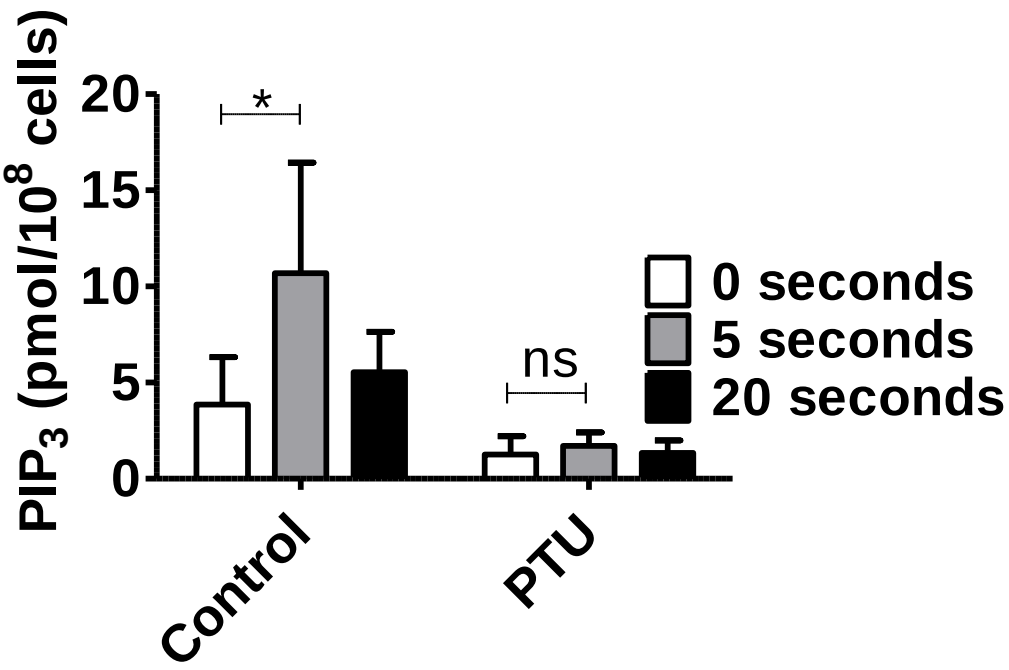

Figure 7.7. PIP_3 production during global stimulation with cAMP in *grlJ*$^-$/*Q8NHA5*$^+$ cells following ten minute incubation with phosphate buffer or phenylthiourea (3mM). A mass ELISA was used to quantify PIP_3 production 0, 5 and 20 seconds post stimulation with 1µM cAMP, where a significant change in PIP_3 production was identified 5 seconds following global stimulation in *grlJ*$^-$/*Q8NHA5*$^+$ cells under control conditions. Incubation with phenylthiourea (3mM) (PTU), resulted in no significant changes in PIP_3 production 5 seconds after global stimulation with cAMP. The figure is representative of triplicate experiments using a 2-way ANOVA for statistical comparisons. Error bars represent standard error of the mean (SEM). * $P<0.05$, ns= not significant.

7.6. Discussion

Previous experiments reported in this thesis identified GrlJ as a G-protein coupled receptor involved in phenylthiourea detection, and an acute block in *Dictyostelium* cell behaviour **(Chapter 5)**. Additional analysis showed detection of phenylthiourea through GrlJ inhibited PIP_3 production following stimulation with cAMP **(Chapter 6)**. This mechanism contrasts to current molecular mechanisms of phenylthiourea detection in mammals (Kinnamon, 2011). With regards to phenylthiourea and its structurally related analogue, propylthiouracil, the current understanding of *TAS2R38* polymorphisms resulting in different taster status, is however insufficient, owing to the substantial variability in taster status (Hayes et al., 2008). Previous genome wide association research has identified the variation in *TAS2R38* single nucleotide polymorphisms accounts for only 49% of variability observed in propylthiouracil detection thresholds (Genick et al., 2011). In this chapter, an uncharacterised human protein, Q8NHA5, was identified to be involved in phenylthiourea detection **(Table 7.1)**.

7.6.1. Identification of an uncharacterised human protein

Dictyostelium contains a large number of G-protein coupled receptors, (~0.5% of the genome), the proportion of which places the amoeba between fungi and animals in evolutionary distance (Prabhu and Eichinger, 2006). Within the genome, *Dictyostelium* contains seventeen genes encoding $GABA_B$-like receptors, belonging to the family three group of G-protein coupled receptors (Prabhu and Eichinger, 2006). To date, only two of these receptors, GrlE (Anjard and Loomis, 2006) and GrlB (Wu and Janetopoulos, 2013) receptors are shown to respond to GABA, where GrlJ, identified in this thesis, does not (Prabhu et al., 2007b). In mammals, $GABA_B$ receptors belong to a

phylogenetic group that contains a receptor, CASR, previously shown to be involved in denatonium benzoate detection (Fredriksson et al., 2003; Rogachevskaja et al., 2011), identifying a possible role for bitter tastants in activation of non-T2R receptors. Since the *Dictyostelium* genome contains no recognised T2R receptors, and evidence presented in this thesis indicates the involvement of GrlJ in bitter tastant detection, $GABA_B$ receptors may contain a binding site for which bitter tastants such as phenylthiourea can regulate receptor activity.

A database search for proteins with sequence similarity to GrlJ identified an uncharacterised human protein, Q8NHA5, sharing low homology **(Table 7.1)**, that showed high homology with $GABA_B$ subunit 1 receptor isoforms **(Figure 7.2** and **7.3)**. $GABA_B$ receptors are G-protein coupled receptors, located pre- and post- synaptically throughout the human central nervous system (Terunuma et al., 2010), lungs (Chapman et al., 1993) and the gastrointestinal tract (Nakajima et al., 1996). These receptors comprise of $GABA_B$ subunit 1 and 2 receptors, which form heterodimers, both of which are essential in producing functional $GABA_B$ receptors (White et al., 1998). Ligand binding of GABA to $GABA_B$ receptors involves a venus fly trap domain, shown only to exist in $GABA_B$ subunit 1 receptors, where $GABA_B$ subunit 2 receptors are involved in receptor activation (Rondard et al., 2011). $GABA_B$ receptors are targets of many diseases, where receptor agonism is used to treat skeletal muscle spasticity, pain and drug addiction (Bowery, 2006). Activation of $GABA_B$ receptors also provides a broncho-protective effect, relaxing airway smooth muscle, reducing coughing and bronchospasm (Chapman et al., 1993). Interestingly, bitter tastants also cause bronchodilation by activation of T2R receptors in the lungs, making them a target for novel therapeutic drugs in

asthma treatment (Liggett, 2013; An et al., 2012). This evidence provides a potential complementary role for T2R and $GABA_B$ receptor agonism, where activation of these receptors may induce similar signalling cascades.

In the gastrointestinal tract, activation of $GABA_B$ receptors with baclofen results in increased gastric contractility (Symonds et al., 2003; Rotondo et al., 2010) and decreased gastric volume (Rotondo et al., 2010). Despite this, activation of $GABA_B$ receptors after injection with baclofen (2mg/kg) results in delayed gastric emptying of liquids (Symonds et al., 2003) and also causes conditioned taste aversion to saccharin in rats (Wilson et al., 2011). This evidence suggests activation $GABA_B$ receptors located within the central nervous system may promote digestion and transport of nutrients through the gastrointestinal tract. Interestingly, baclofen is also regarded as a moderately bitter tasting compound, which requires a masking agent if administered orally (Janardhan et al., 2010). This data suggests compounds which activate $GABA_B$ receptors may also have aversive qualities that inhibit gastric motility upon activation in the gastrointestinal tract. Alternatively, agonists such as baclofen could activate aversive receptors in the gastrointestinal tract, such as T2R receptors, which may delay gastric emptying and cause conditioned taste aversion.

Agonists of $GABA_B$ receptors are used to treat a range of neurological disorders in humans such as schizophrenia, bipolar disorder, depression and epilepsy (Bowery, 2006; Fatemi et al., 2011). Interestingly, bitter taster status, which is dependent on *TAS2R38* polymorphisms, has also been linked to epilespy (Pal et al., 2004). This evidence provides another possible link

between T2R receptors and $GABA_B$ receptors, particularly the TAS2R38 receptor, which is responsible for phenylthiourea sensitivity.

Despite sharing little homology, comparison of mammalian T2R receptors and $GABA_B$ receptors, identified the requirement for N-linked glycosylation sites, in maturation and localisation to the cell membrane (Reichling et al., 2008; White et al., 1998; Maehashi and Huang, 2009; Rands et al., 1990). Whilst T2R receptors contain a conserved N-glycosylation site in the second extracellular loop (Reichling et al., 2008; Maehashi and Huang, 2009), $GABA_B$ receptors contain N-glycosylation sites in the N-terminus of the protein (White et al., 1998). Determination of N-glycosylation sites in GrlJ, Q8NHA5 and $GABA_{B1B}$ receptors identified a number of these sites throughout the N-terminus, where some appeared at similar locations on the primary amino acid structure **(Figure 7.3)**. This suggests a possible conserved role for N-linked glycosylation sites in GrlJ, Q8NHA5 and $GABA_{B1B}$ proteins.

7.6.2 Expression of *Q8NHA5* in *Dictyostelium*

Transformation of *Q8NHA5* into *Dictyostelium* cells was confirmed using G418 selection and RT-PCR **(Figure 7.4)**. Using primers specific to *Q8NHA5*, this method clearly identified gene transcription was occurring in *Dictyostelium* cells. Unfortunately, western blot could identify protein levels of Q8NHA5. This may be due to the protein instability resulting in degradation or tight protein folding resulting in reduced antibody binding. Alternatively, a lack of protein levels may be due to cleavage of the FLAG tag, which could be due to *Dictyostelium* proteinases or phosphatases removing the epitope. In human cells, FLAG tags have also been reported as unstable as a result of epitope positioning at the N-terminus of a protein (Quarello et al., 2010). In addition,

triple-tagging with the FLAG epitope has shown relatively poor signals in comparison to other epitope tags (Moqtaderi and Struhl, 2008). Using a more sensitive alternative to western blotting, such as ELISA, may have enhanced sensitivity towards the FLAG epitope attached to the Q8NHA5 protein. Alternatively, use of an antibody specific to Q8NHA5 would be of use in future experiments, as this would rely on detection of the actual protein rather than an epitope tag.

7.6.3. Spore shape analysis of *grlJ*⁻ complemented with *Q8NHA5*

Transformation of *grlJ*⁻ cells with a plasmid expressing *Q8NHA5* tagged with a FLAG tag to form *grlJ*⁻/*Q8NHA5*⁺ cell lines resulted in a partial restoration of *Dictyostelium* spore shape **(Figure 7.5)**. Grl-family proteins may play roles during different stages in *Dictyostelium* development, where GrlJ and GrlA are involved in events post aggregation (Prabhu et al., 2007a; Prabhu et al., 2007b), and GrlB is involved in the formation of mounds (Wu and Janetopoulos, 2013). Since Q8NHA5 partially restores spore shape to those seen in the wild type strain, this $GABA_B$-like protein is likely to provide a similar role to GrlJ in *Dictyostelium* cells.

To date, GABA signalling has only been identified in two proteins GrlB (Wu and Janetopoulos, 2013) and GrlE (Anjard and Loomis, 2006). Interestingly, GrlB and GrlE are involved in different stages of development, where GrlB (Wu and Janetopoulos, 2013) is responsive during early development and GrlE responds to GABA during sporulation (Anjard and Loomis, 2006). Whilst GrlJ is shown not to respond to GABA signalling during sporulation (Prabhu et al., 2007b), GrlJ activation by GABA may occur at a

different stage in development. Q8NHA5 may therefore have supported this role in the absence of GrlJ in *grlJ*$^{-}$/*Q8NHA5*$^{+}$ cells.

7.6.4. Random cell movement analysis of *grlJ*$^{-}$ complemented with *Q8NHA5*

Previous experiments identified in this thesis showed GrlJ is partially responsible for phenylthiourea detection. Exposure of *grlJ*$^{-}$/*Q8NHA5*$^{+}$ cells to phenylthiourea (3mM) in random cell movement resulted in a significant decrease in behaviour, indicating Q8NHA5 was also responsive to the tastant **(Figure 7.6)**. In *Dictyostelium*, regulation of GrlJ results in inhibitory effects on cell behaviour, which is also caused by Q8NHA5. To date, no research has identified phenylthiourea as a receptor agonist to $GABA_B$ receptors in humans. Interestingly, other G-protein coupled receptors belonging to class C receptors, such as CASR (Rogachevskaja et al., 2011) taste type 1 (Kinnamon, 2011) and glutamate receptors (Monastyrskaia et al., 1999) have been associated with bitter, sweet and umami taste transduction respectively. Whilst $GABA_B$ ligands have not been linked with taste transduction, GABA itself has been associated with masking the sensation of bitterness (Rotzoll et al., 2005). Therefore regulation of $GABA_B$ receptors within the gastrointestinal tract may reduce or interfere with bitter taste perception, possibly by masking sensitivity to bitter tastants.

The ability to perceive bitter tastants, particularly in relation to *TAS2R38* polymorphisms has been associated with diseases such hyperthyroidism (Kitchin et al., 1959; Kalow, 1986; Shivaprasad et al., 2012; Shepard and Gartler, 1960) and epilepsy (Pal et al., 2004). This has been related to non-tasters ingesting increased bitter goitrogenic substances found in plants, which

often contain phenylthiourea and derivatives (Kitchin et al., 1959; Pal et al., 2004). Since evidence in this thesis suggests phenylthiourea can activate a homologue of a $GABA_B$ subunit 1 receptor, phenylthiourea-mediated activation could further suppress bitter taste sensitivity in non-tasters, resulting in the increased ingestion of potentially damaging substances in humans. This could also help to explain the variability seen within taster groups previously identified (Hayes et al., 2008).

7.6.5. Involvement of the PI3K pathway

GrlJ-mediated detection of phenylthiourea has been shown in this thesis to occur via inhibition of the PI3K pathway **(Chapter 6)**. To assess the function of GrlJ using Q8NHA5 in *grlJ*$^-$/*Q8NHA5*$^+$ cells, incubation with phenylthiourea resulted in the inhibition of transient PIP_3 production, restoring the wild type phenotype **(Figure 7.7)**. In human cell lines, $GABA_B$ signalling also involves PI3K activity and subsequently phosphorylating PKB/Akt (Lu et al., 2012; Malyala et al., 2008). In *Dictyostelium* PI3K has previously been identified as a downstream target of GrlE activation in GABA signalling during sporulation (Anjard and Loomis, 2006). Since the block in cell behaviour occurs through inhibition of PI3K, regulation of GrlJ and Q8NHA5 could therefore play an inhibitory rather than a stimulatory role on downstream PIP_3 formation. This evidence therefore indicates PI3K signalling also acts downstream to $GABA_B$ receptor activation in both humans and *Dictyostelium*, suggesting a functional role for Q8NHA5 signalling in *Dictyostelium grlJ*$^-$*/Q8NHA5*$^+$ cells.

In *Dictyostelium*, heterotrimeric G-protein coupled receptors are bound one of various Gα subunits in addition to the β subunit and the undiscovered ɣ subunit. Different Gα subunits cause various responses in *Dictyostelium* behaviour where, for example, Gα2 is crucial for cAR activation and

subsequent signal amplification events (Liao et al., 2013). In contrast Gα9 is shown to cause inhibition on cAMP-directed movement, which includes negative regulation of the PI3K pathway (Brzostowski et al., 2004). Grl-family proteins couple to different Gα subunits, where GrlE couples to Gα7 (Anjard et al., 2009), and GrlA couples to Gα4 (Anjard et al., 2009). This data suggests different Grl-family proteins bind to different Gα-subunits, which may therefore interact with different molecular signalling pathways in *Dictyostelium* behaviour. Heterotrimeric G-protein dissociation from $GABA_B$ receptors such as GrlJ and Q8NHA5 with a subunit such as Gα9 in *Dictyostelium* is consistent with the inhibition in PIP_3 formation shown. Interestingly, Gα9 (along with Gα11) was identified in the REMI mutagenesis screen as resistant to phenylthiourea **(Appendix 6)**. Further research may therefore identify Gα9 to bind to GrlJ.

In mammals, $GABA_B$ receptor activation results in dissociation of Gαi subunits (Chalifoux and Carter, 2011), which subsequently results in the reduction in adenylyl cyclase activity. These subunits share a high homology with Gα-subunits in *Dictyostelium* (based upon BLAST analysis). Since Q8NHA5-mediated detection of phenylthiourea results in a reduction in PIP_3 formation, the $GABA_B$ receptor is therefore likely to couple to one of the many *Dictyostelium* Gα subunits.

7.7. Summary

A database search for proteins related to GrlJ identified an uncharacterised human receptor, which shares a high homology with $GABA_{B1B}$. Expression of *Q8NHA5* in *GrlJ*$^-$ cells in *Dictyostelium* was identified using RT-PCR. However, due to poor expression or potential cleavage of the FLAG epitope, no fusion protein could be detected could not be detected by western blotting.

Expression of *Q8NHA5* in *grlJ*$^{-}$ cells partially restored wild type spore shape, a wild type response to phenylthiourea, where cell behaviour was blocked in random cell movement, and blocked PIP_3 formation, suggesting inhibition of the PI3K pathway previously described **(Chapter 6)**. These experiments have therefore identified a previously uncharacterised human protein, likely to be a $GABA_B$ receptor component, involved in the detection of the bitter tastant phenylthiourea in *Dictyostelium*. This research could therefore have implications in bitter taste and $GABA_B$ receptor research in the future.

Chapter 8

Discussion

Nausea and vomiting are severe side effects associated with over 50% of currently marketed therapeutic drugs (Parkinson et al., 2011; Holmes et al., 2009). These contraindications can affect clinical response, hinder the progress of some drug treatment courses and reduce patient compliance (Parkinson et al., 2011). In order to predict these unpleasant side effects as early as possible during drug development, animal research is required, which provides an important area for the development of new non-sentient models to comply with the 3R's (reduction, replacement, refinement) principles in research. In the present study, the utility of a biomedical model organism, *Dictyostelium discoideum*, was explored for its potential to predict emetic liability and possibly reduce the number of animals used in emetic and aversive research.

8.1. Can *Dictyostelium* be used as a non-sentient model in emetic and tastant research?

To assess the suitability of *Dictyostelium* as a model for predicting emetic liability, motility assays in a Dunn chamber were used to screen a broad range of emetic and taste aversive compounds for their acute effects on cell behaviour **(Table 3.1)**. Twenty nine emetic and/or taste aversive compounds were screened, seven of which caused significant reversible reductions in cell velocity and/or shape as well as a decrease in cell directionality **(Chapter 3)**. These compounds could be sub-divided into four distinct groups, which were copper salts, T2R receptor ligands, a TRPV1 receptor agonist and a phosphodiesterase IV inhibitor.

Since only seven of twenty nine compounds with known emetic effects in mammals affected *Dictyostelium* behaviour, its use as a general model for predicting emetic liability is limited. Many of the compounds tested were

receptor agonists or inhibitors of receptors that do not exist in *Dictyostelium*. In addition, the short incubation time used to measure acute effects on *Dictyostelium* behaviour may have been too short to allow compounds such as cytotoxic compounds, which cause DNA damage, to affect motility.

Screening of compounds using *Dictyostelium* motility did however identify four different sub-groups of compounds that did block motility. *Dictyostelium* may therefore provide a useful model in the analysis of these compounds in structure-activity relationships or translational studies to identify novel active vanilloids or bitter tastants. For example, the TAS2R receptors 4, 7, 10, 39 and 46 are all activated by multiple bitter tastants, including denatonium benzoate and quinine hydrochloride (Meyerhof et al., 2010). Using *Dictyostelium*, compounds structurally related to bitter tastants such as denatonium benzoate may also help to identify other bitter and non-bitter analogues, which may target specific bitter taste receptors. *Dictyostelium* may also be of potential use to identify the potency of bitter tastants in translational studies. Data obtained in this thesis **(Chapter 3)** has shown *Dictyostelium* detects bitter tastants at concentrations relevant to mammalian thresholds (Hayes et al., 2008; Delwiche et al., 2001; Meyerhof et al., 2010; Nelson and Sanregret, 1997; Peyrot des et al., 2011; Sibert and Frude, 1991). For example, *Dictyostelium* was sensitive to phenylthiourea at concentrations ranging from 1-5mM, which is consistent with phenylthiourea causing calcium release in mouse enteroendocrine cells at 2-5mM. Future research using *Dictyostelium* in translational and structure-activity relationship studies may therefore have potential for use in high throughput screens to identify the potency of other bitter tastants.

8.3. Identification of molecular mechanisms in bitter tastant detection

The ease of using *Dictyostelium* to identify novel protein targets makes the amoeba useful biomedical model (Boeckeler and Williams, 2007; Williams et al., 2006b). By performing a REMI mutagenesis screen, a number of genetic targets potentially involved in bitter tastant detection were identified **(Chapter 4).** This included a G-protein coupled receptor mutant, *grlJ*$^{-}$, which showed partial resistance to phenylthiourea. Whilst ablation of *grlJ* in the Ax2 background used in this thesis resulted in the formation of previously identified malformed spores, an increased growth rate was not observed (Prabhu et al., 2007b) **(Chapter 5)**. This may be due to strain specific differences that have been observed between laboratories. For example, previous research has identified strain specific differences in development using different parent strains to ablate the *gskA* gene (Schilde et al., 2004; Harwood et al., 1995).

REMI mutagenesis screening also identified two racGEFs (*gxcP*$^{-}$ and *gxcKK*$^{-}$), both of which showed resistance to denatonium benzoate in motility, possibly through a parallel pathway. Denatonium benzoate may therefore activate an unidentified receptor, a signalling pathway involving GxcP and GxcKK, or directly regulate a number of racGEFs to inhibit cell behaviour. Further research is required to identify the molecular mechanisms involved in in the regulation of racGEFs by denatonium benzoate.

A final mutant identified in the REMI mutagenesis screen for further analysis, was Pkd2, involved in the detection of naringenin. Ablation of *pkd2* in *Dictyostelium* showed complete resistance to naringenin during random cell movement **(Chapter 4).** This research has since identified a role for naringenin

in inhibiting the formation of polycystic cysts through the Pkd2 receptor in mammalian kidney cell lines (Mark Carew, Kingston University, personal communication; Waheed et al. 2013). Identification of Pkd2 using a REMI mutagenesis screen has therefore supported the role for *Dictyostelium* as a suitable model in biomedical research.

In pursuing the GrlJ-mediated response to phenylthiourea, ablation of *grlJ* in the Ax2 background confirmed the partial resistance in cell behaviour to phenylthiourea. *grlJ*$^{-}$ cells also showed resistance to phenylthiourea in both proliferation (in shaking suspension) and growth on bacterial plates **(Chapter 5)**. GrlJ-mediated cell rounding, induced by phenylthiourea in both motility and random cell movement, suggests an inhibitory effect on F-actin polymerisation, which is partially regulated by PI3K activity (Chen and Iijima, 2012). PI3K activity was also suppressed by phenylthiourea-mediated regulation of GrlJ **(Chapter 6)**. Since macropinocytosis (Lee and Knecht, 2002) and phagocytosis (Chen and Iijima, 2012) are also reliant on PI3K activity and F-actin remodelling, GrlJ-mediated inhibition of cell behaviour may give rise to the observed inhibition of growth in shaking suspension and on bacterial plates.

Since phenylthiourea-mediated regulation of cell behaviour was shown to be G-protein coupled receptor dependent, resulting in the subsequent inhibition of PIP_3 formation, it is likely GrlJ regulates heterotrimeric G-proteins involved in motility **(Figure 8.1)**. However, since GrlJ only showed partial resistance to phenylthiourea, at least one other molecular mechanism must be involved. Previous research has identified four key signalling mechanisms required for efficient motility, where inhibition of one or two pathways does not inhibit motility (Veltman et al., 2008). Therefore, whilst GrlJ inhibits PIP_3 production and may

also inhibit other pathways (not identified in this thesis), the receptor is unlikely to be responsible for complete inhibition in cell behaviour by phenylthiourea. Since the inhibition of *Dictyostelium* behaviour by phenylthiourea is shown to involve heterotrimeric G-protein activity, it is likely that this other mechanism is also a G-protein coupled receptor **(Figure 8.1)**.

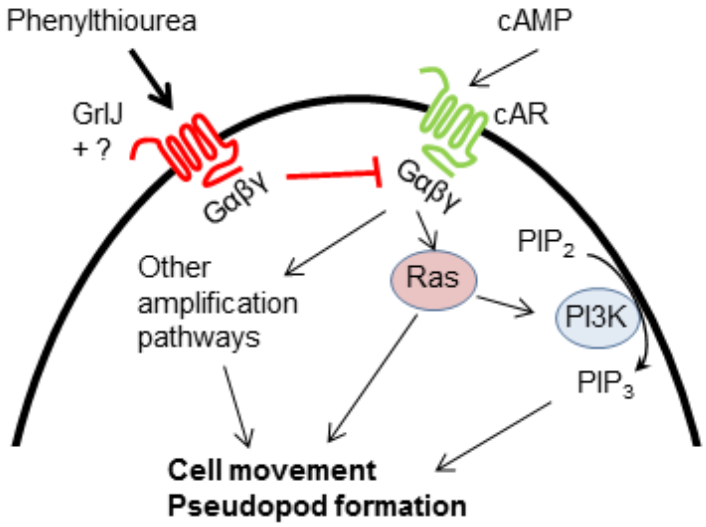

Figure 8.1. Phenylthiourea-mediated regulation of GrlJ on *Dictyostelium* cell behaviour. Under control conditions, during chemotactic and random cell movement, cAMP binds to the cAR receptor, resulting in G-protein dissociation, which activates Ras. PI3K activity is subsequently increased, which converts PIP_2 to PIP_3. Heterotrimeric G-protein and Ras-mediated activation of PI3K along with other amplification pathways results in normal cell behaviour. Detection of phenylthiourea by GrlJ, results in the regulation of heterotrimeric G-proteins, subsequently inhibiting the PI3K pathway and reducing cell behaviour. In addition, heterotrimeric G-protein regulation by an unknown receptor(s) is likely also to inhibit cell behaviour.

GrlJ shares homology with sixteen other Grl-family proteins, few of which have been characterised (Prabhu et al., 2007b). Fourteen of the seventeen Grl-family receptors share similarities ranging from 60% to 74%, and identities ranging from 23% to 44% **(Chapter 7)**. Other Grl-family receptors may therefore also regulate cell behaviour through detection of phenylthiourea. Since *Dictyostelium* is shown to respond to a number of bitter tastants and GrlJ has been identified as a receptor that detects phenylthiourea, further research may also identify bitter tastants as targets for other Grl-family receptors.

A search for related proteins also identified an uncharacterized human protein, Q8NHA5, which shared homology with $GABA_B$ receptors. Transformation of Q8NHA5 into *grlJ*$^-$ cells restored sensitivity to phenylthiourea in cell movement and in PIP_3 production **(Chapter 7)**. This suggests this human $GABA_B$-like receptor may be involved in phenylthiourea detection (Robery et al. 2013). In humans, activation of $GABA_B$ receptors also inhibits PI3K activity, resulting in decreased PIP_3 production in a similar manner to that shown for *Dictyostelium* (Lu et al., 2012; Malyala et al., 2008).

In humans, $GABA_B$ receptors are most commonly targeted by the drug baclofen (Janardhan et al., 2010), a bitter tasting compound that is not shown to activate any T2R receptors. Phenylthiourea and baclofen appear to share a degree of structural similarity **(Figure 8.2)**, where both compounds contain an amine group in addition to a benzene ring. Future research may therefore examine a role for baclofen in regulating *Dictyostelium* behavior as well as a role for this compound in GrlJ and/or Q8NHA5 function.

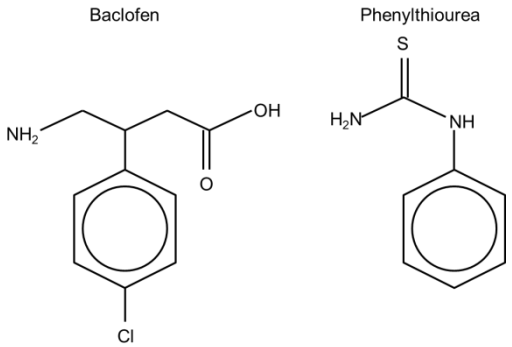

Figure 8.2. Chemical structures of baclofen and phenylthiourea. Both compounds share some structural similarities, such as the presence of an amine group and a benzene ring.

Whilst agonists to $GABA_B$ receptors, such as baclofen, are not known to activate T2R receptors, both types of receptor are shown to regulate common functions in humans, such as causing bronchodilation (Liggett, 2013; Chapman

et al., 1993) suggesting they may share common downstream mechanisms of action. Using compounds that regulate both $GABA_B$ and T2R receptors, such as phenylthiourea, identified in this thesis, could enhance current research into novel treatments for respiratory diseases such as asthma.

$GABA_B$ receptors are targets for multiple disorders of the central nervous system, such as anxiety, depression, drug addiction and neurodegenerative diseases (Kumar et al., 2013). In addition, the $GABA_B$ receptor is a target of anti-spasmodic treatments (Kumar et al., 2013). Since *Dictyostelium* has identified phenylthiourea as potentially regulating a $GABA_B$ receptor, development of novel therapeutic treatments for a range of diseases may in future include compounds such as phenylthiourea or structurally related analogues. *Dictyostelium* may have a potential use for identifying novel $GABA_B$ receptor targeting compounds in a similar way to the discovery of novel potential epilepsy treatments (Chang et al., 2012).

Finally, previous research has identified bitter taster status, which is dependent on single nucleotide polymorphisms on the *TAS2R38* gene resulting in varying sensitivity to compounds such as phenylthiourea, is not sufficient to explain variability in bitter taste sensation (Hayes et al., 2008; Genick et al., 2011). Since $GABA_B$ receptor activation was previously identified to mask bitter tastants (Rotzoll et al., 2005), research in this thesis suggesting a role for phenylthiourea in the activation of a potential $GABA_B$ receptor, may therefore explain the variation in phenylthiourea sensitivity observed in different *TAS2R38* haplotypes.

8.4. Summary

In this thesis, the utility for using *Dictyostelium* as a model for predicting emetic liability was investigated. Although the model is unlikely to provide a reliable predictor to a wide range of emetic compounds, it did show a response to multiple bitter compounds. Pursuing the bitter taste response in *Dictyostelium* identified a G-protein coupled receptor, GrlJ, as responsible for partial inhibition of cell behavior by phenylthiourea and controlling the block in PIP_3 production. Finally an uncharacterized human protein, Q8NHA5, was then identified as a likely $GABA_B$ receptor that restored sensitivity of *grlJ*$^-$ cells to phenylthiourea, suggesting this human protein may function as a target for the bitter tastant.

References

Adler,E., Hoon,M.A., Mueller,K.L., Chandrashekar,J., Ryba,N.J., and Zuker,C.S. (2000). A novel family of mammalian taste receptors. Cell *100*, 693-702.

Aizawa,H., Katadae,M., Maruya,M., Sameshima,M., Murakami-Murofushi,K., and Yahara,I. (1999). Hyperosmotic stress-induced reorganization of actin bundles in Dictyostelium cells over-expressing cofilin. Genes Cells *4*, 311-324.

Alexander,S.P., Mathie,A., and Peters,J.A. (2011). Guide to Receptors and Channels (GRAC), 5th edition. Br. J. Pharmacol. *164 Suppl 1*, 1-324.

An,S.S., Wang,W.C., Koziol-White,C.J., Ahn,K., Lee,D.Y., Kurten,R.C., Panettieri,R.A., Jr., and Liggett,S.B. (2012). TAS2R activation promotes airway smooth muscle relaxation despite beta(2)-adrenergic receptor tachyphylaxis. Am. J. Physiol Lung Cell Mol. Physiol *303*, L304-L311.

Andrew,N. and Insall,R.H. (2007). Chemotaxis in shallow gradients is mediated independently of PtdIns 3-kinase by biased choices between random protrusions. Nat. Cell Biol. *9*, 193-200.

Andrews,P.L. and Bhandari,P. (1993). Resinferatoxin, an ultrapotent capsaicin analogue, has anti-emetic properties in the ferret. Neuropharmacology *32*, 799-806.

Andrews,P.L., Davis,C.J., Bingham,S., Davidson,H.I., Hawthorn,J., and Maskell,L. (1990). The abdominal visceral innervation and the emetic reflex: pathways, pharmacology, and plasticity. Can. J. Physiol Pharmacol. *68*, 325-345.

Andrews,P.L., Dovey,E., Hockaday,J., Hoyle,C.H., Woods,A.J., and Matsuki,N. (2000a). The development of the emetic reflex in the house musk shrew, Suncus murinus. Brain Res. Dev. Brain Res. *121*, 29-34.

Andrews,P.L. and Horn,C.C. (2006). Signals for nausea and emesis: Implications for models of upper gastrointestinal diseases. Auton. Neurosci. *125*, 100-115.

Andrews,P.L., Kovacs,M., and Watson,J.W. (2001). The anti-emetic action of the neurokinin(1) receptor antagonist CP-99,994 does not require the presence of the area postrema in the dog. Neurosci. Lett. *314*, 102-104.

Andrews,P.L., Okada,F., Woods,A.J., Hagiwara,H., Kakaimoto,S., Toyoda,M., and Matsuki,N. (2000b). The emetic and anti-emetic effects of the capsaicin analogue resiniferatoxin in Suncus murinus, the house musk shrew. Br. J. Pharmacol. *130*, 1247-1254.

Andrews,P.L., Rapeport,W.G., and Sanger,G.J. (1988). Neuropharmacology of emesis induced by anti-cancer therapy. Trends Pharmacol. Sci. *9*, 334-341.

Andrews,P.L. and Rudd,J.A. (2004). The Role of Tachykinins and the Tachykinin NK1 Receptor in Nausea and Emesis. In Handbook of Experimental Pharmacology, P.Holzer, ed. (Berlin: Springer Verlag), pp. 359-440.

Andrews,P.L., Torii,Y., Saito,H., and Matsuki,N. (1996). The pharmacology of the emetic response to upper gastrointestinal tract stimulation in Suncus murinus. Eur. J. Pharmacol. *307*, 305-313.

Andrews,P.L.R. and Davis,C.J. (1993). The mechanism of emesis induced by anti-cancer therapies. In Emesis in anti-cancer therapy - mechanisms and treatment, P.L.R.Andrews and G.J.Sanger, eds. (London, UK: Hall Medical), pp. 113-161.

Andrews,P.L.R. and Sanger,G.J. (1993). The problem of emesis in anti-cancer therapy: An introduction. In Emesis in anti-cancer therapy - mechanisms and treatment, P.L.R.Andrews and G.J.Sanger, eds. (London, UK: Hall Medical), pp. 1-7.

Anjard,C. and Loomis,W.F. (2006). GABA induces terminal differentiation of Dictyostelium through a GABAB receptor. Development *133*, 2253-2261.

Anjard,C., Su,Y., and Loomis,W.F. (2009). Steroids initiate a signaling cascade that triggers rapid sporulation in Dictyostelium. Development *136*, 803-812.

Aoki,M., Fukunaga,M., Sugimoto,T., Hirano,Y., Kobayashi,M., Honda,K., and Yamada,T. (2001). Studies on mechanisms of low emetogenicity of YM976, a novel phosphodiesterase type 4 inhibitor. J. Pharmacol. Exp. Ther. *298*, 1142-1149.

Araki,T., van Egmond,W.N., van Haastert,P.J., and Williams,J.G. (2010). Dual regulation of a Dictyostelium STAT by cGMP and Ca2+ signalling. J. Cell Sci. *123*, 837-841.

Araya,M., Chen,B., Klevay,L.M., Strain,J.J., Johnson,L., Robson,P., Shi,W., Nielsen,F., Zhu,H., Olivares,M., Pizarro,F., and Haber,L.T. (2003). Confirmation of an acute no-observed-adverse-effect and low-observed-adverse-effect level for copper in bottled drinking water in a multi-site international study. Regul. Toxicol. Pharmacol. *38*, 389-399.

Araya,M., McGoldrick,M.C., Klevay,L.M., Strain,J.J., Robson,P., Nielsen,F., Olivares,M., Pizarro,F., Johnson,L.A., and Poirier,K.A. (2001). Determination of an acute no-observed-adverse-effect level (NOAEL) for copper in water. Regul. Toxicol. Pharmacol. *34*, 137-145.

Arul,D. and Subramanian,P. (2013). Naringenin (Citrus Flavonone) Induces Growth Inhibition, Cell Cycle Arrest and Apoptosis in Human Hepatocellular Carcinoma Cells. Pathol. Oncol. Res.

Asano,Y., Nagasaki,A., and Uyeda,T.Q. (2008). Correlated waves of actin filaments and PIP3 in Dictyostelium cells. Cell Motil. Cytoskeleton *65*, 923-934.

Bader,S., Kortholt,A., and van Haastert,P.J. (2007). Seven Dictyostelium discoideum phosphodiesterases degrade three pools of cAMP and cGMP. Biochem. J. *402*, 153-161.

Bagorda,A., Mihaylov,V.A., and Parent,C.A. (2006). Chemotaxis: moving forward and holding on to the past. Thromb. Haemost. *95*, 12-21.

Baines,A., Parkinson,K., Sim,J.A., Bragg,L., Thompson,C.R., and North,R.A. (2013). Functional properties of five Dictyostelium discoideum P2X receptors. J. Biol. Chem.

Bannink,E.O., Sauerbrey,M.L., Mullins,M.N., Hauptman,J.G., and Obradovich,J.E. (2008). Actinomycin D as rescue therapy in dogs with relapsed or resistant lymphoma: 49 cases (1999--2006). J. Am. Vet. Med. Assoc. *233*, 446-451.

Bavan,S., Straub,V.A., Blaxter,M.L., and Ennion,S.J. (2009). A P2X receptor from the tardigrade species Hypsibius dujardini with fast kinetics and sensitivity to zinc and copper. BMC. Evol. Biol. *9*, 17.

Bear,J.E., Rawls,J.F., and Saxe,C.L., III (1998). SCAR, a WASP-related protein, isolated as a suppressor of receptor defects in late Dictyostelium development. J. Cell Biol. *142*, 1325-1335.

Benson,P.W., Hooker,J.B., Koch,K.L., and Weinberg,R.B. (2012). Bitter taster status predicts susceptibility to vection-induced motion sickness and nausea. Neurogastroenterol. Motil. *24*, 134-40, e86.

Bhandari,P., Bingham,S., and Andrews,P.L. (1992). The neuropharmacology of loperamide-induced emesis in the ferret: the role of the area postrema, vagus, opiate and 5-HT3 receptors. Neuropharmacology *31*, 735-742.

Blaise,C., Gagne,F., Ferard,J.F., and Eullaffroy,P. (2008). Ecotoxicity of selected nano-materials to aquatic organisms. Environ. Toxicol. *23*, 591-598.

Bobkov,I.G. (1964). On the role of nodular ganglia of the vagus nerve in the emetic response to aconitine and veratrine. Fiziol. Zh. SSSR Im I. M. Sechenova *50*, 187-192.

Boeckeler,K. and Williams,R.S. (2007). *Dicytostelium* as a Biomedical Model. In Encyclopedia of Life Sciences, John Wiley & Sons Ltd.

Bolourani,P., Spiegelman,G.B., and Weeks,G. (2006). Delineation of the roles played by RasG and RasC in cAMP-dependent signal transduction during the early development of Dictyostelium discoideum. Mol. Biol. Cell *17*, 4543-4550.

Borison,H.L. and Fairbanks,V.F. (1952). Mechanism of veratrum-induced emesis in the cat. J. Pharmacol. Exp. Ther. *105*, 317-325.

Borison,H.L. and McCarthy,L.E. (1983). Neuropharmacology of chemotherapy-induced emesis. Drugs *25 Suppl 1*, 8-17.

Bosgraaf,L., Russcher,H., Smith,J.L., Wessels,D., Soll,D.R., and van Haastert,P.J. (2002). A novel cGMP signalling pathway mediating myosin phosphorylation and chemotaxis in Dictyostelium. EMBO J. *21*, 4560-4570.

Bosgraaf,L. and van Haastert,P.J. (2009). Navigation of chemotactic cells by parallel signaling to pseudopod persistence and orientation. PLoS. One. *4*, e6842.

Bowery,N.G. (2006). GABAB receptor: a site of therapeutic benefit. Curr. Opin. Pharmacol. *6*, 37-43.

Brauchi,S., Orta,G., Mascayano,C., Salazar,M., Raddatz,N., Urbina,H., Rosenmann,E., Gonzalez-Nilo,F., and Latorre,R. (2007). Dissection of the components for PIP2 activation and thermosensation in TRP channels. Proc. Natl. Acad. Sci. U. S. A *104*, 10246-10251.

Breshears,L.M., Wessels,D., Soll,D.R., and Titus,M.A. (2010). An unconventional myosin required for cell polarization and chemotaxis. Proc. Natl. Acad. Sci. U. S. A *107*, 6918-6923.

Brunert,D., Klasen,K., Corey,E.A., and Ache,B.W. (2010). PI3Kgamma-dependent signaling in mouse olfactory receptor neurons. Chem. Senses *35*, 301-308.

Brzostowski,J.A., Parent,C.A., and Kimmel,A.R. (2004). A G alpha-dependent pathway that antagonizes multiple chemoattractant responses that regulate directional cell movement. Genes Dev. *18*, 805-815.

Bufe,B., Breslin,P.A., Kuhn,C., Reed,D.R., Tharp,C.D., Slack,J.P., Kim,U.K., Drayna,D., and Meyerhof,W. (2005). The molecular basis of individual differences in phenylthiocarbamide and propylthiouracil bitterness perception. Curr. Biol. *15*, 322-327.

Burlando,B., Evangelisti,V., Dondero,F., Pons,G., Camakaris,J., and Viarengo,A. (2002). Occurrence of Cu-ATPase in Dictyostelium: possible role in resistance to copper. Biochem. Biophys. Res. Commun. *291*, 476-483.

Burnstock,G. and Verkhratsky,A. (2009). Evolutionary origins of the purinergic signalling system. Acta Physiol (Oxf) *195*, 415-447.

Caicedo,A., Pereira,E., Margolskee,R.F., and Roper,S.D. (2003). Role of the G-protein subunit alpha-gustducin in taste cell responses to bitter stimuli. J. Neurosci. *23*, 9947-9952.

Caicedo,A. and Roper,S.D. (2001). Taste receptor cells that discriminate between bitter stimuli. Science *291*, 1557-1560.

Carter,S.K., Bakowski,M.T., and Hellman,K. (1981). Chemotherapy of Cancer. (New York, USA: John Wiley and Sons).

Chalifoux,J.R. and Carter,A.G. (2011). GABAB receptor modulation of synaptic function. Curr. Opin. Neurobiol. *21*, 339-344.

Chandrashekar,J., Mueller,K.L., Hoon,M.A., Adler,E., Feng,L., Guo,W., Zuker,C.S., and Ryba,N.J. (2000). T2Rs function as bitter taste receptors. Cell *100*, 703-711.

Chang,P., Orabi,B., Deranieh,R.M., Dham,M., Hoeller,O., Shimshoni,J.A., Yagen,B., Bialer,M., Greenberg,M.L., Walker,M.C., and Williams,R.S. (2012). The antiepileptic drug valproic acid and other medium-chain fatty acids acutely reduce phosphoinositide levels independently of inositol in Dictyostelium. Dis. Model. Mech. *5*, 115-124.

Chapman,R.W., Hey,J.A., Rizzo,C.A., and Bolser,D.C. (1993). GABAB receptors in the lung. Trends Pharmacol. Sci. *14*, 26-29.

Charest,P.G., Shen,Z., Lakoduk,A., Sasaki,A.T., Briggs,S.P., and Firtel,R.A. (2010). A Ras signaling complex controls the RasC-TORC2 pathway and directed cell migration. Dev. Cell *18*, 737-749.

Chen,C.L. and Iijima,M. (2012). Myosin I: A new pip(3) effector in chemotaxis and phagocytosis. Commun. Integr. Biol. *5*, 294-296.

Chen,C.L., Wang,Y., Sesaki,H., and Iijima,M. (2012). Myosin I links PIP3 signaling to remodeling of the actin cytoskeleton in chemotaxis. Sci. Signal. *5*, ra10.

Chen,L., Iijima,M., Tang,M., Landree,M.A., Huang,Y.E., Xiong,Y., Iglesias,P.A., and Devreotes,P.N. (2007). PLA2 and PI3K/PTEN pathways act in parallel to mediate chemotaxis. Dev. Cell *12*, 603-614.

Chen,M.C., Wu,S.V., Reeve,J.R., Jr., and Rozengurt,E. (2006). Bitter stimuli induce Ca2+ signaling and CCK release in enteroendocrine STC-1 cells: role of L-type voltage-sensitive Ca2+ channels. Am. J. Physiol Cell Physiol *291*, C726-C739.

Cheng,F.H., Andrews,P.L., Moreaux,B., Ngan,M.P., Rudd,J.A., Sam,T.S., Wai,M.K., and Wan,C. (2005). Evaluation of the anti-emetic potential of anti-migraine drugs to prevent resiniferatoxin-induced emesis in Suncus murinus (house musk shrew). Eur. J. Pharmacol. *508*, 231-238.

Chu,K.M., Ngan,M.P., Wai,M.K., Yeung,C.K., Andrews,P.L., Percie du Sert,N., Lin,G., and Rudd,J.A. (2010a). Olvanil, a non-pungent vanilloid enhances the gastrointestinal toxicity of cisplatin in the ferret. Toxicol. Lett. *192*, 402-407.

Chu,K.M., Ngan,M.P., Wai,M.K., Yeung,C.K., Andrews,P.L., Percie du Sert,N., and Rudd,J.A. (2010b). Olvanil: a non-pungent TRPV1 activator has anti-emetic properties in the ferret. Neuropharmacology *58*, 383-391.

Chung,C.Y. and Firtel,R.A. (2002). Signaling pathways at the leading edge of chemotaxing cells. J. Muscle Res. Cell Motil. *23*, 773-779.

Clapp,T.R., Trubey,K.R., Vandenbeuch,A., Stone,L.M., Margolskee,R.F., Chaudhari,N., and Kinnamon,S.C. (2008). Tonic activity of G-alpha gustducin regulates taste cell responsivity. FEBS Lett. *582*, 3783-3787.

Correa,E.A., Hogestatt,E.D., Sterner,O., Echeverri,F., and Zygmunt,P.M. (2010). In vitro TRPV1 activity of piperine derived amides. Bioorg. Med. Chem. *18*, 3299-3306.

Cosson,P. and Soldati,T. (2008). Eat, kill or die: when amoeba meets bacteria. Curr. Opin. Microbiol. *11*, 271-276.

Costall,B. and Naylor,R.J. (1992). Neuropharmacology of emesis in relation to clinical response. Br. J. Cancer Suppl *19*, S2-S7.

Criton,M. and Le Mellay-Hamon,V. (2008). Analogues of N-hydroxy-N'-phenylthiourea and N-hydroxy-N'-phenylurea as inhibitors of tyrosinase and melanin formation. Bioorg. Med. Chem. Lett. *18*, 3607-3610.

Cubeddu,L., Hoffmann,I., and Fuenmayor,N. (1992). Serotonin and emesis--from animals to humans: a discussion of Professor Naylor's paper. Br. J. Cancer Suppl *19*, S9-11.

Cubeddu,L.X., Bonisch,H., Gothert,M., Molderings,G., Racke,K., Ramadori,G., Miller,K.J., and Schworer,H. (2000). Effects of metformin on intestinal 5-hydroxytryptamine (5-HT) release and on 5-HT3 receptors. Naunyn Schmiedebergs Arch. Pharmacol. *361*, 85-91.

Cushny (1918). A text-book of pharmacology and therapeutics or the action of drugs in health and disease. (London: J & A Churchill).

Czikora,A., Lizanecz,E., Bako,P., Rutkai,I., Ruzsnavszky,F., Magyar,J., Porszasz,R., Kark,T., Facsko,A., Papp,Z., Edes,I., and Toth,A. (2012). Structure-activity relationships of vanilloid receptor agonists for arteriolar TRPV1. Br. J. Pharmacol. *165*, 1801-1812.

Davis,T.G., Peterson,J.J., Kou,J.P., Capper-Spudich,E.A., Ball,D., Nials,A.T., Wiseman,J., Solanke,Y.E., Lucas,F.S., Williamson,R.A., Ferrari,L., Wren,P., Knowles,R.G., Barnette,M.S., and Podolin,P.L. (2009). The identification of a novel phosphodiesterase 4 inhibitor, 1-ethyl-5-{5-[(4-methyl-1-piperazinyl)methyl]-1,3,4-oxadiazol-2-yl}-N-(tet rahydro-2H-pyran-4-yl)-1H-pyrazolo[3,4-b]pyridin-4-amine (EPPA-1), with improved therapeutic index using pica feeding in rats as a measure of emetogenicity. J. Pharmacol. Exp. Ther. *330*, 922-931.

Delwiche,J.F., Buletic,Z., and Breslin,P.A. (2001). Relationship of papillae number to bitter intensity of quinine and PROP within and between individuals. Physiol Behav. *74*, 329-337.

Depoortere,R., Barret-Grevoz,C., Bardin,L., and Newman-Tancredi,A. (2008). Apomorphine-induced emesis in dogs: differential sensitivity to established and novel dopamine D2/5-HT(1A) antipsychotic compounds. Eur. J. Pharmacol. *597*, 34-38.

Dong,X.P., Wang,X., and Xu,H. (2010). TRP channels of intracellular membranes. J. Neurochem. *113*, 313-328.

Dormann,D., Weijer,G., Parent,C.A., Devreotes,P.N., and Weijer,C.J. (2002). Visualizing PI3 kinase-mediated cell-cell signaling during Dictyostelium development. Curr. Biol. *12*, 1178-1188.

Eglen,R.M., Lee,C.H., Smith,W.L., Johnson,L.G., Whiting,R.L., and Hegde,S.S. (1993). RS 42358-197, a novel and potent 5-HT3 receptor antagonist, in vitro and in vivo. J. Pharmacol. Exp. Ther. *266*, 535-543.

Eichinger,L., Pachebat,J.A., Glockner,G., Rajandream,M.A., Sucgang,R., Berriman,M., Song,J., Olsen,R., Szafranski,K., Xu,Q., Tunggal,B., Kummerfeld,S., Madera,M., Konfortov,B.A., Rivero,F., Bankier,A.T., Lehmann,R., Hamlin,N., Davies,R., Gaudet,P., Fey,P., Pilcher,K., Chen,G., Saunders,D., Sodergren,E., Davis,P., Kerhornou,A., Nie,X., Hall,N., Anjard,C., Hemphill,L., Bason,N., Farbrother,P., Desany,B., Just,E., Morio,T., Rost,R., Churcher,C., Cooper,J., Haydock,S., van,D.N., Cronin,A., Goodhead,I., Muzny,D., Mourier,T., Pain,A., Lu,M., Harper,D., Lindsay,R., Hauser,H., James,K., Quiles,M., Madan,B.M., Saito,T., Buchrieser,C., Wardroper,A., Felder,M., Thangavelu,M., Johnson,D., Knights,A., Loulseged,H., Mungall,K., Oliver,K., Price,C., Quail,M.A., Urushihara,H., Hernandez,J., Rabbinowitsch,E., Steffen,D., Sanders,M., Ma,J., Kohara,Y., Sharp,S., Simmonds,M., Spiegler,S., Tivey,A., Sugano,S., White,B., Walker,D., Woodward,J., Winckler,T., Tanaka,Y., Shaulsky,G., Schleicher,M., Weinstock,G., Rosenthal,A., Cox,E.C., Chisholm,R.L., Gibbs,R., Loomis,W.F., Platzer,M., Kay,R.R., Williams,J., Dear,P.H., Noegel,A.A., Barrell,B., and Kuspa,A. (2005). The genome of the social amoeba Dictyostelium discoideum. Nature *435*, 43-57.

Ezak,M.J., Hong,E., Chaparro-Garcia,A., and Ferkey,D.M. (2010). Caenorhabditis elegans TRPV channels function in a modality-specific pathway to regulate response to aberrant sensory signaling. Genetics *185*, 233-244.

Fackler,O.T. and Grosse,R. (2008). Cell motility through plasma membrane blebbing. J. Cell Biol. *181*, 879-884.

Faix,J., Kreppel,L., Shaulsky,G., Schleicher,M., and Kimmel,A.R. (2004). A rapid and efficient method to generate multiple gene disruptions in Dictyostelium discoideum using a single selectable marker and the Cre-loxP system. Nucleic Acids Res. *32*, e143.

Fatemi,S.H., Folsom,T.D., and Thuras,P.D. (2011). Deficits in GABA(B) receptor system in schizophrenia and mood disorders: a postmortem study. Schizophr. Res. *128*, 37-43.

Feit,I.N., Medynski,E.J., and Rothrock,M.J. (2001). Ammonia differentially suppresses the cAMP chemotaxis of anterior-like cells and prestalk cells in Dictyostelium discoideum. J. Biosci. *26*, 157-166.

Fetting,J.H., Wilcox,P.M., Sheidler,V.R., Enterline,J.P., Donehower,R.C., and Grochow,L.B. (1985). Tastes associated with parenteral chemotherapy for breast cancer. Cancer Treat. Rep. *69*, 1249-1251.

Fountain,S.J. (2010). Neurotransmitter receptor homologues of Dictyostelium discoideum. J. Mol. Neurosci. *41*, 263-266.

Francione,L., Smith,P.K., Accari,S.L., Taylor,P.E., Bokko,P.B., Bozzaro,S., Beech,P.L., and Fisher,P.R. (2009). Legionella pneumophila multiplication is enhanced by chronic AMPK signalling in mitochondrially diseased Dictyostelium cells. Dis. Model. Mech. *2*, 479-489.

Francione,L.M., Annesley,S.J., Carilla-Latorre,S., Escalante,R., and Fisher,P.R. (2010). The Dictyostelium model for mitochondrial disease. Semin. Cell Dev. Biol.

Frank,M.E., Bouverat,B.P., MacKinnon,B.I., and Hettinger,T.P. (2004). The distinctiveness of ionic and nonionic bitter stimuli. Physiol Behav. *80*, 421-431.

Fredriksson,R., Lagerstrom,M.C., Lundin,L.G., and Schioth,H.B. (2003). The G-protein-coupled receptors in the human genome form five main families. Phylogenetic analysis, paralogon groups, and fingerprints. Mol. Pharmacol. *63*, 1256-1272.

Friedberg,F. and Rivero,F. (2010). Single and multiple CH (calponin homology) domain containing multidomain proteins in Dictyostelium discoideum: an inventory. Mol. Biol. Rep. *37*, 2853-2862.

Fujiwara-Sawada,M., Imanishi,T., Yoshida,A., and Baba,J. (2003). Possible involvement of peripheral serotonin 5-HT3 receptors in fluvoxamine-induced emesis in Suncus murinus. J. Pharm. Pharmacol. *55*, 271-274.

Fukui,H., Yamamoto,M., Ando,T., Sasaki,S., and Sato,S. (1993a). Increase in serotonin levels in the dog ileum and blood by cisplatin as measured by microdialysis. Neuropharmacology *32*, 959-968.

Fukui,H., Yamamoto,M., Sasaki,S., and Sato,S. (1993b). Involvement of 5-HT3 receptors and vagal afferents in copper sulfate- and cisplatin-induced emesis in monkeys. Eur. J. Pharmacol. *249*, 13-18.

Fukui,H., Yamamoto,M., Sasaki,S., and Sato,S. (1994). Possible involvement of peripheral 5-HT4 receptors in copper sulfate-induced vomiting in dogs. Eur. J. Pharmacol. *257*, 47-52.

Funamoto,S., Milan,K., Meili,R., and Firtel,R.A. (2001). Role of phosphatidylinositol 3' kinase and a downstream pleckstrin homology domain-containing protein in controlling chemotaxis in dictyostelium. J. Cell Biol. *153*, 795-810.

Gaddum,J.H. (1961). Zinc sulphate 1% vomiting in a few minutes. In Pharmacology, (London: Oxford University Press), p. 266.

Garcia,G.L. and Parent,C.A. (2008a). Signal relay during chemotaxis. J. Microsc. *231*, 529-534.

Garcia,G.L. and Parent,C.A. (2008b). Signal relay during chemotaxis. J. Microsc. *231*, 529-534.

Garcia,R., Nguyen,L., and Brazill,D. (2013). Dictyostelium discoideum SecG interprets cAMP-mediated chemotactic signals to influence actin organization. Cytoskeleton (Hoboken.).

Gayatri,R. and Chatterjee,S. (1991). Effects of chlorpromazine on growth and development of Dictyostelium discoideum. Microbios *68*, 97-107.

Genick,U.K., Kutalik,Z., Ledda,M., Destito,M.C., Souza,M.M., Cirillo,C.A., Godinot,N., Martin,N., Morya,E., Sameshima,K., Bergmann,S., and le,C.J. (2011). Sensitivity of genome-wide-association signals to phenotyping strategy: the PROP-TAS2R38 taste association as a benchmark. PLoS. One. *6*, e27745.

Gerisch,G. and Keller,H.U. (1981). Chemotactic reorientation of granulocytes stimulated with micropipettes containing fMet-Leu-Phe. J. Cell Sci. *52*, 1-10.

Gerisch,G., Schroth-Diez,B., Muller-Taubenberger,A., and Ecke,M. (2012). PIP3 waves and PTEN dynamics in the emergence of cell polarity. Biophys. J. *103*, 1170-1178.

Glendinning,J.I., Yiin,Y.M., Ackroff,K., and Sclafani,A. (2008). Intragastric infusion of denatonium conditions flavor aversions and delays gastric emptying in rodents. Physiol Behav. *93*, 757-765.

Gold,H., Greiner,T., Cattell,M., Modell,W., Gluck,J., and Marsh,R. (1952). Difference in the relation of cardiac to emetic actions in oral and parenteral digitalization. Am. J. Med. *13*, 124-144.

Goury-Sistla,P., Nanjundiah,V., and Pande,G. (2012). Bimodal distribution of motility and cell fate in Dictyostelium discoideum. Int. J. Dev. Biol. *56*, 263-272.

Green,B.G. and Hayes,J.E. (2003). Capsaicin as a probe of the relationship between bitter taste and chemesthesis. Physiol Behav. *79*, 811-821.

Hansen,S.R., Janssen,C., and Beasley,V.R. (1993). Denatonium benzoate as a deterrent to ingestion of toxic substances: toxicity and efficacy. Vet. Hum. Toxicol. *35*, 234-236.

Harwood,A.J., Plyte,S.E., Woodgett,J., Strutt,H., and Kay,R.R. (1995). Glycogen synthase kinase 3 regulates cell fate in Dictyostelium. Cell *80*, 139-148.

Hayes,J.E., Bartoshuk,L.M., Kidd,J.R., and Duffy,V.B. (2008). Supertasting and PROP bitterness depends on more than the TAS2R38 gene. Chem. Senses *33*, 255-265.

Heaslip,R.J. and Evans,D.Y. (1995). Emetic, central nervous system, and pulmonary activities of rolipram in the dog. Eur. J. Pharmacol. *286*, 281-290.

Hilliard,M.A., Bergamasco,C., Arbucci,S., Plasterk,R.H., and Bazzicalupo,P. (2004). Worms taste bitter: ASH neurons, QUI-1, GPA-3 and ODR-3 mediate quinine avoidance in Caenorhabditis elegans. EMBO J. *23*, 1101-1111.

Hirose,R., Manabe,H., Nonaka,H., Yanagawa,K., Akuta,K., Sato,S., Ohshima,E., and Ichimura,M. (2007). Correlation between emetic effect of

phosphodiesterase 4 inhibitors and their occupation of the high-affinity rolipram binding site in Suncus murinus brain. Eur. J. Pharmacol. *573*, 93-99.

Hoeller,O. and Kay,R.R. (2007). Chemotaxis in the absence of PIP3 gradients. Curr. Biol. *17*, 813-817.

Hoffmann,I.S., Roa,M., Torrico,F., and Cubeddu,L.X. (2003). Ondansetron and metformin-induced gastrointestinal side effects. Am. J. Ther. *10*, 447-451.

Holmes,A.M., Rudd,J.A., Tattersall,F.D., Aziz,Q., and Andrews,P.L. (2009). Opportunities for the replacement of animals in the study of nausea and vomiting. Br. J. Pharmacol. *157*, 865-880.

Horn,C.C., De Jonghe,B.C., Matyas,K., and Norgren,R. (2009). Chemotherapy-induced kaolin intake is increased by lesion of the lateral parabrachial nucleus of the rat. Am. J. Physiol Regul. Integr. Comp Physiol *297*, R1375-R1382.

Horn,C.C., Kimball,B.A., Wang,H., Kaus,J., Dienel,S., Nagy,A., Gathright,G.R., Yates,B.J., and Andrews,P.L. (2013). Why can't rodents vomit? A comparative behavioral, anatomical, and physiological study. PLoS. One. *8*, e60537.

Horn,C.C., Murat,C., Rosazza,M., and Still,L. (2011). Effects of gastric distension and infusion of umami and bitter taste stimuli on vagal afferent activity. Brain Res. *1419*, 53-60.

Horn,C.C., Richardson,E.J., Andrews,P.L., and Friedman,M.I. (2004). Differential effects on gastrointestinal and hepatic vagal afferent fibers in the rat by the anti-cancer agent cisplatin. Auton. Neurosci. *115*, 74-81.

Hornby,P.J. (2001). Central neurocircuitry associated with emesis. Am. J. Med. *111 Suppl 8A*, 106S-112S.

Huang,Y.A., Maruyama,Y., and Roper,S.D. (2008). Norepinephrine is coreleased with serotonin in mouse taste buds. J. Neurosci. *28*, 13088-13093.

Huang,Y.E., Iijima,M., Parent,C.A., Funamoto,S., Firtel,R.A., and Devreotes,P. (2003). Receptor-mediated regulation of PI3Ks confines PI(3,4,5)P3 to the leading edge of chemotaxing cells. Mol. Biol. Cell *14*, 1913-1922.

Ibarra,N., Pollitt,A., and Insall,R.H. (2005). Regulation of actin assembly by SCAR/WAVE proteins. Biochem. Soc. Trans. *33*, 1243-1246.

Iijima,M. and Devreotes,P. (2002). Tumor suppressor PTEN mediates sensing of chemoattractant gradients. Cell *109*, 599-610.

Iijima,M., Huang,Y.E., and Devreotes,P. (2002). Temporal and spatial regulation of chemotaxis. Dev. Cell *3*, 469-478.

Iijima,M., Huang,Y.E., Luo,H.R., Vazquez,F., and Devreotes,P.N. (2004). Novel mechanism of PTEN regulation by its phosphatidylinositol 4,5-bisphosphate binding motif is critical for chemotaxis. J. Biol. Chem. *279*, 16606-16613.

Insall,R., Kuspa,A., Lilly,P.J., Shaulsky,G., Levin,L.R., Loomis,W.F., and Devreotes,P. (1994). CRAC, a cytosolic protein containing a pleckstrin

homology domain, is required for receptor and G protein-mediated activation of adenylyl cyclase in Dictyostelium. J. Cell Biol. *126*, 1537-1545.

Intelmann,D., Haseleu,G., and Hofmann,T. (2009). LC-MS/MS quantitation of hop-derived bitter compounds in beer using the ECHO technique. J. Agric. Food Chem. *57*, 1172-1182.

Ishimaru,Y., Okada,S., Naito,H., Nagai,T., Yasuoka,A., Matsumoto,I., and Abe,K. (2005). Two families of candidate taste receptors in fishes. Mech. Dev. *122*, 1310-1321.

Isono,K. and Morita,H. (2010). Molecular and cellular designs of insect taste receptor system. Front Cell Neurosci. *4*, 20.

Janardhan,D., Sreekanth,J., Kumar,P.T.P., and Krishna,M.V. (2010). Formulation and evaluation of baclofen orally disintegrating tablets. International Journal of Pharmaceutical Sciences and Nanotechnology *2*, 733-738.

Janetopoulos,C., Ma,L., Devreotes,P.N., and Iglesias,P.A. (2004). Chemoattractant-induced phosphatidylinositol 3,4,5-trisphosphate accumulation is spatially amplified and adapts, independent of the actin cytoskeleton. Proc. Natl. Acad. Sci. U. S. A *101*, 8951-8956.

Jang,W. and Gomer,R.H. (2011). Initial cell type choice in Dictyostelium. Eukaryot. Cell *10*, 150-155.

Javid,F.A. and Naylor,R.J. (2002). The effect of serotonin and serotonin receptor antagonists on motion sickness in Suncus murinus. Pharmacol. Biochem. Behav. *73*, 979-989.

Jin,T., Xu,X., Fang,J., Isik,N., Yan,J., Brzostowski,J.A., and Hereld,D. (2009). How human leukocytes track down and destroy pathogens: lessons learned from the model organism Dictyostelium discoideum. Immunol. Res. *43*, 118-127.

Jin,T., Xu,X., and Hereld,D. (2008). Chemotaxis, chemokine receptors and human disease. Cytokine *44*, 1-8.

Johannessen,S.I. and Henriksen,O. (1979). Comparative steady state serum levels of valproic acid administered as two different formulations--Deprakine and Orfiril. Acta Neurol. Scand. *60*, 371-374.

Jorenby,D.E., Smith,S.S., Fiore,M.C., Hurt,R.D., Offord,K.P., Croghan,I.T., Hays,J.T., Lewis,S.F., and Baker,T.B. (1995). Varying nicotine patch dose and type of smoking cessation counseling. JAMA *274*, 1347-1352.

Kae,H., Kortholt,A., Rehmann,H., Insall,R.H., van Haastert,P.J., Spiegelman,G.B., and Weeks,G. (2007). Cyclic AMP signalling in Dictyostelium: G-proteins activate separate Ras pathways using specific RasGEFs. EMBO Rep. *8*, 477-482.

Kalow,W. (1986). Ethnic differences in reactions to drugs and xenobiotics. Caffeine and other drugs. Prog. Clin. Biol. Res. *214*, 331-341.

Kamimura,Y., Xiong,Y., Iglesias,P.A., Hoeller,O., Bolourani,P., and Devreotes,P.N. (2008). PIP3-independent activation of TorC2 and PKB at the cell's leading edge mediates chemotaxis. Curr. Biol. *18*, 1034-1043.

Kan,K.K., Jones,R.L., Ngan,M.P., and Rudd,J.A. (2002). Actions of prostanoids to induce emesis and defecation in the ferret. Eur. J. Pharmacol. *453*, 299-308.

Kan,K.K., Jones,R.L., Ngan,M.P., and Rudd,J.A. (2003). Action of prostanoids on the emetic reflex of Suncus murinus (the house musk shrew). Eur. J. Pharmacol. *477*, 247-251.

Kang,R., Kae,H., Ip,H., Spiegelman,G.B., and Weeks,G. (2002). Evidence for a role for the Dictyostelium Rap1 in cell viability and the response to osmotic stress. J. Cell Sci. *115*, 3675-3682.

Karniol,I.G., Dalton,J., and Lader,M.H. (1978). Acute and chronic effects of lithium chloride on physiological and psychological measures in normals. Psychopharmacology (Berl) *57*, 289-294.

Kataria,R., Xu,X., Fusetti,F., Keizer-Gunnink,I., Jin,T., van Haastert,P.J., and Kortholt,A. (2013). Dictyostelium Ric8 is a nonreceptor guanine exchange factor for heterotrimeric G proteins and is important for development and chemotaxis. Proc. Natl. Acad. Sci. U. S. A *110*, 6424-6429.

Kawata,T. (2011). STAT signaling in Dictyostelium development. Dev. Growth Differ. *53*, 548-557.

Kayashima,N., Iwasaki,M., and Hayama,T. (1978a). Site of emetic action of oral copper sulfate in dogs. (II) Importance of lower duodenum. Jpn. J. Pharmacol. *28*, 797-801.

Kayashima,N., Tanaka,M., Iwasaki,M., and Hayama,T. (1978b). Site of emetic action of oral copper sulfate in dogs. (I) Thresholds of various portions of gastrointestinal tract to locally applied copper sulfate. Jpn. J. Pharmacol. *28*, 775-781.

Kim,U.K., Jorgenson,E., Coon,H., Leppert,M., Risch,N., and Drayna,D. (2003). Positional cloning of the human quantitative trait locus underlying taste sensitivity to phenylthiocarbamide. Science *299*, 1221-1225.

Kimmel,A.R. and Faix,J. (2006). Generation of multiple knockout mutants using the Cre-loxP system. Methods Mol. Biol. *346*, 187-199.

King,J.S. and Insall,R.H. (2008). Chemotaxis: TorC before you Akt.. Curr. Biol. *18*, R864-R866.

King,J.S. and Insall,R.H. (2009). Chemotaxis: finding the way forward with Dictyostelium. Trends Cell Biol. *19*, 523-530.

King,J.S., Teo,R., Ryves,J., Reddy,J.V., Peters,O., Orabi,B., Hoeller,O., Williams,R.S., and Harwood,A.J. (2009). The mood stabiliser lithium suppresses PIP3 signalling in Dictyostelium and human cells. Dis. Model. Mech. *2*, 306-312.

Kinnamon,S.C. (2011). Taste receptor signalling - from tongues to lungs. Acta Physiol (Oxf) *204*, 158-168.

Kissin,I. and Szallasi,A. (2011). Therapeutic targeting of TRPV1 by resiniferatoxin, from preclinical studies to clinical trials. Curr. Top. Med. Chem. *11*, 2159-2170.

Kitchin,F.D., Howel-Evans,W., Clarke,C.A., McConnel,R.B., and Sheppard,P.M. (1959). P.T.C. taste response and thyroid disease. Br. Med. J. *1*, 1069-1074.

Knetsch,M.L., Schafers,N., Horstmann,H., and Manstein,D.J. (2001). The Dictyostelium Bcr/Abr-related protein DRG regulates both Rac- and Rab-dependent pathways. EMBO J. *20*, 1620-1629.

Knox,A.P., Strominger,N.L., Battles,A.H., and Carpenter,D.O. (1993). Behavioral studies of emetic sensitivity in the ferret. Brain Res. Bull. *31*, 477-484.

Kortholt,A., Bolourani,P., Rehmann,H., Keizer-Gunnink,I., Weeks,G., Wittinghofer,A., and van Haastert,P.J. (2010). A Rap/phosphatidylinositol 3-kinase pathway controls pseudopod formation [corrected]. Mol. Biol. Cell *21*, 936-945.

Kortholt,A., Kataria,R., Keizer-Gunnink,I., van Egmond,W.N., Khanna,A., and van Haastert,P.J. (2011). Dictyostelium chemotaxis: essential Ras activation and accessory signalling pathways for amplification. EMBO Rep. *12*, 1273-1279.

Kortholt,A., King,J.S., Keizer-Gunnink,I., Harwood,A.J., and van Haastert,P.J. (2007). Phospholipase C regulation of phosphatidylinositol 3,4,5-trisphosphate-mediated chemotaxis. Mol. Biol. Cell *18*, 4772-4779.

Kris,M.G., Cubeddu,L.X., Gralla,R.J., Cupissol,D., Tyson,L.B., Venkatraman,E., and Homesley,H.D. (1996). Are more antiemetic trials with a placebo necessary? Report of patient data from randomized trials of placebo antiemetics with cisplatin. Cancer *78*, 2193-2198.

Kumar,K., Sharma,S., Kumar,P., and Deshmukh,R. (2013). Therapeutic potential of GABA receptor ligands in drug addiction, anxiety, depression and other CNS disorders. Pharmacol. Biochem. Behav.

Kusakabe,Y., Yasuoka,A., Asano-Miyoshi,M., Iwabuchi,K., Matsumoto,I., Arai,S., Emori,Y., and Abe,K. (2000). Comprehensive study on G protein alpha-subunits in taste bud cells, with special reference to the occurrence of Galphai2 as a major Galpha species. Chem. Senses *25*, 525-531.

Kuwayama,H. and van Haastert,P.J. (1998). Chemotactic and osmotic signals share a cGMP transduction pathway in Dictyostelium discoideum. FEBS Lett. *424*, 248-252.

Kyte,J. and Doolittle,R.F. (1982). A simple method for displaying the hydropathic character of a protein. J. Mol. Biol. *157*, 105-132.

Laffan,R.J. and Borison,H.L. (1957). Emetic action of nicotine and lobeline. J. Pharmacol. Exp. Ther. *121*, 468-476.

Lalueza-Fox,C., Gigli,E., de la Rasilla,M., Fortea,J., and Rosas,A. (2009a). Bitter taste perception in Neanderthals through the analysis of the TAS2R38 gene. Biol. Lett. *5*, 809-811.

Lalueza-Fox,C., Gigli,E., de la Rasilla,M., Fortea,J., and Rosas,A. (2009b). Bitter taste perception in Neanderthals through the analysis of the TAS2R38 gene. Biol. Lett. *5*, 809-811.

Langridge,P.D. and Kay,R.R. (2006). Blebbing of Dictyostelium cells in response to chemoattractant. Exp. Cell Res. *312*, 2009-2017.

Langridge,P.D. and Kay,R.R. (2007). Mutants in the Dictyostelium Arp2/3 complex and chemoattractant-induced actin polymerization. Exp. Cell Res. *313*, 2563-2574.

Lee,E. and Knecht,D.A. (2002). Visualization of actin dynamics during macropinocytosis and exocytosis. Traffic. *3*, 186-192.

Lehmann,D.M., Seneviratne,A.M., and Smrcka,A.V. (2008). Small molecule disruption of G protein beta gamma subunit signaling inhibits neutrophil chemotaxis and inflammation. Mol. Pharmacol. *73*, 410-418.

Li,G., Alexander,H., Schneider,N., and Alexander,S. (2000). Molecular basis for resistance to the anticancer drug cisplatin in Dictyostelium. Microbiology *146 (Pt 9)*, 2219-2227.

Li,H., Yang,L., Fu,H., Yan,J., Wang,Y., Guo,H., Hao,X., Xu,X., Jin,T., and Zhang,N. (2013). Association between Galphai2 and ELMO1/Dock180 connects chemokine signalling with Rac activation and metastasis. Nat. Commun. *4*, 1706.

Li,L., Norrelykke,S.F., and Cox,E.C. (2008). Persistent cell motion in the absence of external signals: a search strategy for eukaryotic cells. PLoS. One. *3*, e2093.

Liao,X.H., Buggey,J., Lee,Y.K., and Kimmel,A.R. (2013). Chemoattractant Stimulation of TORC2 is Regulated by Receptor/G protein Targeted Inhibitory Mechanisms that Function Upstream and Independently of an Essential GEF/Ras Activation Pathway in Dictyostelium. Mol. Biol. Cell.

Liggett,S.B. (2013). Bitter taste receptors on airway smooth muscle as targets for novel bronchodilators. Expert. Opin. Ther. Targets. *17*, 721-731.

Lilly,P., Wu,L., Welker,D.L., and Devreotes,P.N. (1993). A G-protein beta-subunit is essential for Dictyostelium development. Genes Dev. *7*, 986-995.

Lilly,P.J. and Devreotes,P.N. (1994). Identification of CRAC, a cytosolic regulator required for guanine nucleotide stimulation of adenylyl cyclase in Dictyostelium. J. Biol. Chem. *269*, 14123-14129.

Liman,E.R. (2007). TRPM5 and taste transduction. Handb. Exp. Pharmacol. 287-298.

Lindley,K.J. and Andrews,P.L. (2005). Pathogenesis and treatment of cyclical vomiting. J. Pediatr. Gastroenterol. Nutr. *41 Suppl 1*, S38-S40.

Liu,Y.L., Malik,N., Sanger,G.J., Friedman,M.I., and Andrews,P.L. (2005). Pica--a model of nausea? Species differences in response to cisplatin. Physiol Behav. *85*, 271-277.

Loovers,H.M., Postma,M., Keizer-Gunnink,I., Huang,Y.E., Devreotes,P.N., and van Haastert,P.J. (2006). Distinct roles of PI(3,4,5)P3 during chemoattractant signaling in Dictyostelium: a quantitative in vivo analysis by inhibition of PI3-kinase. Mol. Biol. Cell *17*, 1503-1513.

Lu,F.F., Su,P., Liu,F., and Daskalakis,Z.J. (2012). Activation of GABA(B) receptors inhibits protein kinase B/glycogen synthase kinase 3 signaling. Mol. Brain *5*, 41.

Ludlow,M.J., Durai,L., and Ennion,S.J. (2009). Functional characterization of intracellular Dictyostelium discoideum P2X receptors. J. Biol. Chem. *284*, 35227-35239.

MacWilliams,H.K. and Bonner,J.T. (1979). The prestalk-prespore pattern in cellular slime molds. Differentiation *14*, 1-22.

Maehashi,K. and Huang,L. (2009). Bitter peptides and bitter taste receptors. Cell Mol. Life Sci. *66*, 1661-1671.

Makale,M.T. and King,G.L. (1992). Surgical and pharmacological dissociation of cardiovascular and emetic responses to intragastric $CuSO_4$. Am. J. Physiol *263*, R284-R291.

Malyala,A., Zhang,C., Bryant,D.N., Kelly,M.J., and Ronnekleiv,O.K. (2008). PI3K signaling effects in hypothalamic neurons mediated by estrogen. J. Comp Neurol. *506*, 895-911.

Manahan,C.L., Iglesias,P.A., Long,Y., and Devreotes,P.N. (2004). Chemoattractant signaling in dictyostelium discoideum. Annu. Rev. Cell Dev. Biol. *20*, 223-253.

Matsuki,N., Ueno,S., Kaji,T., Ishihara,A., Wang,C.H., and Saito,H. (1988). Emesis induced by cancer chemotherapeutic agents in the Suncus murinus: a new experimental model. Jpn. J. Pharmacol. *48*, 303-306.

McBride,C.S., Arguello,J.R., and O'Meara,B.C. (2007). Five Drosophila genomes reveal nonneutral evolution and the signature of host specialization in the chemoreceptor superfamily. Genetics *177*, 1395-1416.

McMains,V.C., Liao,X.H., and Kimmel,A.R. (2008). Oscillatory signaling and network responses during the development of Dictyostelium discoideum. Ageing Res. Rev. *7*, 234-248.

McMains,V.C., Myre,M., Kreppel,L., and Kimmel,A.R. (2010). Dictyostelium possesses highly diverged presenilin/{gamma}-secretase that regulates growth and cell-fate specification and can accurately process human APP: a system for functional studies of the presenilin/{gamma}-secretase complex. Dis. Model. Mech.

McQuade,K.J., Nakajima,A., Ilacqua,A.N., Shimada,N., and Sawai,S. (2013). The green tea catechin epigallocatechin gallate (EGCG) blocks cell motility, chemotaxis and development in Dictyostelium discoideum. PLoS. One. *8*, e59275.

Meili,R., Ellsworth,C., and Firtel,R.A. (2000). A novel Akt/PKB-related kinase is essential for morphogenesis in Dictyostelium. Curr. Biol. *10*, 708-717.

Meili,R., Ellsworth,C., Lee,S., Reddy,T.B., Ma,H., and Firtel,R.A. (1999). Chemoattractant-mediated transient activation and membrane localization of Akt/PKB is required for efficient chemotaxis to cAMP in Dictyostelium. EMBO J. *18*, 2092-2105.

Meyerhof,W., Batram,C., Kuhn,C., Brockhoff,A., Chudoba,E., Bufe,B., Appendino,G., and Behrens,M. (2010). The molecular receptive ranges of human TAS2R bitter taste receptors. Chem. Senses *35*, 157-170.

Miller,A.D. and Leslie,R.A. (1994). The area postrema and vomiting. Front Neuroendocrinol. *15*, 301-320.

Miranda,C.L., Stevens,J.F., Helmrich,A., Henderson,M.C., Rodriguez,R.J., Yang,Y.H., Deinzer,M.L., Barnes,D.W., and Buhler,D.R. (1999). Antiproliferative and cytotoxic effects of prenylated flavonoids from hops (Humulus lupulus) in human cancer cell lines. Food Chem. Toxicol. *37*, 271-285.

Misty,R., Martinez,R., Ali,H., and Steimle,P.A. (2006). Naringenin is a novel inhibitor of Dictyostelium cell proliferation and cell migration. Biochem. Biophys. Res. Commun. *345*, 516-522.

Monastyrskaia,K., Lundstrom,K., Plahl,D., Acuna,G., Schweitzer,C., Malherbe,P., and Mutel,V. (1999). Effect of the umami peptides on the ligand binding and function of rat mGlu4a receptor might implicate this receptor in the monosodium glutamate taste transduction. Br. J. Pharmacol. *128*, 1027-1034.

Moqtaderi,Z. and Struhl,K. (2008). Expanding the repertoire of plasmids for PCR-mediated epitope tagging in yeast. Yeast *25*, 287-292.

Muller-Taubenberger,A. (2006). Application of fluorescent protein tags as reporters in live-cell imaging studies. Methods Mol. Biol. *346*, 229-246.

Na,J., Tunggal,B., and Eichinger,L. (2007). STATc is a key regulator of the transcriptional response to hyperosmotic shock. BMC. Genomics *8*, 123.

Nakajima,K., Tooyama,I., Kuriyama,K., and Kimura,H. (1996). Immunohistochemical demonstration of GABAB receptors in the rat gastrointestinal tract. Neurochem. Res. *21*, 211-215.

Nakayama,H., Yamakuni,H., Nakayama,A., Maeda,Y., Imazumi,K., Matsuo,M., and Mutoh,S. (2004). Diphenidol has no actual broad antiemetic activity in dogs and ferrets. J. Pharmacol. Sci. *96*, 301-306.

Nellen,W., Silan,C., and Firtel,R.A. (1984). DNA-mediated transformation in Dictyostelium discoideum: regulated expression of an actin gene fusion. Mol. Cell Biol. *4*, 2890-2898.

Nelson,R.D., Quie,P.G., and Simmons,R.L. (1975). Chemotaxis under agarose: a new and simple method for measuring chemotaxis and spontaneous migration of human polymorphonuclear leukocytes and monocytes. J. Immunol. *115*, 1650-1656.

Nelson,S.L. and Sanregret,J.D. (1997). Response of pigs to bitter-tasting compounds. Chem. Senses *22*, 129-132.

Ngai,J., Inngjerdingen,M., Berge,T., and Tasken,K. (2009). Interplay between the heterotrimeric G-protein subunits Galphaq and Galphai2 sets the threshold for chemotaxis and TCR activation. BMC. Immunol. *10*, 27.

Niijima,A., Jiang,Z.Y., Daunton,N.G., and Fox,R.A. (1987). Effect of copper sulphate on the rate of afferent discharge in the gastric branch of the vagus nerve in the rat. Neurosci. Lett. *80*, 71-74.

O'Donnel,S., Webb,J.K., and Shine,R. (2010). Conditioned taste aversion enhances the survival of an endangered predator imperilled by a toxic invader. Journal of Applied Ecology *47*, 558-565.

Oike,H., Nagai,T., Furuyama,A., Okada,S., Aihara,Y., Ishimaru,Y., Marui,T., Matsumoto,I., Misaka,T., and Abe,K. (2007). Characterization of ligands for fish taste receptors. J. Neurosci. *27*, 5584-5592.

Olivares,M., Araya,M., Pizarro,F., and Uauy,R. (2001). Nausea threshold in apparently healthy individuals who drink fluids containing graded concentrations of copper. Regul. Toxicol. Pharmacol. *33*, 271-275.

Osinski,M.A., Uchic,M.E., Seifert,T., Shaughnessy,T.K., Miller,L.N., Nakane,M., Cox,B.F., Brioni,J.D., and Moreland,R.B. (2005). Dopamine D2, but not D4, receptor agonists are emetogenic in ferrets. Pharmacol. Biochem. Behav. *81*, 211-219.

Pakes,N.K., Jayasinghe,S.N., and Williams,R.S. (2011). Bio-electrospraying and aerodynamically assisted bio-jetting the model eukaryotic Dictyostelium discoideum: assessing stress and developmental competency post treatment. J. R. Soc. Interface.

Pakes,N.K., Veltman,D.M., Rivero,F., Nasir,J., Insall,R., and Williams,R.S. (2012a). The Rac GEF ZizB regulates development, cell motility and cytokinesis in Dictyostelium. J. Cell Sci. *125*, 2457-2465.

Pakes,N.K., Veltman,D.M., and Williams,R. (2012b). Zizimin and Dock guanine nucleotide exchange factors in cell function and disease. Small GTPases. *4*.

Pal,S.K., Sharma,K., Pathak,A., Sawhney,I.M., and Prabhakar,S. (2004). Possible relationship between phenylthiocarbamide taste sensitivity and epilepsy. Neurol. India *52*, 206-209.

Parker,L.A., Limebeer,C.L., Rock,E.M., Litt,D.L., Kwiatkowska,M., and Piomelli,D. (2009). The FAAH inhibitor URB-597 interferes with cisplatin- and nicotine-induced vomiting in the Suncus murinus (house musk shrew). Physiol Behav. *97*, 121-124.

Parkinson,J., Muthas,D., Clark,M., Boyer,S., Valentin,J.P., and Ewart,L. (2011). Application of data mining and visualization techniques for the prediction of drug-induced nausea in man. Toxicol. Sci.

Parsons,J.A. and Summers,R.J. (1971). Cat assay for the emetic action of digitalis and related glycosides (digitoxin, digoxin, lanatoside C, ouabain and calactin). Br. J. Pharmacol. *42*, 143-152.

Peracino,B., Borleis,J., Jin,T., Westphal,M., Schwartz,J.M., Wu,L., Bracco,E., Gerisch,G., Devreotes,P., and Bozzaro,S. (1998). G protein beta subunit-null mutants are impaired in phagocytosis and chemotaxis due to inappropriate regulation of the actin cytoskeleton. J. Cell Biol. *141*, 1529-1537.

Percie du Sert,N., Rudd,J.A., Apfel,C.C., and Andrews,P.L. (2010). Cisplatin-induced emesis: systematic review and meta-analysis of the ferret model and the effects of 5-HT(3) receptor antagonists. Cancer Chemother. Pharmacol.

Percie du Sert,N., Rudd,J.A., Moss,R., and Andrews,P.L. (2009). The delayed phase of cisplatin-induced emesis is mediated by the area postrema and not the abdominal visceral innervation in the ferret. Neurosci. Lett. *465*, 16-20.

Percie du Sert,N., Holmes,A.M., Wallis,R., and Andrews,P.L. (2012). Predicting the emetic liability of novel chemical entities: a comparative study. Br. J. Pharmacol. *165*, 1848-1867.

Peyrot des,G.C., Beauchamp,G.K., Stern,R.M., Koch,K.L., and Breslin,P.A. (2011). Bitter taste induces nausea. Curr. Biol. *21*, R247-R248.

Pierce,K.L., Premont,R.T., and Lefkowitz,R.J. (2002). Seven-transmembrane receptors. Nat. Rev. Mol. Cell Biol. *3*, 639-650.

Pingle,S.C., Matta,J.A., and Ahern,G.P. (2007). Capsaicin receptor: TRPV1 a promiscuous TRP channel. Handb. Exp. Pharmacol. 155-171.

Pollard,T.D. and Borisy,G.G. (2003). Cellular motility driven by assembly and disassembly of actin filaments. Cell *112*, 453-465.

Pollera,C.F., Nardi,M., Marolla,P., Pinnaro,P., Terzoli,E., and Giannarelli,D. (1989). Effective control of CMF-related emesis with high-dose dexamethasone: results of a double-blind crossover trial with metoclopramide and placebo. Am. J. Clin. Oncol. *12*, 524-529.

Postma,M., Roelofs,J., Goedhart,J., Loovers,H.M., Visser,A.J., and van Haastert,P.J. (2004). Sensitization of Dictyostelium chemotaxis by

phosphoinositide-3-kinase-mediated self-organizing signalling patches. J. Cell Sci. *117*, 2925-2935.

Postma,M. and van Haastert,P.J. (2009). Mathematics of experimentally generated chemoattractant gradients. Methods Mol. Biol. *571*, 473-488.

Prabhu,Y. and Eichinger,L. (2006). The Dictyostelium repertoire of seven transmembrane domain receptors. Eur. J. Cell Biol. *85*, 937-946.

Prabhu,Y., Mondal,S., Eichinger,L., and Noegel,A.A. (2007a). A GPCR involved in post aggregation events in Dictyostelium discoideum. Dev. Biol. *312*, 29-43.

Prabhu,Y., Muller,R., Anjard,C., and Noegel,A.A. (2007b). GrlJ, a Dictyostelium GABAB-like receptor with roles in post-aggregation development. BMC. Dev. Biol. *7*, 44.

Pronin,A.N., Tang,H., Connor,J., and Keung,W. (2004). Identification of ligands for two human bitter T2R receptors. Chem. Senses *29*, 583-593.

Pronin,A.N., Xu,H., Tang,H., Zhang,L., Li,Q., and Li,X. (2007). Specific alleles of bitter receptor genes influence human sensitivity to the bitterness of aloin and saccharin. Curr. Biol. *17*, 1403-1408.

Punta,M., Coggill,P.C., Eberhardt,R.Y., Mistry,J., Tate,J., Boursnell,C., Pang,N., Forslund,K., Ceric,G., Clements,J., Heger,A., Holm,L., Sonnhammer,E.L., Eddy,S.R., Bateman,A., and Finn,R.D. (2012). The Pfam protein families database. Nucleic Acids Res. *40*, D290-D301.

Quarello,P., Garelli,E., Carando,A., Brusco,A., Calabrese,R., Dufour,C., Longoni,D., Misuraca,A., Vinti,L., Aspesi,A., Biondini,L., Loreni,F., Dianzani,I., and Ramenghi,U. (2010). Diamond-Blackfan anemia: genotype-phenotype correlations in Italian patients with RPL5 and RPL11 mutations. Haematologica *95*, 206-213.

Rands,E., Candelore,M.R., Cheung,A.H., Hill,W.S., Strader,C.D., and Dixon,R.A. (1990). Mutational analysis of beta-adrenergic receptor glycosylation. J. Biol. Chem. *265*, 10759-10764.

Raper,K.B. (1935). *Dictyostelium Discoideum*, a new species of slime mould from decaying forest leaves. J. Agricultural Research *50*, 135-147.

Reichling,C., Meyerhof,W., and Behrens,M. (2008). Functions of human bitter taste receptors depend on N-glycosylation. J. Neurochem. *106*, 1138-1148.

Richards,C.A. and Andrews,P.L. (2007). Emesis as a model system for the study of functional bowel disease. J. Pediatr. Gastroenterol. Nutr. *45 Suppl 2*, S120-S126.

Riera,C.E., Vogel,H., Simon,S.A., Damak,S., and le,C.J. (2009). Sensory attributes of complex tasting divalent salts are mediated by TRPM5 and TRPV1 channels. J. Neurosci. *29*, 2654-2662.

Riera,C.E., Vogel,H., Simon,S.A., and le,C.J. (2007). Artificial sweeteners and salts producing a metallic taste sensation activate TRPV1 receptors. Am. J. Physiol Regul. Integr. Comp Physiol *293*, R626-R634.

Rivero,F., Koppel,B., Peracino,B., Bozzaro,S., Siegert,F., Weijer,C.J., Schleicher,M., Albrecht,R., and Noegel,A.A. (1996). The role of the cortical cytoskeleton: F-actin crosslinking proteins protect against osmotic stress, ensure cell size, cell shape and motility, and contribute to phagocytosis and development. J. Cell Sci. *109 (Pt 11)*, 2679-2691.

Rivers,D.B., Dani,M.P., and Richards,E.H. (2009). The mode of action of venom from the endoparasitic wasp Pimpla hypochondriaca (hymenoptera: ichneumonidae) involves Ca+2-dependent cell death pathways. Arch. Insect Biochem. Physiol *71*, 173-190.

Robery,S., Mukanowa,J., Percie du Sert,N., Andrews,P.L., and Williams,R.S. (2011). Investigating the effect of emetic compounds on chemotaxis in Dictyostelium identifies a non-sentient model for bitter and hot tastant research. PLoS. One. *6*, e24439.

Rogachevskaja,O.A., Churbanov,G.D., Bystrova,M.F., Romanov,R.A., and Kolesnikov,S.S. (2011). Stimulation of the extracellular Ca(2)(+)-sensing receptor by denatonium. Biochem. Biophys. Res. Commun. *416*, 433-436.

Rondard,P., Goudet,C., Kniazeff,J., Pin,J.P., and Prezeau,L. (2011). The complexity of their activation mechanism opens new possibilities for the modulation of mGlu and GABAB class C G protein-coupled receptors. Neuropharmacology *60*, 82-92.

Rossler,P., Boekhoff,I., Tareilus,E., Beck,S., Breer,H., and Freitag,J. (2000). G protein betagamma complexes in circumvallate taste cells involved in bitter transduction. Chem. Senses *25*, 413-421.

Rossler,P., Kroner,C., Freitag,J., Noe,J., and Breer,H. (1998). Identification of a phospholipase C beta subtype in rat taste cells. Eur. J. Cell Biol. *77*, 253-261.

Rotondo,A., Serio,R., and Mule,F. (2010). Functional evidence for different roles of GABAA and GABAB receptors in modulating mouse gastric tone. Neuropharmacology *58*, 1033-1037.

Rotzoll,N., Dunkel,A., and Hofmann,T. (2005). Activity-guided identification of (S)-malic acid 1-O-D-glucopyranoside (morelid) and gamma-aminobutyric acid as contributors to umami taste and mouth-drying oral sensation of morel mushrooms (Morchella deliciosa Fr.). J. Agric. Food Chem. *53*, 4149-4156.

Rozengurt,E. and Sternini,C. (2007). Taste receptor signaling in the mammalian gut. Curr. Opin. Pharmacol. *7*, 557-562.

Rudd,J.A. and Wai,M.K. (2001). Genital grooming and emesis induced by vanilloids in Suncus murinus, the house musk shrew. Eur. J. Pharmacol. *422*, 185-195.

Ryan, R. S. M. British National Formulary. 63. 2012. British Medical Association and Royal Pharmaceutical Society.
Ref Type: Edited Book

Saito,R., Takano,Y., and Kamiya,H.O. (2003). Roles of substance P and NK(1) receptor in the brainstem in the development of emesis. J. Pharmacol. Sci. *91*, 87-94.

Sakurai,T., Misaka,T., Ishiguro,M., Masuda,K., Sugawara,T., Ito,K., Kobayashi,T., Matsuo,S., Ishimaru,Y., Asakura,T., and Abe,K. (2010). Characterization of the beta-D-glucopyranoside binding site of the human bitter taste receptor hTAS2R16. J. Biol. Chem. *285*, 28373-28378.

Sanger,G.J. and Andrews,P.L. (2006). Treatment of nausea and vomiting: gaps in our knowledge. Auton. Neurosci. *129*, 3-16.

Sanger,G.J., Holbrook,J.D., and Andrews,P.L. (2011). The translational value of rodent gastrointestinal functions: a cautionary tale. Trends Pharmacol. Sci.

Sasaki,A.T., Janetopoulos,C., Lee,S., Charest,P.G., Takeda,K., Sundheimer,L.W., Meili,R., Devreotes,P.N., and Firtel,R.A. (2007). G protein-independent Ras/PI3K/F-actin circuit regulates basic cell motility. J. Cell Biol. *178*, 185-191.

Sawano,S., Seto,E., Mori,T., and Hayashi,Y. (2005). G-protein-dependent and -independent pathways in denatonium signal transduction. Biosci. Biotechnol. Biochem. *69*, 1643-1651.

Schilde,C., Araki,T., Williams,H., Harwood,A., and Williams,J.G. (2004). GSK3 is a multifunctional regulator of Dictyostelium development. Development *131*, 4555-4565.

Schioth,H.B., Nordstrom,K.J., and Fredriksson,R. (2007). Mining the gene repertoire and ESTs for G protein-coupled receptors with evolutionary perspective. Acta Physiol (Oxf) *190*, 21-31.

Scott,A.M., Powell,G.M., Upshall,D.G., and Curtis,C.G. (1990). Pulmonary toxicity of thioureas in the rat. Environ. Health Perspect. *85*, 43-50.

Scott,T.R. and Giza,B.K. (1987). A measure of taste intensity discrimination in the rat through conditioned taste aversions. Physiol Behav. *41*, 315-320.

Seeley,R.J., Blake,K., Rushing,P.A., Benoit,S., Eng,J., Woods,S.C., and D'Alessio,D. (2000). The role of CNS glucagon-like peptide-1 (7-36) amide receptors in mediating the visceral illness effects of lithium chloride. J. Neurosci. *20*, 1616-1621.

Seymour,M.T. (1993). The pharmacokinetics and pharmacodynamics of chemotherapeutic agents. In Emesis in anti-cancer therapy - mechanisms and treatment, P.L.R.Andrews and G.J.Sanger, eds. (London, UK: Hall Medical), pp. 9-44.

Shepard,T.H. and Gartler,S.M. (1960). Increased incidence of non-tasters of phenylthiocarbamide among congenical athyreotic cretins. Science *131*, 929.

Shi,P. and Zhang,J. (2006). Contrasting modes of evolution between vertebrate sweet/umami receptor genes and bitter receptor genes. Mol. Biol. Evol. *23*, 292-300.

Shivaprasad,H.S., Chaithra,P.T., Kavitha,P., and Malini,S.S. (2012). Role of phenylthiocarbamide as a genetic marker in predicting the predisposition of disease traits in humans. J. Nat. Sci. Biol. Med. *3*, 43-47.

Sibert,J.R. and Frude,N. (1991). Bittering agents in the prevention of accidental poisoning: children's reactions to denatonium benzoate (Bitrex). Arch. Emerg. Med. *8*, 1-7.

Sievers,F., Wilm,A., Dineen,D., Gibson,T.J., Karplus,K., Li,W., Lopez,R., McWilliam,H., Remmert,M., Soding,J., Thompson,J.D., and Higgins,D.G. (2011). Fast, scalable generation of high-quality protein multiple sequence alignments using Clustal Omega. Mol. Syst. Biol. *7*, 539.

Sillo,A., Bloomfield,G., Balest,A., Balbo,A., Pergolizzi,B., Peracino,B., Skelton,J., Ivens,A., and Bozzaro,S. (2008). Genome-wide transcriptional changes induced by phagocytosis or growth on bacteria in Dictyostelium. BMC. Genomics *9*, 291.

Smith,J.E., Paton,J.F., and Andrews,P.L. (2002). An arterially perfused decerebrate preparation of Suncus murinus (house musk shrew) for the study of emesis and swallowing. Exp. Physiol *87*, 563-574.

Smith,P.B. and Crespi,C. (2002). Thiourea toxicity in mouse C3H/10T1/2 cells expressing human flavin-dependent monooxygenase 3. Biochem. Pharmacol. *63*, 1941-1948.

Stephens,L., Milne,L., and Hawkins,P. (2008). Moving towards a better understanding of chemotaxis. Curr. Biol. *18*, R485-R494.

Sternini,C. (2007). Taste receptors in the gastrointestinal tract. IV. Functional implications of bitter taste receptors in gastrointestinal chemosensing. Am. J. Physiol Gastrointest. Liver Physiol *292*, G457-G461.

Storr,M.A. and Sharkey,K.A. (2007). The endocannabinoid system and gut-brain signalling. Curr. Opin. Pharmacol. *7*, 575-582.

Strehle,A., Schleicher,M., and Faix,J. (2006). Trix, a novel Rac guanine-nucleotide exchange factor from Dictyostelium discoideum is an actin-binding protein and accumulates at endosomes. Eur. J. Cell Biol. *85*, 1035-1045.

Suire,S., Lecureuil,C., Anderson,K.E., Damoulakis,G., Niewczas,I., Davidson,K., Guillou,H., Pan,D., Jonathan,C., Phillip,T.H., and Stephens,L. (2012). GPCR activation of Ras and PI3Kc in neutrophils depends on PLCb2/b3 and the RasGEF RasGRP4. EMBO J. *31*, 3118-3129.

Swiss,E.D. (1952). The emetic properties of veratrum derivatives. J. Pharmacol. Exp. Ther. *104*, 76-86.

Symonds,E., Butler,R., and Omari,T. (2003). The effect of the GABAB receptor agonist baclofen on liquid and solid gastric emptying in mice. Eur. J. Pharmacol. *470*, 95-97.

Szallasi,A. (1994). The vanilloid (capsaicin) receptor: receptor types and species differences. Gen. Pharmacol. *25*, 223-243.

Szolcsanyi,J. (2004). Forty years in capsaicin research for sensory pharmacology and physiology. Neuropeptides *38*, 377-384.

Tabata,N., Ito,M., Tomoda,H., and Omura,S. (1997). Xanthohumols, diacylglycerol acyltransferase inhibitors, from Humulus lupulus. Phytochemistry *46*, 683-687.

Tajima,T., Watanabe,N., Kogawa,Y., Takiguchi,N., Kato,J., Ikeda,T., Kuroda,A., and Ohtake,H. (2001). Chemotaxis of the nematode Caenorhabditis elegans toward cycloheximide and quinine hydrochloride. J. Biosci. Bioeng. *91*, 322-324.

Talavera,K., Yasumatsu,K., Yoshida,R., Margolskee,R.F., Voets,T., Ninomiya,Y., and Nilius,B. (2008). The taste transduction channel TRPM5 is a locus for bitter-sweet taste interactions. FASEB J. *22*, 1343-1355.

Taminato,A., Bagattini,R., Gorjao,R., Chen,G., Kuspa,A., and Souza,G.M. (2002). Role for YakA, cAMP, and protein kinase A in regulation of stress responses of Dictyostelium discoideum cells. Mol. Biol. Cell *13*, 2266-2275.

Tang,L., Franca-Koh,J., Xiong,Y., Chen,M.Y., Long,Y., Bickford,R.M., Knecht,D.A., Iglesias,P.A., and Devreotes,P.N. (2008). tsunami, the Dictyostelium homolog of the Fused kinase, is required for polarization and chemotaxis. Genes Dev. *22*, 2278-2290.

Tao,Y., Howlett,A., and Klein,C. (1996). Nitric oxide inhibits the initiation of cAMP pulsing in D. discoideum without altering receptor-activated adenylate cyclase. Cell Signal. *8*, 26-34.

Teo,R., Lewis,K.J., Forde,J.E., Ryves,W.J., Reddy,J.V., Rogers,B.J., and Harwood,A.J. (2010). Glycogen synthase kinase-3 is required for efficient Dictyostelium chemotaxis. Mol. Biol. Cell *21*, 2788-2796.

Tepper,B.J., White,E.A., Koelliker,Y., Lanzara,C., d'Adamo,P., and Gasparini,P. (2009). Genetic variation in taste sensitivity to 6-n-propylthiouracil and its relationship to taste perception and food selection. Ann. N. Y. Acad. Sci. *1170*, 126-139.

Terbach,N., Shah,R., Kelemen,R., Klein,P.S., Gordienko,D., Brown,N.A., Wilkinson,C.J., and Williams,R.S. (2011). Identifying an uptake mechanism for the antiepileptic and bipolar disorder treatment valproic acid using the simple biomedical model Dictyostelium. J. Cell Sci. *124*, 2267-2276.

Terunuma,M., Pangalos,M.N., and Moss,S.J. (2010). Functional modulation of GABAB receptors by protein kinases and receptor trafficking. Adv. Pharmacol. *58*, 113-122.

Theibert,A. and Devreotes,P.N. (1984). Adenosine and its derivatives inhibit the cAMP signaling response in Dictyostelium discoideum. Dev. Biol. *106*, 166-173.

Tomohiro,D., Mizuta,K., Fujita,T., Nishikubo,Y., and Kumamoto,E. (2013). Inhibition by capsaicin and its related vanilloids of compound action potentials in frog sciatic nerves. Life Sci. *92*, 368-378.

Tordoff,M.G., Alarcon,L.K., and Lawler,M.P. (2008). Preferences of 14 rat strains for 17 taste compounds. Physiol Behav. *95*, 308-332.

Torii,Y., Saito,H., and Matsuki,N. (1991). Selective blockade of cytotoxic drug-induced emesis by 5-HT3 receptor antagonists in Suncus murinus. Jpn. J. Pharmacol. *55*, 107-113.

Torii,Y., Saito,H., and Matsuki,N. (1994). Induction of emesis in Suncus murinus by pyrogallol, a generator of free radicals. Br. J. Pharmacol. *111*, 431-434.

Ueda,M. and Shibata,T. (2007). Stochastic signal processing and transduction in chemotactic response of eukaryotic cells. Biophys. J. *93*, 11-20.

Ueda,T., Ugawa,S., Yamamura,H., Imaizumi,Y., and Shimada,S. (2003). Functional interaction between T2R taste receptors and G-protein alpha subunits expressed in taste receptor cells. J. Neurosci. *23*, 7376-7380.

Ukhanov,K., Brunert,D., Corey,E.A., and Ache,B.W. (2011). Phosphoinositide 3-kinase-dependent antagonism in mammalian olfactory receptor neurons. J. Neurosci. *31*, 273-280.

Ukhanov,K., Corey,E.A., and Ache,B.W. (2013). Phosphoinositide 3-kinase dependent inhibition as a broad basis for opponent coding in Mammalian olfactory receptor neurons. PLoS. One. *8*, e61553.

van Haastert,P.J., Jastorff,B., Pinas,J.E., and Konijn,T.M. (1982). Analogs of cyclic AMP as chemoattractants and inhibitors of Dictyostelium chemotaxis. J. Bacteriol. *149*, 99-105.

van Haastert,P.J., Keizer-Gunnink,I., and Kortholt,A. (2007a). Essential role of PI3-kinase and phospholipase A2 in Dictyostelium discoideum chemotaxis. J. Cell Biol. *177*, 809-816.

van Haastert,P.J., Keizer-Gunnink,I., and Kortholt,A. (2007b). Essential role of PI3-kinase and phospholipase A2 in Dictyostelium discoideum chemotaxis. J. Cell Biol. *177*, 809-816.

van,W.A. and van Haastert,P.J. (1984). Transmethylation inhibitors decrease chemotactic sensitivity and delay cell aggregation in Dictyostelium discoideum. J. Bacteriol. *157*, 368-374.

Varnum,B. and Soll,D.R. (1984). Effects of cAMP on single cell motility in Dictyostelium. J. Cell Biol. *99*, 1151-1155.

Veltman,D.M., Akar,G., Bosgraaf,L., and van Haastert,P.J. (2009). A new set of small, extrachromosomal expression vectors for Dictyostelium discoideum. Plasmid *61*, 110-118.

Veltman,D.M., Keizer-Gunnik,I., and van Haastert,P.J. (2008). Four key signaling pathways mediating chemotaxis in Dictyostelium discoideum. J. Cell Biol. *180*, 747-753.

Veltman,D.M., King,J.S., Machesky,L.M., and Insall,R.H. (2012). SCAR knockouts in Dictyostelium: WASP assumes SCAR's position and upstream regulators in pseudopods. J. Cell Biol. *198*, 501-508.

Veltman,D.M., Roelofs,J., Engel,R., Visser,A.J., and van Haastert,P.J. (2005). Activation of soluble guanylyl cyclase at the leading edge during Dictyostelium chemotaxis. Mol. Biol. Cell *16*, 976-983.

Veltman,D.M. and van Haastert,P.J. (2008). The role of cGMP and the rear of the cell in Dictyostelium chemotaxis and cell streaming. J. Cell Sci. *121*, 120-127.

Verkerke-Van,W., I, Kim,J.Y., Brandt,R., Devreotes,P.N., and Schaap,P. (1998). Functional promiscuity of gene regulation by serpentine receptors in Dictyostelium discoideum. Mol. Cell Biol. *18*, 5744-5749.

Vlahou,G. and Rivero,F. (2006). Rho GTPase signaling in Dictyostelium discoideum: insights from the genome. Eur. J. Cell Biol. *85*, 947-959.

Waligorska,A., Wianecka-Skoczen,M., and Korohoda,W. (2008). Reversible inhibition of movement in the amoebae Dictyostelium discoideum and its effect on chemoattractant recognition. Folia Biol. (Krakow.) *56*, 123-131.

Wang,G.P. and Bushman,F.D. (2006). A statistical method for comparing viral growth curves. J. Virol. Methods *135*, 118-123.

Wang,Y., Chen,C.L., and Iijima,M. (2011). Signaling mechanisms for chemotaxis. Dev. Growth Differ. *53*, 495-502.

Weng,C.J. and Yen,G.C. (2012). Flavonoids, a ubiquitous dietary phenolic subclass, exert extensive in vitro anti-invasive and in vivo anti-metastatic activities. Cancer Metastasis Rev. *31*, 323-351.

White,J.H., Wise,A., Main,M.J., Green,A., Fraser,N.J., Disney,G.H., Barnes,A.A., Emson,P., Foord,S.M., and Marshall,F.H. (1998). Heterodimerization is required for the formation of a functional GABA(B) receptor. Nature *396*, 679-682.

Wilczynska,Z., Happle,K., Muller-Taubenberger,A., Schlatterer,C., Malchow,D., and Fisher,P.R. (2005). Release of Ca2+ from the endoplasmic reticulum contributes to Ca2+ signaling in Dictyostelium discoideum. Eukaryot. Cell *4*, 1513-1525.

Williams,R.S., Boeckeler,K., Graf,R., Muller-Taubenberger,A., Li,Z., Isberg,R.R., Wessels,D., Soll,D.R., Alexander,H., and Alexander,S. (2006a).

Towards a molecular understanding of human diseases using Dictyostelium discoideum. Trends Mol. Med. *12*, 415-424.

Williams,R.S., Boeckeler,K., Graf,R., Muller-Taubenberger,A., Li,Z., Isberg,R.R., Wessels,D., Soll,D.R., Alexander,H., and Alexander,S. (2006b). Towards a molecular understanding of human diseases using Dictyostelium discoideum. Trends Mol. Med. *12*, 415-424.

Williams,R.S., Cheng,L., Mudge,A.W., and Harwood,A.J. (2002). A common mechanism of action for three mood-stabilizing drugs. Nature *417*, 292-295.

Wilson,G.N., Biesan,O.R., Remus,J.L., and Mickley,G.A. (2011). Baclofen alters gustatory discrimination capabilities and induces a conditioned taste aversion (CTA). BMC. Res. Notes *4*, 527.

Wong,C.C., Traynor,D., Basse,N., Kay,R.R., and Warren,A.J. (2011). Defective ribosome assembly in Shwachman-Diamond syndrome. Blood *118*, 4305-4312.

Wu,S.V., Rozengurt,N., Yang,M., Young,S.H., Sinnett-Smith,J., and Rozengurt,E. (2002). Expression of bitter taste receptors of the T2R family in the gastrointestinal tract and enteroendocrine STC-1 cells. Proc. Natl. Acad. Sci. U. S. A *99*, 2392-2397.

Wu,Y. and Janetopoulos,C. (2013). Systematic analysis of gamma-aminobutyric acid (GABA) metabolism and function in the social amoeba Dictyostelium discoideum. J. Biol. Chem.

Xu,X. and Jin,T. (2012). A shortcut from GPCR signaling to Rac-mediated actin cytoskeleton through an ELMO/DOCK complex. Small GTPases. *3*, 183-185.

Xu,X., Muller-Taubenberger,A., Adley,K.E., Pawolleck,N., Lee,V.W., Wiedemann,C., Sihra,T.S., Maniak,M., Jin,T., and Williams,R.S. (2007). Attenuation of phospholipid signaling provides a novel mechanism for the action of valproic acid. Eukaryot. Cell *6*, 899-906.

Yamamoto,K., Nakai,M., Nohara,K., and Yamatodani,A. (2007). The anti-cancer drug-induced pica in rats is related to their clinical emetogenic potential. Eur. J. Pharmacol. *554*, 34-39.

Yamamoto,K., Ngan,M.P., Takeda,N., Yamatodani,A., and Rudd,J.A. (2004). Differential activity of drugs to induce emesis and pica behavior in Suncus murinus (house musk shrew) and rats. Physiol Behav. *83*, 151-156.

Yan,J., Mihaylov,V., Xu,X., Brzostowski,J.A., Li,H., Liu,L., Veenstra,T.D., Parent,C.A., and Jin,T. (2012). A Gbetagamma effector, ElmoE, transduces GPCR signaling to the actin network during chemotaxis. Dev. Cell *22*, 92-103.

Yarmolinsky,D.A., Zuker,C.S., and Ryba,N.J. (2009). Common sense about taste: from mammals to insects. Cell *139*, 234-244.

Yin,X., Gyles,C.L., and Gong,J. (2012). Grapefruit juice and its constituents augment the effect of low pH on inhibition of survival and adherence to intestinal

epithelial cells of Salmonella enterica serovar Typhimurium PT193. Int. J. Food Microbiol. *158*, 232-238.

Yoshida,K. and Soldati,T. (2006). Dissection of amoeboid movement into two mechanically distinct modes. J. Cell Sci. *119*, 3833-3844.

Zhang,S., Charest,P.G., and Firtel,R.A. (2008). Spatiotemporal regulation of Ras activity provides directional sensing. Curr. Biol. *18*, 1587-1593.

Zicha,D., Dunn,G.A., and Brown,A.F. (1991). A new direct-viewing chemotaxis chamber. J. Cell Sci. *99 (Pt 4)*, 769-775.

Zigmond,S.H. (1977). Ability of polymorphonuclear leukocytes to orient in gradients of chemotactic factors. J. Cell Biol. *75*, 606-616.

Zischka,H., Oehme,F., Pintsch,T., Ott,A., Keller,H., Kellermann,J., and Schuster,S.C. (1999). Rearrangement of cortex proteins constitutes an osmoprotective mechanism in Dictyostelium. EMBO J. *18*, 4241-4249.

Zubare-Samuelov,M., Peri,I., Tal,M., Tarshish,M., Spielman,A.I., and Naim,M. (2003). Some sweet and bitter tastants stimulate inhibitory pathway of adenylyl cyclase via melatonin and alpha 2-adrenergic receptors in Xenopus laevis melanophores. Am. J. Physiol Cell Physiol *285*, C1255-C1262.

Appendices

Compound	Concentration (mM)	Velocity (pre) (μm/sec)	Velocity (post) (μm/sec)	P-value (Velocity)	Aspect (pre)	Aspect (post)	P-value (Aspect)
5-flurouracil	0.25	0.2111±0.002	0.1680±0.003	ns	2.573±0.034	2.192±0.024	ns
Actinomycin D	0.7	0.2211±0.003	0.1229±0.002	ns	2.575±0.023	2.106±0.015	ns
Cisplatin	0.3	0.1474±0.002	0.1827±0.002	ns	2.682±0.018	3.119±0.031	ns
Cycloheximide	5	0.2266±0.004	0.1903±0.002	ns	2.525±0.027	2.267±0.033	ns
Methotrexate	0.25	2.2197±0.003	0.2165±0.003	ns	2.352±0.017	2.470±0.023	ns
Streptozotocin	0.001	0.1891±0.002	0.1669±0.0022	ns	2.277±0.020	2.125±0.019	ns
Vincristine	0.001	0.2564±0.003	0.2451±0.003	ns	2.582±0.014	2.355±0.018	ns
5-hydroxytryptamine	0.1	0.1649±0.002	0.1907±0.002	ns	3.086±0.032	2.958±0.022	ns
Apomorphine HCl	1	0.1496±0.003	0.1488±0.002	ns	3.020±0.030	2.852±0.024	ns
Substance P	0.001	0.1843±0.003	0.1555±0.003	ns	2.914±0.015	2.973±0.028	ns
Nicotine	0.1	0.1300±0.004	0.1178±0.003	ns	2.594±0.035	2.682±0.022	ns
Loperamide HCl	0.1	0.1250±0.002	0.7288±0.002	ns	2.582±0.018	2.337±0.018	ns
Veratridine HCl	0.5	0.1785±0.003	0.1899±0.003	ns	2.784±0.043	2.800±0.137	ns
Fluoxetine	0.0065	0.1576±0.002	0.2101±0.001	ns	2.893±0.017	1.807±0.023	ns
Digoxin	0.001	0.1334±0.003	0.0798±0.002	ns	2.595±0.025	2.019±0.014	ns
Pyrogallol	10	0.2038±0.003	0.1787±0.004	ns	2.990±0.022	2.749±0.028	ns
Lithium Cl	10	0.2151±0.004	0.2164±0.004	ns	2.532±0.020	2.451±0.031	ns
Metformin	10	0.1392±0.003	0.1150±0.003	ns	2.724±0.023	2.638±0.027	ns
$PGF_{2\alpha}$	0.1	0.1673±0.003	0.1765±0.003	ns	3.034±0.033	3.164±0.034	ns

Appendix 1. Summary of non-effective compounds on *Dictyostelium* cell behaviour (velocity and aspect). Emetic compounds showing no effect on *Dictyostelium* behaviour included cytotoxic agents (5-fluorouracil, actinomycin D, cisplatin, cycloheximide, methotrexate, streptozotocin and vincristine), receptor agonists (5-hydroxytryptamine, apomorphine hydrochloride, substance P, nicotine, loperamide hydrochloride,and veratridine hydrochloride), a selective serotonin reuptake inhibitor (fluoxetine), an extracellular enzyme inhibitor (digoxin), a free radical generator (pyrogallol), a central nervous system depressant (lithium chloride), an enteroendocrine cell stimulant (metformin) and a prostaglandin ($PGF_{2\alpha}$). Mean velocity and aspect pre- and post-addition of each compound has been summarised, where no significant difference was observed. Statistical analyses were performed using 2-tailed paired Student t-tests, where a minimum of 30 cells were measured in each of three replicates. ns = not significant.

NCBI Number	Gene	Organism	Number of *Dictyostelium* BLAST Hits	Highest E-value
7442	TRPV1	*H. Sapiens*	>10	0.001
51393	TRPV2	*H. Sapiens*	5	0.0006
162514	TRPV3	*H. Sapiens*	8	6.00E-05
59341	TRPV4	*H. Sapiens*	4	0.002
56302	TRPV5	*H. Sapiens*	>10	5.00E-09
55503	TRPV6	*H. Sapiens*	7	2.00E-05
193034	TRPV1	*M. musculus*	>10	4.00E-04
22368	TRPV2	*M. musculus*	1	1.00E-04
246788	TRPV3	*M. musculus*	10	2.00E-05
63873	TRPV4	*M. musculus*	3	5.00E-03
194352	TRPV5	*M. musculus*	>10	5.00E-06
64177	TRPV6	*M. musculus*	>10	6.00E-09
177117	OSM-9	*C. elegans*	>10	5.00E-06
188314	OCR-2	*C. elegans*	>10	5.00E-07

Appendix 2. BLAST analysis of the *Dictyostelium* genome for proteins showing amino acid similarity to TRPV receptors from multiple species. Potential homologues are defined by an E-value of less than $1.00E^{-40}$, thus *Dictyostelium* does not contain proteins showing significant sequence similarity to be considered as homologues.

NCBI Number	Gene	Organism	Number of *Dictyostelium* BLAST Hits	Highest E-value
50834	TAS2R1	*H. sapien*	0	N/A
50831	TAS2R3	*H. sapien*	0	N/A
50832	TAS2R4	*H. sapien*	0	N/A
54429	TAS2R5	*H. sapien*	0	N/A
50837	TAS2R7	*H. sapien*	0	N/A
50836	TAS2R8	*H. sapien*	0	N/A
50835	TAS2R9	*H. sapien*	0	N/A
50839	TAS2R10	*H. sapien*	0	N/A
50838	TAS2R13	*H. sapien*	0	N/A
50840	TAS2R14	*H. sapien*	0	N/A
50833	TAS2R16	*H. sapien*	0	N/A
259294	TAS2R19	*H. sapien*	0	N/A
259295	TAS2R20	*H. sapien*	0	N/A
259293	TAS2R30	*H. sapien*	0	N/A
259290	TAS2R31	*H. sapien*	0	N/A
5726	TAS2R38	*H. sapien*	0	N/A
259285	TAS2R39	*H. sapien*	0	N/A
259286	TAS2R40	*H. sapien*	0	N/A
259287	TAS2R41	*H. sapien*	1	0.034
353164	TAS2R42	*H. sapien*	0	N/A
259289	TAS2R43	*H. sapien*	0	N/A
259291	TAS2R45	*H. sapien*	0	N/A
259292	TAS2R46	*H. sapien*	0	N/A
259296	TAS2R50	*H. sapien*	0	N/A
338398	TAS2R60	*H. sapien*	0	N/A
387339	TAS2R102	*M. musculus*	0	N/A
667992	TAS2R103	*M. musculus*	0	N/A
387340	TAS2R104	*M. musculus*	0	N/A
57252	TAS2R105	*M. musculus*	0	N/A
387341	TAS2R106	*M. musculus*	0	N/A
387342	TAS2R107	*M. musculus*	0	N/A
387343	TAS2R109	*M. musculus*	0	N/A
387344	TAS2R110	*M. musculus*	0	N/A
387345	TAS2R113	*M. musculus*	0	N/A
387346	TAS2R114	*M. musculus*	0	N/A
112408	TAS2R116	*M. musculus*	0	N/A
353166	TAS2R117	*M. musculus*	0	N/A
57254	TAS2R119	*M. musculus*	0	N/A
387348	TAS2R120	*M. musculus*	0	N/A
353167	TAS2R123	*M. musculus*	0	N/A
387351	TAS2R124	*M. musculus*	0	N/A
387352	TAS2R125	*M. musculus*	0	N/A
387353	TAS2R126	*M. musculus*	0	N/A

387354	TAS2R129	*M. musculus*	0	N/A
387511	TAS2R134	*M. musculus*	0	N/A
387512	TAS2R135	*M. musculus*	0	N/A
353165	TAS2R136	*M. musculus*	0	N/A
387616	TAS2R140	*M. musculus*	0	N/A
387514	TAS2R143	*M. musculus*	0	N/A
664690	TAS2R200.1	*D.rerio*	0	N/A
553134	TAS2R200.2	*D.rerio*	0	N/A
798975	TAS2R202	*D.rerio*	0	N/A
36094	GR47A	*D. melanogastar*	0	N/A
117484	GR59B	*D. melanogastar*	0	N/A
38935	GR66A	*D. melanogastar*	0	N/A
117498	GR22E	*D. melanogastar*	0	N/A
117349	GR22F	*D. melanogastar*	0	N/A
117492	GR22B	*D. melanogastar*	0	N/A
178236	QUI-1	*C. elegans*	>10	2.00E-19
177117	OSM-9	*C. elegans*	>10	5.00E-06
188314	OCR-2	*C. elegans*	>10	5.00E-07

Appendix 3. BLAST analysis of the *Dictyostelium* genome for proteins showing amino acid similarity to known bitter receptors from multiple species. Potential homologues are defined by an E-value of less than $1.00E^{-40}$, thus *Dictyostelium* does not contain proteins showing significant sequence similarity to be considered as homologues. N/A = Not applicable.

NCBI Number	Gene	Organism	Number of *Dictyostelium* BLAST Hits	Highest E-value
29850	TRPM5	*H. Sapiens*	0	N/A
56843	TRPM5	*M. musculus*	0	N/A

Appendix 4. BLAST analysis of the *Dictyostelium* genome for proteins showing amino acid similarity to TRPM5 receptors from human and mouse. Potential homologues are defined by an E-value of less than $1.00E^{-40}$, thus *Dictyostelium* does not contain proteins showing significant sequence similarity to be considered as homologues. N/A = Not applicable.

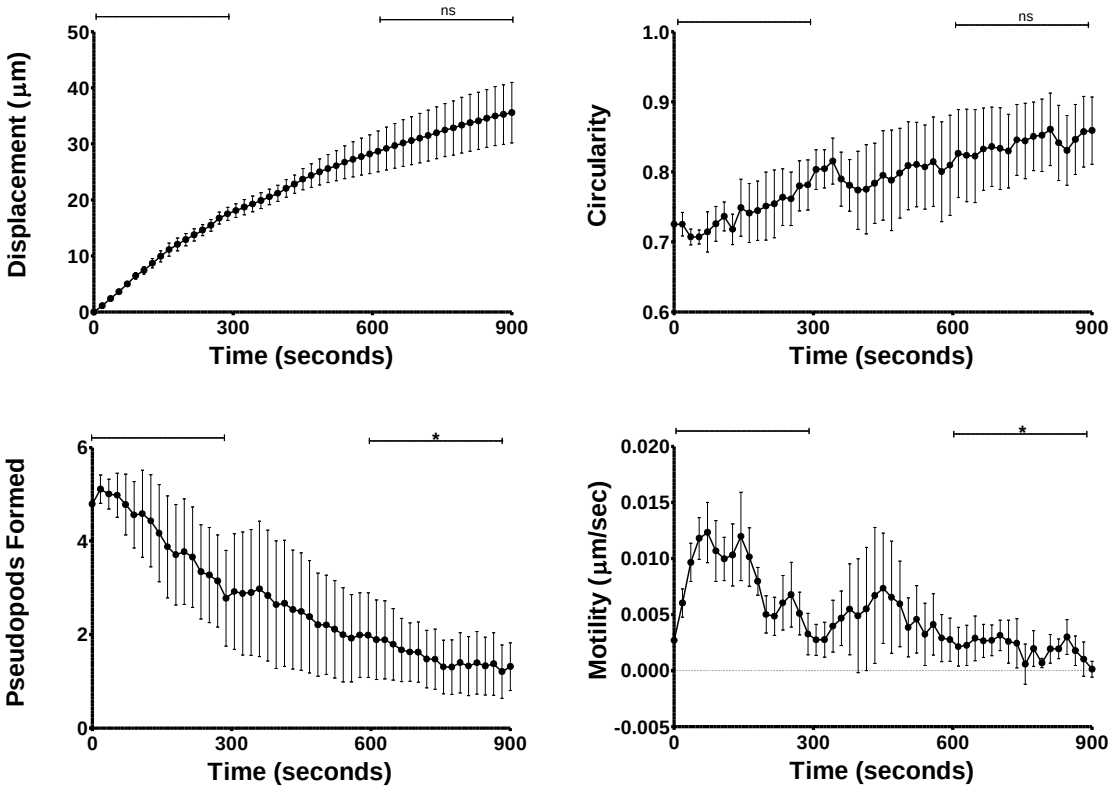

Appendix 5. Analysis of *Dictyostelium* wild-type cells during random cell movement following exposure to curcumin (5μM) after 288 seconds. Cell behaviour was measured during random cell movement, with data from 30 cells quantified every 18 seconds over a 900 second period with the addition of curcumin (5μM) after 288 seconds. **(A)** Displacement. No significant change was observed between the first 288 and final 288 seconds of the assay **(B) Circularity**. No significant change was observed between the first 288 and final 288 seconds of the assay. **(C)** Protrusion formation. A significant decrease in protrusion formation was identified between the first and final 288 seconds of the assay ($P<0.05$). **D:** Motility. A significant decrease in cell motility was identified between the first 288 and final 288 seconds of the assay ($P<0.05$) Data from A-D is presented as mean of triplicate experiments analysing a 10 cells in each. Statistical analyses were performed using paired two-tailed Student t-tests comparing average values from T=0-288 and T=612-900 seconds as indicated. ns = not significant.

Chemical	Gene Name A	Gene Name B	Gene Product A	Gene Product B
P	*abcC3*		ABC transporter C family protein	
V	abcC8		ABC transporter C family protein	
D, V	*abcG12*		ABC transporter G family protein	
P	*abcG9*		ABC transporter G family protein	
V	*acsA*		acetyl-CoA synthetase	
N	*adcF*		arrestin domain-containing protein	
P	*agpB*		1-acylglycerol-3-phosphate O-acyltransferase	
N, V	*arcC*		actin related protein 2/3 complex, subunit 3	
D	*arfGAP*		Arf GTPase activating protein	
D, N, P, V	*armc8*	*DDB_G0269732*	armadillo repeat-containing protein	DnaJ homolog subfamily member 1
P, N	*chr3:958029*			
V	*cinC*		elongation factor 2, vegetative specific protein H6	
N, V	cprA		cysteine protease	
D	*cupC*	*cupD*	calcium up-regulated protein	calcium up-regulated protein
D, N, P, V	*DDB_G0267590*		GRAM domain-containing protein	
V	DDB_G0267824	*DDB_G0267822*		
D, P	*DDB_G0268150*	*DDB_G0268148*	Pseudogene	
V	DDB_G0268242			
D	*DDB_G0268250*			
V	DDB_G0268902		long stretch of CAA (cationic amino acid)	
D, N, P, V	*DDB_G0269022*	*DDB_G0268874*		
N	*DDB_G0269090*			
D	*DDB_G0269308*		Pseudogene	
P	*DDB_G0269478*	*act31*		actin related protein
D, N, V	*DDB_G0269760*		BTB/POZ domain-containing protein.	

V	DDB_G0269998	rnf10		RING zinc finger-containing protein
V	*DDB_G0270300*			
N	*DDB_G0270796*		Pseudogene	
D	*DDB_G0270856*		RabGAP/TBC domain-containing protein	
D, N, P, V	*DDB_G0271296*	*DDB_G0271294*		
P	*DDB_G0272160*			
D	*DDB_G0272282*		protein serine/threonine kinase	
V	DDB_G0272450	G0272290_RTE		
V	DDB_G0272965	DDB_G0272670		
D, N, P, V	*DDB_G0272999*		putative Ca2+ channel. polycystin-2-like protein	
N	*DDB_G0273017*		isocitrate lyase	
D, P, V	*DDB_G0273629*	*DDB_G0273627*		
N	*DDB_G0274199*	*DDB_G0274197*	putative metallophosphoesterase	methyltransferase type 12 protein
P	*DDB_G0275117*			
D	*DDB_G0275393*	*DDB_G0275329*		
N, P, V	*DDB_G0276263*			
P	*DDB_G0276327*	*DDB_G0276271*		
N, V	*DDB_G0277069*		Deleted	
P	*DDB_G0277685*			
D	*DDB_G0277769*	*DDB_G0277795*	putative secreted protein; contains a signal sequence	
V	*DDB_G0277777*	*DDB_G0277761*		endoribonuclease L-PSP
D, P	*DDB_G0277795*	*DDB_G0277769*		
D	*DDB_G0278235*	*dhkB*		histidine kinase
D	*DDB_G0278245*	*DDB_G0284605*	Deleted	P-type ATPase, Calcium ATPase
D, V	*DDB_G0278323*	*DDB_G0278663*		coiled-coil domain-containing protein
N, V	*DDB_G0278591*			

D, P	*DDB_G0278663*	*DDB_G0278323*	coiled-coil domain-containing protein	
V	*DDB_G0278761*		NF-X1-type zinc finger-containing protein	
D	*DDB_G0278953*		CBS domain-containing protein	
D	*DDB_G0279203*			
N, P	*DDB_G0279339*	*DDB_G0279341*		
P	*DDB_G0279341*	*DDB_G0279339*		
V	DDB_G0280107			
N, V	*DDB_G0280135*	*DDB_G0280133*	methionine adenosyltransferase beta subunit	putative protein serine/threonine kinase
V	DDB_G0280141			
V	DDB_G0280441	cpiB		cystatin A2. cysteine protease inhibitor
D, N, P	*DDB_G0280593*		Uncharacterised protein KIAA1370	
D	*DDB_G0281447*			
D	*DDB_G0282455*			
V	*DDB_G0282719*	*DDB_G0282827*		
V	DDB_G0282783	DDB_G0282555		similar to a *D. purpureum* protein
D, P, V	*DDB_G0283077*		putative glycoside hydrolase	
P	*DDB_G0283417*		putative protein tyrosine phosphatase	
N	*DDB_G0283719*		DUF1740 family, HAT helix repeat-containing protein	
P	*DDB_G0283753*	*rpl26*		S60 ribosomal protein L26
D	*DDB_G0283967*	*erkB*		extracellular response kinase
D, N, V	*DDB_G0284149*	*DDB_G0284147*	peripheral membrane protein located at Vid vesicles	
D	*DDB_G0284279*		Pseudogene	
D, N, P, V	*DDB_G0284561*			
D, P	*DDB_G0284989*		Deleted	
D, V	*DDB_G0285143*	*osbJ*	Unknown	oxysterol binding family protein, member 10
D, P	*DDB_G0285169*	*DDB_G0285173*		

V	DDB_G0285215		domain similarity to bacterial hypothetical proteins	
N	*DDB_G0285547*	*DDB_G0285545*	TRE3-A ORF2	Ctr copper transporter family protein
V	*DDB_G0285705*		RING zinc finger-containing protein	
D, P	*DDB_G0285747*	*DDB_G0285483*	Deleted	
D	*DDB_G0286053*	*leo1*	Unknown	RNA polymerase II complex component
V	DDB_G0286081			
N	*DDB_G0286175*		Unknown	
V	*DDB_G0286175*	*DDB_G0286141*		
P	*DDB_G0286765*	*DDB_G0286763*	AAA ATPase/BCS1-like protein	
N	*DDB_G0286943*	*DDB_G0286941*	Unknown	
V	DDB_G0286973			
D	*DDB_G0287077*	*gpaC*	protein prenyltransferase alpha subunit	G-protein subunit alpha 3
P	*DDB_G0287085*			
V	DDB_G0287201			
D, P, V	*DDB_G0287491*		paramecium surface antigen repeat-containing protein	
V	DDB_G0287873			
D	*DDB_G0287933*		putative caspase	
D	*DDB_G0288003*	*DDB_G0288001*	EGF-like protein	Putative fatty acyl-CoA synthetase
N	*DDB_G0288035*	*DDB_G0288037*		
D	*DDB_G0288523*		1-acyl-sn-glycerol-3-phosphate acyltransferase gamma	
D, V	*DDB_G0288865*	*agpC*	Uncharacterised N-acyltransferase yjgM	1-acylglycerol-3-phosphate O-acyltransferase
V	*DDB_G0289409*			
D	*DDB_G0289805*	*DDB_G0289777*	TRE3-B	Pseudogene
N	*DDB_G0290305*	*DDB_G0290307*		RNA-binding region containing protein
D	*DDB_G0290307*	*DDB_G0290305*	RNA-binding region RNP-1 protein	

D	*DDB_G0290867*	*jcdF*	Deleted	JmjC protein
D	*DDB_G0291203*		transmembrane protein	
V	DDB_G0291277	DDB_G0291275		mucolipin, putative Ca2+ channel
D	*DDB_G0291394*		Putative lipase YJR107W	
V	DDB_G0291924			
V	*DDB_G0291968*			
D, N	*DDB_G0292236*		contains a signal peptide	
V	*DDB_G0293032*			
V	DDB_G0293282			
V	DDB_G0293440			
V	DDB_G0293486	fncI	TRE3-C ORF1	Fanconi anemia group I protein
D	*DDB_G0293492*		glycoside hydrolase family 25 protein	
D	*DDB_G0293548*	*empB*		emp24/gp25L/p24 family protein B
V	DDB_G0293662			
V	*DDB_G0294174*	*DDB_G0267208*		DIRS1 ORF1 fragment
D	*DDB_G0295725*	*DDB_G0278603*	Unknown	
D, P	*dhKE*		/HisK family protein kinase	
V	*eif2b1*	*panC*	translation initiation factor eIF-2B alpha subunit	pantoate-beta-alanine ligase
V	*eif3H*		translation initiation factor 3 (eIF3) subunit H	
D, V	eIF4g	DDB_G0275393	eukaryotic translation initiation factor 4 gamma	
D	*elp3*		elongation protein 3	
D	*exdl2B*	*exdl2A*	3'-5' exonuclease protein	3'-5' exonuclease protein
D	*fnKD-2*	*fnKD-1*	FNIP repeat-containing protein	FNIP repeat-containing kinase
D	*fnkE*		putative protein serine/threonine kinase	
D	*forJ*	*DDB_G0287061*	formin homology domain-containing protein	Rab GTPase domain-containing protein
D, V	*frmC*		leucine-rich repeat-containing protein (LRR)	

D	*fuk*	*DDB_G0269680*	Fucokinase	FG-GAP repeat containing protein 2
P, V	*gacE*		RhoGAP domain-containing protein	
V	*gbpC*	*DDB_G0291109*	RasGEF domain-containing protein	
P	*gbpD*		RasGEF domain-containing/ cyclic GMP-binding protein	
D	*glnA3*	*DDB_G0279473*	glutamate-ammonia ligase	NADH oxidase domain-containing protein
D, P	*gnd*		6-phosphogluconate dehydrogenase (decarboxylating	
V	gpaE		G-protein subunit alpha 5	
P	*gpaI*		G-protein subunit alpha 9	
D, P	*gpaK*		G-protein subunit alpha 11	
P	*grlJ*	*DDB_G0272442*	G-protein-coupled receptor (GPCR) family 3 protein 9	
P	*gxcH*		PH domain-containing/RhoGEF protein	
N, V	*gxcI*		RhoGEF domain-containing protein	
V	*gxcP*		pleckstrin homology (PH) domain-containing protein	
D	*impA*		FKBP-type peptidylprolyl cis-trans isomerase (PPIase)	
P	*impaI*		Inositol monophosphatase (IMPase)	
D, N, P	*kif11*		kinesin family member 11	
N	*lmpA*		lysosomal integral membrane glycoprotein	
D	*lysA*		WD-40 repeat-containing protein	
N	*lysS*	*mrpl17*	lysine-tRNA ligase	ribosomal protein L17, mitochondrial
N	*mcfA*		transmembrane protein, mitochondrial substrate carrier	
D	*memo1*		Mediator of ErbB2-driven cell motility	
D, N, V	*mhkB*		myosin heavy chain kinase B	
D	*mlh3*		MutL DNA mismatch repair protein	
N, V	*mlh3*		MutL DNA mismatch repair protein	
V	*nol9*	*parG*	NUC156 family protein	poly (ADP-ribose) glycohydrolase

V	noxC		NADPH oxidase flavocytochrome	
N	*ponB*	*DDB_G0286245*	putative actin binding protein	
P	*psaB*		puromycin-sensitive aminopeptidase-like protein	
D, V	*purL*		phosphoribosylformylglycinamide synthase	
P, V	*rabR*	*DDB_G0271978*	Rab GTPase	Pseudogene
P	*ranbp1*		Ran binding protein 1 domain-containing protein	
P	*rasV*		Ras GTPase	
D, N	*rasW*		Ras GTPase	
V	rpa1	DDB_G0275951	RNA polymerase I, largest subunit	putative transmembrane protein
D	*rpl13a*		protein component of the large (60S) ribosomal subunit	
D	*rpl26*		protein component of the large (60S) ribosomal subunit	
V	*rpl3*	*DDB_G0291924*	60S ribosomal protein L3	
D	*rpl32*	*DDB_G0271978*	S60 ribosomal protein L32	
P	*rpl35a*	*nek2*	S60 ribosomal protein L35a	protein serine/threonine kinase
V	*rpl6*	*psmC5*	60S ribosomal protein L6	26S proteasome subunit ATPase 5
D, V	*rvb2*	*DDB_G0280773*	RuvB-like protein 2	
P	*samm50*	*limG*	sorting and assembly machinery like protein	LIM-type zinc finger-containing protein
P	*sec31*		WD40 repeat-containing protein	
P	*sibC*		von Willebrand factor domain-containing protein	
D	*spt6*		SH2 domain-containing protein	
P	*syn8A*		syntaxin 8/ t-SNARE family protein	
V	*tal*	*DDB_G0280945*	Transaldolase	
V	*tgrA_ps3*	*cpnF*	immunoglobulin E-set family gene	phospholipid-binding protein
V	*tgrH_ps1*	*dcp2*	immunoglobulin E-set family gene	mRNA-decapping enzyme 2
P	*thoc1*	*DDB_G0275497*	putative THO1 protein (nuclear matrix protein p84)	

P	*tRNA-Ser-GCU-1*		serine transfer RNA	
V	*tRNA-Tyr-GUA-5*	DDB_G0285545	tyrosine transfer RNA	Ctr copper transporter family protein
N	*ube2c*	*DDB_G0278773*	ubiquitin-conjugating enzyme E2	vesicle-associated membrane protein
D	*ublcp1-2*	*ublcp1-1*	ubiquitin-like CTD phosphatase 1	ubiquitin-like CTD phosphatase 1
D	*udKA*		uridine kinase, uridine phosphokinase	
P, V	*usp39*		SAP DNA-binding domain-containing protein	
D, P	*wrnip1*		Werner helicase-interacting protein 1	
V	*ykt6*	dus4l	v-SNARE family protein	tRNA-dihydrouridine synthase 4-like
N	*zntB*	*crlE*	zinc/iron permease	G-protein-coupled receptor family protein

Appendix 6. REMI mutants showing resistance to tastants. Insertions in 187 genes that were found to convey resistance to bitter tastants denatonium benzoate (D), phenylthiourea (P), naringenin (N) and/or valproic acid (V). Gene names and a brief gene description have been indicated. Where two genes have been listed, the blasticidin and barcode insertion has occurred upstream or downstream of each gene, where it is unclear exactly which gene has been affected.

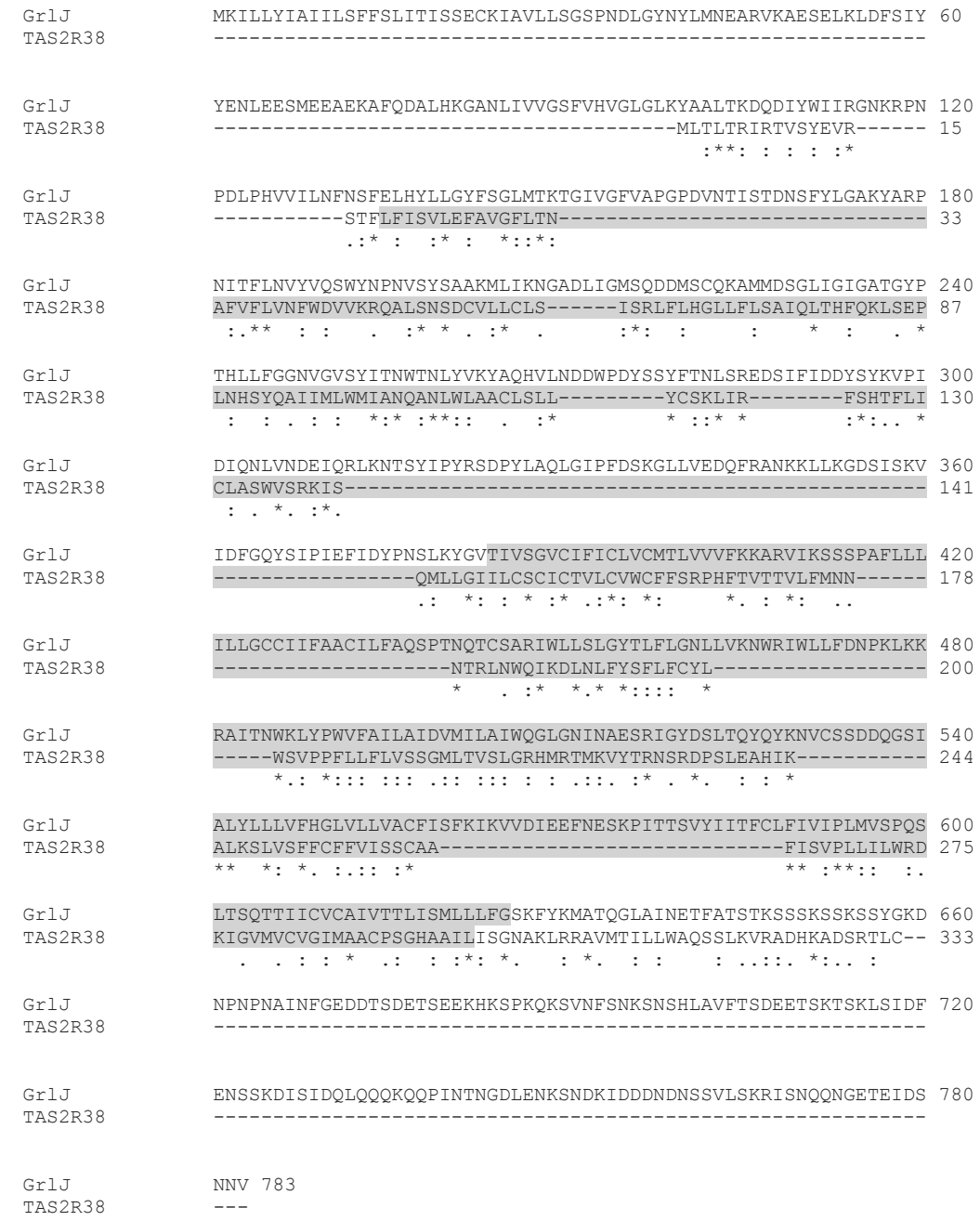

Appendix 7. Amino acid homology between GrlJ and TAS2R38. *Dictyostelium* GrlJ and human TAS2R38, responsible for phenylthiourea detection, were aligned using Clustal Omega. Low sequence homology is seen in the transmembrane regions (highlighted in grey), where only a small region of the transmembrane domains of the two proteins overlap.

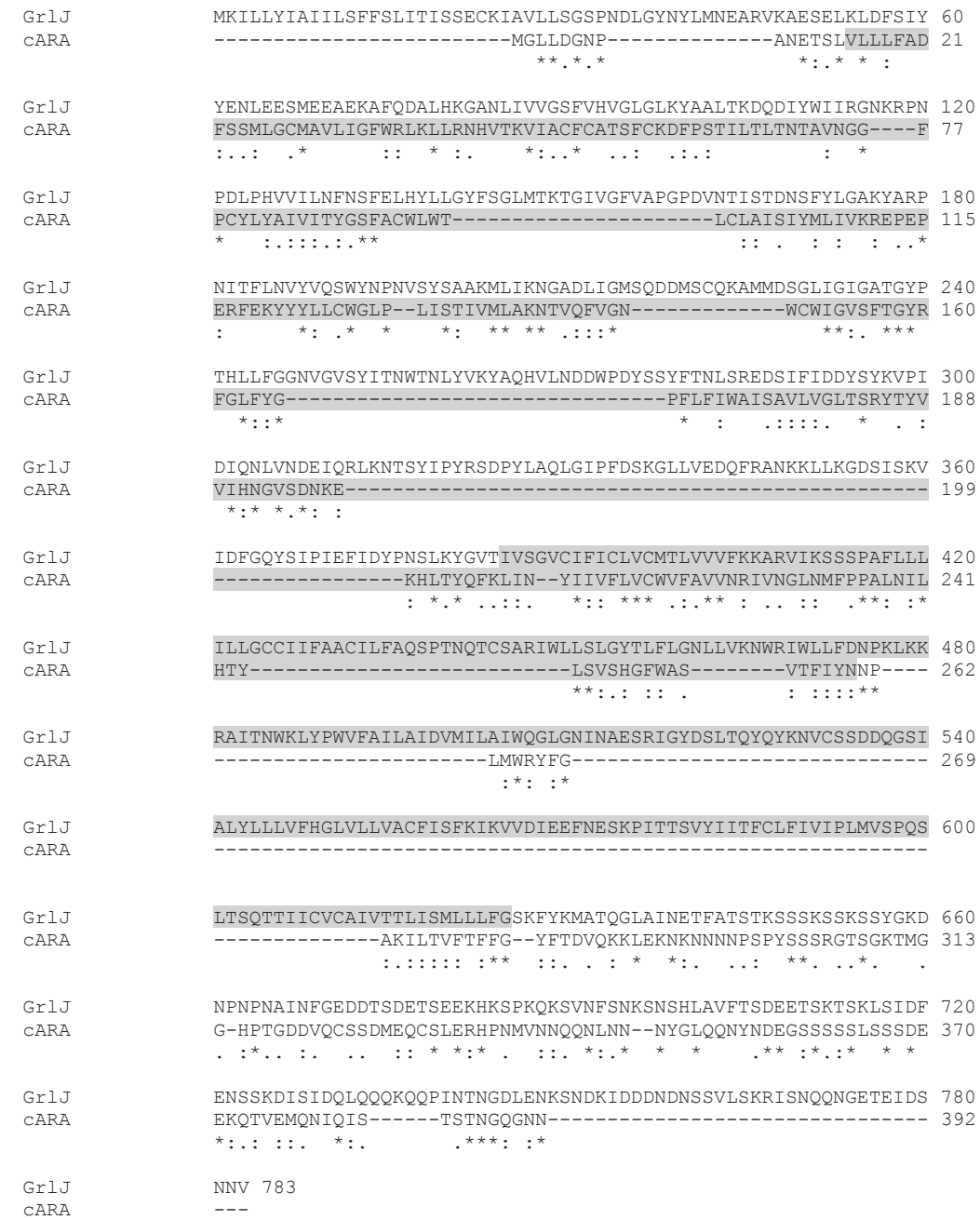

Appendix 8. Amino acid homology between GrlJ and cARA. *Dictyostelium* GrlJ and cARA, responsible for cAMP signal detection, were aligned using Clustal Omega. Low sequence homology homology is seen in the transmembrane regions (highlighted in grey), where only a small region of the transmembrane domains of the two proteins overlap.

Publications

Investigating the effect of emetic compounds on chemotaxis in *Dictyostelium* identifies a non-sentient model for bitter and hot tastant research

Steven Robery[1], Janina Mukanowa[1], Nathalie Percie du Sert[2], Paul L. R. Andrews[2], Robin S. B. Williams[1,*]

[1]Centre for Biomedical Sciences, School of Biological Sciences, Royal Holloway University of London, Egham TW20 0EX, UK

[2]Division of Biomedical Sciences, St George's University of London, London SW17 0RE, UK

2011, *PlosOne*

Abstract

Novel chemical entities (NCEs) may be investigated for emetic liability in a range of unpleasant experiments involving retching, vomiting or conditioned taste aversion/food avoidance in sentient animals. We have used a range of compounds with known emetic /aversive properties to examine the possibility of using the social amoeba, *Dictyostelium discoideum*, for research into identifying and understanding emetic liability, and hence reduce adverse animal experimentation in this area. Twenty eight emetic or taste aversive compounds were employed to investigate the acute (10 min) effect of compounds on *Dictyostelium* cell behaviour (shape, speed and direction of movement) in a shallow chemotactic gradient (Dunn chamber). Compound concentrations were chosen based on those previously reported to be emetic or aversive in *in vivo* studies and results were recorded and quantified by automated image analysis. *Dictyostelium* cell motility was rapidly and strongly inhibited by four structurally distinct tastants (three bitter tasting compounds - denatonium benzoate, quinine hydrochloride, phenylthiourea, and the pungent constituent of chilli peppers - capsaicin). In addition, stomach irritants (copper chloride and copper sulphate), and a phosphodiesterase IV inhibitor also rapidly blocked movement. A concentration-dependant relationship was established for five of these compounds, showing potency of inhibition as capsaicin (IC_{50}=11.9±4.0μM) > quinine hydrochloride (IC_{50}=44.3±6.8μM) > denatonium benzoate (IC_{50}=129±4μM) > phenylthiourea (IC_{50}=366±5μM) > copper sulphate (IC_{50}=1433±3μM). In contrast, 21 compounds within the cytotoxic and receptor agonist/antagonist classes did not affect cell behaviour. Further analysis of bitter and pungent compounds showed that the effect on cell behaviour was reversible and not cytotoxic, suggesting an uncharacterised molecular mechanism of action for these compounds. These results therefore demonstrate that *Dictyostelium* has potential as a non-sentient model in the analysis of the molecular effects of tastants, although it has limited utility in identification of emetic agents in general.

A novel human receptor involved in bitter tastant detection identified using the model organism *Dictyostelium discoideum*

Steven Robery[1], Richard Tyson[2], Christopher Dinh[3], Adam Kuspa[3], Angelika A Noegel[4], Till Bretschneider[2], Paul L R Andrews[5], Robin S B Williams[1]

[1]Centre for Biomedical Sciences, School of Biological Sciences, Royal Holloway University of London, Egham TW20 0EX, UK

[2]Molecular Organization and Assembly in Cells, University of Warwick, Coventry, CV4 7AL, UK

[3]Department of Biochemistry and Molecular Biology, Baylor College of Medicine, Houston, Texas 77030, USA

[4]Institute of Biochemistry I, Medical Faculty, University of Cologne, Cologne, Germany

[5]Division of Biomedical Sciences, St George's University of London, London SW17 0RE, UK

2013 *Journal Cell Science*

Abstract

Detection of substances tasting bitter to humans occurs in diverse organisms including the social amoeba, Dictyostelium discoideum. To establish a molecular mechanism for bitter tastant detection in Dictyostelium, we screened a mutant library for resistance to a commonly used bitter standard, phenylthiourea. This approach identified a G-protein coupled receptor mutant, grlJ$^-$, showing a significantly increased tolerance to phenylthiourea in growth, survival and movement. This mutant was not resistant to a structurally dissimilar potent bitter tastant, denatonium benzoate, suggesting it is not a target for at least one other bitter tastant. Analysis of the cell signalling pathway involved in the detection of phenylthiourea showed dependence upon heterotrimeric G-protein and phosphatidylinositol 3-kinase activity, suggesting this signalling pathway is responsible for phenylthiourea cellular effects. This is further supported by a phenylthiourea-dependent block in the transient cAMP-induced production of PIP_3 in wild type but not grlJ$^-$cells. Finally, we have identified an uncharacterized human protein gamma-aminobutyric acid (GABA) type B receptor subunit 1 isoform with weak homology to GrlJ that restored grlJ$^-$ sensitivity to phenylthiourea in cell movement and PIP_3 regulation. Our data thus identifies a novel pathway for the detection of the standard bitter tastant, phenylthiourea, in Dictyostelium and implicates a poorly characterized human protein in phenylthiourea dependent cell responses.

Naringenin inhibits the growth of *Dictyostelium* and MDCK-derived cysts in a polycystin-2 (TRPP2)-dependent manner

Abdul Waheed[1], Marthe Ludtmann[2], Nicholl Pakes[2], Steven Robery[2], Adam Kuspa[3], Christopher Dinh[3], Deborah Baines[1], Robin S B Williams[2], Mark Carew[1]

[1]School of Pharmacy & Chemistry, Kingston University, Penrhyn Road, Kingston upon Thames, Surrey, KT1 2EE, UK

[2]Centre for Biomedical Sciences, School of Biological Sciences, Royal Holloway University of London, Egham TW20 0EX, UK

[3]Department of Biochemistry and Molecular Biology, Baylor College of Medicine, Houston, Texas 77030, USA

2013 *British Journal of Pharmacology*

Abstract

BACKGROUND AND PURPOSE: Identifying and characterising potential new therapeutic agents to target cell proliferation may provide improved treatments for neoplastic disorders such as cancer and polycystic diseases.

EXPERIMENTAL APPROACH: We used the simple, tractable biomedical model Dictyostelium to investigate the molecular mechanism of naringenin, a dietary flavonoid with antiproliferative and chemopreventive actions in vitro and in animal models of carcinogenesis. We then translated these results to a mammalian kidney model, MDCK renal tubule cells, growing in culture and as cysts in a collagen matrix.

KEY RESULTS: Naringenin inhibited Dictyostelium growth, but not development, with an EC50 of 50-100 μM. Screening of a library of random gene knockout mutants identified a mutant lacking polycystin-2 that was resistant to the effect of naringenin on growth and random cell movement. Polycystin-2 (TRPP2) is a divalent cation channel, where mutations in the protein give rise to type 2 autosomal dominant polycystic kidney disease. Naringenin inhibited MDCK cell growth with an EC50 of 28 μM, and inhibited cyst growth with an EC50 of 3-10 μM. Knockdown of polycystin-2 levels by siRNA in this model conferred partial resistance to naringenin such that cysts treated with 3 and 10 μM naringenin were larger following polycystin-2 knockdown compared to controls. Naringenin did not affect chloride secretion.

CONCLUSIONS AND IMPLICATIONS: The action of naringenin on cell growth in the phylogenetically diverse systems of Dictyostelium and mammalian kidney cells, suggests a conserved effect mediated by polycystin-2 (TRPP2). Further studies will investigate naringenin as a potential new therapeutic agent in ADPKD.